ZooKeys 694: 1–10 (2017)
doi: 10.3897/zookeys.694.14616
http://zookeys.pensoft.net

RESEARCH ARTICLE

A peer-reviewed open-access journal
ZooKeys
Launched to accelerate biodiversity research

Two new species and two new records of fungus-feeding Phlaeothripinae from China (Thysanoptera, Phlaeothripidae)

Chao Zhao[1], Xiaoli Tong[1]

1 *Department of Entomology, College of Agriculture, South China Agricultural University, Guangzhou 510642, China*

Corresponding author: *Xiaoli Tong* (xtong@scau.edu.cn)

Academic editor: *L. Mound* | Received 20 June 2017 | Accepted 3 August 2017 | Published 29 August 2017

http://zoobank.org/695583A6-6338-43FD-99C0-86371EACD7C6

Citation: Zhao C, Tong X (2017) Two new species and two new records of fungus-feeding Phlaeothripinae from China (Thysanoptera, Phlaeothripidae). ZooKeys 694: 1–10. https://doi.org/10.3897/zookeys.694.14616

Abstract

Two new species of fungivorous Phlaeothripinae, *Mystrothrips levis* **sp. n.** and *Urothrips lancangensis* **sp. n.**, are described from China. *Pentagonothrips antennalis* Haga & Okajima and *Plectrothrips bicolor* Okajima are newly recorded in China.

Keywords

leaf litter thrips, *Mystrothrips*, new species, *Urothrips*

Introduction

The species of fungivorous Phlaeothripinae belong to *Phlaeothrips* lineage, which are usually taken from dead branches or leaf-litter and feed on fungal hyphae (Mound 2013, Minaei 2013, Dang et al. 2014). The fungivorous Phlaeothripinae fauna of China was poorly known until 30 years ago, so that only 46 species in 18 genera of this group were reported from this country (Tong and Zhang 1989). Recently, the Chinese fungivorous Phlaeothripinae was well reviewed by Dang and Qiao (2014), and subsequently three additional species of the group were recorded from China (Zhao and Tong 2016, Tong and Zhao 2017). Up to the present, 98 species and 31 genera

of fungus-feeding Phlaeothripinae are recorded from China. As a large country which is across the Palaearctic and Oriental regions, China harbors an enormous diversity of Thysanoptera, yet the thrips fauna remains poorly understood. This is especially true for the group of fungus-feeding Phlaeothripinae. During recent surveys of the thrips fauna in southern China, some species of fungus-feeding Phlaeothripinae have been collected. The aim of the present paper is to describe two new species and two newly recorded species of the group from China.

Materials and methods

All thrips specimens were extracted by using Tullgren funnels from leaf litter, and then sorted and preserved in 90% alcohol. Examined specimens were mounted into Canada balsam using the method outlined by Zhang et al. (2006). Slide-mounted specimens were examined and photographed under ZEISS Imager A1 microscope with a digital camera attached. All specimens in this study were collected from leaf-litter unless otherwise noted. All type specimens are deposited in the Insect Collection, South China Agricultural University (**SCAU**).

Taxonomy

***Mystrothrips levis* sp. n.**
http://zoobank.org/5399B364-0B5C-4B37-A2F5-896C751EF8A6
Figs 1–8

Material examined (females and males all apterous). Holotype. Female aptera: **CHINA**, Guangdong: Guangzhou City, South China Botanical Garden (23Guangdong: Guan), in leaf litter of bamboo, 9.viii.2014 (Chao Zhao).

Paratypes. 8 females 2 males, collected with holotype; 5 females 1 male, the same locality but collected on 20.xi.2015 (Chao Zhao).

Description. Female aptera (Fig. 1). Body and antennae uniformly brown. All legs yellowish brown except for tarsi yellow.

Head (Fig. 3) almost as long as broad; dorsal surface smooth medially but with polygonal reticulation between eyes and faint reticulation laterally and posteriorly; cheeks slightly convex and weakly constricted just behind eyes; eyes small and bulging, slightly less than 1/4 of head length; postocular setae long and expanded at apex, approximately half of head length; ocelli absent; postocellar setae and mid-dorsal setae as long as eyes, pointed at apex. Antennae 8-segmented (Fig. 8), approximately 2.5 times as long as head; segments III and IV with two and three sense cones, respectively; segments II–V sculptured; segment VIII strongly constricted at base. Maxillary stylets nearly retracted to postocular setae, approximately one-third of head width apart medially.

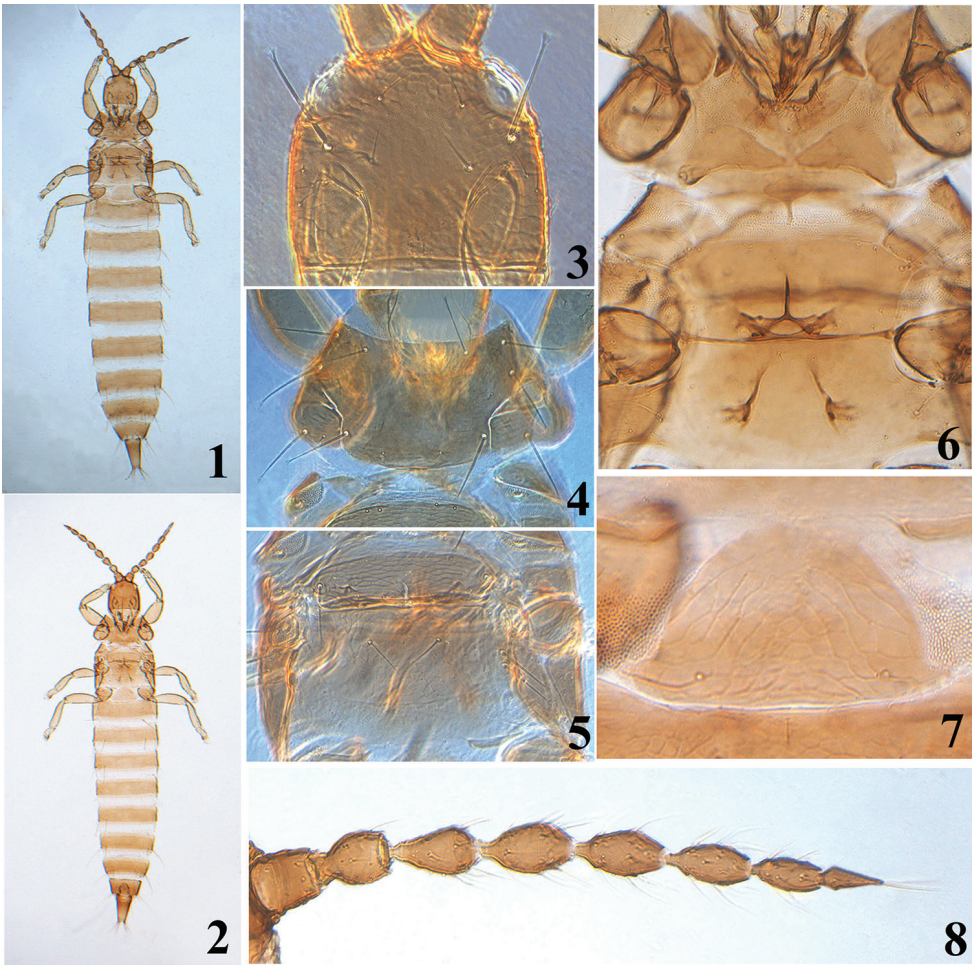

Figures 1–8. *Mystrothrips levis* sp. n. **1** female **2** male **3** head **4** pronotum **5** meso- and metanotum **6** ventral view of thorax **7** pelta **8** antenna.

Pronotum dorsal surface almost smooth but with faint transverse lines anteriorly; notopleural sutures complete; five pairs of major setae long and expanded (Fig. 4). Basantra present but small; ferna and prospinasternum well-developed. Mesonotum sculptured with distinctly transverse reticulation, and a pair of well-developed long lateral setae expanded at apex; mesopresternum eroded medially, divided into two small irregular lateral plates. Metanotum weakly sculptured with polygonal reticulation, a pair of long and acute setae situated medially (Fig. 5); meso- and metasternum smooth; metathoracic sternopleural sutures absent (Fig. 6); mesoeusternum anterior margin entire, mesothoracic furcae united together medially, but metathoracic furcae separated. Fore tarsal tooth absent.

Pelta nearly semicircular in shape with short lateral lobes, distinctly reticulate, a pair of campaniform sensilla present (Fig. 7); abdominal tergites weakly sculptured with reticulation, without developed sigmoid wing retaining setae; S1 and S2 setae on

tergites II–VIII well-developed, long and expanded at apex; S1 setae on tergite II much longer than S2, approximately 3.0 times as long as S2; tergites III–VII with S1 and S2 setae subequal in length; S1 on tergite VIII approximately 0.7 times as long as S2; tergite IX with S1 and S2 setae subequal in length, longer than tube, weakly pointed or blunt at apex; abdominal sternites II–VIII with a transverse row of 8–16 discal setae medially, each sternite bearing two pairs of long and pointed setae arising in front of posterior margin. Tube approximately 4/5 of head length; anal setae shorter than tube.

Measurements **(holotype female in microns).** Distended body length 2030. Head length 190, width 185; eyes length 50; postocular setae length 75. Antennae length 470, segments I–VIII length (width) as follows: 49(43); 53(41); 68(32); 67(34); 65(34); 61(30); 54(24); 52(12). Pronotum median length 140, width across median part 310; length of major setae: pronotum anteromarginal setae 48, anteroangular setae 68, midlateral setae 90, posteroangular setae 85, epimeral setae 80. Metanotum median setae 40. Pelta length 100, width at base 170. Abdominal tergite IX S1 setae length 190, intermediate setae length 85, S2 length 190. Tube length 155, width at base 93, at apex 42; anal setae length 135.

Male aptera (Fig. 2): Similar to apterous female in color and structure but smaller. Fore tarsal tooth present; tergite IX with S1 setae approximately 3.0 times as long as S2; sternites without pore plate.

Measurements **(paratype male in microns).** Distended body length 1620. Head length 160, width 155; eyes length 35; postocular setae length 70. Antennae length 375, segments I–VIII length (width) as follows: 34(36); 44(29); 50(32); 50(31); 55(28); 50(25); 45(20); 45(13). Pronotum median length 125, width across median part 260; length of major setae: pronotum anteromarginal setae 60, anteroangular setae 45, midlateral setae 73, posteroangular setae 66, epimeral setae 63. Metanotum median setae 30. Pelta length 65, width at base 110. Abdominal tergite IX setae S1 length 145, intermediate setae length 60, S2 length 45. Tube length 130, width at base 80, at apex 32; anal setae length 110.

Distribution. China (Guangdong).

Etymology. The specific epithet, *levis*, is from the Latin adjective, meaning "smooth", and refers to the dorsal surface of head and pronotum which are largely smooth. In contrast, most species of this genus are sculptured with distinct polygonal reticulation on head and pronotum.

Remarks. Of the seven species worldwide listed in the genus *Mystrothrips* (ThripsWiki 2017), two are recorded from China. *M. longantennus* Wang, Tong & Zhang is from southern China, and *M. flavidus* Okajima is widespread from China (Guangxi, Guangdong and Taiwan) to Japan (Okajima 2006, Wang et al. 2008, Dang and Qiao 2014). The new species is most similar to *M. flavidus* in color and structure, but it can be distinguished from the latter by (1) head and pronotum largely smooth (vs sculptured with polygonal reticulation entirely in *M. flavidus*); (2) antennae uniformly brown (versus antennae segments I and II distinctly lighter than remaining segments in *M. flavidus*); (3) pelta semicircular with short lateral lobes (vs broadly trapezoidal in *M. flavidus*); (4) S1 and S2 setae on abdominal tergite IX much longer than tube (vs shorter than tube in *M. flavidus*).

***Pentagonothrips antennalis* Haga & Okajima**
Figs 9, 10

Pentagonothrips antennalis Haga & Okajima, 1979: 147.

Material examined. CHINA, Hunan: 2 females and 1 male, Zhuzhou City, Yanling County, Shennong Valley (26°29'N, 114°01'E), in leaf litter, 16. ix. 2014 (Chao Zhao). **Hubei:** 1 male, Huanggang City, Yingshan County, Taohuachong (30°99'04"N, 116°02'76"E), in leaf litter, 23.iv.2014 (Chao Zhao).

Diagnosis. Dorsal surface of body entirely reticulate; head longer than width, cheeks distinctly incut behind eyes; postocular setae well-developed with expanded at apex. Antennae 7-segmented, morphological segments VII and VIII fused with an incomplete suture, segments III and IV with two and three sense cones, respectively. Maxillary stylets short, wide apart. Pronotum with five pairs of well-developed major setae, strongly expanded at apex. Basantra absent. Fore tarsal tooth present in both sexes. Pelta transverse, shaped as a squashed ellipse, with distinctly polygonal reticulation. Sternite VIII with pair of stout or leaf-like posteromarginal setae submedially. Tube short than head. Pore plate of male absent.

Distribution. China (Hunan, Hubei); Japan.

Remarks. The monobasic genus, *Pentagonothrips*, was originally established from Japan (Haga and Okajima 1979, Okajima 2006). *P. antennalis* is here recorded from China for the first time. This species is closely related to the species of the genus *Mystrothrips* Priesner in shape and structure. However, it can be separated from *Mystrothrips* by the following characters: Antennae 7-segmented; mesopresternum weak and membranous; anterior margin of mesoeusternum with a longitudinal median division (mesoeusternum anterior margin entire in *Mystrothrips*); mesothoracic furcae closely fused together medially as well as metathoracic furcae joined together medially (but metathoracic furcae separated in *Mystrothrips*).

***Plectrothrips bicolor* Okajima**
Figs 11, 12

Plectrothrips bicolor Okajima, 1981: 313.

Material examined. CHINA, Guangdong: 1 female, Guangzhou City, Arboretum of South China Agricultural University (23°09'N, 113°21'E), in leaf litter, 20.xi.2004 (Jun Wang); 1 male, Guangzhou City, Dafushan Forest Park (22°57'N, 113°18'E), in leaf litter of *Litchi chinensis*,17.iv.2016 (Chao Zhao).

Diagnosis. Body bicolored, yellow and brown. Head, thorax and tube brown, abdomen yellowish brown; all legs yellow; antennal segments II and III yellow, remaining segments brown. Head longer than broad, dorsal surface smooth except weakly sculptured posterolaterally. Antennal segments III and IV with two and three sense cones,

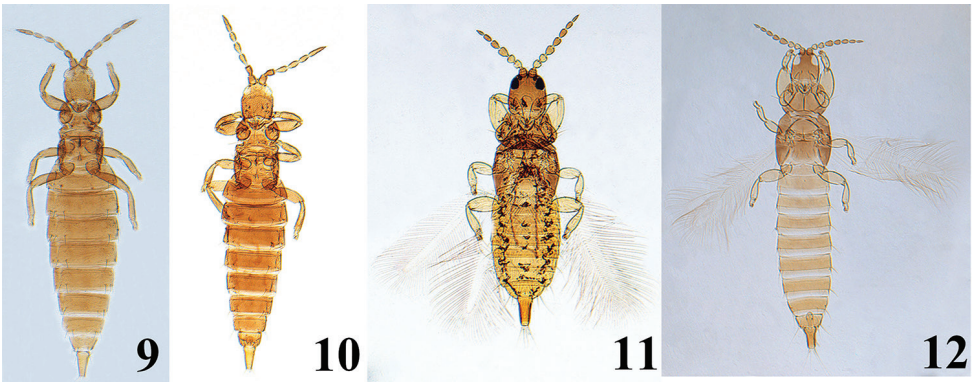

Figures 9–12. *Pentagonothrips antennalis* Haga & Okajima: **9** female **10** male *Plectrothrips bicolor* Okajima: **11** female **12** male.

respectively, segment VI with two sense cones. Maxillary stylets short, maxillary bridge developed and arched. Pronotum smooth, surrounded by stippled membrane with a distinct median longitudinal line. Metanotum with longitudinal striae medially. Mid tibia and hind tibia with one and two apical spur-like stout setae, respectively. Forewing parallel-sided with seven duplicated cilia. Pelta irregularly triangular with slender lateral lobes and a pair of campaniform sensilla. Abdominal tergites II–VII each with a pair of wing retaining setae; sternites V–VII with a pair of worm-like reticulate areas in both sexes; tergite IX S1 and S2 setae pointed, S1 setae longer than S2 but shorter than tube; tergite IX in male with a small median projection on posterior margin.

Distribution. China (Guangdong); Japan; Indonesia.

Remarks. This genus now includes 32 species in the world (ThripsWiki 2017), of which three species have been reported from China (Dang et al. 2014). *P. bicolor*, originally described from Japan and Indonesia (Okajima 1981, 2006), is here newly recorded from mainland China. This species is extracted from leaf litter by using Tullgren funnels in the present study. In contrast, most species of the genus are usually collected under bark of decayed trees.

Urothrips lancangensis sp. n.

http://zoobank.org/B5B5318F-4ADA-49EE-928F-9C8CA9299354
Figs 13–19

Material examined (females and males all apterous). Holotype. Female aptera, **CHINA**, Yunnan province, Pu'er City, Lancang County, Nuozhadu Nature Reserve (22°30'N,100°34'E, alt. 1840m), 5.xi.2016 (Chao Zhao).

Paratypes. 6 females, 3 males, collected with holotype.

Description. Female aptera (Fig. 13): Body bicolored, yellow and brown; largely yellow except head, pronutum, fore and hind femora and abdominal tergites I–IV(V)

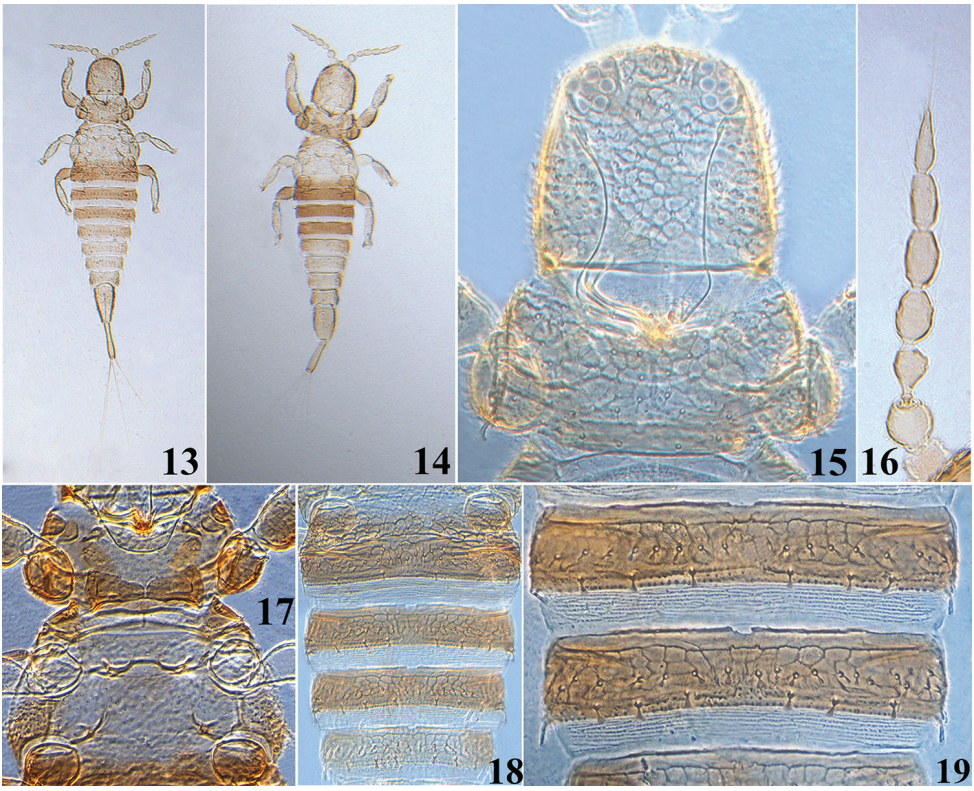

Figures 13–19. *Urothrips lancangensis* sp. n. **13** female **14** male **15** head and pronotum **16** antenna **17** pro, meso and meta sternum **18** abdominal tergites I–V 19 abdominal tergites III–IV.

brown; antennal segments II–VII tinged with light brown; tergites V–IX yellow shaded with brown laterally; tube yellow with extreme apex brown.

Head (Fig. 15) as long as or a little shorter than broad; head broadly rounded in front, without any prominent setae on anterior margin, weakly produced between antennae ventrally; cheeks slightly convex; dorsal surface sculptured with polygonal reticulation except tuberculate laterally and small setae weakly expended at apex. Eyes with approximately 10 facets dorsally, but absent ventrally; ocelli absent. Antennae arising ventrally, with 7 visible segments and distinct from each other (Fig. 16); segment VII without suture between morphological segments VII and VIII; segment III with one simple sense cone, situated outside of apex; IV with two simple sense cones, each approximately two-thirds as long as the segment; segments VI and VII each with one outer simple sense cone. Maxillary stylets retracted to compound eyes, approximately half of head width apart medially.

Pronotum transverse and rectangular (Fig. 15), approximately 2.3 times as wide as long and 0.6 times as long as head; dorsal surface sculptured with polygonal reticulation and many small setae expended at apex; epimeral setae well developed and expanded at apex. Basantra reduced to a pair of small plates laterally; ferna well devel-

oped. Meso- and metanotum with small setae expanded at apex and faintly reticulate; meta-epimeron bulging with wart-like small tubercles and one well- developed seta expanded at apex, more slender than pronotal epimeral setae. Mesopresternum complete and transverse; mesoeusternum anterior margin entire; mesothoracic furcae fused together medially, but metathoracic furcae widely separated (Fig. 17). Fore tarsus with a hook-like hamus on external margin.

Abdomen broadest at segment II and tapering evenly to the tube. Abdominal tergite I transverse and distinctly sculptured, closely fused to tergite II, and clearly separated from metanotum (Fig. 18); tergites II–VIII sculptured with polygonal reticulation at anterior half and with a transverse row of 10–22 short, dilated and fan-shaped setae medially, and each with three pairs of short, fan-shaped setae in front of posterior margin (Figs 18, 19); tergites III–VIII each with a pair of well-developed posterolateral setae blunt at apex; tergite IX faintly reticulate, approximately 2.5 times as long as distal wide. Tube weakly reticulate, slightly shorter than head length, constracted submedially and weakly convex near apex; tube with three pairs of anal setae; the longest lateral anal setae approximately 3.5 times as long as tube, but median dorsal pair shorter than the lateral two pairs.

Measurements (holotype female in microns). Body length 1400. Head length 180; maximum width 190. Pronotum length 110; median width 250; epimeral setae 20. Metathoracic epimeral setae 20. Abdominal tergite IX length 120, basal width 75, distal width 40. Tube length 130, basal width 22, apical width 25; anal setae 430. Antennal segments I–VIII length (width) as follows: 20(36), 28 (31), 37 (23), 39 (24), 45 (20), 40 (15), 47 (12).

Male aptera. (Fig. 14). Color and structure similar to apterous female, but body smaller.

Measurements (paratype male in microns). Body length 1050. Head length 160; maximum width 160. Pronotum length 90; median width 185; epimeral setae 13. Metathoracic epimeral setae 13. Abdominal tergite IX length 105, basal width 55, distal width 40. Tube length 115, basal width 20, apical width 22; anal setae 370. Antennal segments I–VIII length (width) as follows: 22(33), 23 (31), 32 (19), 29 (22), 33 (20), 31(17), 39(13).

Distribution. China (Yunnan).

Etymology. The specific epithet is named after the type locality, Lancang County, Yunnan Province, China.

Remarks. There are ten species recognized in this genus (ThripsWiki 2017), of which three are recorded from China (Tong and Zhao 2017). The new species described here shares morphological affinities with *Urothrips tarai* (Stannard, 1970), particularly in the shape of antennae, but it can be differentiated from the latter by the following diagnostic characters: (1) head broadly rounded in front (vs slightly produced in *U. tarai*); (2) dorsal surfaces of head and pronotum largely sculptured with polygonal reticulation (vs head and pronotum distinctly tuberculate and without reticulation in *U. tarai*); (3) major body setae on head, pronotum, especially on abdominal tergites are stout, dilated and fan-shaped at apex (in *U. tarai*, the major body setae are fine and pointed except epimeral, meta-epimeron and abdominal tergites III–VIII posterolateral setae); (4) fore femora brown (while fore femora yellow in *U. tarai*).

Acknowledgements

This study was funded by the National Natural Science Foundation of China (No. 31372236), the Key Project for National Groundwork of Science & Technology (No. 2013FY111500-5-3) and the Pilot Programme of Biodiversity Survey and Assessment (No. 2016HB2096001006). The first author would like to thank Dr. Xingmin Wang (South China Agricultural University) for his assistance during collecting trips. We also acknowledge the helpful comments and suggestions provided by the editor and referees.

References

Dang LH, Mound LA, Qiao GX (2014) Conspectus of the Phlaeothripinae genera from China and Southeast Asia (Thysanoptera, Phlaeothripidae). Zootaxa 3807(1): 1–82. http://dx.doi.org/10.11646/zootaxa.3807.1.1

Dang LH, Qiao GX (2014) Key to the fungus-feeder Phlaeothripinae species from China (Thysanoptera: Phlaeothripidae). Zoological Systematics 39(3): 313–358. http://159.226.67.68/EN/10.11865/zs20140301

Haga K, Okajima S (1979) A new glyptothripine genus and species (Thysanoptera: Phlaeothripidae) from Japan. Annotationes Zoologicae Japonensis 52: 146–150. http://ci.nii.ac.jp/naid/110003353225

Minaei K (2013) The *Phlaeothrips*-lineage of fungus feeding thrips (Thysanoptera: Phlaeothripidae) in Iran with a new species of *Hindsiothrips*. Zootaxa 3599: 279–290. http://dx.doi.org/10.11646/zootaxa.3599.3.5

Mound LA (2013) Order Thysanoptera Haliday, 1836. In: Zhang Z-Q (Ed.) Animal biodiversity: An outline of higher-level classification and survey of taxonomic richness. Zootaxa 3703: 1–82. http://dx.doi.org/10.11646/zootaxa.3703.1.11

Okajima S (1981) A revision of the tribe Plectrothripini of fungus-feeding Thysanoptera (Phlaeothripidae: Phlaeothripinae). Systematic Entomology 6: 291–336. http://dx.doi.org/10.1111/j.1365-3113.1981.tb00441.x

Okajima S (2006) The Insects of Japan. Vol. 2. The suborder Tubulifera (Thysanoptera). Touka-Shobo Co. Ltd., Fukuoka, 720 pp.

Stannard LJ (1970) New genera and species of Urothripini (Thysanoptera: Phlaeothripidae). Proceedings of the Royal Entomological Society of London, Series B (Taxonomy) 39: 114–124. https://doi.org/10.1111/j.1365-3113.1970.tb00264.x

ThripsWiki (2017) ThripsWiki–providing information on the World's thrips. http://thrips.info/wiki/Main_Page [25 July 2017]

Tong XL, Zhang WQ (1989) A report on the fungus-feeding thrips of Phlaeothripinae from China (Thysanoptera: Phlaeothripidae). Journal of South China Agricultural University 10(3): 58–66.

Tong XL, Zhao C (2017) Review of fungus-feeding urothripine species from China, with descriptions of two new species (Thysanoptera: Phlaeothripidae). Zootaxa 4237(2): 307–320. https://doi.org/10.11646/zootaxa.4237.2.5

Ulitzka MR, Mound LA (2014) New generic synonyms in the Palaeotropical genus Urothrips (Thysanoptera: Phlaeothripinae) with one new species from Seychelles. Zootaxa 3755 (6): 595–600. doi: 10.11646/zootaxa.3755.6.6.

Wang J, Tong XL, Zhang WQ (2008) A new species of *Mystrothrips* Priesner from China (Thysanoptera, Phlaeothripidae). Entomological News 119(4): 366–370. https://doi.org/10.3157/0013-872X-119.4.366

Zhang HR, Okajima S, Mound LA (2006) Collecting and slide preparation methods for thrips. Chinese Bulletin of Entomology 43(5): 725–728. Avaliable from: http://www.ent-bull.com.cn/asp/qikan/manage/wenzhang/06050725.pdf [Accessed 5 May. 2017]

Zhao C, Tong X (2016) A new species of *Baenothrips* Crawford from China (Thysanoptera, Phlaeothripidae). ZooKeys 636: 67–75. https://doi.org/10.3897/zookeys.636.10706

ZooKeys 694: 11–30 (2017)
doi: 10.3897/zookeys.694.13802
http://zookeys.pensoft.net

RESEARCH ARTICLE

A peer-reviewed open-access journal
ZooKeys
Launched to accelerate biodiversity research

Eight new species of *Batrisodes* Reitter from China (Coleoptera, Staphylinidae, Pselaphinae)

Ri-Xin Jiang[1], Zi-Wei Yin[1]

1 *Department of Biology, Shanghai Normal University, 100 Guilin Road, Shanghai, 200234, P. R. China*

Corresponding author: *Zi-Wei Yin* (pselaphinae@gmail.com)

Academic editor: *A. Brunke* | Received 23 May 2017 | Accepted 28 July 2017 | Published 29 August 2017

http://zoobank.org/994183A2-3B14-4F5F-BF49-A2F34D82709E

Citation: Jiang R-X, Yin Z-W (2017) Eight new species of *Batrisodes* Reitter from China (Coleoptera, Staphylinidae, Pselaphinae). ZooKeys 694: 11–30. https://doi.org/10.3897/zookeys.694.13802

Abstract

Eight new species of the genus *Batrisodes* Reitter are described from continental China, seven of which were found in association with ants: *B. abdominalis* **sp. n.** and *B. tianmuensis* **sp. n.** with an *Ectomomyrmex* ant from Zhejiang; *B. grossus* **sp. n.** with an *Odontomachus* ant from Guangxi; *B. simianshanus* **sp. n.** with an *Aphaenogaster* ant from Chongqing; *B. qiului* **sp. n.** with a *Pheidole* ant, *B. xuhaoi* **sp. n.** with a *Lasius* ant, and *B. zhouchaoi* **sp. n.** with *Lasius* and *Nylanderia* ants from Sichuan. *Batrisodes zethus* **sp. n.** was collected from a leaf litter sample.

Keywords

Batrisodes, China, myrmecophilous, new species, Pselaphinae

Introduction

Eleven species of the genus *Batrisodes* Reitter are currently known to occur in China, scattered in Zhejiang, Hunan, Sichuan, Yunnan, Xizang (Tibet), Ningxia, and Taiwan (Besuchet 1981; Nomura 2007; Yin and Li 2013; Yin et al. 2011, 2015; Jiang and Yin 2016). This number is apparently at a low level in contrast to the 150 described species in the Holarctic region (Chandler 1997; Schülke and Smetana 2015).

Here, another eight new species are added to the Chinese fauna based on newly acquired material, seven of them were collected from ant colonies. This further demonstrates the high morphological disparity among members of *Batrisodes*, which, however, makes it more difficult to determine a synapomorphy for the genus.

Materials and methods

All type material is housed in the Insect Collection of Shanghai Normal University, Shanghai, China (**SNUC**).

The collecting data of the material are quoted verbatim. The Chinese translation of each locality below provincial level is included in parentheses at the first appearance in the text. Each type specimen bears the following label: 'HOLOTYPE (red) (or PARATYPE (yellow)), ♂ (or ♀), *Batrisodes* + specific name sp. n., det. Jiang and Yin 2017, SNUC'.

Dissected parts of dead beetles were preserved in Euparal on plastic slides that were placed on the same pin with the specimen. Habitus images were taken using a Canon 7D camera in conjunction with a Canon MP-E 65 mm f/2.8 1-5X Macro Lens, and a Canon MT-24EX Macro Twin Lite Flash was used as light source. Images of the morphological details were made using a Canon G9 camera mounted on an Olympus CX31 microscope under reflected or transmitted light. Zerene Stacker (version 1.04) was used for image stacking. All images were modified and grouped into plates in Adobe Photoshop CS5 Extended.

The following abbreviations are applied

AL	length of the dorsally visible part of the abdomen (posterior to elytra) along the midline;	**HL**	length of the head from the anterior clypeal margin to the occipital constriction;
AnL	length of the antenna;	**HW**	width of the head across eyes;
AW	maximum width of the abdomen;	**PL**	length of the pronotum along the midline;
EL	length of the elytra along the suture;		
EW	maximum width of the elytra;	**PW**	maximum width of the pronotum.

Length of the body is a sum of HL + PL + EL + AL.

Taxonomy

***Batrisodes abdominalis* sp. n.**
http://zoobank.org/E4EC7778-BD22-4790-BEE0-F5D505543627
Figure 1

Type material (1 ex.). **Holotype: CHINA:** ♂, labeled 'China: Zhejiang Prov., Linan County (临安县), West Tianmushan (西天目山), 06.v.2012, 1200 m, Wen-Xuan Bi leg.' (SNUC).

Diagnosis of male. The new species can be separated from other Chinese *Batrisodes* species by the following combination of characters: all antennomeres longer than wide; antennomeres X and XI each with a small denticle on the ventral side;

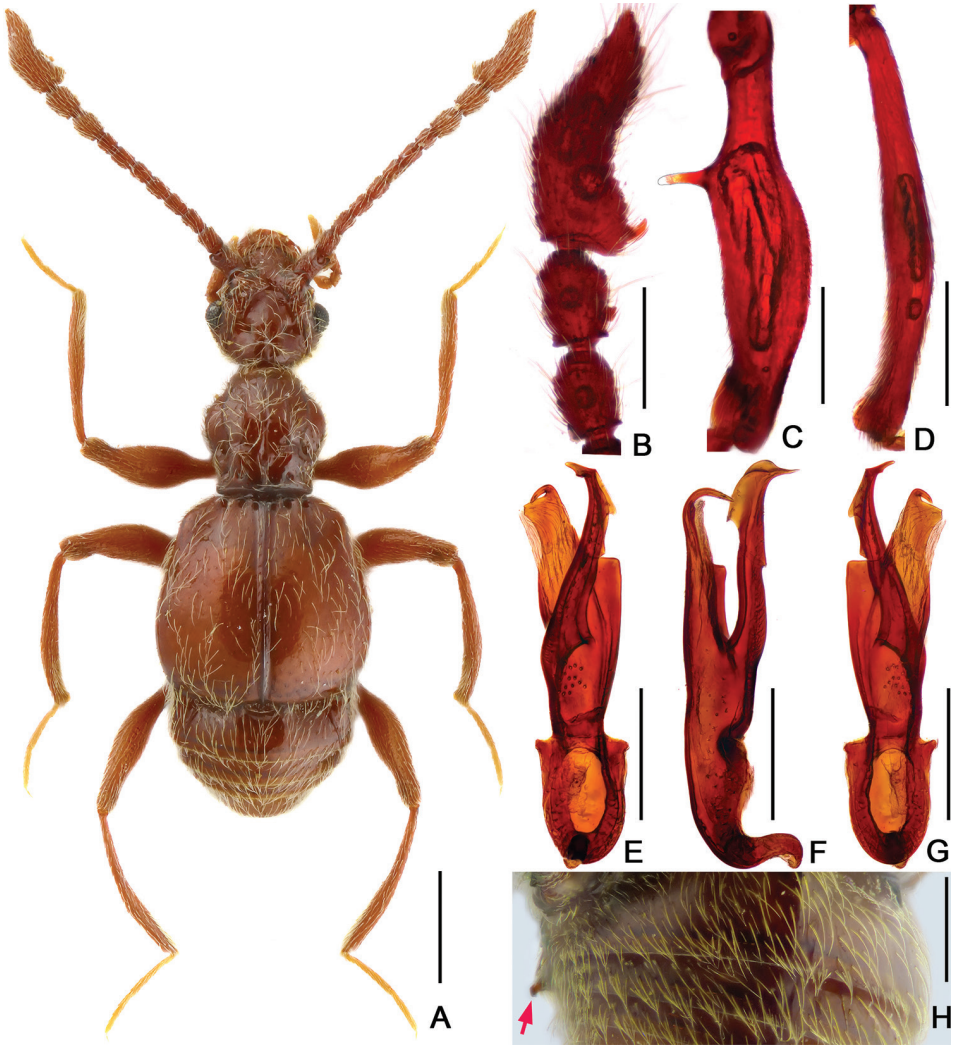

Figure 1. *Batrisodes abdominalis*, male. **A** Habitus **B** Antennal club **C** Mesofemur **D** Mesotibia **E–G** Aedeagus, in ventral (**E**), lateral (**F**), and dorsal (**G**) views **H** Abdominal segments V–VI, in lateral view. Scale bars: 0.5 mm (**A**); 0.2 mm (**B–H**).

mesofemur with a long protuberance near base, sternite V with a small spine at middle, and the slender, asymmetrical aedeagus with an elongate dorsal lobe.

Description. Male. (Fig. 1A), Body reddish brown, BL 2.62 mm. Head slightly wider than long, HL 0.51 mm, HW 0.57 mm, rectangular and covered with short hair, with large vertexal foveae, antennal tubercles prominent; area between moderately raised antennal tubercles concave and impunctate; clypeus slightly punctate, with round anterior margin; lateral longitudinal carinae slight, extending from level of eyes to head base, lacking median vertexal carina. Each eye composed of about 75 facets; Antennomeres II–XI longer than wide, IX–X (Fig. 1B) slightly enlarged, X with small denticle near basal 1/3;

XI largest, nearly 2.5 times as long as X, with small denticle near base. Pronotum longer than wide, PL 0.63 mm, PW 0.55 mm, disc slightly convex, with small median antebasal foveae, median and lateral longitudinal sulci distinct; lateral antebasal fovea large and distinct; outer and inner basolateral foveae small but distinct. Elytra wider than long, without punctation and covered with sparse short hair, EL 0.89 mm, EW 0.97 mm, each elytron with three distinct basal foveae, discal striae shallow and unobvious. Mesofemora (Fig. 1C) with long distinct ventral spine near 1/3; mesotibiae (Fig. 1D) with short obtuse apical spine. Abdomen much wider than long, AL 0.59 mm, AW 0.81 mm; tergite IV longest, more than twice longer than next, with obvious oblique marginal carinae; sternite V (Fig. 1H) with small spine at middle. Aedeagus (Fig. 1E–G) slender and asymmetrical, median lobe simple with two elongate lobes. Length of aedeagus 0.61 mm.

Female. Unknown.

Distribution. East China: Zhejiang.

Host ant. *Ectomomyrmex* sp.

Biology. The new species was collected from an ant colony nesting under a stone.

Etymology. The specific epithet refers to the small spine on male sternite V.

***Batrisodes grossus* sp. n.**

http://zoobank.org/3C6404B4-F33D-47BA-8EAA-38340B8BA1A9

Figs 2–3, 12

Type material (5 exs). **Holotype: CHINA:** ♂, labeled 'China: Guangxi, Jinxiu County (金秀县), Dayao Mountain (大瑶山), 16 km (十六公里), 24°08'11"N, 110°14'28"E, beech forest, rotten wood, colony of ant, 1100 m, 17.vii.2014, Zhong Peng leg.' (SNUC). **Paratypes: CHINA:** 4 ♀♀, same label data as the holotype (SNUC).

Diagnosis of male. The new species can be separated from other Chinese *Batrisodes* species by the following combination of characters: head dorsum, pronotum, and elytra roughly punctate, antennomeres III–V wider than VI–X, mesotrochanter, mesofemur, and mesotibia spinose, and slightly asymmetrical aedeagus expanded at the apex.

Description. Male. (Fig. 2A), Body reddish brown, BL 2.58 mm. Head approximately as long as wide, near trapezoidal, rough and covered with short hair, HL 0.46 mm, HW 0.50 mm, with large vertexal foveae, antennal tubercles prominent; area between moderately raised antennal tubercles concave; clypeus punctate, with round anterior margin; lateral longitudinal carinae slight, extending from level of eyes to head base, lacking median vertexal carina. Each eye composed of about 50 facets. Antennomeres II–X (Fig. 3A) moniliform, III–V slightly expanded, XI largest, nearly 2.5 times as long as X. Punctate pronotum slightly wider than long, PL 0.52 mm, PW 0.59 mm, disc slightly convex; with small median antebasal foveae, median and lateral longitudinal sulci distinct; lateral antebasal fovea large and distinct; outer and inner basolateral foveae small but distinct. Elytra as wide as long, with large uniform punctation and covered with long moderate-length hair, EL 0.87 mm, EW 0.87 mm; each elytron with three small but distinct basal foveae, discal striae shallow and unobvious.

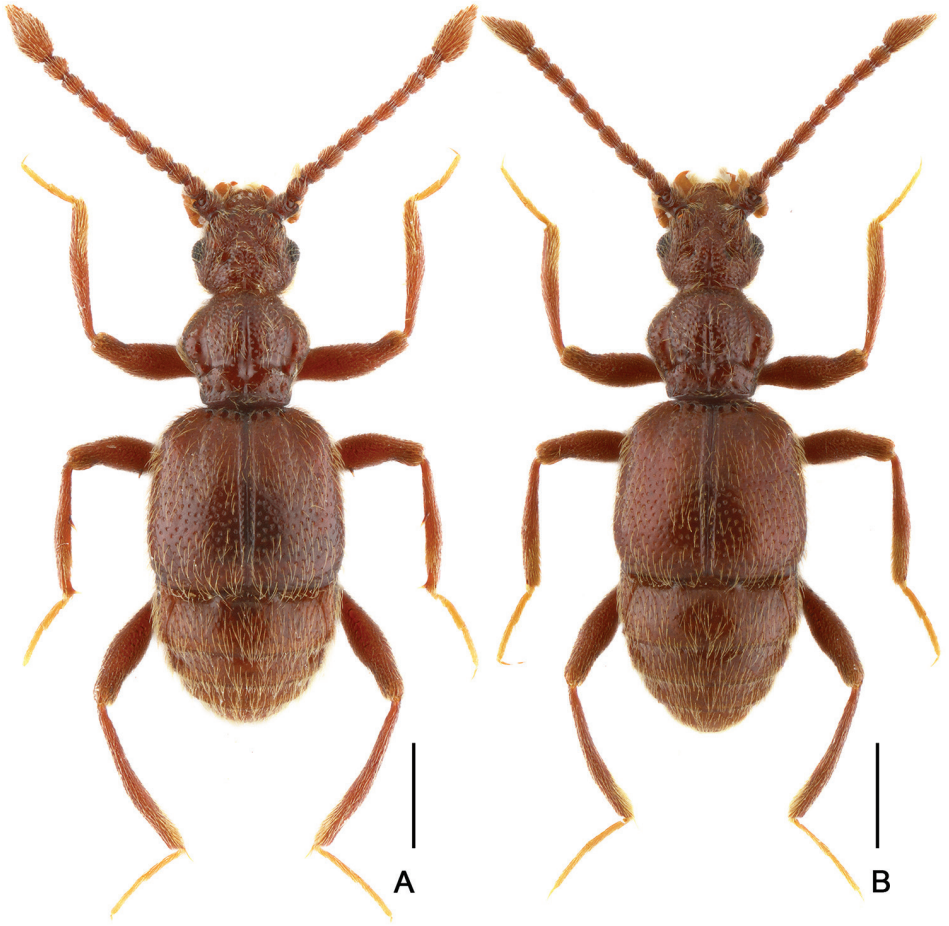

Figure 2. Dorsal habitus of *Batrisodes grossus*. **A** Male **B** Female. Scale bars: 0.5 mm.

Mesotrochanter (Fig. 3B) with distinct triangular short spine; mesofemora (Fig. 3B) with thin but distinct ventral spine at middle; mesotibiae (Fig. 3C) with small ventral denticle near middle and an acute triangular apical spine. Abdomen wider than long, AL 0.73 mm, AW 0.85 mm; tergite IV longest, approximately 1.5 times as long as next, with strongly oblique marginal carinae. Length of aedeagus (Fig. 3D–E) 0.35 mm; median lobe simple, flattened, apical obviously expanded, nearly symmetrical.

Female (Fig. 2B). Similar to male, antennomere III–V normal; each eye composed of about 40 facets; legs lacking denticle and spine; tergite VIII (Fig. 3F) semicircular; sternite VIII (Fig. 3G) transverse; symmetrical genital complex (Fig. 3H) slightly sclerotized. Measurements of body parts: BL 2.45–2.53 mm, HL 0.45–0.46 mm, HW 0.50–0.51 mm, PL 0.49–0.52 mm, PW 0.58–0.60 mm, EL 0.81–0.84 mm, EW 0.87–0.88 mm, AL 0.70–0.71 mm, AW 0.83–0.84 mm.

Distribution. Southwestern China: Yunnan.

Host ant. *Odontomachus* sp.

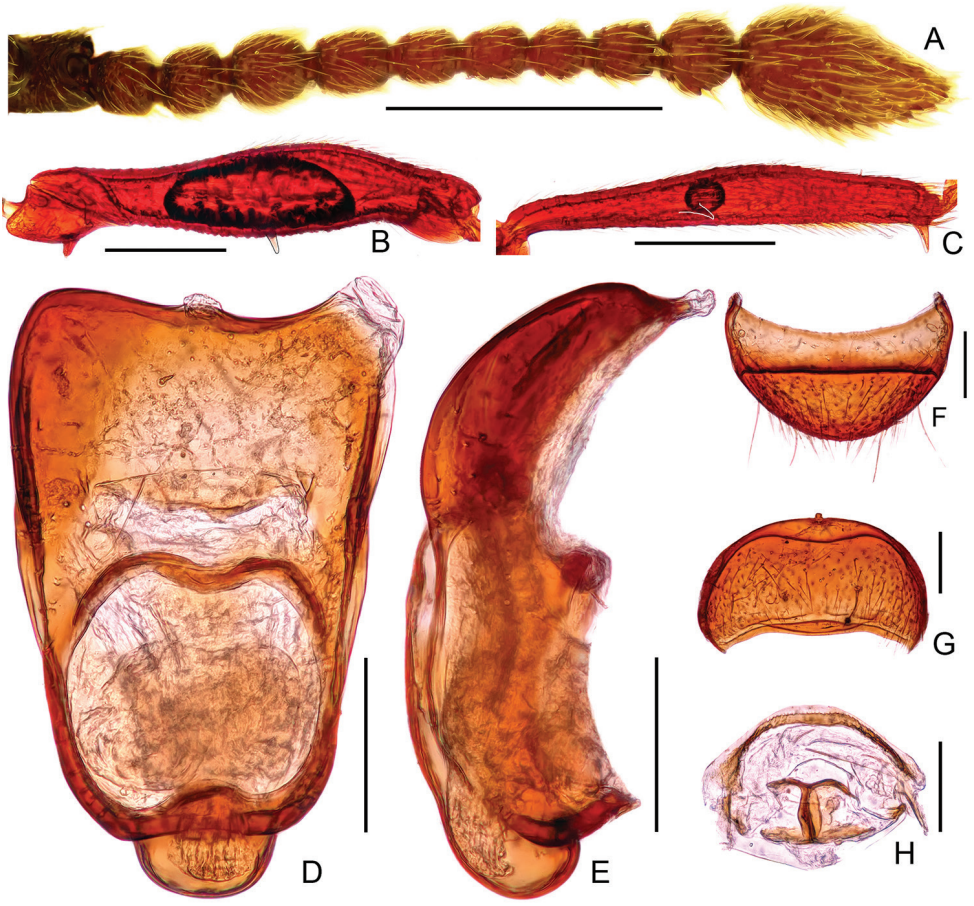

Figure 3. Diagnostic features of *Batrisodes grossus* (**A–E** Male **F–H** Female). **A** Antenna **B** Mesotrochanter and mesofemur **C** Mesotibia **D–E** Aedeagus, in ventral (**D**), and lateral (**E**) views (**F**) Tergite VIII **G** Sternite VIII **H** Genital complex. Scale bars: 0.2 mm (**A–C**); 0.1 mm (**D–H**).

Biology. All adults were collected from an *Odontomachus* colony in a tree hole (Fig. 12).

Etymology. The specific epithet refers to the roughly punctate body surface of the new species.

***Batrisodes qiului* sp. n.**
http://zoobank.org/7308BE97-B8E4-4701-AB67-91FA45B34D9D
Fig. 4

Type material (1 ex.). **Holotype: CHINA:** ♂, labeled 'China: Sichuan, Luzhou City, Gulin County (古蔺县), Honglong Lake (红龙湖), 28°07'17"N, 105°46'53"E, 1620 m, 30.iv.2017, ant nest in rotten wood, Lu Qiu leg.' (SNUC)

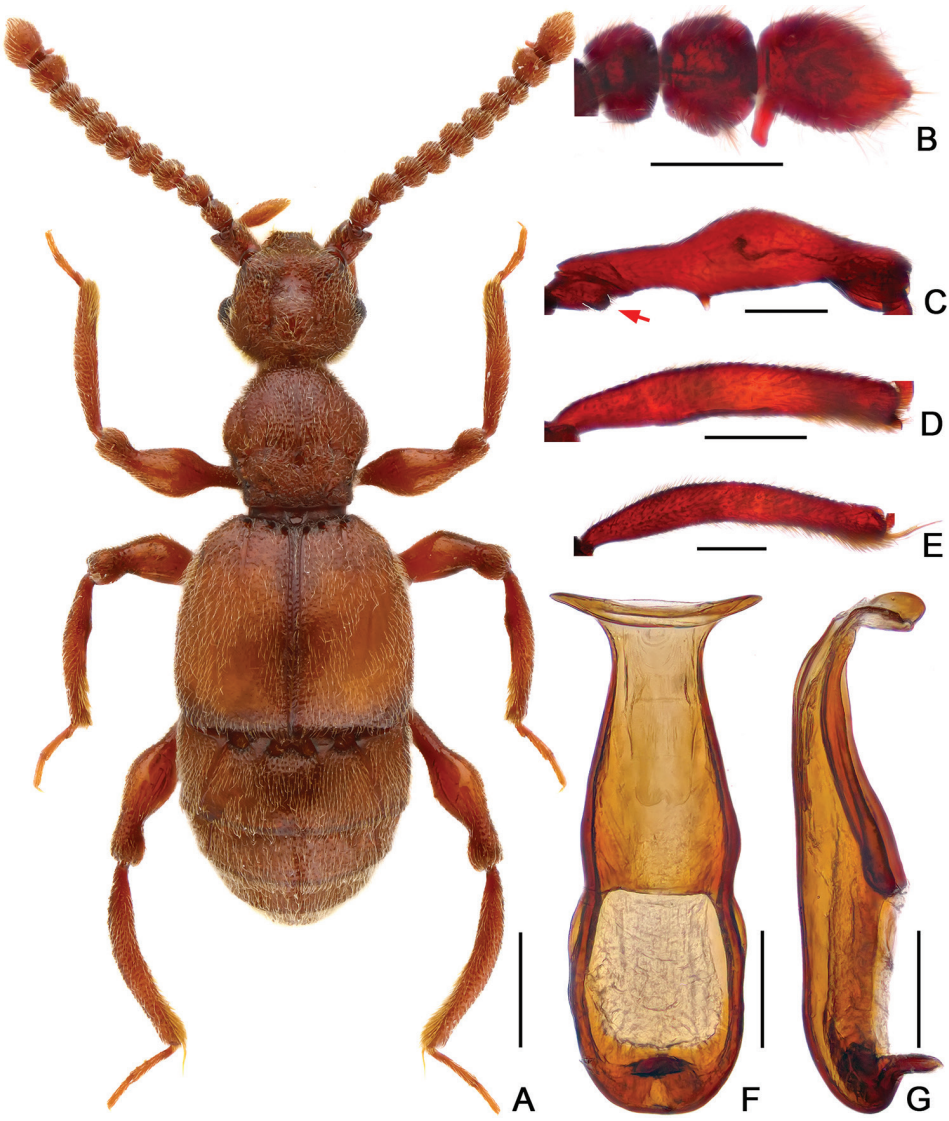

Figure 4. Diagnostic features of *Batrisodes qiului*, male. **A** Dorsal habitus **B** Antennal club **C** Mesotrochanter and mesofemur **D** Mesotibia **E** Metatibia **F–G** Aedeagus, in ventral (**F**), and lateral (**G**) views. Scale bars: 0.5 mm (**A**); 0.2 mm (**B–E**); 0.1 mm (**F–G**).

Diagnosis of male. The new species can be easily separated from other *Batrisodes* species in China by the following combination of characters: moniliform antennomeres, antennomeres XI with a large projection at the base, mesotrochanter with an abrupt projection at the ventral margin, mesofemur with a small spine at middle, and simple, slender aedeagus distinctly expanded at the apex.

Description. Male. (Fig. 4A), Body reddish brown, BL 3.05 mm. Head slight wider than long, near rectangular, rough and covered with short hair, HL 0.60 mm, HW 0.66

mm, with small but obvious vertexal foveae, antennal tubercles prominent; area between moderately raised antennal tubercles concave; clypeus slightly punctate, with round anterior margin; lateral longitudinal carinae unobvious, lacking median vertexal carina. Each eye composed of about 60 facets. Antennomeres II–XI moniliform, XI (Fig. 4B) largest, with distinct, apically-truncate basal denticle. Pronotum nearly as long as wide, PL 0.65 mm, PW 0.64 mm, disc slightly convex; with distinct median antebasal foveae, lateral longitudinal sulci present; lateral antebasal fovea distinct; outer and inner basolateral foveae small and not distinct. Elytra wider than long, EL 0.93 mm, EW 1.07 mm; each elytron with three small but distinct basal foveae, discal striae shallow and short. Mesotrochanter (Fig. 4C) with abrupt projection at ventral margin; mesofemora (Fig. 4C) with short but distinct ventral spine at basal 2/5; mesotibiae (Fig. 4D) slightly expanded at basal 1/3, with small apical spine; metatibiae (Fig. 4E) with long apical tuft of setae. Abdomen wider than long, AL 0.87 mm, AW 1.05 mm; tergite IV (first visible tergite) longest, approximately twice as long as next, with obvious oblique marginal carinae; tergite V–VI with obvious oblique marginal carinae. Aedeagus (Fig. 4F–G) slender, length 0.45 mm; median lobe simple, flattened and symmetrical, expanded at the apex.

Female. Unknown.

Distribution. Southwestern China: Sichuan.

Host ant. *Pheidole* sp.

Biology. All adults were collected from an ant nest in rotten wood.

Etymology. The specific epithet is dedicated to our friend Lu Qiu, who collected this new species and sent the material to us for study.

***Batrisodes simianshanus* sp. n.**

http://zoobank.org/67946A0E-7D8D-4B5E-AEAB-B9C55D77F2BB

Figs 5–6, 13

Type material (8 exs). **Holotype: CHINA:** ♂, labeled 'China: Chongqing, Simian Shan N. R. (四面山自然保护区), Sunzigou (笋子沟), 28°41'47"N, 106°22'49"E, 751 m, 06.iii.2016, ant nest under rock, XU Hao & QIU Jianyue leg.' (SNUC). **Paratypes: CHINA:** 1 ♂, 3 ♀♀, same label data as the holotype (SNUC); 2 ♂♂, 1 ♀, labeled 'China, Chongqing City, Jiangjin District (江津区), Simianshan N. R. (四面山自然保护区), Motianling (摩天岭), ant nest under rock, 28°38'03"N, 106°22'59"E, 1220 m, 30.iv.2016, XU Hao & QIU Jianyue leg.' (SNUC).

Diagnosis of male. *Batrisodes simianshanus* can be separated from all other Chinese congeners by the following combination of characters: ocular canthi present, antennomere XI with a small, acute denticle at mesal margin, pronotum lacking outer and inner basolateral foveae, median antebasal foveae small, mesofemur with a distinct ventral protuberance near base, mesotibiae with small apical spine, and symmetrical, robust aedeagus with the endophallus bearing a pair of elongate lateral sclerites.

Description. Male. (Fig. 5A), Body reddish brown, BL 3.18–3.20 mm. Head wider than long, near rectangular, rough and covered with short hair HL 0.62–

Figure 5. Dorsal habitus of *Batrisodes simianshanus*. **A** Male **B** Female. Scale bars: 0.5 mm.

0.63 mm, HW 0.68 mm, with large vertexal foveae, antennal tubercles prominent; area between obviously raised antennal tubercles concave and without hair; clypeus slightly punctate, with round anterior margin; lateral longitudinal carinae slight, extending from level of eyes to head base. Each eye composed of about 60 facets and with one short ocular spine. Antennomeres II–X moniliform, IX–XI (Fig. 6A) slightly expanded, XI large and longest, with small denticle near base. Pronotum nearly as long as wide, PL 0.69–0.70 mm, PW 0.65–0.68 mm, disc slightly convex; with much small media antebasal foveae, median and lateral longitudinal sulci shallow and unclear; lateral antebasal fovea large and distinct, without outer and inner basolateral foveae. Elytra slight wider than long, EL 0.99–1.01 mm, EW 1.14–1.16 mm; each elytron with three small but distinct basal foveae, discal striae shallow and short. Profemora (Fig. 6B) expanded at middle, mesofemora (Fig. 6C) with

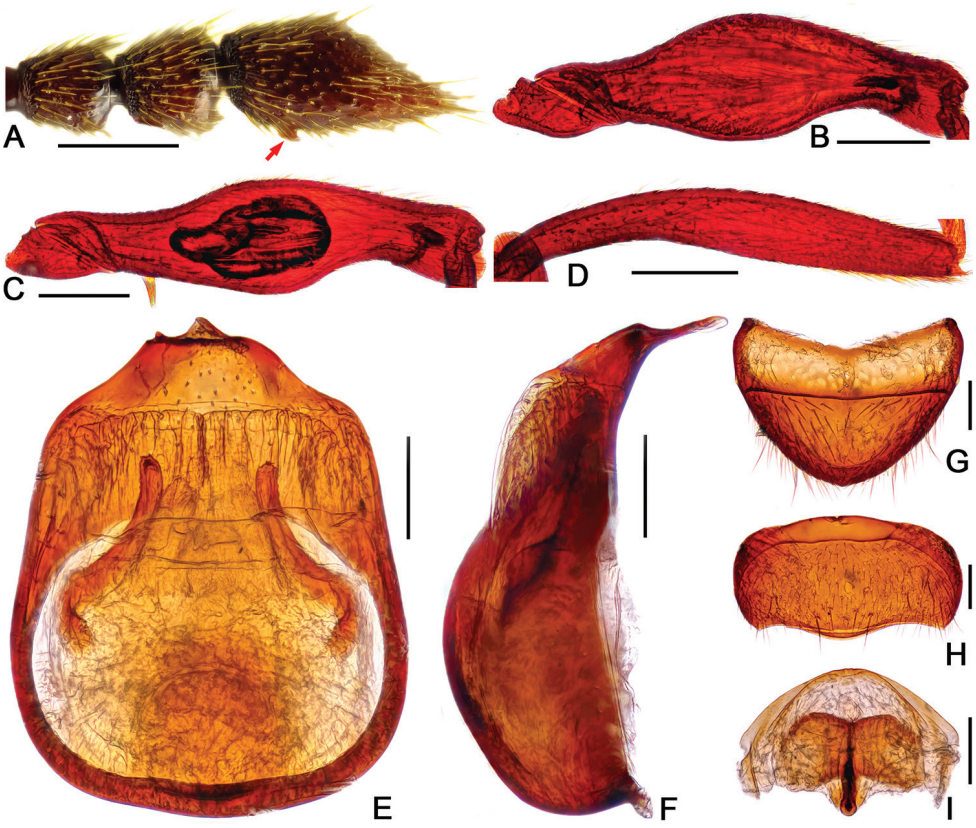

Figure 6. Diagnostic features of *Batrisodes simianshanus* (**A–F** Male **G–I** Female). **A** Antennal club (arrow indicates ventral denticle). **B** Protrochanter and profemur **C** Mesotrochanter and mesofemur **D** Mesotibia **E–F** Aedeagus, in ventral (**E**), and lateral (**F**) views (**G**) Tergite VIII (**H**) Sternite VIII (**I**) Genital complex. Scale bars: 0.2 mm (**A–D**); 0.1 mm (**E–I**).

thin but distinct ventral protuberance near base and expanded at middle; mesotibiae (Fig. 6D) with small and indistinct triangular apical spine. Abdomen wider than long, AL 0.85–0.89 mm, AW 1.04–1.09 mm; tergite IV longest, twice as long as next, with shallow but distinct oblique marginal carinae. Aedeagus (Fig. 6E–F) symmetrical and robust, median lobe simple, with pair of elongate lateral sclerites, length of aedeagus 0.44 mm.

Female (Fig. 5B). Similar to male, antennomere IX–XI less expanded, XI lacking denticle; each eye composed of about 50 facets; legs simple; tergite VIII (Fig. 6G) semicircular; sternite VIII (Fig. 6H) transverse; symmetrical genital complex (Fig. 6I) slightly sclerotized. Measurements of body parts: BL 3.01–3.04 mm, HL 0.62–0.63 mm, HW 0.63–0.64 mm, PL 0.66–0.68 mm, PW 0.65–0.66 mm, EL 0.98–0.99 mm, EW 1.10–1.12 mm, AL 0.74–0.75 mm, AW 1.04–1.09 mm.

Distribution. Southwestern China: Chongqing.

Host ant. *Aphaenogaster* sp.

Biology. All adults were collected from ant colonies nested on the ground under stones (Fig 13).

Etymology. The specific epithet refers to the type locality of the new species, the Simianshan Nature Reserve.

***Batrisodes tianmuensis* sp. n.**

http://zoobank.org/EF6FF910-56BE-4AAE-A73C-D7411C002B58

Fig. 7

Type material. (1 ex.). **Holotype: CHINA:** ♂, labeled 'China: Zhejiang, Linan County, West Tianmushan, 13.iv.2017, 310 m, 30°18'54"N, 119°26'35"E, ant nest under rock, Song Xiaobin leg.' (SNUC).

Diagnosis of male. *Batrisodes tianmuensis* can be separated from all other Chinese congeners by the following combination of characters: antennomeres XI strongly concave at the ventral margin and with an acute basal projection, smooth pronotum lacking median antebasal foveae and inner and outer basolateral foveae, mesofemur with a small ventral spine at middle, mesotibia with a blunt apical protuberance, and aedeagus with an elongate, broad dorsal lobe suddenly pointed at the apex.

Description. Male. (Fig. 7A), Body reddish brown, BL 2.52 mm. Head wider than long, rectangular and covered with sparse short hair, HL 0.51 mm, HW 0.57 mm, with small vertexal foveae; antennal tubercles prominent; area between moderately raised antennal tubercles concave and impunctate; clypeus slightly punctate, with round anterior margin; lateral longitudinal carinae slight, extending from level of eyes to head base, lacking median vertexal carina. Each eye composed of about 55 facets. Antennomeres II–X moniliform, XI (Fig. 7B) largest, approximately 3 times as long as X, strongly concave at mesal surface, with acute denticle near base. Pronotum slightly longer than wide, PL 0.55 mm, PW 0.52 mm, smooth with sparse short hair; disc slightly convex, without median antebasal foveae and median longitudinal sulci; lateral longitudinal sulci shallow, lateral antebasal fovea small and indistinct; lacking outer and inner basolateral foveae. Elytra wider than long, smooth and covered with sparse short hair, EL 0.87 mm, EW 0.99 mm; each elytron with three small basal foveae, discal striae shallow and indistinct. Mesofemora (Fig. 7C) with small thin ventral spine near middle; mesotibiae (Fig. 7D) with small triangular apical spine. Abdomen much wider than long, AL 0.62 mm, AW 0.95 mm; tergite IV longest, nearly 2.5 times as long as next, with shallow oblique marginal carinae. Aedeagus (Fig. 7E–G) strongly asymmetrical, median lobe with long, broad dorsal lobe pointed at apex; length of aedeagus 0.49 mm.

Female. Unknown.

Distribution. East China: Zhejiang.

Host ant. *Ectomomyrmex* sp.

Biology. The new species was collected from an ant colony nesting under a stone.

Etymology. The specific epithet refers to the type locality of the new species, the West Tianmu Mountain.

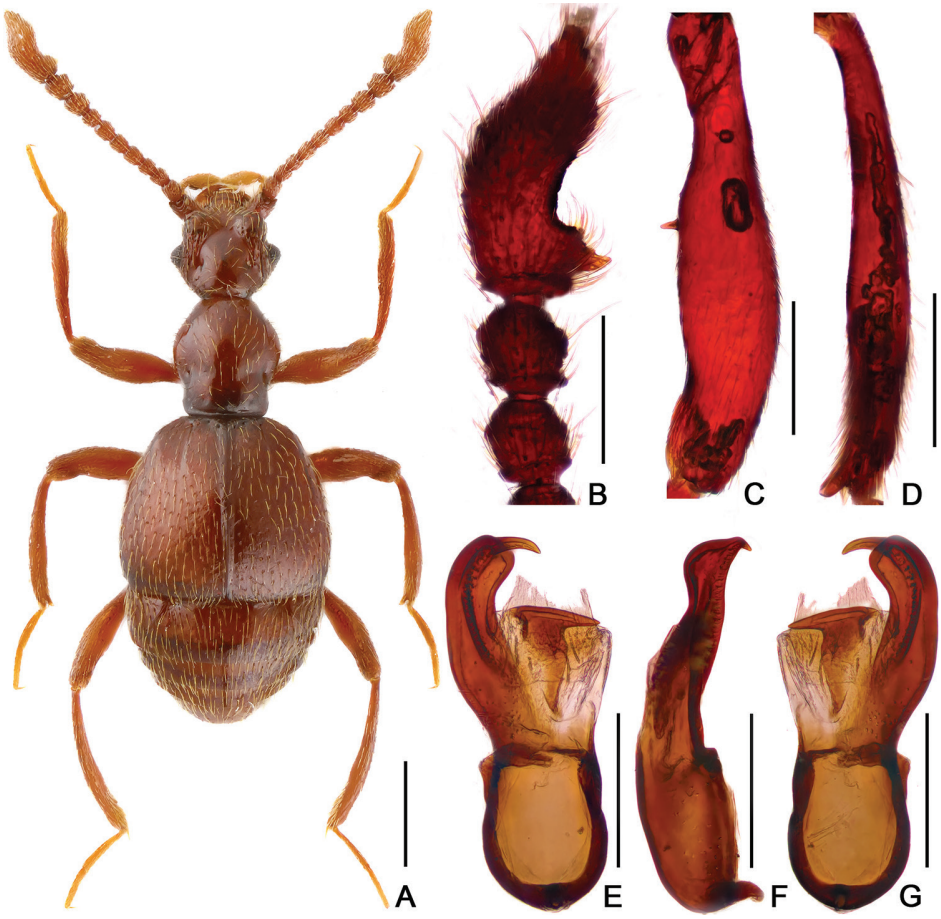

Figure 7. Diagnostic features of *Batrisodes tianmuensis*, male. **A** Dorsal habitus **B** Antennal club **C** Mesotrochanter and mesofemur **D** Mesotibia **E–G** Aedeagus, in ventral (**E**), lateral (**F**), and dorsal (**G**) views. Scale bars: 0.5 mm (**A**); 0.2 mm (**B–G**).

***Batrisodes xuhaoi* sp. n.**
http://zoobank.org/401C578A-AA7F-459E-80DA-AD99CB5B216A
Figs 8–9, 14

Type material (5 exs). **Holotype: CHINA:** ♂, labeled 'China: Sichuan, Luding County (泸定县), Gonggashan N. R. (贡嘎山自然保护区), Hongshitan (红石滩), ant nest under rock, 29°48'10"N, 102°03'42"E, 2740 m, 24.vi.2016, XU Hao & QIU Jianyue leg.' (SNUC). **Paratypes: CHINA:** 3 ♂♂, 1 ♀, same label data as the holotype (SNUC).

Diagnosis of male. *Batrisodes xuhaoi* can be separated from all other Chinese congeners by the following combination of characters: stout general habitus, moniliform antennomeres, antennomere XI with a thick projection at base, profemur strongly expanded near middle, mesotrochanter expanded at ventral margin, mesofemur with

Figure 8. Dorsal habitus of *Batrisodes xuhaoi*. **A** Male **B** Female. Scale bars: 0.5 mm.

a small ventral spine at middle, mesotibia with acute spines at middle and apex, and asymmetrical, elongate aedeagus broadened at the apex.

Description. Male. (Fig. 8A), Body reddish brown, BL 2.76–2.80 mm. Head wider than long, near trapezoidal, rough and covered with short hair, HL 0.50–0.51 mm, HW 0.62–0.63 mm, with large vertexal foveae, antennal tubercles prominent; area between moderately raised antennal tubercles obviously concave; clypeus slightly punctate, with round anterior margin; lateral longitudinal carinae short and slight, extending from level of eyes to head base, lacking median vertexal carina. Each eye composed of about 50 facets. Antennomeres II–XI moniliform, XI (Fig. 9A) large, with distinct, apically-truncate basal denticle. Pronotum as long as wide, PL 0.63–0.64 mm, PW 0.63–0.64 mm, disc slightly convex; with distinct median antebasal foveae, median and lateral longitudinal sulci present; lateral antebasal fovea large and distinct; outer and inner basolateral foveae small but distinct. Elytra wider than long, EL 0.85–0.86 mm, EW 0.92–0.94 mm; each elytron with three small but distinct basal foveae, discal striae shallow and short. Profemora (Fig. 9B) strongly expanded at middle, mesofemora (Fig. 9C)

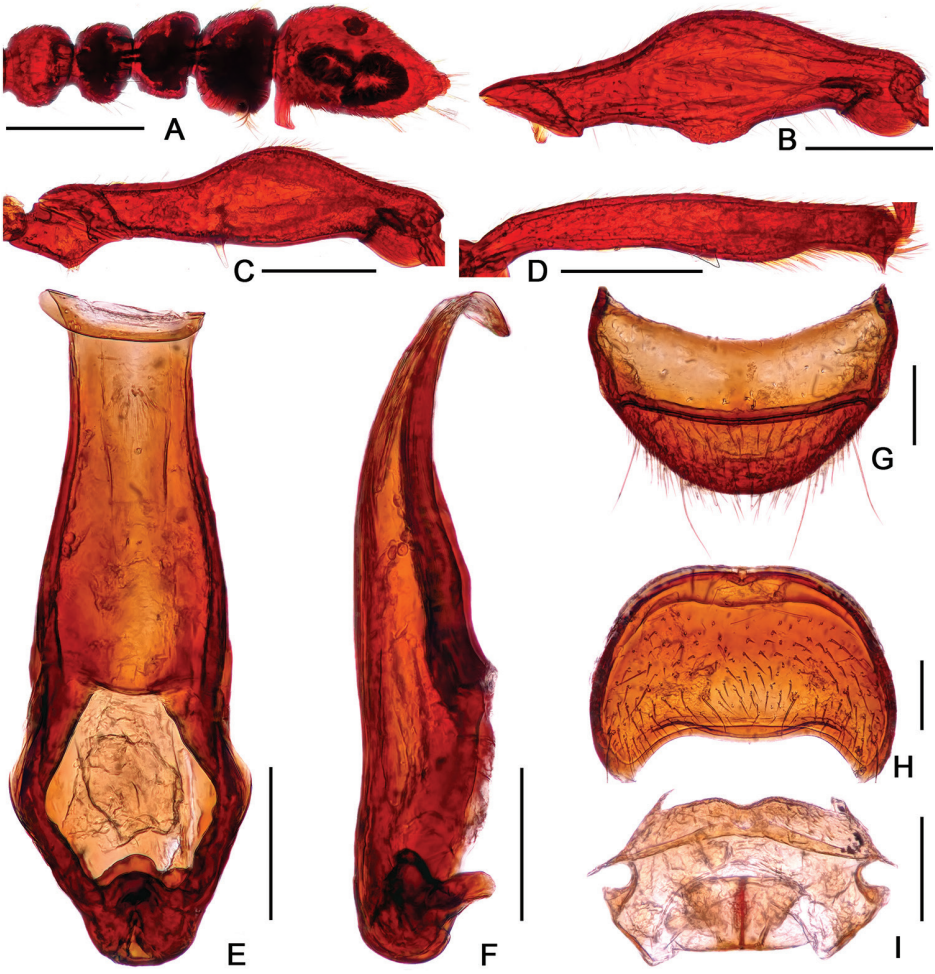

Figure 9. Diagnostic features of *Batrisodes xuhaoi* (**A–F** Male **G–I** Female). **A** Antennal club **B** Profemur **C** Mesotrochanter and mesofemur **D** Mesotibia **E–F** Aedeagus, in ventral (**E**), and lateral (**F**) views (**G**) Tergite VIII (**H**) Sternite VIII (**I**) Genital complex. Scale bars: 0.2 mm (**A–D**); 0.1 mm (**E–I**).

with thin but distinct ventral spine near middle; mesotibiae (Fig. 9D) slightly swollen at apical 1/3, with small ventral denticle near middle and small triangular apical spine. Abdomen wider than long, AL 0.77–0.80 mm, AW 0.90–0.93 mm; tergite IV (first visible tergite) longest, nearly twice as long as next, with strongly oblique marginal carinae; tergite V–VI with obvious oblique marginal carinae. Aedeagus (Fig. 9E–F) nearly symmetrical, slender, length 0.44 mm, median lobe simple, flattened, broadened at apex.

Female (Fig. 8B). General habitus similar to male, antennomere XI lacking basal denticle; each eye composed of about 40 facets; legs lacking denticle and spine; tergite VIII (Fig. 9G) semicircular; sternite VIII (Fig. 9H) transverse; symmetrical genital complex (Fig. 9I) slightly sclerotized. Measurements of body parts: BL 2.82 mm, HL

0.51 mm, HW 0.64 mm, PL 0.65 mm, PW 0.64 mm, EL 0.88 mm, EW 0.96 mm, AL 0.78 mm, AW 0.93 mm.

Distribution. Southwestern China: Sichuan.

Host ant. *Lasius* sp.

Biology. All adults were collected from ant colonies nesting on the ground under stones (Fig. 14).

Etymology. The specific epithet is dedicated to Hao Xu, co-collector of the type series.

***Batrisodes zethus* sp. n.**

http://zoobank.org/79C51DBA-2BE7-4CC4-B4AB-7D94F5DB9080

Fig. 10

Type material (1 ex.). **Holotype: CHINA:** ♂, labeled 'China: Hunan, Liuyang City, Daweishan National Forest Park (大围山国家森林公园), 28°25'25"N, 114°07'06"E, 1391 m, 03. vi.2017, Jiang, Liu & Hu leg.' (SNUC)

Diagnosis of male. *Batrisodes zethus* can be separated from all other Chinese congeners by the following combination of characters: habitus stout, antennomere IX strongly protruding laterally, X oblique, XI with a setose longitudinal projection at the lateral surface, mesofemur with a distinct ventral projection at basal 1/3, mesotibia with small tubercles at middle and apex, aedeagus elongate, with numerous spine-like structures at middle of the ventral lobe.

Description. Male. (Fig. 10A), Body reddish brown, BL 2.83 mm. Head wider than long, sub-triangular, roughly punctate and with short setae, HL 0.60 mm, HW 0.66 mm, with large vertexal foveae, antennal tubercles prominent, area between tubercles regularly depressed; clypeus finely punctate, with round anterior margin; lacking lateral longitudinal carinae and median vertexal carina. Each eye composed of about 60 facets. Antennomeres II–VIII moniliform, IX (Fig. 10B) strongly protruding at lateral margins and with long hair at apex, X oblique, XI with a distinct longitudinal projection near middle. Pronotum slightly wider than long, PL 0.58 mm, PW 0.62 mm, covered with fine, short hair, disc slightly convex; with small but , distinct mediobasal impression, lateral longitudinal sulci present; lateral antebasal fovea large and distinct; outer and inner basolateral foveae small. Elytra wider than long, uniformly punctate; EL 0.87 mm, EW 1.04 mm; each elytron with three large basal foveae, discal striae shallow, extending to half elytral length. Mesofemora (Fig. 10C) with thick, long projection at basal 1/3; mesotibiae (Fig. 10D) with small, blunt projection at middle and apex; Abdomen wider than long, AL 0.78 mm, AW 0.97 mm; tergite IV (first visible tergite) longest, nearly 1.5 times as long as next, with oblique marginal carinae; tergite V–VI each with oblique marginal carinae. Aedeagus (Fig. 10E–G) asymmetrical, median lobe with many spine-like structures at apical half.

Female. Unknown.

Distribution. Central China: Hunan.

Biology. This new species was collected from leaf litter.

Etymology. Zethus is the son of Zeus and Antiope.

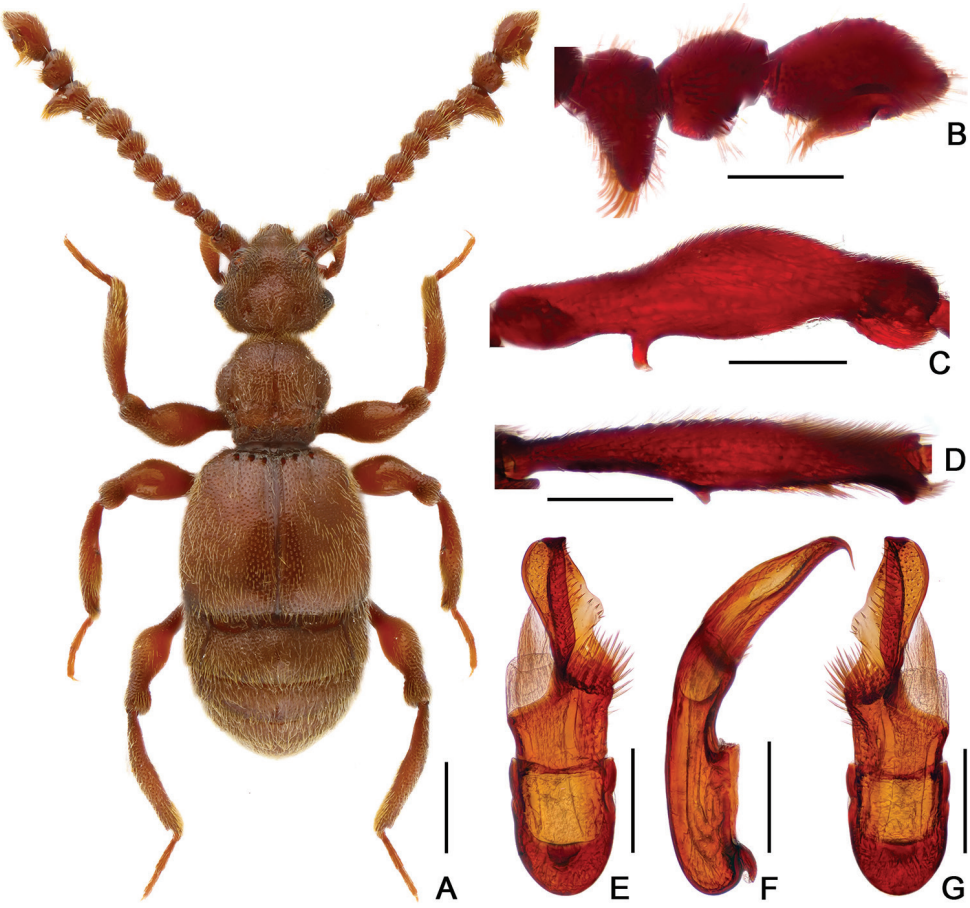

Figure 10. Diagnostic features of *Batrisodes zethus*, male. **A** Dorsal habitus **B** Antennal club **C** Mesotrochanter and mesofemur **D** Mesotibia **E–G** Aedeagus, in ventral (**E**), lateral (**F**), and dorsal (**G**) views. Scale bars: 0.5 mm (**A**); 0.2 mm (**B–G**).

***Batrisodes zhouchaoi* sp. n.**
http://zoobank.org/31133048-37CD-4B88-BBAE-76BFBA4D73B5
Fig. 11

Type material (2 exs). **Holotype: CHINA:** ♂, labeled 'China: Sichuan, Chengdu City (成都市), Dujiangyan City (都江堰市), Zipingpu Township (紫坪铺镇), Lingyan-guan-yin-shan (灵岩观音山), 31.03°N, 103.61°E, 1180 m, 03.iv.2017, ant nest under rock, Zhou Chao & He Li leg.' (SNUC). **Paratypes: CHINA:** 1 ♂, same collecting data as the holotype, except 'ant colony under bark,' (SNUC).

Diagnosis. *Batrisodes zhouchaoi* can be readily separated from all other Chinese congeners by the following combination of characters: antennomere X strongly transverse, with a small denticle at mesal margin, XI with a small denticle base; pronotum distinctly winder than long; mesotrochanter with a blunt ventral projection, mesofem-

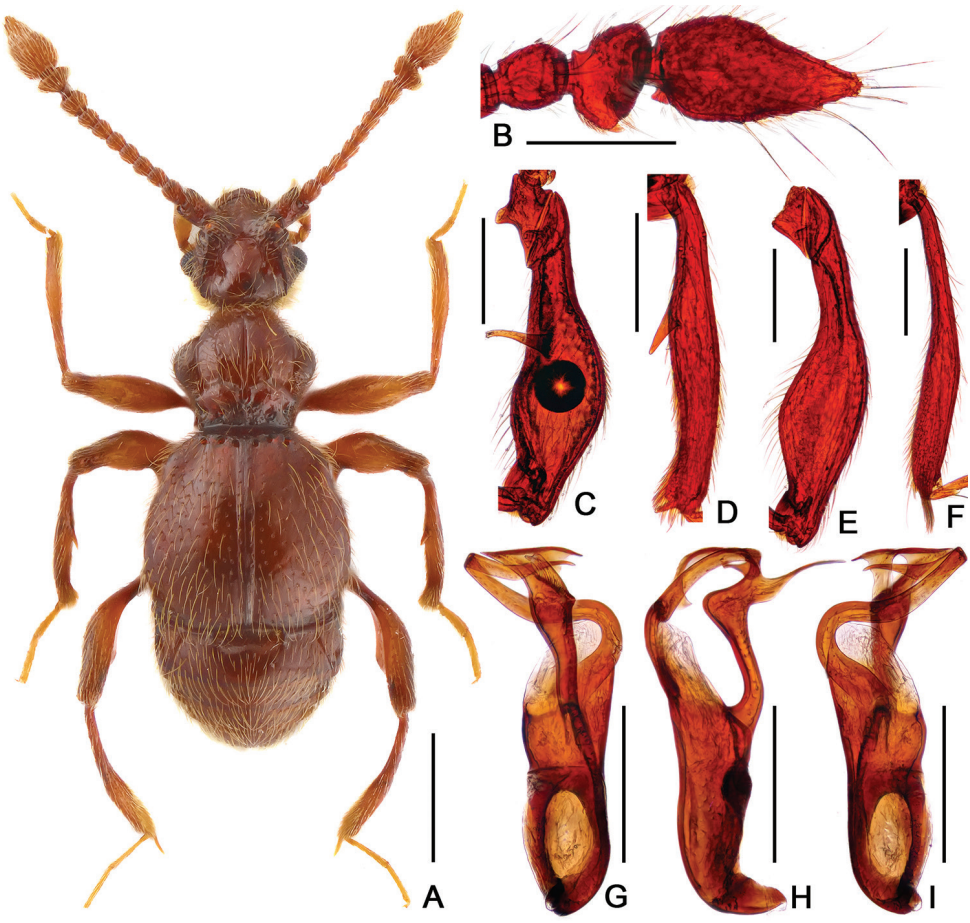

Figure 11. Diagnostic features of *Batrisodes zhouchaoi*, male. **A** Dorsal habitus **B** Antennal club **C** Mesotrochanter and mesofemur **D** Mesotibia **E** Metatrochanter and metafemur **F** Metatibia **G–I** Aedeagus, in ventral (**G**), lateral (**H**), and dorsal (**I**) views. Scale bars: 0.5 mm (**A**); 0.2 mm (**B–I**).

ora with a long ventral protuberance at middle, mesotrochanter protuberant ventrally, metafemora expanded along the ventral margin; aedeagus strongly asymmetrical, with elongate, twisted ventral and dorsal lobes.

Description. Male. (Fig. 11A), Body reddish brown, BL 2.18–2.19 mm. Head wider than long, near rectangular, and covered with short hair HL 0.45–0.46 mm, HW 0.50–0.51 mm, with large vertexal foveae, antennal tubercles prominent and punctate; area between obviously raised antennal tubercles concave and sparsely pubescent; clypeus slightly punctate, with round anterior margin; lateral longitudinal carinae extending from above eyes to occipital constriction. Each eye composed of about 55 facets. Antennomeres II–IX moniliform, X (Fig. 11B) much wider than long with small denticle near middle, XI (Fig. 11B) largest and with small denticle near base. Pronotum wider than long, PL 0.48–0.50 mm, PW 0.55–

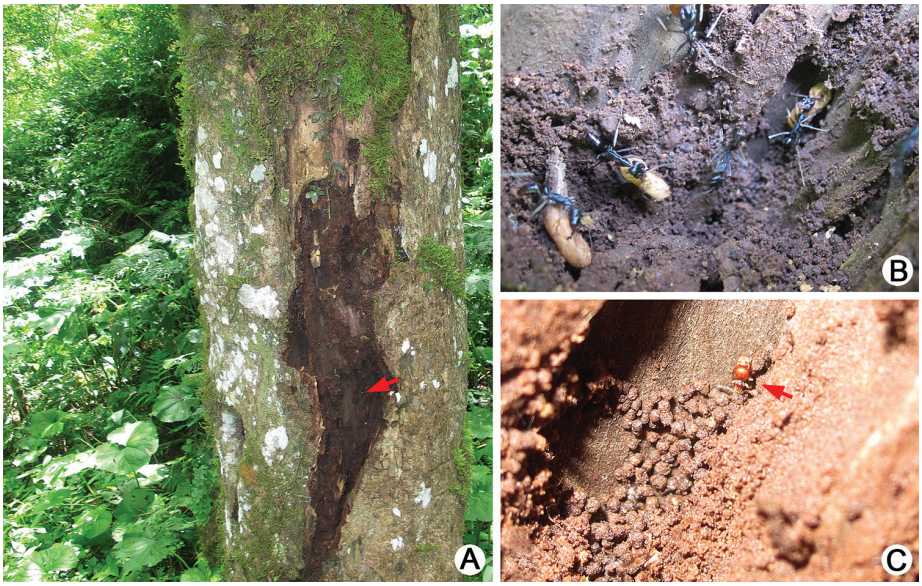

Figure 12. Habitat of *Batrisodes grossus*. **A** Colony of host ant under bark **B** A closer view of ant colony **C** A living *Batrisodes grossus* walking inside the nest.

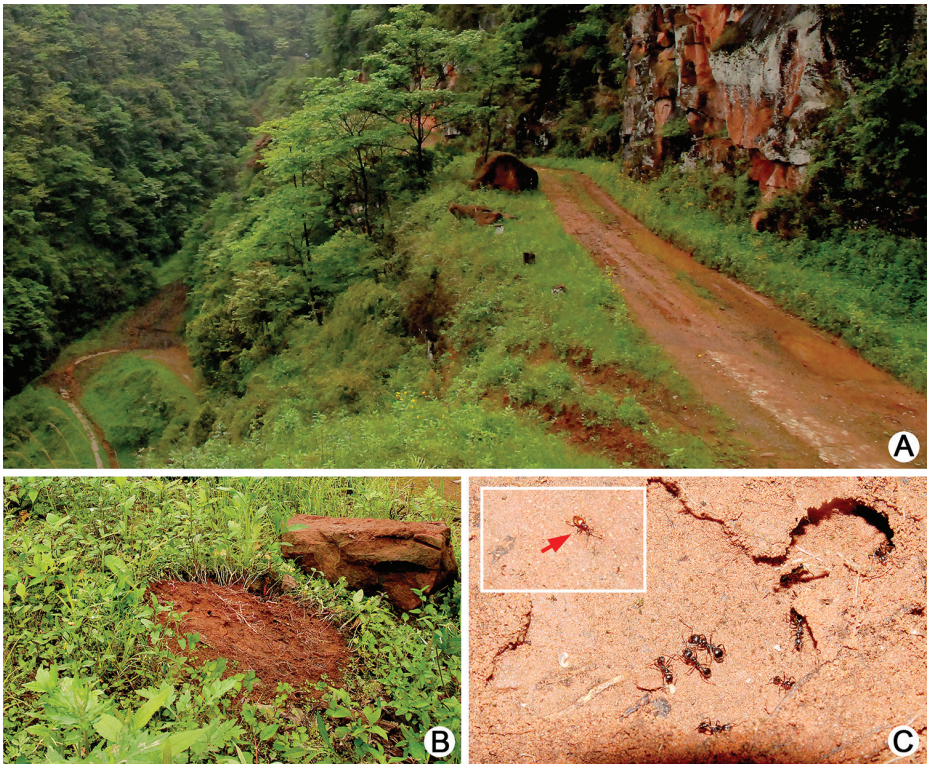

Figure 13. Habitat of *Batrisodes simianshanus*. **A** General environment **B** Ant nest exposed after the stone was turned over **C** A closer view of ant nest and a living *Batrisodes simianshanus* walking on the surface of ant nest.

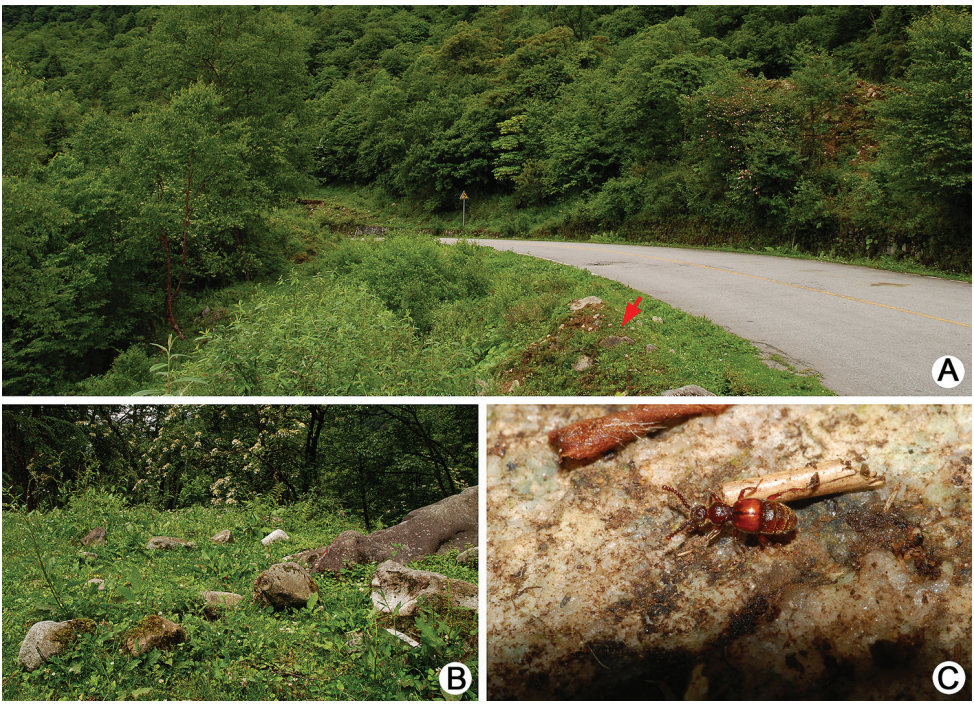

Figure 14. Habitat of *Batrisodes xuhaoi*. **A** General environment **B** A closer view of the habitat **C** A living *Batrisodes xuhaoi* walking on the underside of the stone.

0.56 mm, disc slightly convex; with small antebasal foveae, median and lateral longitudinal sulci clear; lateral antebasal fovea large and distinct, outer and inner basolateral foveae distinct. Elytra slight wider than long, EL 0.74–0.75 mm, EW 0.77–0.78 mm; each elytron with three large basal foveae, discal striae shallow and short. Mesotrochanter (Fig. 11C) with blunt, short spine; mesofemora (Fig. 11C) expanded at apical 1/3 and with long and distinct ventral spine at middle; mesotibiae (Fig. 11D) with distinct ventral denticle spine near middle and a small triangular apical denticle; metafemora (Fig. 11E) expanded along ventral margin, metatibiae (Fig. 11F) with long apical tuft of setae. Abdomen wider than long, AL 0.48–0.51 mm, AW 0.72–0.74 mm; tergite IV longest, three times as long as next, with distinct oblique marginal carinae. Aedeagus (Fig. 11G–I) slender and asymmetrical, median lobe simple with two elongate and twisted lobe; length of aedeagus 0.48 mm.

Female. Unknown.

Distribution. Southwestern China: Sichuan.

Host ant. *Lasius* sp. and *Nylanderia* sp.

Biology. All adults were collected from ant colonies nesting under stone or bark.

Etymology. The new species is named after Chao Zhou, who collected this new species and sent us the material as a gift.

Acknowledgments

We thank the following colleagues and friends for collecting and providing the material: Wen-Xuan Bi (Shanghai), Zhong Peng, Xiao-Bin Song, and Yi-Xiao Liu (Shanghai Normal University, Shanghai), Lu Qiu and Jian-Yue Qiu (Southwest University, Chongqing), Hao Xu (Hunan Agricultural University, Changsha), Chao Zhou (Chengdu). Hao Ran (Guangxi Normal University, Guangxi) helped to identify the host ants. Peter Hlaváč (Prague, Czech) and Adam Brunke (Ottawa, Canada) critically commented on the manuscript. The present study was supported by grants of the National Natural Science Foundation of China (No. 31501874), and Science and Technology Commission of Shanghai Municipality (No. 15YF1408700).

References

Besuchet C (1981) Contribution à l'étude des *Batrisodes* paléarctiques (Coleoptera: Pselaphidae). Revue Suisse de Zoologie 88: 275–296. https://doi.org/10.5962/bhl.part.82372

Chandler DS (1997) A catalog of the Coleoptera of America north of Mexico. Family: Pselaphidae. United States Department of Agriculture, Agriculture Handbook 529–31, Washington DC, 118 pp.

Jiang RX, Yin ZW (2016) Two new species of *Batrisodes* Reitter (Coleoptera: Staphylinidae: Pselaphinae) from China. Zootaxa 4205: 194–200. https://doi.org/10.11646/zootaxa.4205.2.9

Nomura S (2007) Two new species of the genus *Batrisodes* (Coleoptera, Staphylinidae, Pselaphinae) from Taiwan. Elytra 35: 76–84.

Schülke M, Smetana A (2015) Family Staphylinidae Latreille, 1802. In: Löbl I, Löbl D (Eds) Catalogue of Palaearctic Coleoptera, Hydrophiloidea – Staphylinoidea, Revised and Updated Edition. Brill, Leiden/Boston, 304–1134.

Yin ZW, Li LZ (2013) *Batrisodes* (*Excavodes*) *simplex* sp. n. (Coleoptera: Staphylinidae: Pselaphinae): a second species of the genus from continental China. Deutsche Entomologische Zeitschrift 60: 261–266.

Yin ZW, Nomura S, Zhao MJ (2011) Taxonomic study on *Batrisodellus* Jeannel of China, with discussion on the systematic position of *Batrisodellus callissimus* Nomura & Wang, 1991. Spixiana 34: 33–38.

Yin ZW, Shen JW, Li LZ (2015) New species and new combinations of Asian *Batrisodes* Reitter (Coleoptera, Staphylinidae, Pselaphinae), and synonymy of *Batrisodellus* Jeannel with *Batrisodes*. Deutsche Entomologische Zeitschrift 62: 45–54. https://doi.org/10.3897/dez.62.4539

ZooKeys 694: 31–39 (2017)
doi: 10.3897/zookeys.694.12863
http://zookeys.pensoft.net

RESEARCH ARTICLE

A peer-reviewed open-access journal
ZooKeys
Launched to accelerate biodiversity research

A new species of the subgenus *Scymnus* from Pakistan (Coleoptera, Coccinellidae)

Azad Rashid[1], Xiaosheng Chen[2], Baoli Qiu[1], Xingmin Wang[1]

1 *Key Laboratory of Bio-Pesticide Innovation and Application, Engineering Technology Research Center of Agricultural Pest Biocontrol, Guangdong Province; Department of Entomology, South China Agricultural University, Guangzhou 510640, China* **2** *Department of Forestry Protection, College of Forestry and Landscape Architecture, South China Agricultural University, Guangzhou, 510640, China*

Corresponding author: *Baoli Qiu* (baileyqiu@scau.edu.cn); *Xingmin Wang* (wangxmcn@scau.edu.cn)

Academic editor: *M. Thomas* | Received 23 March 2017 | Accepted 21 July 2017 | Published 29 August 2017

http://zoobank.org/7C6E63B1-A91F-44C8-9CE4-4456C2EBFA3B

Citation: Rashid A, Chen X, Qiu B, Wang X (2017) A new species of the subgenus *Scymnus* from Pakistan (Coleoptera, Coccinellidae). ZooKeys 694: 31–39. https://doi.org/10.3897/zookeys.694.12863

Abstract

A new species, *Scymnus* (*Scymnus*) *contortubus* Rashid, Chen & Wang, **sp. n.**, is described and illustrated from Pakistan. A diagnosis, remarks, illustrations, and a distribution map are provided of the new species and its most similar congener, *S.* (*S.*) *nubilus* Mulsant.

Keywords

Coccinelloidea, Coccidulini, entomology, new species, Pakistan, taxonomy

Introduction

The subgenus *Scymnus* was established by Mulsant, 1850 with *Coccinella rufipes* Fabricius, 1798 as the type species, based on the presence of an 11-segmented antenna and the incomplete abdominal postcoxal line.

The genus *Scymnus* Kugelann, 1794 belonged to the tribe Scymnini Mulsant, 1846 in the subfamily Scymninae (Sasaji 1968; Kovář 1996). However, Ślipiński (2007) presented a two-subfamily system, moving the genus *Scymnus* to the tribe Coccidulini in the subfamily Coccinellinae. Further studies based upon molecular

and morphological characters supported Ślipiński's (2007) division of Coccinellidae in two subfamilies, Coccinellinae and Microweiseinae (Giorgi et al. 2009; Seago et al. 2011). Recent study on the Cucujoidea (Robertson et al. 2015) has recovered Coccinellidae as belonging to the superfamily Coccinelloidea together with eight other families of the former Cerylonid Series.

Members of the genus *Scymnus* Kugelann, 1794 are predatory and mostly feed on aphids, adelgids, and scale insects, playing an important role in regulating pest populations (Chen et al. 2016). Prior to the present study, 58 species were reported in the subgenus *Scymnus* (*Scymnus*) from the Oriental Region and only one species, *S.* (*S.*) *nubilus* Mulsant, 1850, has been known to exist in Pakistan (Poorani, 2002; Chen et al. 2013). In this paper, another species is described, and a diagnosis of the subgenus with distribution pattern of both species is presented.

Materials and methods

Specimens were collected from different localities in Pakistan during 2015–2016 and were preserved in 85% ethanol. A Zeiss Stemi 305 microscope was used for observing external morphology followed by the dissection of male and female genital structures. After dissection, genitalia were cleared in 10% solution of NaOH and placed in a drop of neutral balsam onto glass slides for further studies.

SteREO Discovery V20 (Zeiss) microscope with an ocular micrometer was used for all measurements, which are presented in millimetres. The following abbreviations are used:

TL total length from clypeus to apex of elytra,
TW total width across both elytra at widest part,
TH total height in highest part of elytra,
HW head width in widest part including eyes,
PL pronotal length across the central area from anterior to basal margin of pronotum,
PW pronotal width across widest part,
EL elytral length along suture including scutellum,
EW elytral width, equivalent to TW.

An AxioCam HRc digital camera attached to the stereoscope, (SteREO Discovery V20) was used for photographs of the whole bodies of beetles. Composite images were generated with AXIO VISION REL. 4.8 software and edited using ADOBE PHOTOSHOP CC. 2017.

A compound microscope, Olympus BX51 attached to a Coolsnap-Procf & CRI Micro*Color camera was used for the preparation of illustrations of the morphological characters of male genitalia. Morphological terminology of Ślipiński (2007) was followed. Type specimens are deposited in the Department of Entomology, South China Agricultural University, Guangzhou, China.

Taxonomy

Genus *Scymnus* Kugelann, 1794

Subgenus *Scymnus* Kugelann, 1794

Scymnus Kugelann, 1794: 545. Type species: designated by Westwood 1838: 43, *Scymnus nigrinus* Kugelann, 1794.

Anisoscymnus Crotch, 1874: 273. Type species: *Coccinella rufipes* Fabricius, 1798, by original designation.

Diagnosis. Members of the subgenus *Scymnus* can be easily distinguished by the following combination of characters: body small, oval or elongate oval; antennae 11-segmented (Fig. 1f); prosternum having distinct carinae, nearly reaching the anterior margin (Fig. 1b); abdominal postcoxal line incomplete, recurved forward, never reaching lateral margin of ventrite; area surrounding by postcoxal line sparsely punctate; abdomen with six ventrites, 5th and 6th abdominal ventrites in male truncate or emarginate apically in male (Fig. 1i); female genitalia with distinct infundibulum.

Distribution. Worldwide (Chen et al. 2013).

Scymnus (*Scymnus*) *contortubus* Rashid, Chen & Wang, sp. n.

http://zoobank.org/C6D02733-EB0F-4EC9-964D-4F6FABBCC6C2

Figs 1, 2

Etymology. The species name is derived from Latin (*contortum* = twisted and *tubus* = tube) referring to a curved, tube-like apex of penis.

Diagnosis. This species is separated by the presence of a stout penis with a curved apex (Fig. 2d) and parameres with long, dense setae on both the apex and inner side (Fig. 2f–g). In *S.* (*S.*) *nubilus*, the most similar congener, penis is slender (Fig. 3e) and parameres have sparse long setae only at apices (Fig. 3g–h).

Description. TL: 1.8 mm, TW: 1.3 mm, TH: 0.7 mm, HW: 0.6 mm, TL/TW: 1.38, PL/PW: 0.33, EL/ EW: 1.07.

Body oval, distinctly convex, dorsum with dense white pubescence. Head brown with black vertex. Antennae and mouthparts brown. Pronotum black with lateral margins reddish brown. Elytra reddish brown with broad black U-shaped sutural stripe, extending 5/6 length of elytral suture (Fig. 2a–c). Lateral margins of elytra coarsely punctate. Prothoracic hypomeron reddish brown. Prosternum, mesoventrite, and metaventrite black. Elytral epipleuron yellowish brown with both margins black. Legs reddish brown.

Head small, width 0.66 times of pronotal width (HW/PW= 0.6/0.9). Head with fine punctures, same size as eye facets, separated by 0.5–1.0 diameters (Fig. 2b). Eyes densely faceted, with dense hairs, interocular distance 0.47 times head width. Pronotum width 0.69 times of elytral width (PW/EW=0.9/1.3), pronotal punctures sparse,

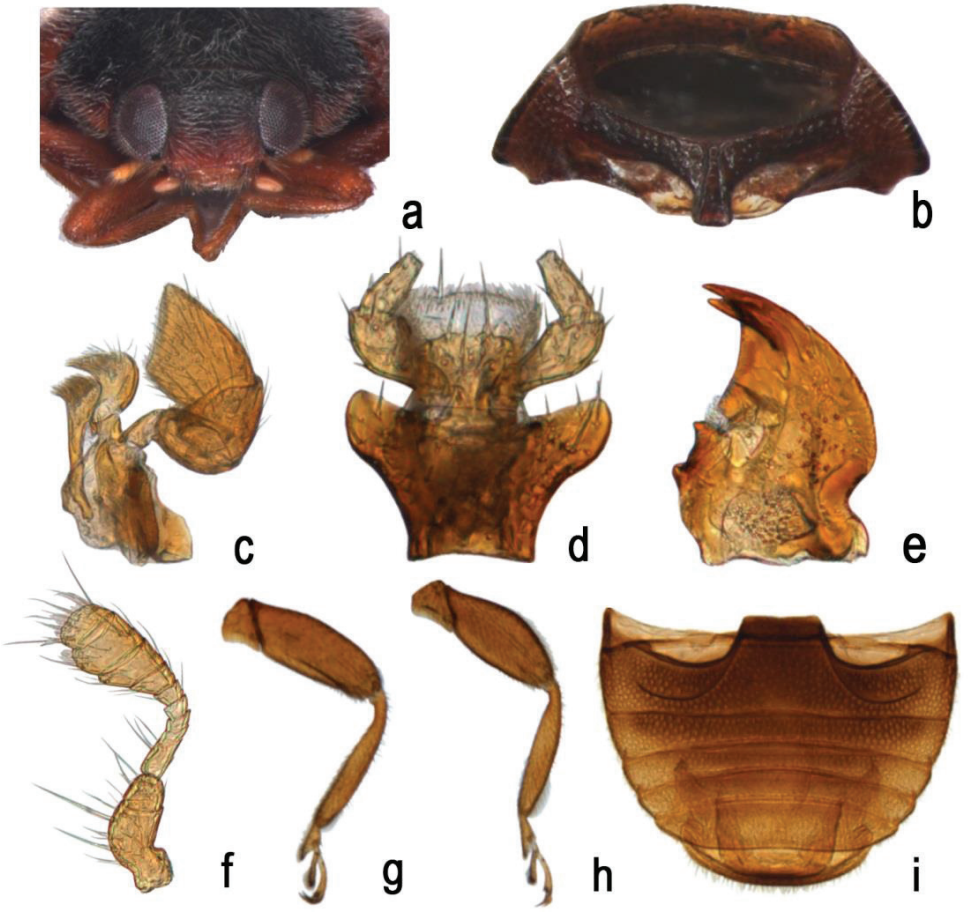

Figure 1. *Scymnus* (*Scymnus*) *contortubus* Rashid, Chen & Wang, sp. n.: **a** head, frontal **b** prothorax, antero-ventral **c** maxilla **d** labium **e** mandible **f** antenna **g** fore leg **h** hind leg **i** abdomen, male.

slightly coarser than those on head, 1.0–2.0 diameters apart. Elytral punctures coarse, separated by 2.0–4.0 diameters. Prosternal carinae distinct extending to anterior margin and slightly converging anteriorly. Prosternal process T-shaped, twice as long as its width at base. Abdominal postcoxal lines incomplete, extending to 6/7 length of ventrite and slightly recurved toward base of ventrite; area surrounding postcoxal line with dense granular punctures, distributed unevenly (Fig. 2e).

Male genitalia: Penis stout (Fig. 2d). Penis capsule with long inner process and short dilated outer one. Apex of penis strongly recurved towards inner side with thread-like appendage. Tegmen stout, with penis guide parallel-sided from base to nearly half length, tapering gradually to a blunt apex in ventral view. In lateral view, penis guide with sides parallel at basal 2/3, then abruptly constricted to pointed apex. Parameres stout; slightly longer than penis guide, with dense, long setae on apical and inner margins (Fig. 2f–g).

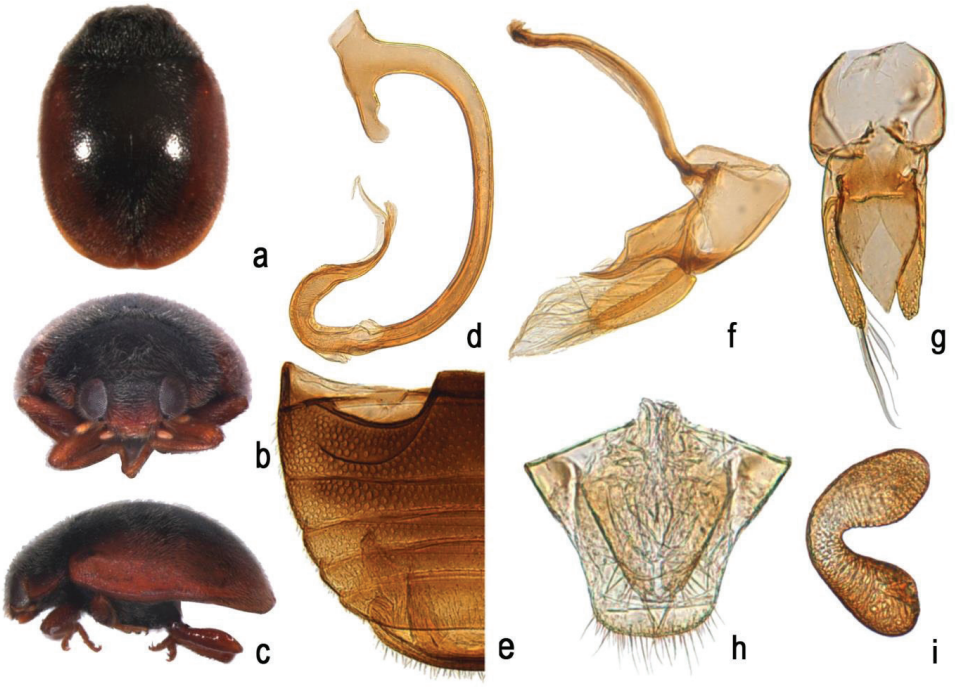

Figure 2. *Scymnus* (*Scymnus*) *contortubus* Rashid, Chen & Wang, sp. n.: **a** dorsal view **b** anterior view **c** lateral view **d** penis **e** abdomen **f** tegmen, lateral view **g** tegmen, ventral view **h** ovipositor **i** spermatheca.

Female genitalia: Coxites elongate triangular, 2.5 times as long as wide, tapering to blunt apices, each with long terminal setae (Fig. 2h); infundibulum present; spermatheca C-shaped (Fig. 2i).

Types. Holotype, Male, **PAKISTAN**: (Kashmir). Arja Mountains, No. SCAU (E) 16579, [N33°57 27.80, E073°39 54.04"], *ca*. 940 m, 28.X.2015, Huo LZ leg; Paratypes: (86) 2♂1♀, same data as holotype; 8♂1♀ Rawalakot, [N33°52 07.93", E073°43 46.49"] *ca*. 1668 m; 28.X.2015, Huo LZ leg; 12♂ 10♀ Mirpur, [N33°28 23.07", E073°52 57.94"] *ca*. 500–610 m, 26.X.2015; Huo LZ leg; (Khyber Pakhtunkhwa) 5♂ 5♀, Balakot, [N34°33 27.62", E073°21 25.08"] *ca*. 1093 m; 15.X.2015; Wang XM leg; 1♂ Birote, [N34°03 27.54", E073°30 00.32"] *ca*. 789 m; 13.X.2015; Wang XM leg; 4♂ 2♀ Arab khan, [N34°25 20.73", E073°18 44.21"] *ca*. 104 m; 16.X.2015; Wang XM leg; 5♂ 6♀ Shung, [N34°52 31.52", E072°54 12.46"] *ca*. 656 m; 17.X.2015; Wang XM leg; 9♂ ♀7 Parehna, [N34°21 32.17", E073°04 53.75"] *ca*. 775 m; 19.X.2015; Wang XM leg; 1♂ 1♀ Paras, [N34°39 23.53", E073°30 13.91"] *ca*. 1364 m; 15.X.2015; Wang XM leg; (Punjab) 1♂ 2♀ Salgran, [N33°49, 33.96", E073°17 09.48"] *ca*. 857 m; 13.X.2015; Wang XM leg; 2♂ 1♀ Gokina [N33°46, 03.26", E073°04 37.78"] *ca*. 1090 m; 11.X.2015; Wang XM leg.

Distribution. Pakistan (Kashmir, Khyber Pakhtunkhwa, Punjab).

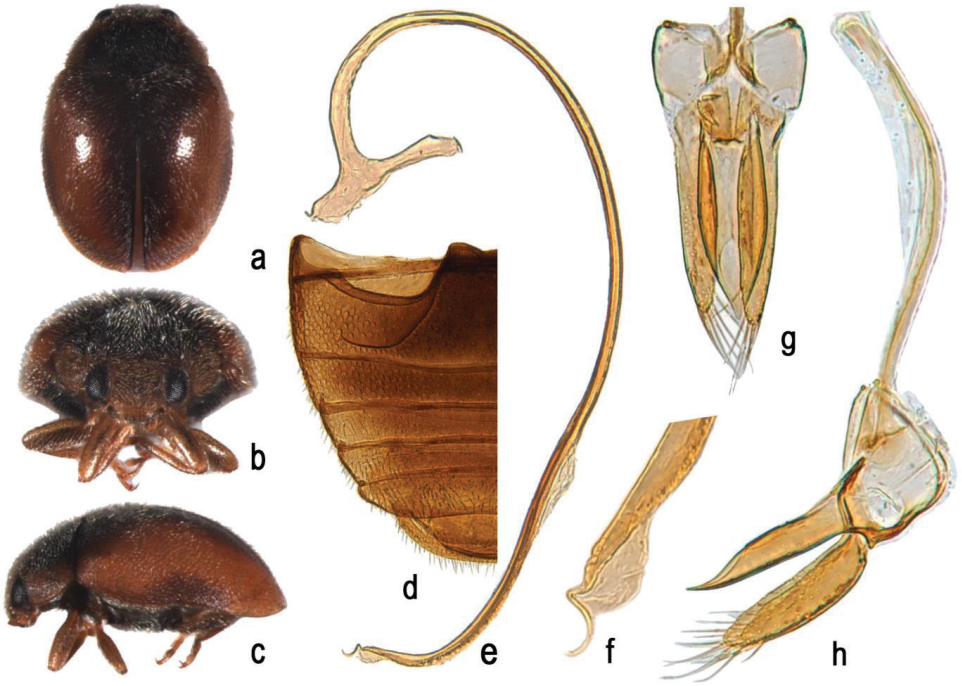

Figure 3. *Scymnus* (*Scymnus*) *nubilus* Mulsant: **a** dorsal view **b** anterior view **c** lateral view **d** abdomen **e** penis **f** apex of penis **g** tegmen, ventral view **h** tegmen, lateral view.

Scymnus (*Scymnus*) *nubilus* Mulsant, 1850

Fig. 3

Scymnus nubilus Mulsant, 1850: 972; Bielawski 1972: 293; Booth and Pope 1989: 359; Canepari 2001: 207; Chen et al. 2013: 438.

Scymnus (*Scymnus*) *nubilus*: Korschefsky 1931: 143; Kapur 1972: 311; Miyatake 1985: 9; Yu and Pang 1992: 44; Poorani 2002: 358; Kovář 2007: 590; Yu 2011: 131; Chen et al. 2013: 438.

Remarks. *Scymnus* (*S.*) *nubilus* Mulsant can be easily confused with *S.* (*S.*) *contortubus* sp. n. and other *Scymnus* species due to their similar colouration. However it can be distinguished from other species by the long and slender penis with nearly S-shaped tip (Fig. 3e–f). Diagnostic are also: the tegmen stout (Fig. 3g–h), the penis guide nearly parallel along 2/3 of basal length, converging to pointed apex in ventral view (Fig. 3g), in lateral view abruptly narrowing from apical 1/3 length to apex; parameres with long apical setae (Fig. 3h).

Material examined. PAKISTAN (Kashmir) 1♀ 2♂, Mirpur, [N33°28 23.07", E073°52 57.94"] *ca.* 500–610 m, 26.X.2015, Huo LZ leg. (Khyber Pakhtunkhwa) 1♀ 1♂, Besham [N34°59 51.61", E072°54 21.34"] *ca.* 750 m, 18.10.2015, Wang XM leg; 1♂ Arab khan, [N34°25 20.73", E073°18 44.21"] *ca.* 1043 m, 16.X.2015,

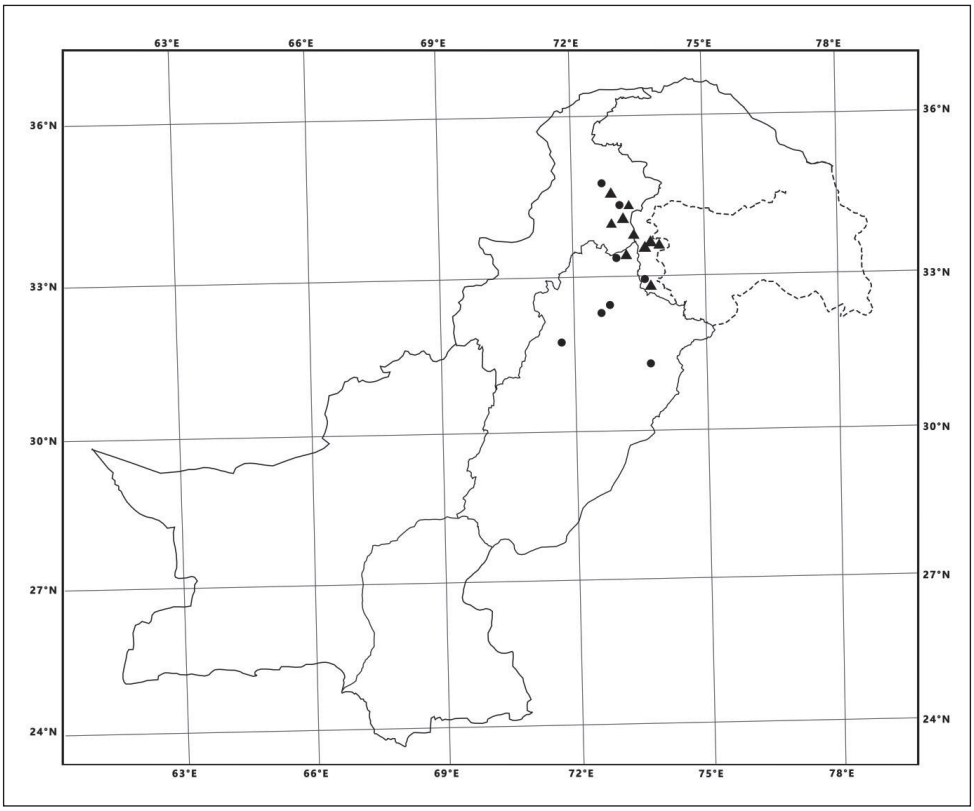

Figure 4. Distribution map: *Scymnus* (*Scymnus*) *contortubus* Rashid, Chen & Wang, sp. n. (▲) and *Scymnus* (*Scymnus*) *nubilus* Mulsant (●).

Wang XM leg. (Punjab) 1♀, Chakwal, [N32°55 33.23", E072°44 56.91"] *ca*. 515 m, 20.X.2015, Wang XM leg; 3♂, Kallar kahar, [N32°46 20.29", E072°42 56.28"] *ca*. 648 m, 21.X.2015, Wang XM leg; 3♀ 1♂, Margalla [N33°44 00.16", E073°02 12.16"] *ca*. 609 m, 10.X.2015, Wang XM leg; 1♂, Pai khel [N32°45 57", E071°34 21"] *ca*. 226m , 17.IX.2016, Rashid A leg; 2♂, Khurianwala, [N31°31 41.54", E073°14 50.86"], *ca*. 192 m, 22.X.2015, Wang XM leg.

Distribution. Pakistan (Kashmir, Khyber Pakhtunkhwa, Punjab), China, Japan, India, Sri Lanka, Burma, Nepal, Micronesia, Portugal, La Réunion, African Region.

Acknowledgements:

The authors sincerely thank Dr. Shaukat Ali (South China Agricultural University, China) for making arrangements for survey in Pakistan. We are deeply indebted to three anonymous reviewers for their constructive and valuable comments and suggestions on our manuscript. We are grateful to Mr. Huo Lizhi and Li Wenjing (South

China Agricultural University, China) for their efforts in collecting coccinellids. The research was supported by National Natural Science Foundation of China (31501884, 31601878), Guangdong Natural Science Foundation (2017 for XSC), Biodiversity survey and evaluation pilot Programme, Science and Technology Planning Project of Guangdong Province (2015A030302069), Science and Technology Partnership Program, Ministry of Science and Technology of China (KY201402014), Science and Technology Program of Guangzhou, China (201509010023).

References

Bielawski R (1972) Die marienkafer (Coleoptera: Coccinellidae) aus Nepal. Fragmenta Faunistica 18: 283–312. https://doi.org/10.3161/00159301FF1972.18.16.283

Booth RG, Pope RD (1989) A review of the type material of Coccinellidae (Coleoptera) described by F.W. Hope, and by E. Mulsant in the Hope Entomological Collections, Oxford. Entomologica scandinavica 20: 343–370. https://doi.org/10.1163/187631289X00366

Canepari C (2001) The identity of *Nephus levaillanti* (Coleoptera: Coccinellidae). Bollettino della Societa Entomologica Italiana 133(3): 207–211.

Chen X, Canepari C, Wang X, Ren S (2016) Revision of the subgenus *Orthoscymnus* Canepari of *Scymnus* Kugelann (Coleoptera, Coccinellidae), with descriptions of four new species. ZooKeys 552: 91–107. https://doi.org/10.3897/zookeys.552.6167

Chen X, Wang X, Ren S (2013) A review of the subgenus *Scymnus* of *Scymnus* from China (Coleoptera, Coccinellidae). Annales Zoologici 63(3): 417–499. https://doi.org/10.3161/000345413X672483

Fabricius JC (1798) Supplementum entomologiciae systematicae. Hafniae.

Giorgi JA, Vandenberg NJ, McHugh JV, Forrester JA, Ślipiński SA, Miller KB, Shapiro LR, Whiting MF (2009) The evolution of food preferences in Coccinellidae. Biological Control 51: 215–231. https://doi.org/10.1016/j.biocontrol.2009.05.019

Kapur AP (1972) The Coccinellidae (Coleoptera) of Goa. Records of the Zoological Survey of India 66(1–4): 309–320.

Korschefsky R (1931) Coleopterorum Catologus. Pars 118. Coccinellidae. I. Berlin, 224 pp.

Kovář I (1996) Phylogeny. In: Hodek I, Honěk A (Eds) Ecology of Coccinellidae. Kluwer Academic Publishers, Dordrecht, 19–31. https://doi.org/10.1007/978-94-017-1349-8_2

Kovář I (2007) New nomenclatorial and taxonomic acts and comments. Coccinellidae, In: Lobl I, Smetana A (Eds) Catalogue of Palaearctic Coleoptera. Apollo books, Stenstrup, 568–631.

Kugelann JG (1794) Verzeichniss der in eigigen Gegenden Preussens bis jetzt entdeckten Käfer-Arten, nebst kurzen Nachrichten von denselben. Neuestes Magazin für die Liebhaber der Entomologie 1(5): 513–582.

Miyatake M (1985) Coccinellidae collected by the Hokkaido University expedition to Nepal Himalaya, 1968 (Coleoptera). Insecta Matsumurana (New Series) 30: 1–33.

Mulsant E (1846) Securipalpes. Histoire Naturelle des Coleopteres de France, 1 pl. Paris 4: 380.

Mulsant E (1850) Species de Coleopteres trimeres securipalpes. Annales des Sciences Physiques et Naturelles d'Agriculture et d'Industrie Lyon 2: 1–1104. https://doi.org/10.5962/bhl.title.8953

Poorani J (2002) An annotated checklist of the Coccinellidae (Coleoptera) (excluding Epilachninae) of the Indian sub-region. Oriental Insects 36: 307–383. https://doi.org/10.1080/00305316.2002.10417335

Robertson JA, Ślipiński A, Moulton M, Shockley FW, Giorgi A, Lord NP, McKenna DD, Tomaszewska W, Forrester J, Miller KB, Whiting MF, McHugh JV (2015) Phylogeny and classification of Cucujoidea and the recognition of a new superfamily Coccinelloidea (Coleoptera: Cucujiformia). Systematic Entomology 40: 745–778. https://doi.org/10.1111/syen.12138

Sasaji H (1968) Phylogeny of the family Coccinellidae (Coleoptera). Etizenia 35: 1–37.

Seago AE, Giorgi JA, Li JH, Ślipiński A (2011) Phylogeny, classification and evolution of ladybird beetles (Coleoptera: Coccinellidae) based on simultaneous analysis of molecular and morphological data. Molecular Phylogenetics and Evolution 60: 137–151. https://doi.org/10.1016/j.ympev.2011.03.015

Ślipiński A (2007) Australian ladybird beetles (Coleoptera: Coccinellidae): their biology and classification. ABRS, Canberra, 286 pp.

Westwood JO (1838) Synopsis of the genera of British insects [paginated separately], published with 'An introduction to the modern classification of insects, founded on the natural habits and corresponding organisations of the different families (2 vols)'. Longman, Orme, Brown, Green, and Longmans, London, 1–48.

Yu GY, Pang XF (1992) A review of Chinese *Scymnus* Kugelann (Coleoptera: Coccinellidae). Journal of South China Agricultural University 13(4): 39–47. [In Chinese with English summary]

Yu GY (2011) The Coccinellidae of Taiwan. Chemical Industry Press, Beijing, 198 pp. [In Chinese with English summary]

ZooKeys 694: 41–70 (2017)
doi: 10.3897/zookeys.694.13097
http://zookeys.pensoft.net

REVIEW ARTICLE

A peer-reviewed open-access journal
ZooKeys
Launched to accelerate biodiversity research

A review of the occurrence and diversity of the sphragis in butterflies (Lepidoptera, Papilionoidea)

Ana Paula S. Carvalho[1,2], Albert G. Orr[3], Akito Y. Kawahara[1,2]

1 *Entomology and Nematology Department, University of Florida, 1881 Natural Area Dr, Gainesville, FL 32608, United States* **2** *McGuire Center for Lepidoptera and Biodiversity, Florida Museum of Natural History, University of Florida, 3215 Hull Road, Gainesville, FL, 32611 United States* **3** *Environmental Futures Research Institute, Griffith University, Nathan, QLD 4111, Australia*

Corresponding author: *Ana Paula S. Carvalho* (acarvalho@ufl.edu)

Academic editor: *T. Simonsen* | Received 6 April 2017 | Accepted 7 August 2017 | Published 29 August 2017

http://zoobank.org/6C1FA2F3-C274-4652-A1FA-D5C8570C4ABA

Citation: Carvalho APS, Orr AG, Kawahara AY (2017) A review of the occurrence and diversity of the sphragis in butterflies (Lepidoptera, Papilionoidea). ZooKeys 694: 41–70. https://doi.org/10.3897/zookeys.694.13097

Abstract

Males of many butterfly species secrete long-lasting mating plugs to prevent their mates from copulating with other males, thus ensuring their sperm will fertilize all future eggs laid. Certain species have further developed a greatly enlarged, often spectacular, externalized plug, termed a sphragis. This distinctive structure results from complex adaptations in both male and female genitalia and is qualitatively distinct from the amorphous, internal mating plugs of other species. Intermediate conditions between internal plug and external sphragis are rare. The term sphragis has often been misunderstood in recent years, hence we provide a formal definition based on accepted usage throughout most of the last century. Despite it being a highly apparent trait, neither the incidence nor diversity of the sphragis has been systematically documented. We record a sphragis or related structure in 273 butterfly species, representing 72 species of Papilionidae in 13 genera, and 201 species of Nymphalidae in 9 genera. These figures represent respectively, 13% of Papilionidae, 3% of Nymphalidae, and 1% of known butterfly species. A well-formed sphragis evolved independently in at least five butterfly subfamilies, with a rudimentary structure also occurring in an additional subfamily. The sphragis is probably the plesiomorphic condition in groups such as Parnassius (Papilionidae: Parnassiinae) and many Acraeini (Nymphalidae: Heliconiinae). Some butterflies, such as those belonging to the *Parnassius simo* group, have apparently lost the structure secondarily. The material cost of producing the sphragis is considerable. It is typically offset by production of a smaller spermatophore, thus reducing the amount of male-derived nutrients donated to the female during mating for use in oogenesis and/or somatic maintenance. The sphragis potentially represents one of the clearest

examples of mate conflict known. Investigating its biology should yield testable hypotheses to further our understanding of the selective processes at play in an 'arms race' between the sexes. This paper provides an overview, which will inform future study.

Keywords
Ditrysia, mate conflict, mating plug, Nymphalidae, Papilionidae, sperm guarding, sperm precedence, sexual competition

Introduction

Male butterflies, like most animals, typically maximize their reproductive success by mating with as many females as possible. Conversely, for females, one copulation is normally sufficient to provide sperm to fertilize all the eggs that they can produce. Female butterflies possess sperm storage organs which can maintain vital sperm from a single mating for their entire life (Chapman 1969, Parker 1970, 1984, Ferro and Akre 1975, Ehrlich and Ehrlich 1978, Walker 1980, Thornhill and Alcock 1983, Drummond 1984, Gwynne 1984, Orr 1988, Solensky and Oberhauser 2009, Klowden 2013). However, females frequently mate more than once. This may result from the need for: more male-derived nutrients received during copulation, more sperm (especially if their first mate was depleted), increasing the genetic quality of the fertilized eggs by mating with a fitter male, increased genetic diversity of offspring in an unpredictable environment, or reducing the energy loss and risk of harm involved in resisting the attempts of copulation with new males. With many factors potentially influencing female mating, there is great interspecific variation in female mating frequencies, ranging from obligate monandry to regular polyandry (Scott 1972, Walker 1980, Thornhill and Alcock 1983, Knowlton and Greenwell 1984, Arnqvist and Nilsson 2000, Blanckenhorn et al. 2002, Wedell 2005).

When female insects mate more than once, it is often the sperm of the final male to mate which fertilizes most (or all) of the female's remaining eggs, a process termed "last male sperm precedence" (Labine 1966, Parker 1970, Boggs and Watt 1981, Simmons 2001). Males of all Lepidoptera, except Micropterigidae (Sonnenschein and Hauser 1990), produce infertile (apyrene) sperm, which may play a role in blocking those of a previous partner (Silberglied et al. 1984). Therefore, when a male mates, it is generally in his interest to prevent the female from mating again. Conversely, if the female benefits from polyandry, counter-mechanisms to overcome male paternity assurance strategies may evolve.

Although many strategies are found among insects to prevent females from remating, with females evidently complicit in some cases (Parker 1970, 1984, Gilbert 1976, Thornhill and Alcock 1983, T. Chapman and Patridge 1996, Orr 1999a, Simmons 2001, Hosken et al. 2009, Shuker and Simmons 2014), in butterflies the most common strategy is for the male to produce a mating plug which physically blocks the copulatory opening (Labine 1966, Parker 1970, Ehrlich and Ehrlich 1978, Drummond 1984, Orr and Rutowski 1991, Matsumoto and Suzuki 1995, Orr 1995). Mat-

ing plugs also occur in mammals, nematodes and in many arthropod groups, such as spiders, wasps, and flies (Gillies 1956, Thornhill and Alcock 1983, Timmermeyer et al. 2010, Uhl et al. 2010, Hirt et al. 2017). However, only in those of the ditrysian Lepidoptera, a group to which all butterflies belong, can the plug be potentially permanent because it does not impede oviposition. This stems from the unique arrangement of the female genital ducts in the Ditrysia. The copulatory opening (ostium bursae) is located ventrally on the eighth segment, typically within a shallow pocket, the sinus vaginalis, and is completely separate from the oopore, which exits terminally between the paired ovipositor lobes (papillae anales) and through which eggs pass during oviposition (Eaton 1988, Scoble 1992). Therefore, not only can the plug be permanent, it can also be large and externally elaborate, covering large parts of the female's abdomen, in which case it is termed a sphragis.

The history and nature of the sphragis

The production of a sphragis, one of the more extreme male strategies that has evolved to prevent the female from remating, occurs only in certain butterflies. It was first clearly described by Linnaeus (1746) for the parnassiine swallowtail *Parnassius apollo* (Linnaeus 1758) and was subsequently discussed in more than 140 publications before 1918 (Bingham 1907, Houlbert 1916, Bryk 1919). The term 'sphragis' (plural: *sphragides*), which means 'seal' in Greek, was first used by Eltringham (1912), who described the structure found in many *Acraea* Fabricius, 1807 species (Nymphalidae: Heliconiinae) as a "*wax-like seal [produced] after pairing*". The term was also used by Waterhouse and Lyell (1914) for the postcopulatory 'seal' in *Cressida cressida* (Fabricius, 1775) (Papilionidae: Troidini) and by Bryk (1919), who applied the term to the structure in most genera where a sphragis is recognized as occurring today. With this level of sustained attention over the decades, it is clear that the sphragis is a recognizable phenomenon deserving special investigation. However, there has been recent confusion in the use of the term, hence there is a need to clarify its meaning. We therefore define the sphragis as: an external formation, originating from male accessory glands, with a well-defined, species-specific structure, fixed to the female abdomen following insemination, where it blocks the ostium bursae.

The form of the sphragis is consistent within a species, it is shaped by complex adaptations in the male genitalia, and it is wholly or mainly external to the female abdomen. In these respects, sphragides differ qualitatively from smaller amorphous internal mating plugs. In almost all sphragis-bearing species, the female external genitalia are strongly modified from the ditrysian groundplan; these modifications have in turn influenced the form of the sphragis (Orr 1988, 1995). Intermediate states, where they occur, involve highly sophisticated male and/or female adaptations (Orr 1988).

Specialized features of sphragides in different species have been identified by several authors (Bryk 1918, Ackery 1975, Pierre 1985a, Orr 1988, 1999a, Matsumoto and Suzuki 1995). In some, the sphragis incorporates long scales derived from specialized

tufts on the male genitalia (Pierre 1985a, Orr and Kitching 2010, Matsumoto, Orr & Yago *in prep*.). These may reinforce the structure of the sphragis and/or provide bulk by increasing the sphragis in size and weight. In others, the sphragis is densely tiled with short flat scales which may make it slippery and difficult for other males to grasp. In both cases, the scales seem to hinder sphragis removal by other males (Pierre 1985a, Orr 1999b). The sphragis is also frequently hollow, greatly increasing its bulk, or is intricately sculptured, often including projections which potentially make access to the female genitalia difficult. Moreover, an elaborate girdle, which encircles the female abdomen, is often associated with the sphragis, holding it tightly in place. It sometimes incorporates strengthening scales.

One oft-cited misconception is that the 'waxy' sphragis can dissolve in water (Drummond 1984, Epstein 1987, Sourakov and Emmel 1997), supposedly explaining the high incidence of sphragis-bearing species in semiarid habitats. This fallacy originated from a misreading by Hinton (1964) of the French abstract of Tykac (1951), which was originally published in Czech (Orr 1988).

Formation of the sphragis

The sphragis is produced from a viscous secretion which is molded within membranous or sclerotized pockets in the male genitalia, sometimes being extruded gradually as it hardens, so that the final product is far larger than any cavity in the male's body (Bryk 1918, Takakura 1967, Matsumoto 1987, Orr 1988, 1995). Hardening may occur on contact with air, but this process is not understood. It is also possible that sphragis formation is mediated by enzymatic action, at least in some species (Orr 1995). The sphragidal fluid varies among species, with some producing an almost clear vitreous secretion, and others a secretion with an appearance similar to the lipoprotein mass found in a fresh spermatophore (Orr 1995). The precise composition of the sphragis has not been established, but it is known to contain high protein levels (Orr 1988), and its waxy appearance suggests a lipid element. All sphragis-bearing species that have been investigated exhibit hypertrophied, paired accessory glands and it is generally accepted that these secrete the sphragidal fluid (Eltringham 1925, Ehrlich 1961, Orr 1988, 1995, 2002). It is known that the spermatophore, which in most butterflies is a thick hollow structure formed from lipoprotein (Boggs and Gilbert 1979, Orr 1988), is secreted by a glandular region of the ductus ejaculatorius simplex (Callahan and Cascio 1963), or ejaculatory duct, which leads directly to the aedeagus.

Production of the sphragis is a substantial male material investment, which apparently occurs at the expense of the spermatophore. A great deal of material needs to be repurposed to build the sphragis. The amount of accessory gland secretion (including the spermatophore, and spermatophylax), which females could potentially metabolize and utilize for oogenesis or somatic maintenance (Boggs and Gilbert 1979, Boggs and Watt 1981, Orr 1988, 1995), is thus reduced in its subsequent transfer to the female. Even while producing a small spermatophore, males are limited in the number of

sphragides they can produce (Orr 1988, 1995). It is common to find specimens (both in the field and in museum collections) with frail or incomplete sphragides. These were probably produced by males that recently mated or had mated several times previously, and thus had exhausted the resources necessary to produce a sphragis of normal bulk (Orr 1988). It has been estimated that males of the *Heteronympha penelope* Waterhouse, 1937 (Nymphalidae: Satyrinae) require 7–10 days after mating to recover the resources necessary to produce another sphragis, and can only produce 3–4 effective sphragides in their lifetime (Orr 2002). Available measurements indicate that the investment involved in the production of each sphragis varies between about 3–20% of the male's body weight, depending on the species (Table 1) (Orr 1988).

Behavioral specialization

Presence of the sphragis is typically associated with specific behavioral patterns. Courtship behavior is absent or rudimentary in almost all sphragis-bearing species (Epstein 1987, Matsumoto 1987, Orr 1988, Tyler et al. 1994, Sourakov and Emmel 1997). Mates are secured, often by pursuit and aerial capture, with mating taking place in mid-air or on the ground (Larsen 1991, 2005). Matsumoto (1987) reported that males of *Luehdorfia japonica* Leech, 1889 (Parnassiinae) seize females in midair, carry them to the ground, and copulate with them. Similar behavior has been analyzed in detail in the Australian sphragis-bearing troidine *C. cressida* (Orr 1988, 1999b). In this species, large males often capture and mate with the smaller females in mid-air but relatively smaller males carry females to the ground to mate. *Cressida cressida* males are significantly larger than females, an unusual condition in butterflies, but this disparity probably relates to their strong territorial behavior, rather than to success at forced copulation (Orr 1999b).

Function of the sphragis

All experimental evidence (Matsumoto 1987, Orr 1988), indicates that the sphragis functions as a physical barrier, preventing a new male from penetrating the female's ostium bursae and reinseminating her. In his monumental work, *Grundzüge der Sphragidologie*, Bryk (1918, 1919, 1930, 1950) effectively dismissed much fanciful speculation that had taken place in the preceding 170 years, arguing that the sphragis serves as a physical barrier to insemination. This conclusion was reached earlier by Marshall (1901, 1902), based on his observations of *Acraea* (Heliconiinae) mating in nature, and Haude (1913), based on observations of *Parnassius*. Eltringham (1925) reached this conclusion, noting at the time '*indeed it would seem that more has been written about [the sphragis], and with less result, than about most features of insect structure*'. Because the sphragis blocks only the genital opening of the female, the ovipositor is unobstructed (Labine 1964), although the sphragis can be so large in many species it can be a distinct encumbrance and ac-

Table 1. Percentage of male investment in the sphragis based on male's weight. Data adapted from Orr (1988).

	Male investiment on the sphragis (% body weight)
Parnassius glacialis (Papilionidae: Parnassiinae)	20.5 ± 2.7
Parnassius apollo (Papilionidae: Parnassiinae)	7.4 ± 2.5
Luehdorfia japonica (Papilionidae: Parnassiinae)	9.8 ± 5.7
Cressida cressida (Papilionidae: Papilioninae)	6.7 ± 1.1
Euryades corethrus (Papilionidae: Papilioninae)	8.6 ± 1.0
Parides proneus (Papilionidae: Papilioninae)	3.1 ± 1.5
Acraea serena (Nymphalidae: Heliconiinae)	3.3 ± 0.4
Acraea anemosa (Nymphalidae: Heliconiinae)	6.1 ± 0.9
Acraea andromacha (Nymphalidae: Heliconiinae)	3.1 ± 0.2

cidental blocking of the oopore has been reported (van der Poorten and van der Poorten 2016). The size and shape of the sphragis could potentially be important in preventing males from being able to grasp the female with their valvae (Orr 1995). Moreover, Orr and Rutowski (1991) showed that the sphragis of *C. cressida* might have the secondary function of providing a visual cue to males indicating that a female has already mated. In their study, females with intact sphragides were less likely to be pursued by males when compared with females where the sphragis was experimentally trimmed or removed. Supporting this hypothesis is the observation that females of *C. cressida* have evolved a specialized posture, that when in flight, allows the sphragis to be seen clearly from behind (Orr and Rutowski 1991, Orr 1999b). It is conceivable that in other sphragis-bearing species, males might also be able to visually assess whether mating is possible depending on the development of the sphragis (Orr and Rutowski 1991). Apart from its large size, the sphragis often stands out with strong color contrast to the rest of the body, possibly increasing its apparency, but if this occurs it is surely a secondary function (Orr 1999b).

The taxonomic distribution of the sphragis

In the most comprehensive comparative survey to date, Orr (1988) examined the presence or absence of mating plugs, the relative investment in spermatophore versus plug, as well as female genital anatomy in over 160 species, including sphragis-bearing species and others representing a range of plugging strategies in the Papilionidae, Pieridae and Nymphalidae. Bryk (1919, 1935b) surveyed the sphragis of several Papilionidae and Palaearctic Nymphalidae genera, while Ackery (1975) focused on Parnassiinae. Although most sphragis-bearing genera recognized by contemporary taxonomic arrangements were included, no study so far has provided a comprehensive survey of all species. The morphology of the sphragis and associated male and female genitalia are well documented in widely scattered literature for African *Acraea* (Eltringham 1912, 1925, van Son 1963, Pierre 1985a, 1988, 1992a, 1992b, Orr 1988), but the sphragis in Neotropical *Acraea* (Paluch et al. 2003) has received less attention.

The present state of knowledge

Studies on the biology of the sphragis in living butterflies have mostly focused on *C. cressida* in the Troidini (Orr 1988), *Luehdorfia* and *Parnassius* in the Parnassiinae (Matsumoto 1987), and *H. penelope* in the Satyrinae (Orr 2002). Some less detailed observations are also available for the genus *Acraea* in the Heliconiinae (Marshall 1901, Eltringham 1912, Epstein 1987, Orr 1988).

A large body of published information exists on the occurrence and diversity of the sphragis, but it is largely obscure, scattered, old and often published in languages other than English. There is a need for this information to be collated and for several conspicuous gaps to be filled. In this paper we aim to provide an overview of the subject and develop a dataset to inform future investigation. We present the first comprehensive review of the structural variability of the sphragis across all butterflies, illustrating the variety of forms that these can take. All species of butterflies in which a well-defined sphragis is known to occur are listed based on published information and direct observation of museum specimens. Reports of sphragis occurrence in Erebidae (Rawlins 1992) and Lycaenidae (Bryk 1918, 1919) we dismiss as erroneous.

Bryk (1919) illustrated a sphragis-like structure in the Nymphalidae *Argynnis paphia*, however, subsequent investigation has failed to confirm this observation and it is suggested (Matsumoto pers. comm.) that the structure observed in this case is a result of an accumulation of several mating plugs deposited by one or more males after multiple matings by the female, which could be externally observed.

In addition, as noted previously, sphragis-like formations which may represent incipient sphragis evolution or secondary loss occur in some butterflies (Orr 1995). A complex anomalous structure is also discussed in our analysis. We establish a three point system of categorization for true sphragides based on degree of complexity. Finally, we examine the processes and patterns of sphragis evolution in the context of a currently accepted butterfly phylogeny.

Methods

We examined butterfly specimens in museum collections and searched historical and recent literature for reports, descriptions and illustrations of sphragides or similar external structures (Guenée 1872, Eltringham 1912, Bryk 1935a, Riley 1939, van Son 1963, Saigusa 1973, Ackery 1975, Common and Waterhouse 1981, Saigusa and Lee 1982, Parsons 1983, D'Abrera 1984, 1990, 1995, 1997, Drummond 1984, Pierre 1985a, 1985b, Matsumoto 1987, Miller 1987, Orr 1988, Matsumoto and Suzuki 1995, Penz and Francini 1996, Francini et al. 2004, Paluch et al. 2006, Churkin 2006, Neild 2008, Neild and Romero 2008, Pierre and Bernaud 2009, 2013, Bollino and Racheli 2012, Harada et al. 2012). Museum specimens were studied by APSC and AGO. The former visited the Cornell University Insect Collection, Ithaca, NY, USA (CUIC), Florida Museum of Natural History, McGuire Center for Lepidoptera and Biodiver-

sity, Gainesville, FL, USA (MGCL), and the National Museum of Natural History, Washington DC, USA (USNM). AGO studied specimens in the Australian National Insect Collection, Canberra, Australia, (ANIC), the Natural History Museum, London, UK (BMNH), the Museum Alexander Koenig, Bonn, Germany (ZFMK), and the private collection of the late Prof. Dr. Clas Naumann (Bonn). For our museum specimen searches, we especially targeted Nymphalidae and Papilionidae because only in these families has the sphragis been reliably reported by previous authors. Mated females of all species available to us in each target group (see below) were inspected using a dissecting microscope with the following aims: (1) to confirm and categorize the sphragis in species previously reported to have a sphragis, and (2) to gather new data for any species not mentioned in literature. We also contacted specialists who had studied sphragis-bearing species in order to gather additional unpublished data.

For each species, we tried to examine mated females of at least ten specimens if possible (in a few cases thousands were available). Generally, the minimum combined sample was five specimens. Overall, we directly examined approximately 80% of all sphragis bearing species. We recorded key traits of the sphragis of each species, especially: the presence of male scales attached to the surface or incorporated into its matrix; whether it was mainly hollow or solid; the presence of projections or other specialized sculpturing; and its size relative to the female abdomen. We also examined structures previously classified as protosphragides or vestigial sphragides, and we define an anomalous form as a 'hemi-sphragis'. We targeted the following taxa based on published and unpublished information: Nymphalidae: *Acraea*, *Amauris* Hübner, 1816, *Argynnis* Fabricius 1807, *Dircenna* Doubleday, 1847, *Hestina* Westwood, 1850, *Heteronympha* Wallengren, 1858, *Hipparcha* Fabricius 1807, *Pteronymia* Butler & Druce, 1872, *Sasakia* Moore 1896; Papilionidae: Parnassiinae, *Cressida* Swainson, 1832, *Euryades* Felder & Felder, 1864, *Losaria* Moore, [1902], *Parides* Hübner, 1819, and *Trogonoptera* Rippon, [1890].

In order to show the extent of interspecific variation in sphragis morphology, we digitally imaged the sphragis of representative species using a Canon 5D MKIII camera body and a Canon MP-E 65mm lens. For each image, 10 to 20 image layers (depending on the size of the sphragis) were taken across a series of close-spaced focal planes, using the Automated Macro Rail for Focus Stacking StackShot. These were later stacked using the software Helicon Focus on a PC computer. Figures were edited and assembled using Adobe Photoshop CS4. The taxonomic classification in this study follows Häuser (2005) for Papilionidae, Pierre and Bernaud (2014a) for Acraeini, Lamas (2004) for the Neotropical non-Acraeini Nymphalidae, and LepIndex (Beccaloni et al. 2003) for the remaining Nymphalidae.

Terms related to sphragis-like structures used in this study

- *Protosphragis*: amorphous, non-species-specific version of the sphragis, often facultative in the groups where it is found, and potentially associated with groups in the early evolution of the sphragis.

- *Vestigial sphragis*: non-species specific version of the sphragis, irregular in occurrence, associated with groups believed to be in the process of losing the sphragis.
- *Hemi-sphragis*: semi-internal version of the sphragis, with a complex and regular internal arrangement of lacunae used to increase bulk as well as a regularly striated exposed outer face, associated with complex adaptations in male genitalia, thus equivalent to true sphragides in terms of complexity and regularity of form. Restricted to the troidine genus *Trogonoptera* and figured in Orr (1995).

Based on the traits recorded for each sphragis we developed a system of categorization based on level of complexity. Category 1 (low complexity): a protosphragis or a vestigial sphragis, characterized by being small, amorphous and of facultative occurrence. Category 2 (moderate complexity): a hemi-sphragis, or a well-formed externalized sphragis lacking male scales and essentially solid, of small to medium size. Category 3 (medium complexity): a well formed sphragis incorporating male scales but solid and of simple form, mostly small to medium in size. Category 4 (high complexity): large to very large sphragides, hollow and/or with specialized projections, girdles, or other complex sculpturing, further defined based on absence (Category 4a) or presence (Category 4b) of scales.

Results and discussion

A total of 273 butterflies species in two families – Papilionidae (72 species, 13 genera) and Nymphalidae (201 species, 9 genera) – were recorded as having a sphragis, protosphragis, vestigial sphragis, or hemi-sphragis (Suppl. material 1) (Figures 1–33). These numbers represent 13% of Papilionidae, 3% of Nymphalidae, and 1% of all butterflies (Heppner 1991, Häuser et al. 2005). The 22 sphragis-bearing genera were distributed in 8 tribes within the two families. A well-formed sphragis occurrs in almost all species of *Parnassius*, where it is probably plesiomorphic, and was widespread in *Acraea* (ca 64% of species in the genus). On the other hand, in *Heteronympha* (Figure 13), it occurs in just one out of eight species. The presence of a sphragis in the Ithomiini *Pteronymia* remained undetected until recently (De-Silva et al. *in press*), probably due its small size when compared to other groups, which is consistent with the slim build and small size of butterflies in this genus.

A protosphragis was present in 11 species, vestigial sphragides occurred in 14 species, while a hemi-sphragis is found only in the two known species of the Troidini genus *Trogonoptera* (Suppl. material 1). A girdle was present, at least facultatively, in 23 species and was widespread in some *Parnassius* species-groups, such as in *delphius* (Figure 3) and *acco* groups.

For the species where a sphragis occurs (Suppl. material 1), Category 3 (99 species) and Category 4 (98 species) were most common, together being found in 197 species (72%), whereas Category 1 was least represented, with 25 species (9%) (Table 2). We could not define a category for 16 sphragis-bearing species due to lack of data, which in most cases was due to the small number of specimens available, preventing a

Table 2. Number of species per sphragis category.

	Category 1	Category 2	Category 3	Category 4	Uncertain
Number of species	25	35	99	98	16
Percentage of species	9%	13%	36%	36%	6%

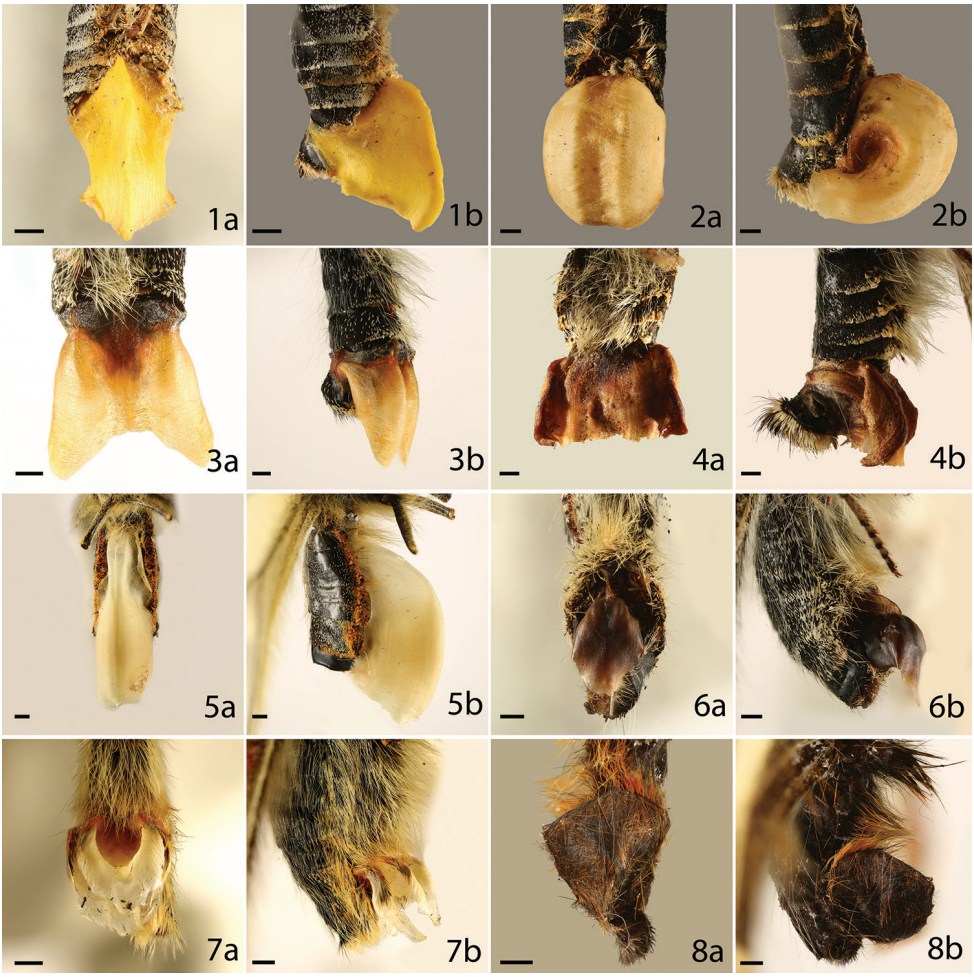

Figures 1–8. Sphragis of butterfly species **a** ventral **b** lateral, category of the sphragis in parenthesis. **1** *Parnassius autocrator* (4) **2** *P. charltonius* (4) **3** *P. delphius* (4) **4** *P. imperator* (4) **5** *P. mnemosyne* (4) **6** *P. phoebus* (4) **7** *P. tenedius* (4) **8** *Luehdorfia chinensis* (3). Scale bar = 1 mm.

confident determination on the complexity of the sphragis. Although most species fit well within our categories, intermediates occurred. Examples include *Allancastria* spp. (Papilionidae: Parnassiinae), in which the sphragis might best be characterized as falling

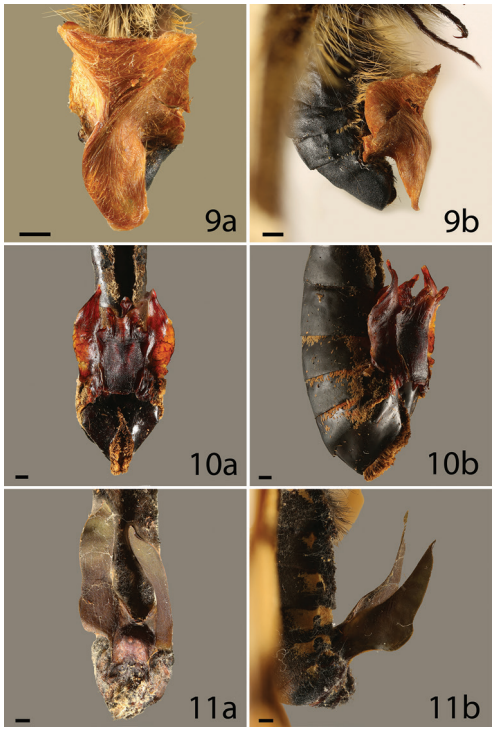

Figures 9–11. Sphragis of butterfly species, **a** ventral **b** lateral, category of the sphragis in parenthesis. **9** *L. puziloi* (4) **10** *Cressida cressida* (4) **11** *Euryades duponchelii* (4). Scale bar = 1 mm.

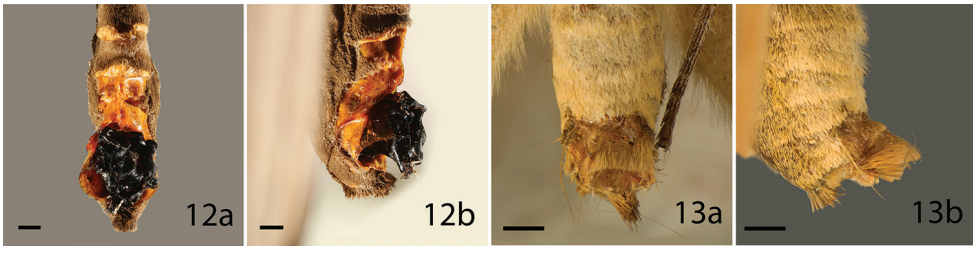

Figures 12, 13. Sphragis of butterfly species, **a** ventral **b** lateral, category of the sphragis in parenthesis. **12** *Amauris niavius* (1) **13** *H. penelope* (4). Scale bar = 1 mm.

between Categories 2 and 3, as well as *Amauris niavius* (Linnaeus, 1758) (Nymphalidae: Danainae) (Figure 12) and *Losaria palu* (Martin, 1912) (Papilionidae: Papilioninae), which could be considered to fall between Categories 1 and 2. We listed these species in Suppl. material 1 based on which category their sphragis best fits. The fact that complex sphragides are more common across butterfly groups might indicate that male adaptations to produce them are subject to strong selection.

Variation in the morphology and color of the sphragis

Four categories of sphragis (including two subcategories) were recognized in terms of structural complexity (Suppl. material 1 and Table 2). As an external, large, and morphologically complex sphragis, there is great variation in size, color and shape (Figures 1–33). For example, the sphragis in species of the *P. mnemosyne* species-group is an enormous, hollow, thin-walled tubular structure, nearly as large as the female abdomen (Figure 5). Our characterizations show that while sphragides are frequently solid, hollowness is relatively common (27%) (Table 3). This could be a strategy to maximize the bulk of the sphragis without increasing mass (Orr 1988), thus optimizing its effectiveness while reducing the material cost to the male in its production, as well as reducing the load carried by the female. Such forms are associated with major adaptations in the male genitalia (Orr 1995). The sphragis of most *Parnassius* species is generally hollow and those of the *P. mnemosyne* group (Figure 5) include the largest sphragides so far measured (in terms of total mass). Based on available data, the sphragis of *P. glacialis* Butler, 1866 represents approximately 20.5% of male dry weight (Orr 1988) (Table 1). Those of *P. imperator* Oberthür, 1883 (Figure 4), *P. charltonius* Gray, (1853) (Figure 2) and *P. acco* Gray, (1853) may be even heavier in relative terms (Orr 1988).

Acraea species exhibit great variation in the form and development of the sphragis. In some, such as *A. natalica* Boisduval, 1847, there is no sphragis or internal mating plug and females mate numerous times with males, which produce small spermatophores (Orr 1988). The form of the female genitalia and the small size of the spermatophore suggests that this species evolved from sphragis-bearing ancestors. Similarly, the sphragis has probably been lost in *A. encedon* (Linnaeus, 1758) and its relatives (Pierre 1985b), but in these species there is an internal plug. The sphragis has therefore apparently been lost independently at least twice in African *Acraea*; in other species the sphragis may be vestigial. In the *Acraea* subgenus *Actinote*, females typically bear a small to medium sized sphragis covered in male scales (Figure 32) (Pierre 1985a). These sphragides tend to be relatively small compared to male mass (see *A. serena* (Fabricius, 1775) in Table 1). Other *Acraea* species bear a medium to large, box-like hollow sphragis (Figure 20), produced in a similar manner to those of *Parnassius* (Orr 1988). These seem to represent a larger investment by the male (see *A. anemosa* Hewitson, 1865 in Table 1) and this is probably true of most hollow sphragides in *Acraea*. Small sphragides incorporating dense, long scales have also been described in *Allancastria* species (Matsumoto et al. *in prep*.) (Papilionidae: Parnassiinae). A medium-sized, scale-covered structure occurs in the *H. penelope*, which produces a largely hollow sphragis (in Figure 13, the sphragis is probably from the male's second mating) (Orr 2002). Numerous scales are incorporated into the large twisted sphragis of *Luedorfia puziloi* (Erschoff, 1872) (Figure 9) and also in the medium-sized flat, shield-like sphragis of *Luehdorfia japonica* Leech, 1889 (Matsumoto 1987). Some medium sized sphragides are probably extremely effective in preventing remating. For example, the sphragis of *C. cressida* is solid with lateral projections, a dorsal keel, and an anterior horn (Orr 1999b), molded within a system of membranes in the male

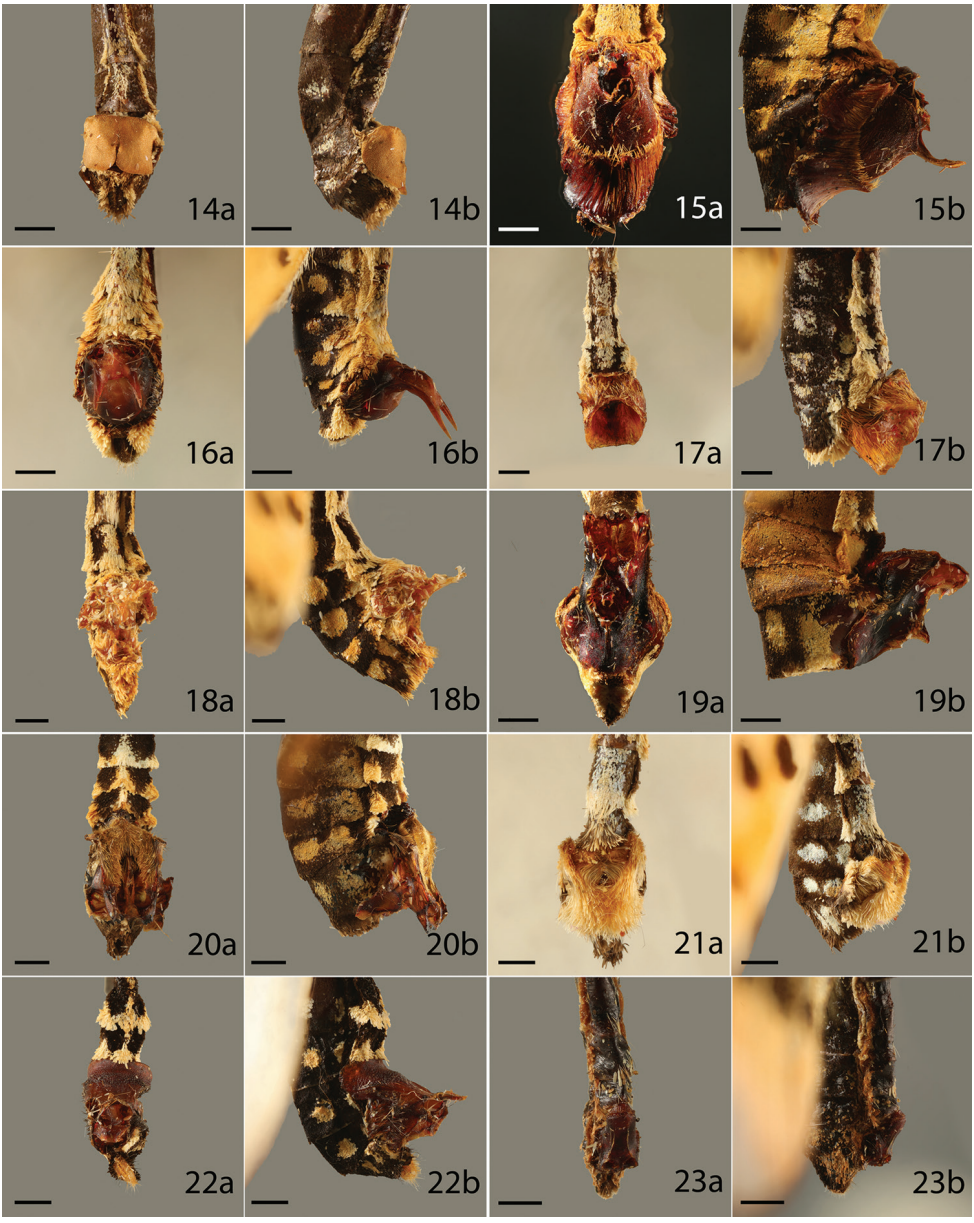

Figures 14–23. Sphragis of butterfly species, **a** ventral, **b** lateral, category of the sphragis in parenthesis. **14** *Acraea kraka* (2) **15** *A. egina* (4) **16** *A. omrora* (4) **17** *A. nohara* (4) **18** *A. oncaea* (3) **19** *A. zetes* (4) **20** *A. endoscota* (4) **21** *A. quirina* (3) **22** *A. igati* (3) **23** *A. hamata* (2). Scale bar = 1 mm.

genitalia and enclosed by valves. It represents about 6.7% of male mass, but is very effective in preventing remating (Orr 1988). The sphragis of some species, notably *Euryades corethrus* (Boisduval, 1836) and *E. duponchelii* (Lucas, 1836) have long projections (Figure 11). This type of sphragis, formed in deep sheaths within the male's body

Table 3. Number of species displaying different sphragis parameters.

Condition	No. of species
Scales	
Yes	145
No	113
Projections and/or girdle	
Yes	60
No	199
Structure	
(Mostly) Hollow	73
(Mostly) Solid	176

(Figure 34) (Miller 1987), potentially make it difficult for subsequent males to grasp the body of mated females to remove the sphragis. In *E. corethrus*, the total mass of the structure is a moderate 8.6% of male body mass (Orr 1988), suggesting efficient use of material. On the other hand, solid small-medium size sphragides lacking scales occur in many *Acraea* species. In these cases the sphragis is formed in a sclerotized mold associated with the male genitalia (van Son 1963, Orr 1988). In *A. andromacha* the sphragis represents 3.1% of male body mass (Table 1), but is not completely effective in preventing remating, with sphragis removal and limited polyandry having been reported (Epstein 1987, Orr 1988).

A girdle occurs in *E. corethrus* (but not in the related *E. duponchelii*) (Bryk 1918) and in several *Parnassius* species such as *P. autocrator* Avinov, 1913 (Figure 1), *P. delphius* (Eversmann, 1843) (Figure 3), and *P. imperator* (Figure 4). It occurs in *P. cephalus* Grum-Grshimailo, 1891, but not in its sister species *P. szechenyii* Frivaldszky, 1886, possibly because the final segment of the abdomen to which the sphragis is attached is unusually deep, making it impossible for the male to encircle the abdomen with his valves (Orr 1988). Recent phylogenies of *Parnassius* (Michel et al. 2008, Omoto et al. 2009) suggest that the girdle has evolved independently at least three times within the genus. The girdle present in a few *Acraea* appears to be a facultative condition, possibly associated with a male's first mating. It loosely encircles the abdomen, but evidently does not grip it tightly above as in girdled papilionid species. The variation in color of the sphragis might reflect differences in the composition of the sphragidal material; this subject deserves further investigation. In the *P. apollo* group (*phoebus,* Figure 6), sister to the remainder of the genus, it is brown and slightly translucent whereas in other species it is whitish (often discolored) and opaque.

Almost all butterfly species in our list display structures that meet our definition of the sphragis, however, we recognized a few unusual intermediate forms. The large, semi-exposed plug of the troidine papilionid *Trogonotera* Rippon, 1890 has internal structure (ordered lacunae) and external, well defined striae, hence we classify it as a 'hemi-sphragis'. The male has a specialized pouch where the plug material is formed into a broad ribbon, which coalesces into a solid body with lacunae (Orr 1988, 1995). The small formation of the troidine papilionid *Parides proneus* (Hübner, 1831), rec-

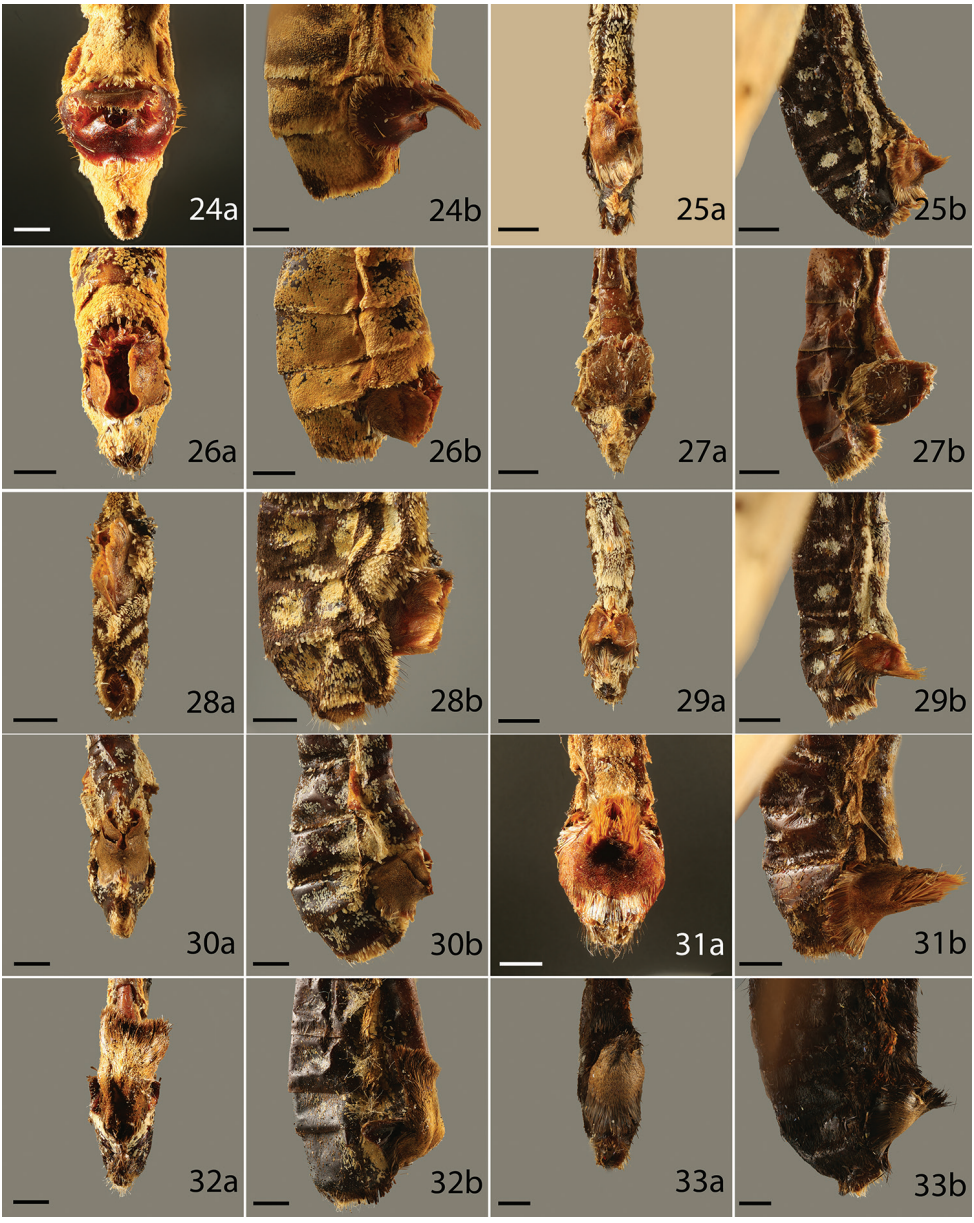

Figures 24–33. Sphragis of butterfly species, **a** ventral **b** lateral, category of the sphragis in parenthesis. **24** *Acraea umbra* (4) **25** *A. quirinalis* (3) **26** *A. pharsalus* (2) **27** *A. serena* (3) **28** *A. althoffi* (3) **29** *A. orestia* (3) **30** *A. pentapolis* (3) **31** *A. issoria* (3) **32** *A. rhodope* (3) **33** *A. ozomene* (3). Scale bar = 1 mm.

ognized by Bryk (1918) as a true sphragis, is regular in shape but is fixed to a bar over the female ostium (Table 1) (Bryk 1918). This structure is comparable in size with the sphragis of many *Acraea* species. The hemi-sphragis of *Trogonoptera* and the small sphragis of *P. proneus* both have an intermediate plug/spermatophore ratio, with ap-

proximately 40% of male secretions being allocated to the sphragis, but the remainder being allocated to the spermatophore and spermatophylax, a granular secretion filling the appendix bursae (Orr 1988, 1995). This intermediate condition is unusual. Species that produce an internal plug typically allocate less than 30% of male accessory gland secretion to the plug, versus 70% to the spermatophore (n=50 species; $\bar{x}$=14.8; s=9) (Orr 1988, 1995). However, sphragis-bearing species allocate between 72% and 99% of accessory secretions to the sphragis, versus less than 30 percent to the spermatophore (n=34 species; $\bar{x}$= 84.1; s=16), resulting in a bimodal frequency distribution of material allocated to sperm guarding (Orr 1988, 1995).

Although the sphragis appears to be an effective structure to prevent remating, there are examples where the female might be able to mate again (Pierre 1985a, Epstein 1987, Matsumoto 1987, Orr 1988, Sourakov and Emmel 1997). For example, a second mating might occur soon after the first mating, while the sphragis of the first male is still relatively soft and can be moved or removed by the second male, or if the first sphragis was unusually frail. Sourakov and Emmel (1997) reported a male of *A. epaea* (Cramer, 1779) on top of a female while she mated with another male, presumably so he too could mate with her. This however, might not guarantee success to the second male; Orr (1988) figured a female of *A. serena* bearing three sphragides congealed into a single mass that incorporated the spermatophores of the second and third males, and which could not possibly have fertilized the female due to the presence of the first sphragis blocking the copulatory opening. In general it is important to appreciate that the presence of a double sphragis, (termed a plethosphragis by Bryk (1924)), does not imply that the second male was able to inseminate that female because as long as the original sphragis remains intact, the spermatophore of the second male remains outside the body of the female. Allowing time for the sphragis to harden could be the reason for protracted mating in *C. cressida*, in which the pair remains coupled for 17 hours or more (Orr 1988).

There are cases known in *Parnassius* species where hardened sphragides have been lost by the female or were removed by subsequent males (Matsumoto and Suzuki 1995, Vlasanek and Konvicka 2009), which would potentially allow additional matings. Moreover, Orr (1988) experimentally induced males of *C. cressida* to mate with caged mated females, and they eventually dissolved the attached sphragis of the first male. However, he noted that the energy and time spent removing the sphragis (around 30 hours) makes this an unlikely occurrence in nature if the sphragis is well formed and would potentially result in the death of one or both butterflies. This process is probably only used as an aid to remove frail sphragides deposited by depleted males (Orr 1999b).

The satyrine nymphalid *H. penelope* is the only species of its genus, and subfamily, bearing a true sphragis (Figure 13) (Orr and Kitching 2010). It does not correspond with all morphological and behavioral adaptations found in other sphragis-bearing butterflies. The external female genitalia are virtually unmodified from the condition found in other species of the genus, whereas all other sphragis-bearing species exhibit profound modifications in this structure, especially exhibiting externalization of the ostium (Orr 2002). However, the highly modified male genitalia are efficient at plug

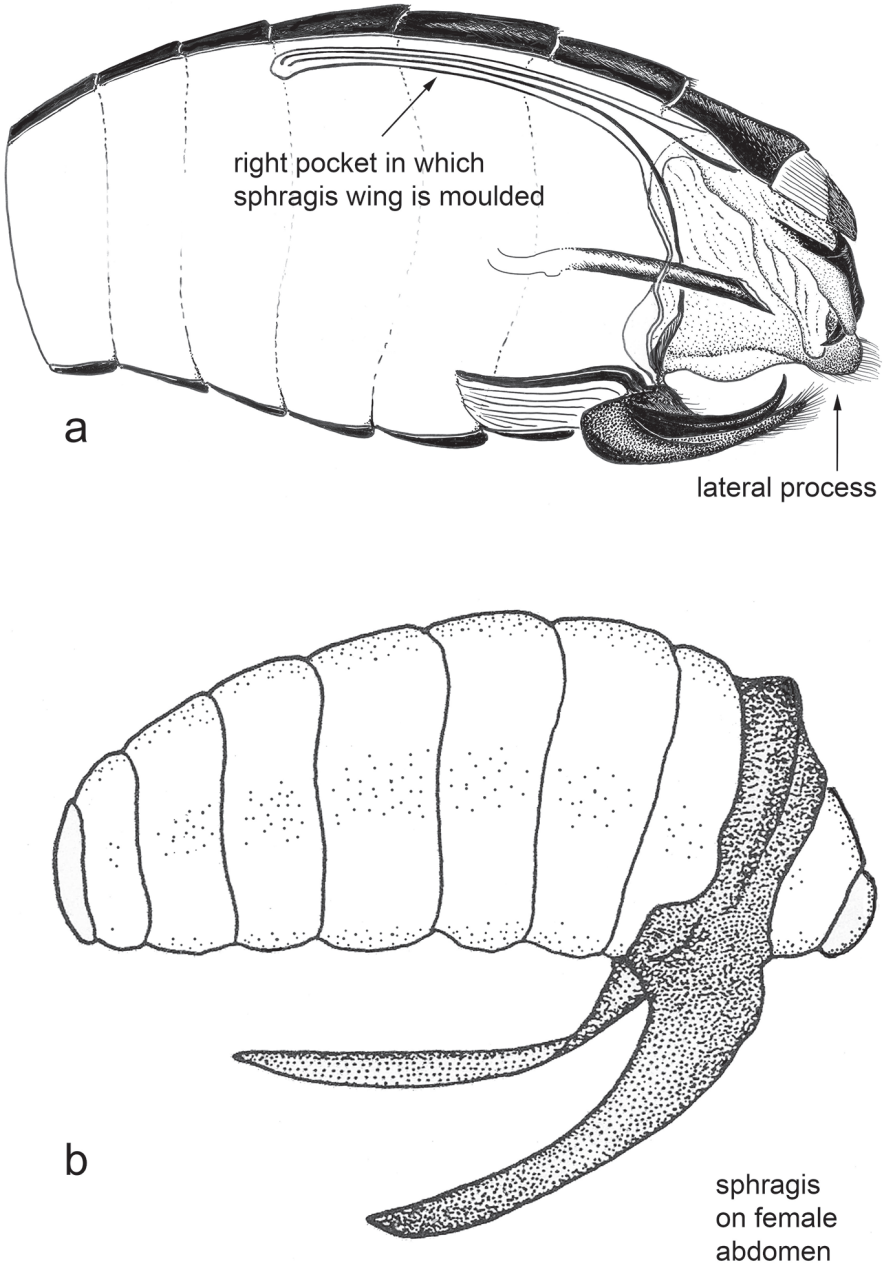

Figure 34. Example of male adaptations associated with sphragis production: **a** parasagittal section of *Euryades corethrus* male showing deep pockets where sphragis wings are molded and other features associated with sphragis production **b** The finished sphragis *in situ* on the female abdomen.

removal. Males bear androconial patches on the wings and exhibit courtship behavior (characteristics often found in polygynous species (Pliske 1975)), although they may facultatively practice aerial capture and forced copulation (Orr 2002).

Towards an understanding of sphragis evolution

The evolution of the sphragis was studied in detail by Orr (1988, 1995, 1999b, 2002) and Matsumoto (1987, Matsumoto and Suzuki 1995). Orr's studies utilized a comparative analysis of genital morphology, reproductive physiology, and behavior in a wide range of sphragis-bearing species. Non-sphragis bearing butterflies in Papilionidae, Pieridae and Nymphalidae were examined for outgroup comparison. Based on an analysis of convergent traits in unrelated lineages, Orr's hypothesis for sphragis evolution is as follows (Figure 35): (1) females of the ancestral, non-sphragis bearing butterfly species benefited from mating with more than one male, most likely due to enhanced material benefits, chiefly protein, gained from the spermatophore; (2) males produced small mating plugs to prevent female remating; (3) females evolved more externalized genitalia (Orr 1988, 1995) (Type 1 of Orr (1995)) that made small mating plugs attached to the spermatophore ineffective and easily removed by males, which simultaneously evolved better mechanisms for physically removing plugs; (4) externalizing the female genitalia made their genitalia more accessible, enabling males to copulate by force, a behavior almost universal in sphragis-bearing species, that increased the chance of female remating; (5) males also responded by producing larger and more complex plugs (sphragides) at the expense of spermatophore size, thereby (6) increasing the pressure on females to mate more than once as the nutritional contribution by males per mating diminished. This led to an escalated arms race where female genitalia became more and more externalized, making it more difficult to affix a sphragis, and more heavily armored to protect them from injury during mating attempts that involved the violent removal of a sphragis. Male genitalia became more specialized to produce sphragides that could not be removed, as they reduced their nutritional contribution via the spermatophore, at the same time increasing plug-removing abilities. The female bursa copulatrix became smaller accordingly, leading to the extreme case where it has completely atrophied in *C. cressida*. This is the 'male wins' scenario, which leads to obligate sphragis formation. Alternatively, males of some species were unable to produce an effective sphragis to counter female anti plugging strategies and so ceased to plug at all and mated as often as possible, a 'female wins' scenario. Orr (1988) suggested this is possibly occurring in certain danaines and also the hyper polyandrous *Acraea natalica*. Part of the reason for this runaway process and the instability of intermediate conditions may lie in the asymmetry of male and female adaptations (Orr 1988).

Furthermore, Orr (1995) suggested that the sphragis evolved independently at least two times in the Papilionidae and two times in Nymphalidae, but recent phylogenetic studies (Braby et al. 2005, Condamine et al. 2012, Simonsen et al. 2012) indicate that eight times across the two butterfly families may be a better minimum estimate for independent sphragis evolution at level 2 or higher (Figure 36). This is supported by

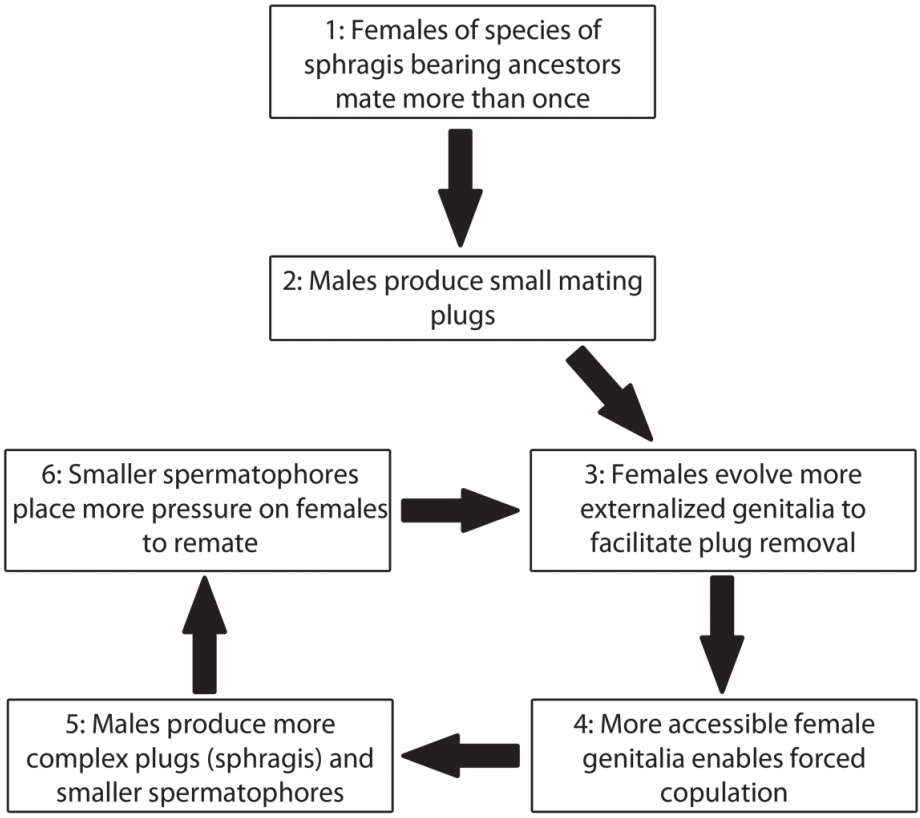

Figure 35. Schematic of the possible process of evolution of the sphragis in butterflies. This assumes a selective landscape where females benefit materially from polyandry and males are continually improving plug-removing ability.

qualitative differences in the sphragis between papilionids and some *Acraea* species, as well as highly specialized external female genitalia evolving non-homologous elements (Orr 1988, 1995) in the two families (Figure 37).

When we include Category 1 in our analysis, the sphragis appears to have arisen in at least six subfamilies in butterflies (Figure 36) and deeper analysis within subfamilies would potentially double this number. Within each of these groups, some species appear to have lost the sphragis completely. For instance, the *Parnassius simo* group is the only species group in *Parnassius* that lacks a sphragis. All species of *Zerynthia* (Papilionidae: Parnassiinae) appear to be in the process of losing the sphragis with vestiges found in some individuals (Matsumoto et al. in prep). Among the 287 described (Pierre and Bernaud 2014b) *Acraea* species, at least 183 have a sphragis or a sphragis-like structure although it is unclear whether the sphragis is plesiomorphic for the genus (Pierre 1985a). Within *Acraea*, the *A. encedon* species-group (subgenus *Actinote*) and *A. natalica* (subgenus *Acraea*), are two of several candidates that have apparently lost the sphragis. Phylogenetic analyses of sphragis-bearing taxa, and their close relatives lacking a sphragis, may reveal whether particular cases are plesiomorphic or derived.

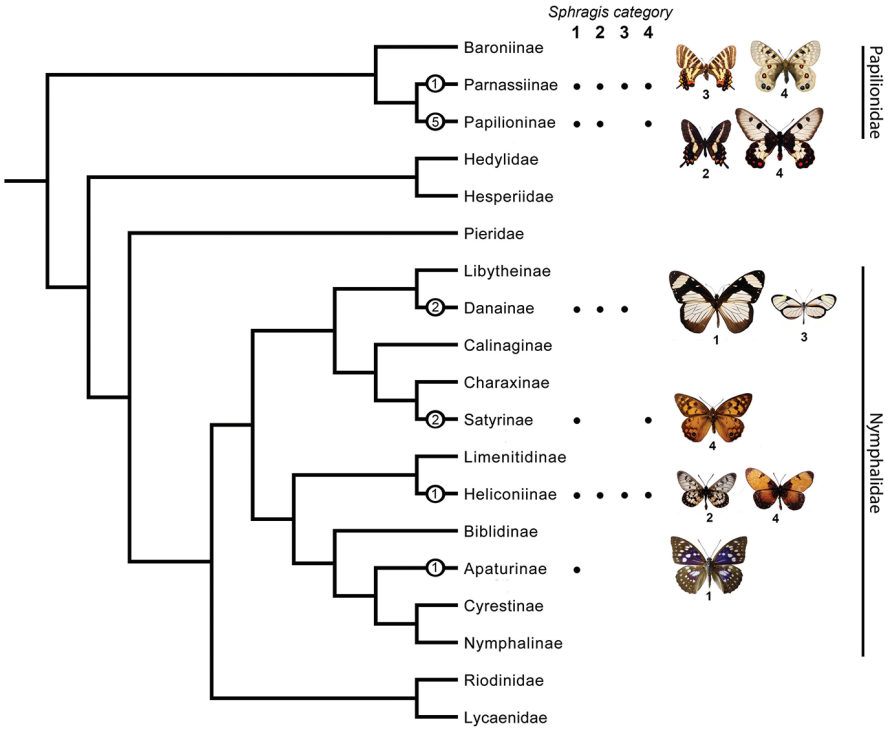

Figure 36. The occurrence of the sphragis in butterfly subfamilies. Dark circles indicate that some species in the clade bear sphragides or a version of it. Numbers inside the dark circles indicate estimation of minimum number of sphragis evolution events. Numbers under butterfly images indicate sphragis category of that species. Tree adapted from the phylogeny of Heikkila et al. (2011).

The two most complex forms of the sphragis (Categories 3 and 4) are found in five out of six subfamilies where the sphragis is found (Figure 36). It could be an indication of strong convergent evolution and positive selection force for the development of complex sphragis structure along butterflies.

In a final twist of the hypothesized evolutionary process, it is possible that in some circumstances the sphragis has become secondarily advantageous to females. Females of *L. japonica* usually mate only once, early in their life (Matsumoto 1987); the same occurs in *E. corethrus* (Nicolás Mega pers. com.) and *C. cressida* (Orr and Rutowski 1991, Orr 1999b). *Cressida* females derive no amino acid nutrients from the miniscule spermatophore (Orr 1988). In these cases, we can wonder if there is any aspect of female choice in these species and how the sphragis has helped this condition. Could females be "losing" in the arms race resulting from the intersexual conflict caused by the sphragis? Can it affect the genetic diversity of the species, considering that females cannot choose the most fit male? Bearing in mind that virgin females do escape copulation attempts (Orr 1999b), is there any feature of forced copulation that allows females to evaluate male sperm quality? These questions should be addressed to fully understand

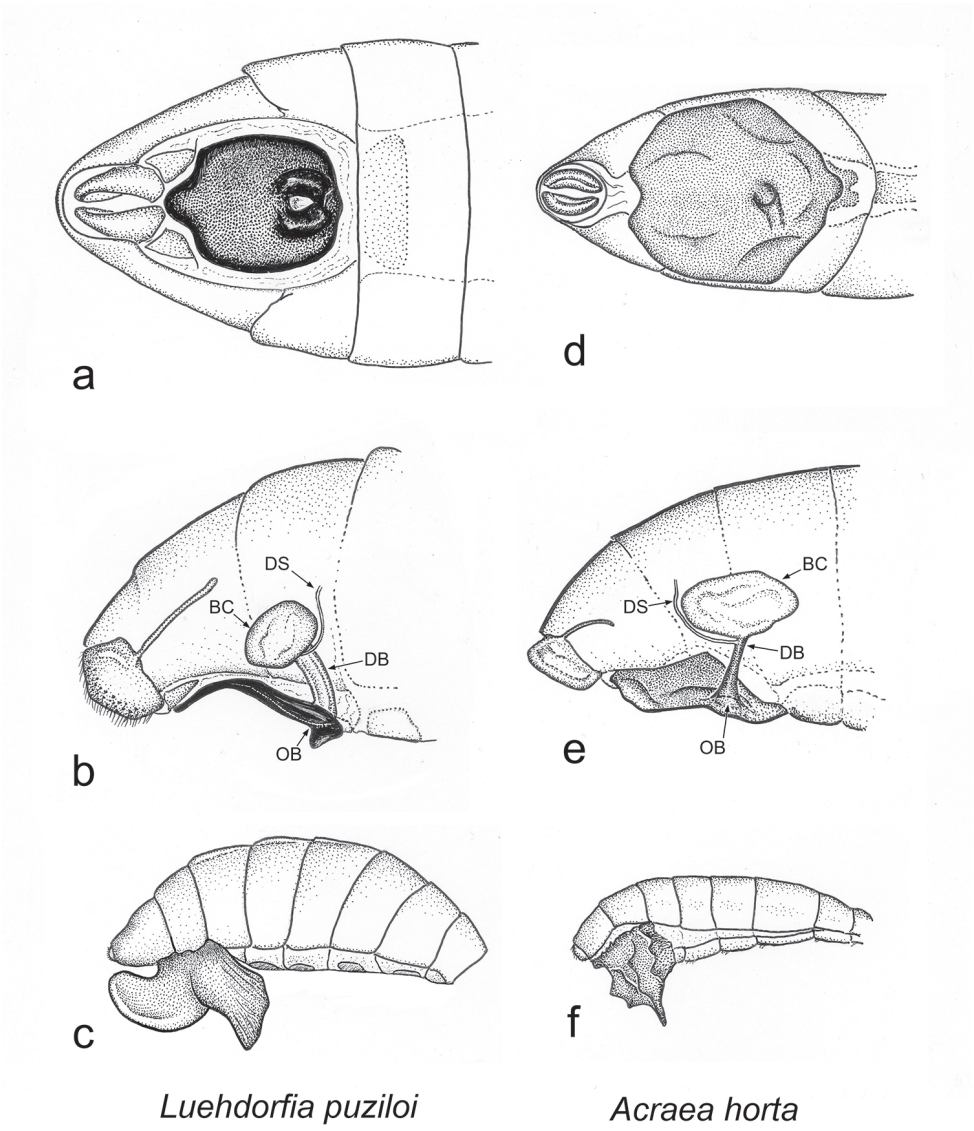

Figure 37. Ventral and parasagittal views of the female genitalia and lateral abdomen with sphragis for *Luehdorfia puziloi* (**a, b, c** respectively), and *Acraea horta* (**d, e, f** respectively), showing convergence in externalization of female genitalia, reduction in the size of the bursa copulatrix, and how the genitalia is covered by the sphragis. BC, bursa copulatrix, DB, ductus bursae; DS, ductus seminalis; OB, ostium bursa.

the effect of the sphragis on butterfly sexual dynamics. For some groups, the presence of the sphragis might be advantageous to females, especially if they receive enough sperm in one copulation and there is no transfer of nutritional substances from the male (Orr 1988). In the case where males visually detect mated females, the sphragis might

prevent a male's mating attempts, which are known to interfere with oviposition and can also cause physical damage to the female (Thornhill and Alcock 1983, Orr 1999b).

It is known that in Papilionidae extremely complex female genitalia occur widely, as well as the numerous externalized forms normally associated with bearing a sphragis (Miller 1987, Orr 1988). Complex female genitalia also occur to a lesser extent in Nymphalidae (Orr 1988), but not in the Hedylidae, Hesperiidae, Riodinidae, or Lycaenidae. Pieridae, as well as the papilionid genus *Battus* Scopoli, 1777, have pilose lobes flanking the ostium (Miller 1987, Orr 1988), which, at least in pierids, appear to be associated with the reception of antiaphrodisiacs from the male (Andersson et al. 2000, 2003, Schulz et al. 2008, Malouines 2016). These may largely obviate the need for mating plugs. A similar phenomenon occurs in *Heliconius* (Gilbert 1976). Data on the incidence of internal mating plugs and mating frequency in butterflies and moths are still too fragmentary for detailed analysis, but available evidence suggests that mating plugs are most common in groups with complex female genitalia. We expect that sphragis formation could only evolve in groups preadapted by having the capacity to produce a large internal mating plug. In general, the positive feedback process (Figure 35) leading to sphragis formation requires female genitalia to become externalized. However, complex genitalia present other possibilities. For example, it has been suggested that some female genital structures may help grip the mating plug (Orr 1988), allowing the male to make a large investment in a nutritious spermatophore, with confidence that a smaller plug would suffice to protect his paternity. If such processes are occurring, it is perhaps not surprising that the sphragis occurs relatively rarely, given that sexual conflict may be resolved in other ways. This is especially likely considering that the sphragis may come at a cost to the species in terms of reduced female fecundity and the disadvantages accruing from the encumbrance of the sphragis itself and attacks from rapacious males. It is possible however that by studying this phenomenon, we may better understand the intersexual dynamics of mating systems in butterflies generally.

Many questions still remain unanswered, especially regarding the processes involved in the evolution of the sphragis. Additionally, more studies are necessary to investigate how the presence of the sphragis may be related to factors such as ecology, especially habitat type and hostplant dispersion, reproductive behavior, and sperm dynamics, however, these topics go beyond the scope of the present study.

Conclusions

This is the first near complete survey of variation and morphological complexity of the sphragis in butterflies to date. This study provides the most comprehensive review on the sphragis, besides suggesting a method of categorization of the structure.

The main outcomes are as follows:

1. A true sphragis was found in 232 species of butterflies from the families Papilionidae and Nymphalidae.

2. The sphragis and related structures can be categorized into roughly four structural types: low complexity (amorphous and facultative), moderate complexity, medium complexity, and high complexity.

3. The sphragis and related structures is found in the Papilionidae subfamilies Parnassiinae and Papilioninae, as well as in the Nymphalidae subfamilies Danainae, Heliconiinae, Apaturinae, and Satyrinae.

4. Based on previously published evidence, the sphragis functions primarily to prevent remating by a secondary male.

Acknowledgments

We especially thank Kazuma Matsumoto (AIES) for his many contributions on Palearctic and Oriental butterflies, especially for sharing his unpublished data on sphragis-like structures in Apaturinae and *Losaria*, for providing literature and allowing access to an unpublished manuscript. Kazuma Matsumoto, along with Jim Miller (USNM), and Christoph L. Häuser (MFN) for important suggestions to improve the quality of this study. Jacques Pierre (MNHN) provided critical information on *Acraea* species. Luísa Mota (UNICAMP) and Keith Willmott (FLMNH) provided valuable information on Ithomiini, as did Nicolás Mega (UFRGS) on South American Troidini. We also thank Phillip Ackery (formerly BMNH), Jason Dombroskie (CUIC), Bryan Harris (USNM), James Liebherr (CUIC), Clas Naumann, Robert Robbins (USNM), Richard Vane Wright (formerly BMNH), Andrew Warren (MGCL), Christoph Häuser (MNHU), John Nielsen (DAWR) and Tommaso Racheli (SUR) for facilitating access to collections, providing loans and donations of vital material and supplying literature. Chris Johns (UF) helped us by supplying the camera equipment. Heinrich Fliedner assisted with philological issues and Richard Peigler (UIW) provided literature resources. Finally, we thank Ryan St Laurent (FLMNH) and Kelly Dexter (FLMNH) for providing preliminary feedback on the manuscript. Ryan St Laurent also helped creating the figures. The National Counsel of Technological and Scientific Development (CNPq/Brazil) funded APSC in this research (Process number: 200814/2015-0) and the Entomology and Nematology Department Student Organization (University of Florida) funded the APSC's trip to USNM. This project was also supported by NSFDEB grant number 1541500 to AYK.

References

Ackery PR (1975) A guide to the genera and species of Parnassiinae (Lepidoptera: Papilionidae). Bulletin of the British Museum 31: 71–105. https://doi.org/10.5962/bhl.part.29484

Arnqvist G, Nilsson T (2000) The evolution of polyandry: multiple mating and female fitness in insects. Animal Behaviour 60: 145–164. https://doi.org/10.1006/anbe.2000.1446

Beccaloni G, Scoble M, Kitching I, Simonsen T, Robinson G, Pitkin B, Hine A, Lyal C (2003) The Global Lepidoptera Names Index (LepIndex). World Wide Web electronic publication. Available from: http://www.nhm.ac.uk/our-science/data/lepindex/ [October 1, 2016]

Bingham CT (1907) The Fauna of British India, including Ceylon and Burma, Butterflies Vol. 2. Taylor and Francis, London, 480 pp. https://doi.org/10.1038/115115c0

Blanckenhorn WU, Hosken DJ, Martin OY, Reim C, Teuschl Y, Ward PI (2002) The costs of copulating in the dung fly *Sepsis cynipsea*. Behavioral Ecology 13: 353–358. https://doi.org/10.1093/beheco/13.3.359

Boggs CL, Gilbert LE (1979) Male Contribution to Egg Production in Butterflies: Evidence for Transfer of Nutrients at Mating. Science 206: 83–84. https://doi.org/10.1126/science.206.4414.83

Boggs CL, Watt WB (1981) Population structure of pierid butterflies IV. Genetic and physiological investment in offspring by male *Colias*. Oecologia 50: 320–324. https://doi.org/10.1007/BF00344970

Bollino M, Racheli T (2012) Butterflies of the World, Supplement 20. Parnassiinae (Partim) Parnassiini (Partim); Luehdorfiini; Zerynthiini (Lepidoptera: Papilionidae). Goecke & Evers, Keltern, 64 pp.

Braby MF, Trueman JWH, Eastwood R (2005) When and where did troidine butterflies (Lepidoptera: Papilionidae) evolve? Phylogenetic and biogeographic evidence suggests an origin in remnant Gondwana in the Late Cretaceous. Invertebrate Systematics 19: 113–143. https://doi.org/10.1071/IS04020

Bryk F (1918) Grundzüge der Sphragidologie. Arkiv för Zoologi 11: 1–38.

Bryk F (1919) Bibliotheca sphragidologica. Archiv für Naturgeschichte 85: 102–183.

Bryk F (1924) Über die Disphragophorie der Schmetterlingsweibchen. Societas Entomologica 12: 45–47.

Bryk F (1930) Monogame Einrichtungen bei Schmetterlingsweibchen. Archiv für Frauenkunde und Konstitutionsforschung 16: 308–313.

Bryk F (1935a) Parnassiidae Pars II. [Parnassiidae Part II]. In: Schulze F, Kükenthal W, Heider K, Hesse R, Abstein C (Eds), Das Tierreich 65. W. de. Gruyter, Berlin, 790 pp.

Bryk F (1935b) Sericinus sphragidophor! Parnassiana 3: 75.

Bryk F (1950) Geographische und individuelle Variabilität der Sphragisbildung (Lepidoptera: Parnassiidae). Entomologisk tidskrift 71: 230–234.

Callahan PS, Cascio T (1963) Histology of the Reproductive Tracts and Transmission of Sperm in the Corn Earworni, *Heliothis zea*. Annals of the Entomological Society of America 56: 535–556. https://doi.org/10.1093/aesa/56.4.535

Chapman RF (1969) The Insects: structure and function. Cambridge University Press, Cambridge, 959 pp.

Chapman T, Patridge L (1996) Sexual conflict as fuel for evolution. Nature 381: 189–190. https://doi.org/10.1038/381189a0

Churkin S (2006) A new species of *Parnassius* Latreille, 1804 from Kyrgyzstan (Lepidoptera, Papilionidae). Helios 7: 142–158.

Common IFB, Waterhouse DF (1981) Butterflies of Australia. Angus and Robertson, Melbourne, xiv, 682 49 of plates pp.

Condamine FL, Silva-Brandão KL, Kergoat GJ, Sperling FAH (2012) Biogeographic and diversification patterns of Neotropical Troidini butterflies (Papilionidae) support a museum model of diversity dynamics for Amazonia. BMC Evolutionary Biology 12. https://doi.org/10.1186/1471-2148-12-82

D'Abrera B (1984) Butterflies of the Neotropical Region: Pt. 2: Danaidae, Ithomiidae, Heliconidae & Morphidae. Hill House Publishers, Malvern, 384 pp.

D'Abrera B (1990) Butterflies of the Holarctic Region: Papilionidae, Pieridae, Danaidae & Satyridae (Partim) Pt. 1. Hill House Publishers, Melbourne, 185 pp.

D'Abrera B (1995) Butterflies of the Neotropical Region: Brassolidae, Acraeidae, Nymphalidae (Partim) Pt. 3. Hill House Publishers, Melbourne, 147 pp.

D'Abrera B (1997) Butterflies of the Afrotropical Region: Papilionidae, Pieridae, Acraeidae, Satyridae Pt. 1. Hill House Publishers, Melbourne, 613 pp.

Drummond BA (1984) Multiple mating and sperm competition in the Lepidoptera. In: Smith RL (Ed.) Sperm competition and the evolution of animal mating systems. Academic Press, London, 291–370. https://doi.org/10.1016/B978-0-12-652570-0.50016-6

Eaton JL (1988) Lepidopteran Anatomy. Wiley-Interscience, Hoboken, 257 pp.

Ehrlich AH, Ehrlich PR (1978) Reproductive Strategies in the Butterflies: I. Mating Frequency, Plugging, and Egg Number. Journal of the Kansas Entomological Society 51: 666–697.

Ehrlich PR (1961) Comparative morphology of the male reproductive system of the butterflies (Lepidoptera: Papilionoidea). 1. Some nearctic species. Microentomology 24: 135–166.

Eltringham H (1912) A Monograph of the African species of the Genus *Acraea*, Fab., with a supplement on those of the Oriental Region. Transactions of the Royal Entomological Society of London 60: 1–369. https://doi.org/10.1111/j.1365-2311.1912.tb02511.x

Eltringham H (1925) III. On the Source of the Sphragidal Fluid in *Parnassius apollo* (Lepidoptera). Transactions of the Royal Entomological Society of London 73: 11–15. https://doi.org/10.1111/j.1365-2311.1925.tb02859.x

Epstein ME (1987) Mating behavior of *Acraea andromacha* (Fabricius) (Nymphalidae) in New Caledonia. Journal of the Lep 41: 119–121.

Ferro DN, Akre RD (1975) Reproductive Morphology and Mechanics of Mating of the Codling Moth, *Laspeyresia pomonella*. Annals of the Entomological Society of America 68: 417–424. https://doi.org/10.1093/aesa/68.3.417

Francini RB, Freitas AVL, Penz CM (2004) Two new species of *Actinote* (Lepidoptera, Nymphalidae) from Southeastern Brazil. Zootaxa 719: 1–10.

Gilbert LE (1976) Postmating Female Odor in *Heliconius* Butterflies: A Male-Contributed Antiaphrodisiac? Science 193: 419–420. https://doi.org/10.1126/science.935877

Gillies MT (1956) A new character for the recognition of nulliparous females of *Anopheles gambiae*. Bulletin of the World Health Organization 15: 451–459.

Guenée MA (1872) Notice sur Divers Lépidoptères du Misée de Genève. Memoires de la Société de physique et d'histoire naturelle de Genève 21: 369–424.

Gwynne DT (1984) Male Mating Effort, Confidence of Paternity, and Insect Sperm Competition. In: Smith RL (Ed.) Sperm competition and the evolution of animal mating systems. Academic Press, London, 177–149. https://doi.org/10.1016/B978-0-12-652570-0.50011-7

Harada M, Wangdi K, Wangdi S, Yago M, Aoki T, Igarashi Y, Yamaguchi S, Watanabe Y, Sherub, Wangdi R, Drukpa S, Saito M, Moriyama Y, Uchiyama T (2012) Rediscovery of Ludlow's Bhutan Glory, *Bhutanitis ludlowi* Gabriel (Lepidoptera: Papilionidae): morphology and biology. Butterflies 10: 4–15.

Haude G (1913) Betrachtungen über den Zweck der Legetasche bei den Parnassierweibchen. Societas entomologica 28: 93–94.

Haüser CL, Jong R de, Lamas G, Robbins RK, Smith C, Vane-Wright RI (2005) Papilionidae – revised GloBIS/GART species checklist (2nd draft). Available from: http://www.insects-online.de/frames/papilio.htm [October 1, 2016]

Heppner JB (1991) Faunal Regions and the Diversity of Lepidoptera. Tropical Lepidoptera 2, supplem: 1–85.

Hinton, HE (1964) Sperm transfer in insects and the evolution of haemocoelic insemination. In: Highnam KC (ed.) Insect Reproduction. Symposium of the Royal Entomological Society of London, 95–107.

Hirt K, Ruch J, Schneider JM (2017) Strategic male mating behaviour in *Argiope lobata*. Animal Behaviour 124: 27–34. https://doi.org/10.1016/j.anbehav.2016.11.030

Hosken DJ, Stockley P, Tregenza T, Wedell N (2009) Monogamy and the battle of the sexes. Annual Review of Entomology 54: 361–378. https://doi.org/10.1146/annurev.ento.54.110807.090608

Houlbert C (1916) Contribution à l'étude das armatures génitales de deus Espèced malgaches appartenant au Genre *Acraea* (Lép. Nymphalidae). Lépidoptérologie Comparée: 135–172. Available from: http://www.biodiversitylibrary.org/item/41276.

Klowden MJ (2013) Physiological Systems in Insects. Elsevier Science, Amsterdam, 697 pp.

Knowlton N, Greenwell SR (1984) Male Sperm Competition Avoidance Mechanisms: The Influence of Female Interests. In: Smith RL (Ed.) Sperm competition and the evolution of animal mating systems. Academic Press, London, 61–84. https://doi.org/10.1016/B978-0-12-652570-0.50009-9

Labine PA (1964) Population biology of the butterfly, *Euphydryas editha*. I. Barriers to Multiple Inseminations. Evolution 18: 335–336. https://doi.org/10.2307/2406408

Labine PA (1966) The Population Biology of the butterfly, *Euphydryas editha*. IV. Sperm precedence - A preliminary report. Evolution 20: 580–586. https://doi.org/10.1111/j.1558-5646.1966.tb03388.x

Lamas G (2004) Checklist: Part 4A. Hesperioidea – Papilionoidea. In: Heppner JB (Ed.) Atlas of Neotropical Lepidoptera. Association for Tropical Lepidoptera, Gainesville.

Larsen TB (1991) The Butterflies of Kenya and Their Natural History. Oxford University Press, Oxford, 640 pp.

Larsen TB (2005) The Butterflies of West Africa. Apollo Books, New York, 865 pp.

Linnaeus C (1746) Fauna svecica, sistens animalia Sveciae regni. Laurentius Salvius, Stockholm, 411 pp.

Marshall GAK (1901) On the female pouch in *Acraea*. The Entomologist 34: 73–75.

Marshall GAK (1902) Five Years' Observations and Experiments (1896–1901) on the Bionomics of South African Insects, chiefly directed to the Investigation of Mimicry and Warning Colours. Transactions of the Entomological Society of London 50: 287–584.

Matsumoto K (1987) Mating patterns of a sphragis-bearing butterfly, *Luehdorfia japonica* Leech (Lepidoptera: Papilionidae), with descriptions of mating behavior. Researches on Population Ecology 29: 97–110. https://doi.org/10.1007/BF02515428

Matsumoto K, Suzuki N (1995) The nature of Mating Plugs and the probability of reinseminarion in Japanese Papilionidae. In: Scriber JM, Tsubaki Y, Lederhouse R (Eds) Swallowtail butterflies: their ecology and evolutionary biology. Scientific Publishers, Gainesville, 145–154.

Michel F, Rebourg C, Cosson E, Descimon H (2008) Molecular phylogeny of Parnassiinae butterflies (Lepidoptera: Papilionidae) based on the sequences of four mitochondrial DNA segments. Annales de la Société entomologique de France (N.S.) 44: 1–36. https://doi.org/10.1080/00379271.2008.10697541

Miller JS (1987) Phylogenetic Studies in the Papilioninae (Lepidoptera: Papilionidae). Bulletin of the American Museum of Natural History 186: 365–512.

Neild AFE (2008) The Butterflies of Venezuela, Part 2: Nymphalidae II (Acraeinae, Libytheinae, Nymphalinae, Ithomiinae, Morphinae). Meridian Publications, London, 275 pp.

Neild AFE, Romero M (2008) Actinote Hübner [1819]. Species account. In: Neild AFE (Ed.) The Butterflies of Venezuela. Part 2: Nymphalidae II (Acraeinae, Libytheinae, Nymphalinae, Ithomiinae, Morphinae). A comprehensive guide to the identification of adult Nymphalidae, Papilionidae, and Pieridae. Meridian Publications, London, 25–46.

Omoto K, Yonezawa T, Shinkawa T (2009) Molecular systematics and evolution of the recently discovered "Parnassian" butterfly (*Parnassius davydovi* Churkin, 2006) and its allied species (Lepidoptera, Papilionidae). Gene 441: 80–88. https://doi.org/10.1016/j.gene.2008.10.030

Orr AG (1988) Mate Conflict and the Evolution of the Sphragis in Butterflies. Griffith University.

Orr AG (1995) The evolution of the sphragis in the Papilionidae and other butterflies. In: Swallowtail butterflies, the ecology and evolutionary biology. Scientific Publisher Inc., Gainesville, 155–164.

Orr AG (1999a) Possible postcopulatory mate guarding in *Ornithoptera eupharion* (Gray) (Lepidoptera: Papilionidae). Australian Entomologist 26: 71–76.

Orr AG (1999b) The Big Greasy, *Cressida cressida* (Papilionidae). In: Kitching RL, Scheermeyer E, Jones RE, Pierce NE (Eds) Biology of Australian Butterflies. Monographs on Australian Lepidoptera 6. CSIRO Publishing, Melbourne, 115–134.

Orr AG (2002) The sphragis of *Heteronympha penelope* Waterhouse (Lepidoptera: Satyridae): its structure, formation and role in sperm guarding. Journal of Natural History 36: 185–196. https://doi.org/10.1080/00222930010022926

Orr AG, Kitching RL (2010) The Butterflies of Australia. Allen & Unwin, Crows Nest, 328 pp.

Orr AG, Rutowski RL (1991) The function of the sphragis in *Cressida cressida* (Fab.) (Lepidoptera: Papilionidae): a visual deterrent to copulation attempts. Journal of Natural History 25: 703–710. https://doi.org/10.1080/00222939100770461

Paluch M, Casagrande MM, Mielke OHH (2003) Tampão genital de *Actinote* Hübner, como caráter taxonômico (Lepidoptera, Nymphalidae, Acraeinae). Revista Brasileira de Entomologia 47: 573–580. https://doi.org/10.1590/S0085-56262003000400007

Paluch M, Casagrande MM, Mielke OHH (2006) Três espécies e duas subespécies novas de *Actinote* Hübner (Nymphalidae, Heliconiinae, Acraeini). Revista Brasileira de Zoologia 23: 764–778. https://doi.org/10.1590/S0101-81752006000300022

Parker GA (1970) Sperm Competition and its evolutionary consequences in the Insects. Biological Reviews 45: 525–567. https://doi.org/10.1111/j.1469-185X.1970.tb01176.x

Parker GA (1984) Sperm Competition and the Evolution of Animal Mating Strategies. In: Smith RL (Ed), Sperm Competition and the Evolution of Animal Mating Systems. Academic Press, London, 1–60. https://doi.org/10.1016/B978-0-12-652570-0.50008-7

Parsons MJ (1983) Notes on the Courtship of *Troides oblongmaculatus* papuensis (Papilionidae) in Papua New Guinea. Journal of the Lepidopterists' Society 37: 83–85.

Penz CM, Francini RB (1996) New species of *Actinote* Hübner (Nymphalidae: Acraeinae) from southeastern Brazil. Journal of the Lepidopterists' Society 50: 309–320.

Pierre J (1985a) Le sphragis chez les Acraeinae (Lepidoptera: Nymphalidae). Annales de la Société Entomologique de France 21: 393–398.

Pierre J (1985b) Systématique évolutive et spéciation chez les Lépidoptères du genre *Acraea* (Nymphalidae). I - Introduction et complexes ultraspécifiques. Annales de la Société entomologique de France 21: 5–27. Available from: http://gallica.bnf.fr/ark:/12148/bpt6k6129393g/f14.

Pierre J (1988) Les *Acraea* du Super-groupe «Egina» Révision et Phylogénie (Lepidoptera: Nymphalidae). Annales de la Société Entomologique de France 24: 263–287.

Pierre J (1992a) Systématique évolutive et cladistique: approche morphologique, spéciation et génation, application chez les *Acraea* (Lepidoptera, Nymphalidae). Bulletin de la Societé entomologique de France 97: 105–118.

Pierre J (1992b) Une nouvelle espèce d'Acraea (Lepidoptera Nymphalidae). Lambillionea 92: 308–310.

Pierre J, Bernaud D (2009) Butterflies of the World 31: Nymphalidae 16: *Acraea*, subgenus *Actinote*. Goecke & Evers, Keltern, 5 pp.

Pierre J, Bernaud D (2013) Butterflies of the World 39: *Acraea*, subgenus *Acraea*. Goecke & Evers, Keltern, 8 pp.

Pierre J, Bernaud D (2014a) Butterflies of the World, Supplément 24, Le genre *Acraea* Fabricius, 1807: Liste systématique, synonymique et liste des noms infrasubspécifiques. Erich Bauer & Thomas Frankenbach, Goecke & Evers, Keltern, 30 pp.

Pierre J, Bernaud D (2014b) Le genre *Acraea* Fabricius, 1807: Liste systématique, synonymique et liste des noms infrasubspécifiques. In: Bauer E, Frankenbach T (Eds) Butterflies of the World, Supplement 24. Goecke & Evers, Keltern, 1–30.

Pliske TE (1975) Courtship Behavior of the Monarch Butterfly, *Danaus plexippus* L. Annals of the Entomological Society of America 68: 143–151. https://doi.org/10.1093/aesa/68.1.143

van der Poorten GM, van der Poorten NE (2016) The Butterfly Fauna of Sri Lanka. Lepodon Books, Toronto, 418 pp.

Rawlins JE (1992) Life History and Systematics of the West Andean Moth *Aucula franclemonti* with Description of a New Species from Ecuador (Lepidoptera: Noctuidae: Agaristinae). Journal of the New York Entomological Society 100: 286–310.

Riley ND (1939) A new species of the genus *Armandia* (Lep. Papilionidae). Entomologist 72: 207–208.

Saigusa T (1973) A phylogeny of the genus *Luehdorfia*. Konchû-to-Shizen 8: 5–18.

Saigusa T, Lee C (1982) A rare papilionid butterfly *Bhutanitis mansfieldi* (Riley): Its rediscovery new subspecies and phylogenetic position. Tyo to Ga 33: 1–24.

Scoble MJ (1992) The Lepidoptera: Form, Function and Diversity. Oxford University Press, Oxford, 420 pp.

Scott JA (1972) Mating of butterflies. Journal of Research on the Lepidoptera 11: 99–127.

Shuker DM, Simmons LW (2014) The evolution of insect mating systems. Oxford University Press, Oxford. https://doi.org/10.1086/681480

Silberglied RE, Shepherd JG, Dickinson J Lou (1984) Eunuchs: The Role of Apyrene Sperm in Lepidoptera? The American Naturalist 123: 255–265. https://doi.org/10.1086/284200

Simmons LW (2001) Sperm Competition and Its Evolutionary Consequences in the Insects. Princeton University Press, Princeton, 456 pp.

Simonsen TJ, de Jong R, Heikkilä M, Kaila L (2012) Butterfly morphology in a molecular age - Does it still matter in butterfly systematics? Arthropod Structure and Development 41: 307–322. https://doi.org/10.1016/j.asd.2012.04.006

Solensky MJ, Oberhauser KS (2009) Sperm precedence in monarch butterflies (*Danaus plexippus*). Behavioral Ecology 20: 328–334. https://doi.org/10.1093/beheco/arp003

van Son G (1963) The butterflies of Southern Africa: Part III Nymphalidae: Acraeinae. In: Transvaal Museum Memoir. Pretoria, 130 pp. [XXIX Plates.]

Sonnenschein M, Hauser CL (1990) Presence of only eupyrene spermatozoa in adult males of the genus *Micropterix* Hübner and its phylogenetic significance (Lepidoptera: Zeugloptera, Micropterigidae). International Journal of Insect Morphology and Embryology 19: 269–276. https://doi.org/10.1016/0020-7322(90)90012-E

Sourakov A, Emmel TC (1997) Mating habits in the genus *Acraea*, with a possible explanation for monosexual populations (Lepidoptera: Nymphalidae: Acraeinae). Tropical Lepidoptera 8: 33–35.

Takakura T (1967) Taiyo-no-ko usubashiro-cho no seikatsu (Life of the child the sun Parnassius glacialis). In: Iwase T (Ed.) Nihon-Konchuki . II. Cho no seikatsu. Kodansha, Tokyo, 75–106.

Thornhill R, Alcock J (1983) The Evolution of Insect Mating Systems. Harvard University Press, Cambridge, 547 pp. https://doi.org/10.4159/harvard.9780674433960

Timmermeyer N, Gerlach T, Guempel C, Knoche J, Pfann JF, Schliessmann D, Michiels NK (2010) The function of copulatory plugs in *Caenorhabditis remanei*: hints for female benefits. Frontiers in zoology 7. https://doi.org/10.1186/1742-9994-7-28

Tykac J (1951) Sphragis či sphragidoid u motýlů. Sphragis ou sphragidoid chez les Lépidoptères. Acta Societatis Entomologicae Cechosloveniae 48: 94–98.

Tyler HA, Brown Jr KS, Wilson KH (1994) Swallowtail Butterflies of the Americas, a study in biological dynamics, ecological diversity, biosystematics and conservation. Scientific Publishers, Gainesville, 375 pp.

Uhl G, Nessler SH, Schneider JM (2010) Securing paternity in spiders? A review on occurrence and effects of mating plugs and male genital mutilation. Genetica 138: 75–104. https://doi.org/10.1007/s10709-009-9388-5

Vlasanek P, Konvicka M (2009) Sphragis in *Parnassius mnemosyne* (Lepidoptera: Papilionidae): male-derived insemination plugs loose efficiency with progress of female flight. Biologia 64: 1206–1211. https://doi.org/10.2478/s11756-009-0207-3

Walker WF (1980) Sperm utilization strategies in nonsocial insects. The American Naturalist 115: 780–799. https://doi.org/10.1086/283600

Waterhouse GA, Lyell G (1914) The butterflies of Australia. A monograph of the Australian Rhophalocera. Angus and Robertson, Sydney, 239 pp.

Wedell N (2005) Female receptivity in butterflies and moths. Journal of Experimental Biology 208: 3433–3440. https://doi.org/10.1242/jeb.01774

Supplementary material 1

Table S1. Sphragis-bearing butterfly species and morphological characteristics of their sphragides

Authors: Ana Paula S. Carvalho, Albert G. Orr, Akito Y. Kawahara

Data type: Microsoft Excel document

Explanation note: G: girdle, VS: vestigial sphragis, PS: protosphragis, HS: hemi-sphragis, *: species is figured in the plates.

Link: https://doi.org/10.3897/zookeys.694.13097.suppl1

ZooKeys 694: 71–93 (2017)
doi: 10.3897/zookeys.694.12785
http://zookeys.pensoft.net

RESEARCH ARTICLE

A peer-reviewed open-access journal
ZooKeys
Launched to accelerate biodiversity research

A new species of the genus *Kurixalus* from Yunnan, China (Anura, Rhacophoridae)

Guohua Yu[1,*], Jishan Wang[1,2,3,*], Mian Hou[4], Dingqi Rao[1], Junxing Yang[1]

1 *Kunming Institute of Zoology, Chinese Academy of Sciences, 32 Jiaochang Donglu, Kunming, Yunnan 650223, China* **2** *Kunming College of Life Science, University of Chinese Academy of Sciences, Kunming, Yunnan 650204, China* **3** *Kunming Institute of survey & design, State Forestry Administration, Kunming, Yunnan 650216, China* **4** *Institute of Continuing Education, Sichuan Normal University, Chengdu, Sichuan 610068, China*

Corresponding author: *Junxing Yang* (yangjx@mail.kiz.ac.cn); *Guohua Yu* (yugh03@mail.kiz.ac.cn)

Academic editor: *A. Herrel* | Received 18 March 2017 | Accepted 2 July 2017 | Published 29 August 2017

http://zoobank.org/C3DD7C0F-E692-42D7-B29A-0E406F08BE08

Citation: Yu G, Wang J, Hou M, Rao D, Yang J (2017) A new species of the genus *Kurixalus* from Yunnan, China (Anura, Rhacophoridae). ZooKeys 694: 71–93. https://doi.org/10.3897/zookeys.694.12785

Abstract

A new species of the genus *Kurixalus* (Anura: Rhacophoridae) is described from Yunnan, China based on morphological and molecular evidence. The new species, *Kurixalus lenquanensis* **sp. n.**, is distinguished from other congeneric species by a combination of (1) smaller body size (SVL in males ranges from 25.0 to 28.9 mm), (2) obtusely pointed snout with no prominence on tip, (3) rough and brown dorsum with darker mark, (4) absence of large dark spots on ventral surface, (5) brownish clouded chin, (6) granular throat, chest, and belly, (7) presence of vomerine teeth, (8) serrated dermal fringes along outer edge of limbs, (9) slight nuptial pad, (10) golden brown iris, and (11) single internal vocal sac. The new species is known only from montane scrub vegetation at the type locality (Lenquan Village, Mengzi City, Yunnan Province) and Yangjiatian Village, Gejiu City, Yunnan Province. Genetically, the new species is nested within a clade of Taiwanese *Kurixalus* and recovered as the sister taxon to *Kurixalus idiootocus* with strong support values, indicating that the ancestor of this new species might have come from Taiwan Island or the ancestor of this new species may have been widespread in southern China and the descendent species in between Taiwan and Yunnan has become extinct.

Keywords

China, *Kurixalus lenquanensis* sp. n., Yunnan

* These authors contributed equally to this work.

Introduction

The genus *Kurixalus* Ye, Fei, & Dubois in Fei 1999 has a wide distribution including eastern India, Indochina, Sunda islands, Philippine archipelago, montane southern China, and adjacent continental islands (Hainan, Taiwan, and Ryukyu Islands); currently 14 species are recognized in this genus (Frost 2017). Owing to its morphological conservativeness, the taxonomy and systematics of this genus was once very confusing. Inger et al. (1999) considered that Chinese and Vietnamese *Kurixalus odontotarsus* (Ye & Fei in Ye et al. 1993) probably belong to *Kurixalus verrucosus* (Boulenger, 1893) or *Kurixalus bisacculus* (Taylor, 1962), Orlov et al. (2002) also considered Vietnamese *K. odontotarsus* as *K. verrucosus*, and *Kurixalus hainanus* (Zhao, Wang, & Shi in Zhao et al. 2005) was thought to be a synonym of *K. odontotarsus* by some authors (e.g. Fei 1999, Fei et al. 2010). However, based on evidence from molecular data, Yu et al. (2010) proposed that *K. odontotarsus*, *K. bisacculus*, and *K. verrucosus* should be treated as three independent species and suggested placing *K. odontotarsus* from Tibet and *K. hainanus* in *K. verrucosus* and *K. bisacculus*, respectively. Moreover, Yu et al. (2010) considered that the distributional range of *K. bisacculus* should be expanded to include most regions of South China. Thus, currently three species of *Kurixalus* (*K. odontotarsus*, *K. bisacculus*, and *K. verrucosus*) are recognized in mainland China and two of them (*K. odontotarsus* and *K. bisacculus*) exist in Yunnan according to Yu et al. (2010).

During recent fieldwork in Yunnan, China (Fig. 1), a small tree frog was discovered that is morphologically similar in appearance with other *Kurixalus* species from Yunnan. It appears to be closely related to *Kurixalus idiootocus* (Kuramoto & Wang, 1987) from Taiwan based on molecular phylogenetic analyses, but it is different from *K. idiootocus* based on the following characters: obtusely pointed snout with no prominence on tip, single internal vocal sac, loreal region oblique, absence of a pair of symmetrical large dark patches on chest, and absence of supernumerary plantar tubercles.

Materials and methods

Sampling. Specimens were collected during fieldwork in Honghe Autonomous Prefecture, Yunnan, China in 2015 and 2016. They were euthanized with diethyl ether anesthesia and fixed by 90% ethanol before being stored in 70% ethanol. Liver tissues were preserved in 99% ethanol. Specimens and tissue samples were deposited at Kunming Institute of Zoology, Chinese Academy of Sciences (KIZ 170175Y–170186Y) and Kunming Institute of Survey & Design, State Forestry Administration (KISD 1506203–1506204).

Morphology. The preserved specimens were examined, measured, and compared with available specimens and published descriptions of currently recognized species of *Kurixalus* from China and neighboring countries (Günther 1858, Boulenger 1893, Annandale 1912, Kuramoto and Wang 1987, Inger et al. 1999, Bossuyt and Dubois 2001, Matsui and Orlov 2004, Mathew and Sen 2008, Nguyen et al. 2014a, Nguyen et al. 2014b, Wu et al. 2016). Measurements were taken using digital calipers to the near-

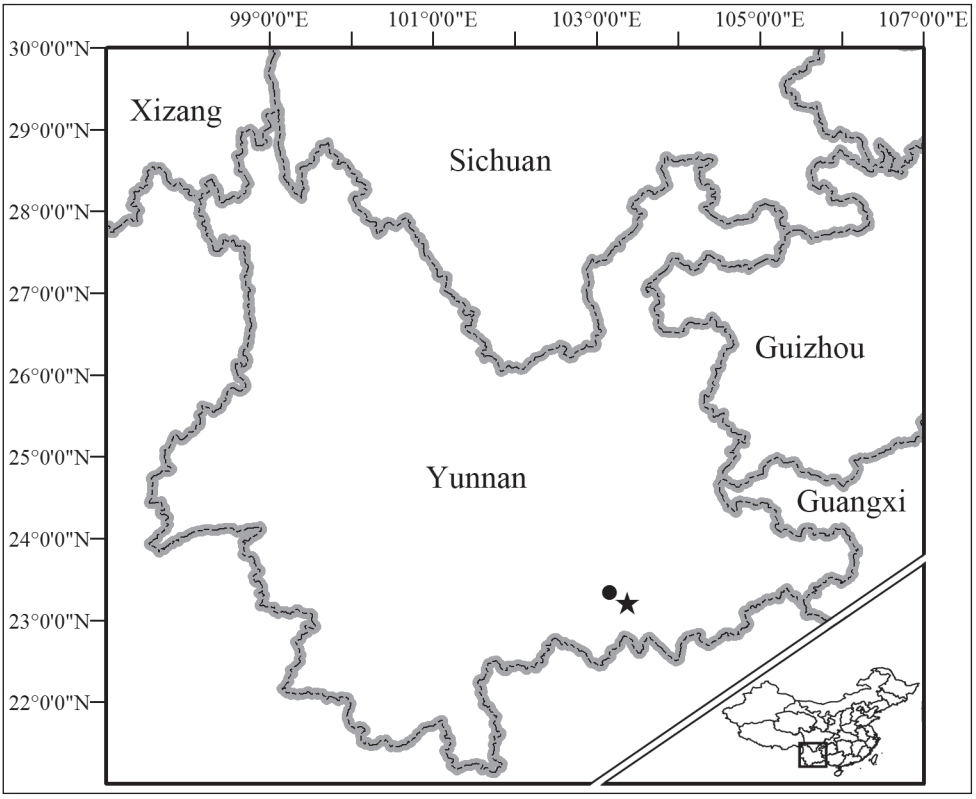

Figure 1. Known distribution of *Kurixalus lenquanensis* sp. n. Filled star indicates the type locality and filled circle indicates Yangjiatian Village.

est 0.1 mm. Morphological terminology follows Fei (1999). Measurements include: snout-vent length (**SVL**, from tip of snout to vent); head length (**HL**, from tip of snout to rear of jaws); head width (**HW**, width of head at its widest point); snout length (**SL**, from tip of snout to anterior border of eye); internarial distance (**IND**, distance between nares); interorbital distance (**IOD**, minimum distance between upper eyelids); upper eyelid width (**UEW**, maximum width of upper eyelid); eye diameter (**ED**, diameter of exposed portion of eyeball); tympanum diameter (**TD**, the greater of tympanum vertical and horizontal diameters); distance from nostril to eye (**DNE**, from nostril to anterior border of eye); forelimb length (**FLL**, from elbow to tip of third finger); tibia length (**TL**, distance from knee to heel); foot length (**FL**, from proximal end of inner metatarsal tubercle to tip of fourth toe); and thigh length (**THL**, from vent to knee).

A multivariate principal component analysis (PCA) was conducted using SPSS 17.0 (SPSS Inc.) based on a correlation matrix of size-standardized measurements (all measurements divided by SVL). Scatter plots of the scores of the first two factors of PCA were used to examine the differentiation among the new species, *K. idiootocus*, *K. bisacculus*, and *K. odontotarsus*.

Molecular analyses. In order to support the generic placement of the new species, the phylogenetic position of the new species was investigated based on molecular data. Total genomic DNA was extracted from liver tissue stored in 99% ethanol. Tissue samples were digested using proteinase K, and subsequently purified following a standard phenol/chloroform isolation and ethanol precipitation. A fragment of the mitochondrial 16S rRNA gene was amplified and sequenced. The primers and experiment protocols used in this study are the same as with Yu et al. (2010). Homologous sequences of other *Kurixalus* species were obtained from GenBank and all new sequences have been deposited in GenBank under Accession Nos. KY768931–KY768944 (Table 1). *Philautus abditus* Inger, Orlov, & Darevsky, 1999 and *Raorchestes menglaensis* (Kou, 1990) were selected as outgrups based on Yu et al. (2013).

Sequences were aligned using CLUSTAL X v1.83 (Thompson et al. 1997) with the default parameters and the alignment was revised by eye. Pairwise distances between species were calculated in MEGA 5 (Tamura et al. 2011). The best substitution model was selected using the Akaike Information Criterion (AIC) in MODELTEST v3.7 (Posada and Crandall 1998). Bayesian phylogenetic inference and Maximum likelihood analysis were performed in MRBAYES 3.1.2 (Huelsenbeck and Ronquist 2001) and RAXMLGUI 1.5b1 (Silvestro and Michalak 2012), respectively, based on the selected substitution model. For the Bayesian analysis, two runs were performed simultaneously with four Markov chains starting from random tree. The chains were run for 4,000,000 generations and sampled every 100 generations. The first 25% of the sampled trees was discarded as burn-in after the standard deviation of split frequencies of the two runs was less than a value of 0.01, and then the remaining trees were used to create a 50% majority-rule consensus tree and to estimate Bayesian posterior probabilities (BPPs). For the maximum likelihood analysis, node support was estimated by 1,000 rapid bootstrap replicates.

Results

Molecular data. The obtained sequence alignment is 870 bp in length. Both Bayesian and maximum likelihood analyses strongly supported that *Kurixalus lenquanensis* sp. n. is in the genus *Kurixalus* and is the sister taxon to *K. idiootocus* (Fig. 2). The average divergence (p-distance) between the new species and other congeneric species ranged from 4.72% to 16.84% (Table 2). This level of divergence in the 16S rRNA gene is indicative of differentiation at the species level in frogs (Fouquet et al. 2007) and is even higher than between other recognized congeners of *Kurixalus* (i.e. *Kurixalus eiffingeri* [Boettger, 1895]/*Kurixalus berylliniris* Wu, Huang, Tsai, Li, Jhang, & Wu, 2016, *K. eiffingeri*/*Kurixalus wangi* Wu, Huang, Tsai, Li, Jhang, & Wu, 2016, *K. berylliniris*/*K. wangi*, *K. bisacculus*/*K. odontotarsus*, *Kurixalus baliogaster* [Inger, Orlov, & Darevsky, 1999]/*K. odontotarsus*, and *K. baliogaster*/*K. bisacculus*; Table 2).

Morphological data. We retained the first two principal components which accounted for 43.7% of the total variance and had eigenvalues above 1.0. Loadings for PC 1 were all positive except for TD and DNE and were most heavily loaded on HW,

Table 1. Sequences used in this study.

Species	Locality	Voucher no.	GenBank no.
Philautus abditus	Krong Pa, Gia Lai, Vietnam	ROM 33145	GQ285673
Raorchestes menglaensis	Lvchuan, Yunnan, China	060821286Rao	GQ285676
Kurixalus appendiculatus	Bukit Sarang, Sarawak, Malaysia	FMNH 267896	JQ060937
Kurixalus eiffingeri	Okinawa Islands, Japan	KUHE 12910	AB933305
Kurixalus idiootocus	Wulai, Taipei, Taiwan	A127	DQ468674
Kurixalus idiootocus	Nan-Tou, Tung Fu, Taiwan	UMFS 5702	DQ283054
Kurixalus idiootocus	Taiwan	KUHE 12979	AB933306
Kurixalus idiootocus	Taiwan	SCUM 061107L	EU215547
Kurixalus idiootocus	Taiwan	CAS 211366	AF458129
Kurixalus berylliniris	Beinan, Taitung, Taiwan	11311 (CE01X)	DQ468669
Kurixalus wangi	Shouka, Pintung, Taiwan	11328 (CE06)	DQ468671
Kurixalus banaensis	Krong Pa, Gia Lai, Vietnam	ROM 32986	GQ285667
Kurixalus viridescens	Hon Ba, Khanh Hoa, Vietnam	VNMN 03802	AB933284
Kurixalus motokawai	Kon Tum, Vietnam	VNMN 03458	LC002888
Kurixalus verrucosus	Nagmung, Kachin, Myanmar	CAS 224381	GU227329
Kurixalus verrucosus	Nagmung, Kachin, Myanmar	CAS 224563	GU227330
Kurixalus verrucosus	Nagmung, Kachin, Myanmar	CAS 225128	GU227331
Kurixalus verrucosus	Tai Nai, Kachin, Myanmar	CAS 231489	GU227332
Kurixalus verrucosus	Mohynin, Kachin, Myanmar	CAS 231491	GU227333
Kurixalus odontotarsus	Mengyang, Yunnan, China	YGH 090175	GU227282
Kurixalus odontotarsus	Mengyang, Yunnan, China	YGH 090176	GU227283
Kurixalus odontotarsus	Caiyanghe, Yunnan, China	YGH 090131	GU227290
Kurixalus odontotarsus	Caiyanghe, Yunnan, China	KIZ 060821030	GU227294
Kurixalus bisacculus	Pingbian, Yunnan, China	YGH 080166	GU227295
Kurixalus bisacculus	Pingbian, Yunnan, China	YGH 080168	GU227296
Kurixalus bisacculus	Jinping, Yunnan, China	KIZ 060821124	KX554511
Kurixalus bisacculus	Thanh Hoa, Vietnam	VNMN 03808	AB933294
Kurixalus bisacculus	Wenshan, Yunnan, China	KIZ 3315	GU227305
Kurixalus bisacculus	Wenshan, Yunnan, China	KIZ 3317	GU227306
Kurixalus bisacculus	Wenshan, Yunnan, China	YGH 090044	GU227299
Kurixalus bisacculus	Wenshan, Yunnan, China	YGH 090046	GU227300
Kurixalus bisacculus	Jingxi, Guangxi, China	YGH 090280	GU227313
Kurixalus bisacculus	Jingxi, Guangxi, China	YGH 090281	GU227314
Kurixalus bisacculus	Libo, Guizhou, China	YGH 090081	GU227307
Kurixalus bisacculus	Nanning, Guangxi, China	YGH 090268	GU227310
Kurixalus bisacculus	Nanning, Guangxi, China	YGH 090270	GU227312
Kurixalus bisacculus	Jinxiu, Guangxi, China	KIZ 060821015	GU227319

Species	Locality	Voucher no.	GenBank no.
Kurixalus bisacculus	Longmeng, Guangdong, China	YGH 090201	GU227320
Kurixalus bisacculus	Longmeng, Guangdong, China	YGH 090202	GU227321
Kurixalus bisacculus	Mt. Wuzhi, Hainan, China	MVZ Herp 236722	JQ060928
Kurixalus bisacculus	Bawangling, Hainan, China	MVZ Herp 236725	JQ060929
Kurixalus bisacculus	Ha Giang, Vietnam	VNMN 01561	AB933287
Kurixalus bisacculus	Pac Ban, Tuyen Quang, Vietnam	ROM 30042	KC465809
Kurixalus bisacculus	Cao Bang, Vietnam	ROM 36726	KC465802
Kurixalus bisacculus	Cao Bang, Vietnam	VNMN 03805	AB933288
Kurixalus bisacculus	Tam Dao, Vinh Phu, Vietnam	MVZ Herp 223857	JQ060931
Kurixalus bisacculus	Tam Dao, Vinh Phu, Vietnam	MVZ Herp 226463	JQ060932
Kurixalus bisacculus	Chi Linh, Hai Duong, Vietnam	ROM 36829	KC465812
Kurixalus bisacculus	Chi Linh, Hai Duong, Vietnam	ROM 36827	KC465813
Kurixalus bisacculus	Pua, Nan, Thailand	THNHM 10051	GU227334
Kurixalus bisacculus	Pua, Nan, Thailand	THNHM 10052	GU227335
Kurixalus baliogaster	Kon Tum, Vietnam	VNMN 03618	AB933300
Kurixalus baliogaster	Gia Lai, Vietnam	VNMN 03812	AB933298
Kurixalus lenquanensis sp. n.	Lenquan, Mengzi, Yunnan, China	KIZ 170175Y	KY768931
Kurixalus lenquanensis sp. n.	Lenquan, Mengzi, Yunnan, China	KIZ 170176Y	KY768932
Kurixalus lenquanensis sp. n.	Lenquan, Mengzi, Yunnan, China	KIZ 170177Y	KY768933
Kurixalus lenquanensis sp. n.	Lenquan, Mengzi, Yunnan, China	KIZ 170178Y	KY768934
Kurixalus lenquanensis sp. n.	Lenquan, Mengzi, Yunnan, China	KIZ 170179Y	KY768935
Kurixalus lenquanensis sp. n.	Lenquan, Mengzi, Yunnan, China	KIZ 170180Y	KY768936
Kurixalus lenquanensis sp. n.	Lenquan, Mengzi, Yunnan, China	KIZ 170181Y	KY768937
Kurixalus lenquanensis sp. n.	Lenquan, Mengzi, Yunnan, China	KIZ 170182Y	KY768938
Kurixalus lenquanensis sp. n.	Lenquan, Mengzi, Yunnan, China	KISD 1506203	KY768939
Kurixalus lenquanensis sp. n.	Lenquan, Mengzi, Yunnan, China	KISD 1506204	KY768940
Kurixalus lenquanensis sp. n.	Yangjiatian, Gejiu, Yunnan, China	KIZ 170183Y	KY768941
Kurixalus lenquanensis sp. n.	Yangjiatian, Gejiu, Yunnan, China	KIZ 170184Y	KY768942
Kurixalus lenquanensis sp. n.	Yangjiatian, Gejiu, Yunnan, China	KIZ 170185Y	KY768943
Kurixalus lenquanensis sp. n.	Yangjiatian, Gejiu, Yunnan, China	KIZ 170186Y	KY768944

IND, and ED (Table 3). No difference was found along the PC 1 axis between the four species. The second principal component (PC 2) accounted for 20.96% of the total variance and loaded heavily and positively on SL and DNE and negatively on FL. Differentiation was found along the PC 2 axis between the new species and *K. idiootocus*, *K. odontotarsus*, and *K. bisacculus* (Fig. 3). The result indicates that the new species differs from *K. idiootocus*, *K. odontotarsus*, and *K. bisacculus* by smaller ratio of SL divided by SVL, smaller ratio of DNE divided by SVL, and higher ratio of FL divided by SVL.

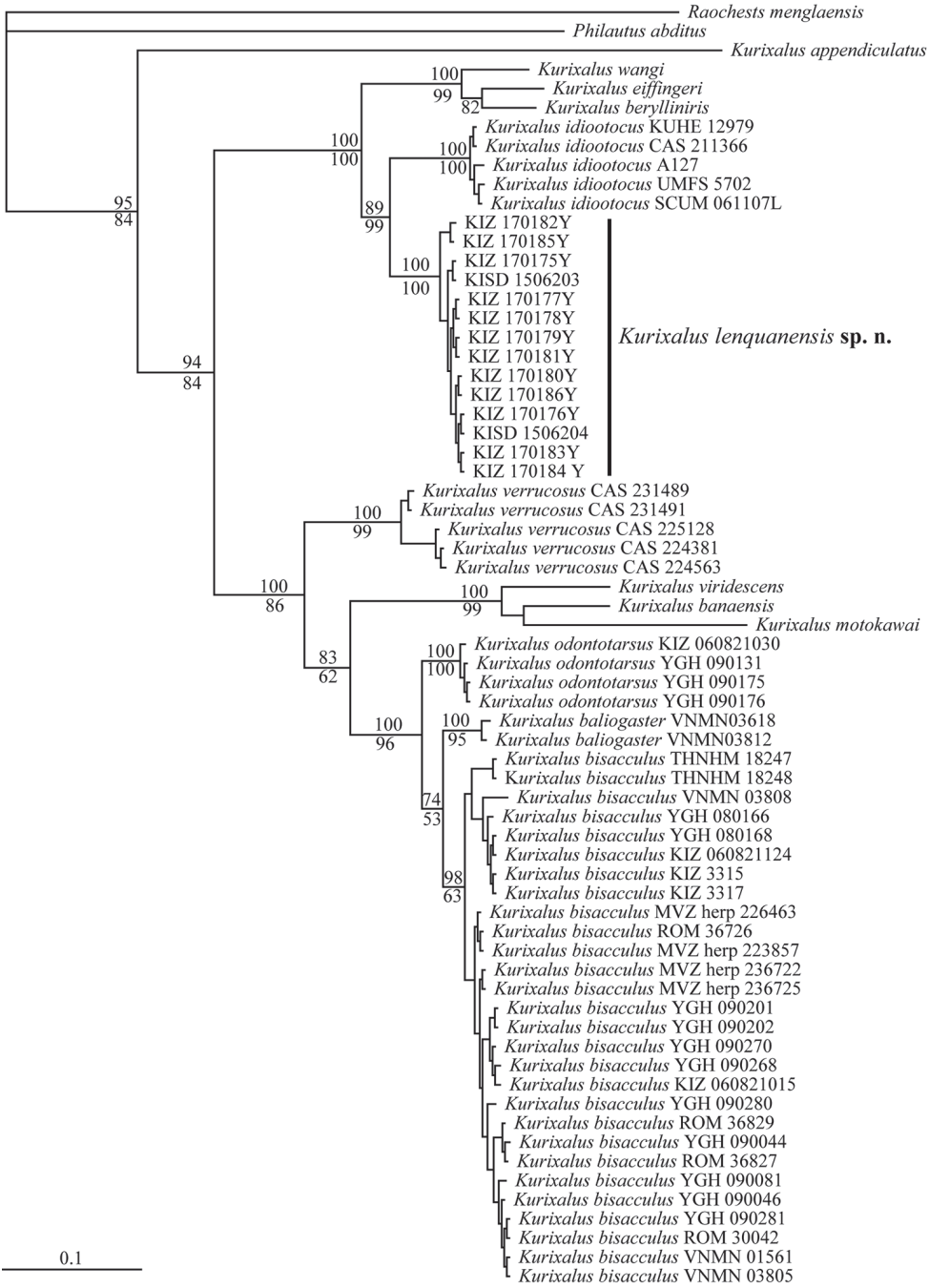

Figure 2. Bayesian phylogram of *Kurixalus* inferred from 870 bp of 16S rRNA gene. Numbers above and below branches are Bayesian posterior probabilities (BPP) and ML bootstrap values (only values above 50% are shown), respectively.

Table 2. Average uncorrected p-distances (%) among members of *Kurixalus* calculated from 16S rRNA gene sequences. Average intraspecific differences (p-distance, %) are shown on the diagonal.

Species	1	2	3	4	5	6	7	8	9	10	11	12	13
1. *K. appendiculatus*	–												
2. *K. eiffingeri*	17.48	–											
3. *K. idiootocus*	17.71	8.07	0.18										
4. *K. berylliniris*	16.29	3.23	6.14	–									
5. *K. wangi*	17.05	3.61	6.52	3.98	–								
6. *K. banaensis*	16.71	12.98	12.48	10.82	11.01	–							
7. *K. viridescens*	18.95	12.76	12.82	11.79	11.41	5.96	–						
8. *K. motokawai*	18.57	14.85	14.06	12.74	12.93	8.76	9.35	–					
9. *K. verrucosus*	16.50	11.70	10.61	10.28	8.96	10.16	10.55	12.87	1.07				
10. *K. odontotarsus*	17.62	12.03	11.60	10.74	10.45	9.02	9.27	11.71	7.22	0.06			
11. *K. bisacculus*	17.59	12.86	12.35	11.65	11.08	9.85	9.77	11.90	7.87	3.03	0.86		
12. *K. baliogaster*	17.55	12.20	11.92	11.59	10.64	9.52	9.18	11.85	8.20	3.44	2.98	0.35	
13. *K. lenquanensis* sp. n.	16.84	7.49	4.72	5.56	5.94	12.51	12.94	14.38	10.47	11.02	11.47	10.98	0.23

Table 3. Factor loadings of the first two principal components of 13 size-adjusted morphometric characteristics of males of *K. lenquanensis* sp. n., *K. idiootocus*, *K. odontotarsus*, and *K. bisacculus*. Absolute values of loading greater than 0.60 in boldface. Abbreviations defined in text.

Character	PC 1	PC 2
Eigenvalue	2.961	2.725
% variation	22.774	20.963
HL	0.376	0.553
HW	**0.715**	0.189
SL	0.369	**0.701**
IND	**0.776**	-0.208
IOD	0.481	-0.443
UEW	0.533	0.416
ED	**0.756**	0.178
TD	-0.19	0.529
FLL	0.437	-0.494
TL	0.362	0.061
FL	0.343	**-0.688**
DNE	-0.068	**0.626**
THL	0.048	-0.232

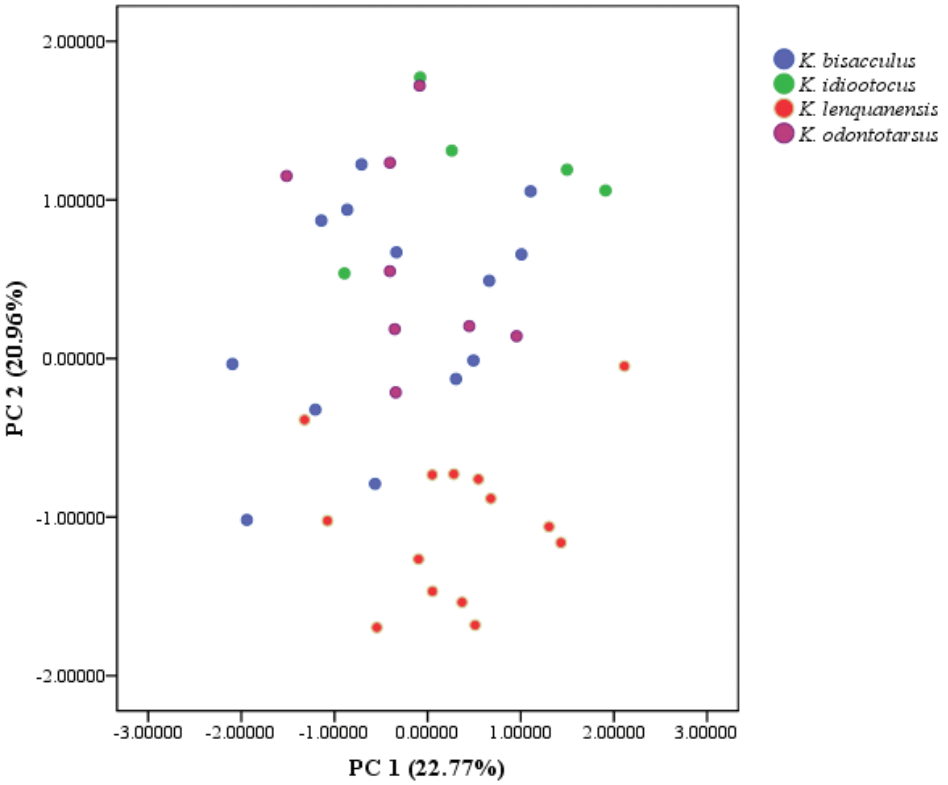

Figure 3. Scatterplot of principal components 1 and 2 of size-adjusted morphometric data for males of *K. lenquanensis* sp. n., *K. idiootocus*, *K. bisacculus*, and *K. odontotarsus*.

Systematics

***Kurixalus lenquanensis* sp. n.**
http://zoobank.org/597FB4AE-5B50-4A57-9400-B6EBB36EAC4F
Figs 4–7

Holotype. KIZ 170180Y (Figs 4–6), an adult male, collected at 20:35 on 5 May 2016 by Guohua Yu from Lenquan Village (23°12'52"N, 103°22'34"E, 1622 m elevation; Fig. 1), Mengzi City, Yunnan Province, China.

Paratype. Thirteen adult males: KIZ 170175Y–170179Y and KIZ 170181Y–170182Y collected at 20:00–22:45 on 5 May 2016 by Guohua Yu from type locality, KISD 1506203–1506204 collected at 21:00–21:30 on 20 June 2015 by Jishan Wang from the same locality as the holotype, and KIZ 170183Y–170186Y collected at 20:00–22:30 on 6 May 2016 by Guohua Yu from Yangjiatian Village (23°20'5.35"N, 103°9'30.33"E; Fig. 1), Gejiu City, Yunnan Province, China.

Type locality. Lenquan Village, Mengzi City, Yunnan Province, China.

Etymology. The name lenquanensis refers to Lenquan Village, the locality where the new species was found.

Diagnosis. The new tree frog species is assigned to the genus *Kurixalus* based on a combination of the following characters: tips of digits enlarged to discs, bearing circum-marginal grooves; small body size (adult males SVL range of 25.0–28.9 mm; Table 4); finger webbing poorly developed and toe webbing moderately developed; serrated dermal fringes along outer edge of forearm and tarsus; an inverted triangle-shaped dark brown mark between eyes; dorsal brown “) (” saddle-shaped or X-shaped marking maybe present; and coarse dorsal and lateral surfaces with small, and irregular tubercles.

Kurixalus lenquanensis sp. n. can be distinguished from its congeners by a combination of the following characters: smaller body size (mean SVL 27 mm in males); obtusely pointed snout with no prominence on tip; curved canthus rostralis; slight nuptial pad; brown dorsal color; rough dorsum; chin clouded with brown; absence of large dark spots on ventral surface; presence of vomerine teeth; gold brown iris; single internal vocal sac; dermal fringes along outer edge of limbs; rough flanks; and granular throat and chest.

Description of holotype. A small rhacophorid (SVL 27.2 mm); HL 89.4% of HW; snout obtusely pointed, no dermal prominence on tip, projecting slightly beyond margin of lower jaw in ventral view; SL (3.7 mm) shorter than ED (4.1 mm); canthus rostralis blunt and curved; lore region oblique, slightly concave; nostril oval, slightly protuberant, closer to tip of snout than eye; IND (2.5 mm) narrower than IOD (2.8 mm) and slightly wider than UEW (2.3 mm); pineal spot absent; pupil oval, horizontal; tympanum distinct (TD 1.6 mm), rounded, less than half ED; supratympanic fold distinct, curves from posterior edge of eye to insertion of arm; vomerine teeth in two oblique patches touching inner front edges of oval choanae; tongue notched posteriorly; single internal vocal sac.

Limbs slender; relative length of fingers is I < II < IV < III. Tips of all four fingers expanded into discs with circum-marginal and transverse ventral grooves; disc on

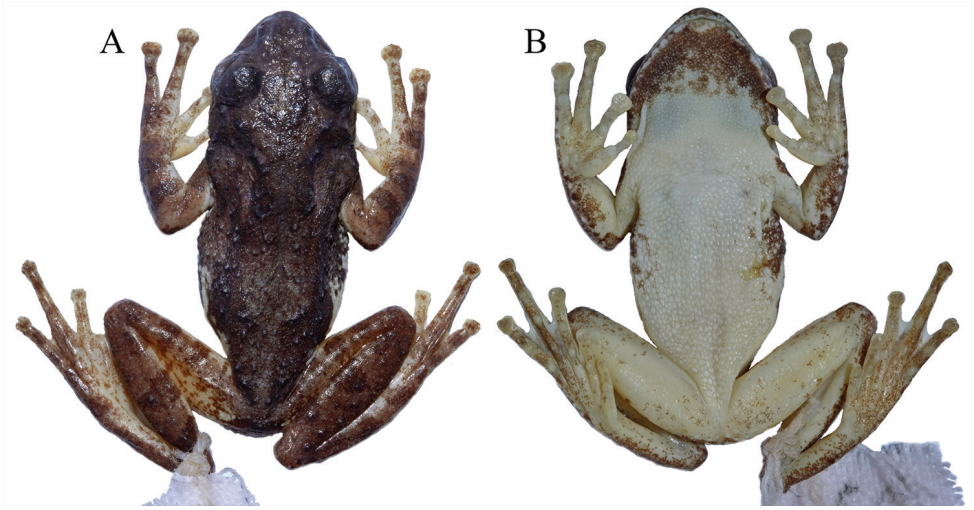

Figure 4. Dorsal **A** and ventral **B** views of the holotype of *Kurixalus lenquanensis* sp. n. in preservative.

Figure 5. Ventral view of hand **A** and foot **B** of the holotype of *Kurixalus lenquanensis* sp. n. in preservative.

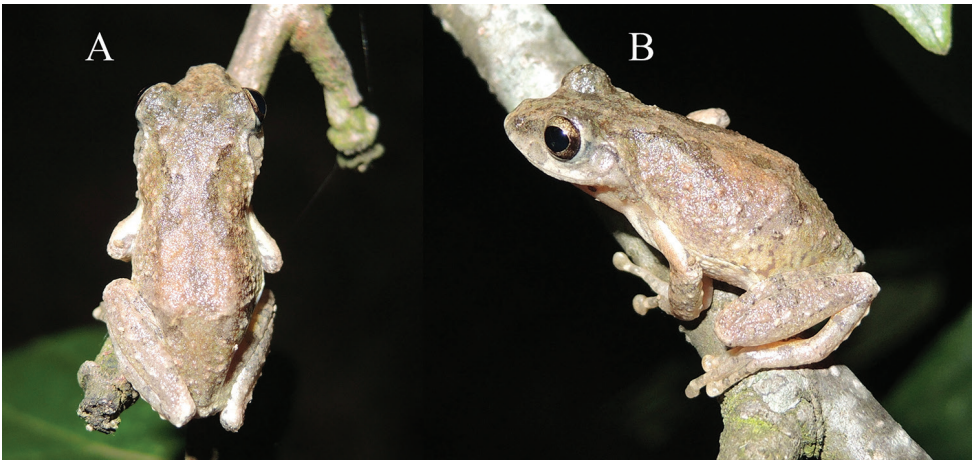

Figure 6. Dorsal **A** and lateral **B** views of the holotype of *Kurixalus lenquanensis* sp. n. in life.

Figure 7. Ventral view of paratype KIZ 170184Y.

finger I small, slightly wider than phalanx width; disc width shorter than tympanum width; relative width of discs is I < II < III < IV. Nuptial pad slight; fingers webbed at base, webbing formula is I2–2.5II2–3.5III3–2.5IV following Myers and Duellman (1982). Fringe of skin on edge of all fingers; subarticular tubercles prominent and rounded, formula 1, 1, 2, 2; supranumerary tubercles present; two metacarpal tubercles, outer slightly narrower than inner; row of white warts forming serrated fringe along outer edge of forearm.

Heels overlapping when legs at right angle to body; relative length of toes is I < II < V < III < IV. Tips of toes expanded into discs with circum-marginal and transverse ventral grooves; toe discs smaller than finger discs; disc on toe I same with width as phalanx width; relative size of discs is I < II < III < IV < V. Webbing moderate on all toes, webbing formula is I2–2.5II1.5–3III1.5–3IV2.75–1.5V. Subarticular tubercles prominent and rounded, formula 1, 1, 2, 3, 2; supernumerary tubercles absent; inner metatarsal tubercle distinct, oval; outer metatarsal tubercle absent; series of tubercles forming serrated dermal fringe along outer edge of tarsus and fifth toe.

Numerous small or large tubercles scattered on top of head, upper eyelids, dorsum, and flanks; patch of white tubercles below vent; white conical tubercle on tibiotarsal articulation; throat and chest finely granulated and abdomen coarsely granulated; dorsal surface of limbs tuberculate and ventral surface of thighs finely granulated.

Color of holotype in life. Iris golden brown; dorsal surface grayish brown with dark brown saddle-shaped mark on dorsum, beginning behind eye; dark brown inverted triangle-shaped mark between eyes; lateral head and tympanic region brown with dark brown spot below canthus; broad dark brown bar along canthus rostralis; limbs dorsally brown with clear dark brown barring; rear, anterior, and venter of thigh light yellow with scattered brown spots, more spots on rear; rear of flank faint yellow with brown spots; chest and abdomen white, nearly immaculate; chin clouded with black.

Color of holotype in preservative. In preservative (Fig. 4), dorsal ground color brown, pattern same as in life. Chest and abdomen white; chin clouded with dark brown; flank dirty white with dark brown spots; rear, anterior, and venter of thigh dirty white with scattered brown spots, more so on rear.

Variations. Morphometric data are summarized in Table 4. Because the holotype and paratypes of the new species are all male, sexual dimorphism could not be determined. Differing from the nearly immaculate abdominal surfaces of the holotype and paratypes from the type locality, abdominal surfaces of three paratypes (KIZ 170183Y, 170184Y, 170186Y) from Yangjiatian, Gejiu are scattered with fine brown spots (Fig. 7). TL is longer than FL in the holotype and most paratypes, but TL is shorter than FL in paratype KIZ 170182Y (Table 4). Additionally, pattern of dark brown mark on dorsum varies among specimens. The holotype and most paratypes have a saddle-shaped dorsal mark, but the two paratypes KISD 1506203 and KISD 1506204 have an X-shaped dorsal mark and the paratype KIZ 170183Y has no obvious dark brown mark on dorsum.

Ecology. At present, the new species is known only from the type locality, Lenquan Village, Mengzi City, Yunnan Province and Yangjiatian Village, Gejiu City, Yunnan Prov-

Table 4. Measurements (mm) of *K. lenquanensis* sp. n. Abbreviations defined in text.

Vouchers no.	SVL	HL	HW	SL	IND	IOD	UEW	ED	TD	DNE	FLL	TL	FL	THL
KIZ 170175Y	26.7	8.1	9.5	3.6	3.0	3.0	2.6	4.2	1.5	2.0	13.3	12.9	11.7	12.5
KIZ 170176Y	26.1	8.2	9.1	3.6	2.6	2.9	2.6	4.0	1.4	1.9	12.8	12.2	11.6	11.7
KIZ 170177Y	27.4	8.2	9.5	3.7	2.8	2.9	2.5	4.3	1.6	1.6	13.5	12.7	12.2	11.8
KIZ 170178Y	27.1	8.3	9.5	3.9	2.6	2.9	2.5	4.1	1.4	2.0	13.1	13.0	12.0	12.1
KIZ 170179Y	27.3	8.5	9.1	3.5	2.4	2.8	2.5	3.9	1.7	1.9	13.5	12.5	12.2	12.4
KIZ 170180Y	27.2	8.1	9.1	3.7	2.5	2.8	2.3	4.1	1.6	1.7	13.8	12.6	12.5	11.7
KIZ 170181Y	28.9	8.9	9.6	4.0	2.7	2.7	2.6	4.3	1.6	2.0	13.3	12.7	12.4	12.2
KIZ 170182Y	27.1	8.2	9.1	3.7	2.7	2.8	2.5	4.3	1.8	1.6	13.7	11.8	12.7	11.7
KISD 1506203	26.7	8.6	9.3	3.4	2.5	2.9	2.5	4.3	1.6	1.6	13.2	11.9	11.7	11.8
KISD 1506204	27.1	8.9	10.0	3.8	2.8	3.1	2.0	4.0	1.6	2.0	13.1	12.2	11.9	11.9
KIZ 170183Y	26.6	8.4	9.8	3.5	2.5	3.1	2.2	3.9	1.5	1.8	13.2	12.5	12.4	12.2
KIZ 170184Y	26.9	8.7	9.7	3.8	2.8	3.0	2.5	4.3	1.5	1.6	13.1	12.5	12.0	12.2
KIZ 170185Y	27.2	8.8	9.8	3.8	2.7	3.1	2.1	3.9	1.8	1.9	13.4	12.2	11.8	11.2
KIZ 170186Y	25.0	8.7	9.7	3.7	2.6	2.9	2.3	3.9	1.5	1.8	12.4	11.6	11.2	10.8

ince (Fig. 1). The holotype was found calling on a tree branch approximately 0.5 m above near a dry puddle in a fruit garden in Lenquan Village (Fig. 8). All other specimens were found on vegetation near the dry puddle in Lenquan Village or vegetation near a reservoir in Yangjiatian Village. Males began to call at about 19:30 when sky was getting dark and all specimens were encountered at night (20:00–22:45). Males called loudly, but no females or eggs were found. *Hyla annectans* (Jerdon, 1870), *Kaloula verrucosa* Boulenger, 1904, and *Microhyla heymonsi* Vogt, 1911 were also encountered at the type locality.

Comparisons. The new species, *Kurixalus lenquanensis* sp. n., is morphologically similar to *K. idiootocus* in that it has a small body size (mean male SVL of 27 mm in new species versus mean male SVL of 27.5 mm in *K. idiootocus*; Table 5). However, the new species can be distinguished from *K. idiootocus* by its obtusely pointed snout with no prominence on tip, absence of a pair of symmetrical large dark patches on chest, single internal vocal sac, and absence of supernumerary plantar tubercles (versus pointed snout with a small prominence on tip, presence of a pair of symmetrical large dark patches on chest, single external vocal sac, and small supernumerary plantar tubercles; Kuramoto and Wang 1987; Figs 9–10). In addition, besides that snout of the new species is shorter than that of *K. idiootocus*, the PCA analysis showed that the new species also differs from *K. idiootocus* by greater ratio of FL divided by SVL (Table 3 and Fig. 3).

Kurixalus lenquanensis sp. n. is distinguished from *K. berylliniris* by gold brown iris, obtusely pointed snout with no prominence on tip, smaller body size, tubercles on upper eyelid, slight nuptial pad, and coarsely granular abdomen (versus emerald to light green iris, pointed snout with a small prominence on tip, larger body size [mean SVL in males = 35 mm], lack of palpebral tubercles, greatly expanded nuptial pad, and smooth abdomen; Wu et al. 2016; Fig. 10).

In addition, the new species can be distinguished from *K. wangi* by a lack of prominence on snout tip, smaller body size, presence of tubercles on dorsum, coarse skin on flanks, and slight nuptial pad (versus pointed snout with small prominence on tip, larger body size [mean SVL in males = 30 mm], absence of tubercles on dorsum, smooth skin on flanks, and greatly expanded nuptial pad; Wu et al. 2016; Fig. 10) and from *K. eiffingeri* by smaller body size, slight nuptial pad, oblique loreal region, and curved canthus rostralis (versus larger body size [mean SVL of 31.1 mm in males], greatly expanded nuptial pad, vertical loreal region, and straight canthus rostralis; Wu et al. 2016).

Kurixalus lenquanensis sp. n. further differs from *Kurixalus appendiculatus* (Günther, 1858) by smaller body size, absence of dermal prominence on snout tip, and tympanum less than half of eye diameter (versus larger body size [male SVL = 30–37 mm], presence of prominence on snout tip, and tympanum half eye diameter; Günther 1858, Inger et al. 1999); from *K. baliogaster* by smaller body size (SVL in males = 25.0–27.4 mm), absence of prominence on obtusely pointed snout tip, absence of large dark spots on ventral surface, tuberculated dorsal and lateral skin, presence of tubercles on eyelids, granular throat, and presence of dermal fringes on limbs (versus larger body size [male SVL = 33.0–33.3 mm], pointed snout with prominence on tip, large dark spots on ventral surface, smooth dorsal and lateral skin, absence of tubercles on eyelids, smooth throat, and absence of dermal fringes on limbs; Inger et al. 1999); and from *Kurixalus banaensis* (Bourret, 1939) by smaller

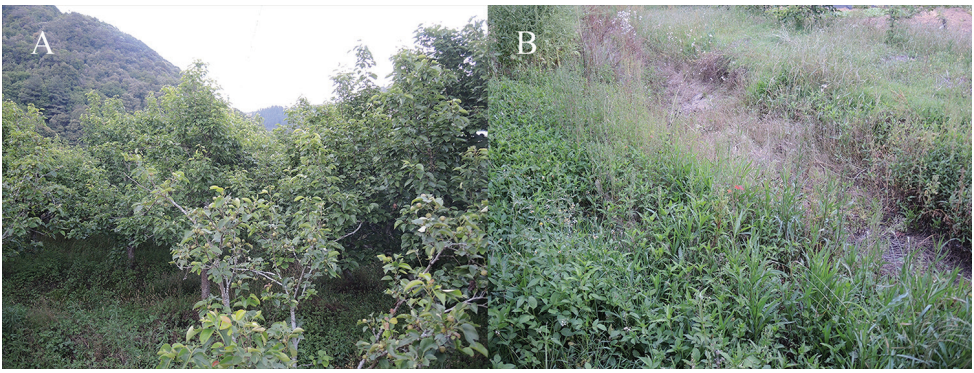

Figure 8. The fruit garden **A** and dry puddle **B** in the fruit garden at type locality of *Kurixalus lenquanensis* sp. n.

body size, obtusely pointed snout being shorter than eye, presence of vomerine teeth, and tuberculate flanks (versus larger body size [mean SVL in males = 29.7 mm], markedly pointed snout being longer than eye, absence of vomerine teeth, and smooth flanks in *K. banaensis*; Nguyen et al. 2014a, Nguyen et al. 2014b, Bossuyt and Dubois 2001).

The new species differs from *Kurixalus viridescens* Nguyen, Matsui, & Duc, 2014 by tuberculate dorsum, brown dorsal color, dark bands on dorsum and limbs, brownish clouded pattern on chin, and presence of vomerine teeth (versus nearly smooth dorsum, uniformly greenish dorsal color, no dark markings on dorsum and limbs, pinkish cream without marking on chin, and absence of vomerine teeth in *K. viridescens*; Nguyen et al. 2014b); from *Kurixalus ananjevae* (Matsui & Orlov, 2004) by smaller body size, presence of vomerine teeth, presence of dermal fringes on limbs, and finely granular throat surface (versus larger body size [32 mm in one male], absence of vomerine teeth, absence of dermal fringes on limbs, and smooth throat surface; Matsui and Orlov 2004); and from *Kurixalus motokawai* Nguyen, Matsui, & Eto, 2014 by obtusely pointed snout tip, presence of vomerine teeth, and clouded chin with brown (versus pointed snout tip, absence of vomerine teeth, and small dark brown spots scattered on chin; Nguyen et al. 2014a)

Currently, two species of *Kurixalus* (*K. bisacculus* and *K. odontotarsus*) are recognized in Yunnan, China (Yu et al. 2010). The new species can be distinguished from *K. bisacculus* and *K. odontotarsus* by smaller body size, absence of large black spots on belly, and obtusely pointed snout with no prominence on tip (versus larger body size [mean SVL in males at more than 33 mm], presence of large black spots on belly, and markedly pointed snout with a prominence on tip extending beyond lower jaw in *K. bisacculus* and *K. odontotarsus*; Table 5; Fig. 9). Moreover, the PCA analysis revealed that the new species further differs from *K. odontotarsus* and *K. bisacculus* by smaller ratio of SL/SVL, smaller ratio of DNE/SVL, and bigger ratio of FL/SVL (Table 3 and Fig. 3).

Additionally, the new species differs from *K. verrucosus* found in Myanmar by smaller body size, snout shorter than diameter of eye, interorbital distance wider than upper eyelid, tympanum less than half of eye diameter, moderate toe webbing, granular throat and chest,

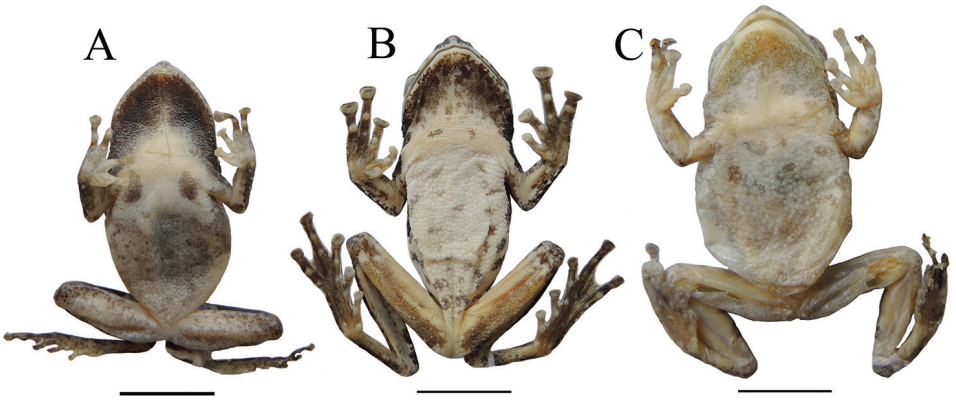

Figure 9. Ventral view of *K. idiootocus* (**A** YGH 140217), *K. odontotarsus* (**B** YGH 090131), and *K. bisacculus* (**C** YGH 090045).

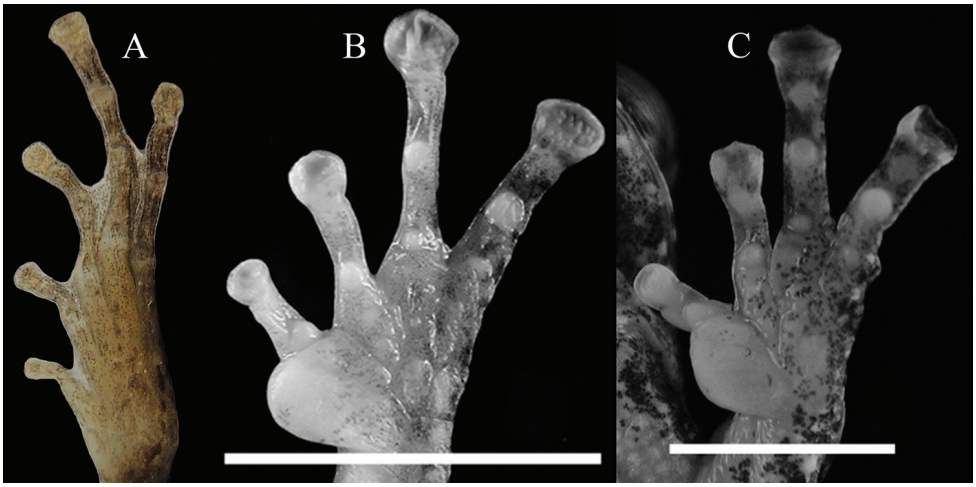

Figure 10. Ventral view of foot of *K. idiootocus* **A** and ventral view of hand of *K. berylliniris* (**B** from Wu et al. 2016) and *K. wangi* (**C** from Wu et al. 2016).

and absence of large brown spots on belly and throat (versus larger body size [mean SVL in males = 29.9 mm], snout as long as diameter of eye, interorbital space as broad as upper eyelid, tympanum half eye diameter, nearly entirely developed toe webbing, smooth throat and chest, and presence of large brown spots on belly and throat; Boulenger 1893); and from *Kurixalus naso* (Annandale, 1912) by smaller body size, obtusely pointed snout with no dermal prominence on tip, moderately developed toe webbing, and absence of large dark spots on chest and belly (versus larger body size [male SVL at more than 30 mm], pointed snout with a dermal prominence on tip, almost completely developed toe webbing, and presence of large dark spots on chest and belly in *K. naso*; Annandale 1912, Mathew and Sen 2008).

Table 5. Comparison of measurements (mm) of *K. lenquanensis* sp. n., *K. idiootocus*, *K. odontotarsus*, and *K. bisacculus*. Abbreviations defined in text.

Measurement	*K. lenquanensis* (n = 14)	*K. idiootocus* (n = 5)	*K. odontotarsus* (n = 8)	*K. bisacculus* (n = 13)
SVL	27.0 ± 0.84 (25.0–28.9)	27.5 ± 1.26 (26.1–29)	33.3 ± 0.91 (32.1–34.3)	33.2 ± 0.96 (31.3–34.4)
HL	8.5 ± 0.29 (8.1–8.9)	9.1 ± 0.32 (8.7–9.5)	10.9 ± 0.24 (10.6–11.3)	10.4 ± 0.29 (10.1–10.9)
HW	9.5 ± 0.3 (9.1–10.0)	9.8 ± 0.37 (9.4–10.3)	11.5 ± 0.46 (11.1–12.3)	11.6 ± 0.61 (10.8–12.8)
SL	3.7 ± 0.16 (3.4–4.0)	4.3 ± 0.21 (4.1–4.6)	4.8 ± 0.27 (4.5–5.3)	4.9 ± 0.41 (4.1–5.7)
IND	2.7 ± 0.16 (2.4–3.0)	2.6 ± 0.08 (2.5–2.7)	3.1 ± 0.21 (2.8–3.4)	3.0 ± 0.20 (2.5–3.2)
IOD	2.9 ± 0.13 (2.7–3.1)	2.9 ± 0.21 (2.8–3.3)	3.5 ± 0.17 (3.2–3.6)	3.4 ± 0.21 (3.1–3.6)
UEW	2.4 ± 0.19 (2.0–2.6)	2.8 ± 0.23 (2.5–3.0)	2.9 ± 0.12 (2.8–3.1)	3.0 ± 0.36 (2.6–3.7)
ED	4.1 ± 0.17 (3.9–4.3)	4.4 ± 0.19 (4.1–4.6)	5.1 ± 0.18 (4.8–5.3)	4.8 ± 0.25 (4.4–5.3)
TD	1.6 ± 0.13 (1.4–1.8)	1.7 ± 0.13 (1.6–1.9)	2.3 ± 0.14 (2.1–2.5)	2.2 ± 0.18 (2.0–2.6)
DNE	1.8 ± 0.17 (1.6–2.0)	1.9 ± 0.11 (1.8–2.1)	2.6 ± 0.21 (2.3–2.9)	2.5 ± 0.17 (2.2–2.7)
FLL	13.2 ± 0.36 (12.4–13.8)	12.7 ± 0.43 (12.1–13.3)	16.1 ± 0.57 (14.8–16.5)	15.9 ± 0.37 (15.5–16.8)
TL	12.4 ± 0.41 (11.6–13.0)	12.4 ± 0.47 (11.9–13.1)	15.5 ± 0.64 (14.3–16.1)	15.8 ± 0.6 (14.9–16.9)
FL	12.0 ± 0.41 (11.2–12.7)	10.5 ± 0.36 (9.9–10.9)	13.9 ± 0.97 (12.4–15.2)	13.9 ± 0.76 (13.1–15.9)
THL	11.9 ± 0.46 (10.8–12.5)	11.9 ± 0.56 (11.4–12.8)	15.4 ± 0.75 (14.2–16.2)	15.4 ± 0.93 (13.9–17)

Discussion

Although morphological synapomorphies of the genus *Kurixalus* are still not very clear (Yu et al. 2013, Nguyen et al. 2014b), intuitively *K. lenquanensis* sp. n. can be placed in *Kurixalus* because of its morphological similarity to other members of the genus (e.g. small body size, inner and outer fingers not opposable, poorly developed finger webbing, moderately developed toe webbing, and serrated dermal fringes on forearm and tarsus). Other small rhacophorid species in the genera *Feihyla*, *Gracixalus*, *Chiromantis*, or *Philautus* generally lack serrated fringes on forearm and tarsus and lack vomerine teeth (Fei 1999, Fei et al. 2010). Additionally, inner (first and second) and outer (third and fourth) fingers are opposable in all species of *Feihyla* and *Chiromantis* (Fei 1999, Fei et al. 2010). This assignment is supported by the molecular data, which indicates that *K. lenquanensis* sp. n. is nested in the genus *Kurixalus* with strong support values.

It is very interesting biogeographically that *K. lenquanensis* sp. n. is nested within a clade consisting of Taiwanese *Kurixalus* with strong support, indicating that the ancestor of the new species may have been from Taiwan Island. Another plausible scenario is that the ancestor of this new species may have been widespread in southern China and the descendent species in between Taiwan and Yunnan has become extinct. Although *K. ananjevae* and *K. naso* are not included in the present study, absence of them would have no impact on the phylogenetic position of the new species because *K. ananjevae* likely does not belong to the genus (Yu et al. 2013), and morphologically, *K. naso* is more similar to members of the *K. odontotarsus* species group than to *K. lenquanensis* sp. n. in body size and ventral color pattern.

Reproductive behavior among Taiwanese relatives of the new species varies; *Kurixalus idiootocus* lays pigmented eggs on land near the edge of water or in depressions where rainfall accumulates (Kuramoto and Wang 1987), whereas *K. eiffingeri*, *K. berylliniris*, and *K. wangi* lay eggs inside tree hollows or cut bamboos with water (Fei et al. 2010, Wu et al. 2016). Although no eggs of *K. lenquanensis* sp. n. were found, reproductive behavior of this new species probably is closer to that of *K. idiootocus* than to that of the other three Taiwanese species because 1) it is the sister taxon to *K. idiootocus* and 2) no tree hollows or cut bamboos were found at the type locality.

Species boundaries among members of the genus *Kurixalus* were previously confusing and our earlier work, based on molecular data (Yu et al. 2010), supported that there are three valid members of *Kurixalus* in mainland China. Therefore, with the new species described here, there are currently four *Kurixalus* species in mainland China: *K. bisacculus*, *K. lenquanensis* sp. n., *K. odontotarsus*, and *K. verrucosus*. However, considering the obvious geographical discontinuity in distribution between *K. lenquanensis* sp. n. and its congeneric relatives from Taiwan Island, additional undiscovered species of *Kurixalus* may exist in south China.

Key to the new species and its congeners

1 Limbs with no serrated dermal fringes **2**
– Limbs with serrated dermal fringes **3**
2 Dorsum smooth; many dark spots scattered on ventral surface ..... ***K. baliogaster***
– Dorsum with small tubercles, no dark spots on ventral surface ..... ***K. ananjevae***
3 Dorsal color uniformly greenish ..... ***K. viridescens***
– Dorsal color not uniformly greenish, generally brownish mixed with dark-marking **4**
4 Iris emerald to light green ..... ***K. berylliniris***
– Iris golden **5**
5 Nuptial pad greatly expanded **6**
– Nuptial pad slight **7**
6 Tubercles on lateral margin of finger IV connected with dermal fringe; venter whitish with very little pigmentation; loreal region oblique; canthus rostralis curved ..... ***K. wangi***
– Tubercles on lateral margin of finger IV separated from each other; venter with numerous fine brownish dots, especially in the gular region; loreal region vertical; canthus rostralis straight ..... ***K. eiffingeri***
7 Vomerine teeth absent **8**
– Vomerine teeth present **9**
8 Snout tip less markedly pointed; lateral fringes on limbs and infra-cloacal tubercles less developed; lateral sides areolate ..... ***K. motokawai***
– Snout tip markedly pointed; lateral fringes on limbs and infra-cloacal tubercles developed; flanks smooth ..... ***K. banaensis***
9 Smaller body size (adult male SVL less than 30 mm) **10**
– Bigger body size (generally adult male SVL greater than 30 mm) **11**
10 Snout obtusely pointed with no prominence on tip; absence of a pair of symmetrical large dark patches on chest; single internal vocal sac ..... ***K. lenquanensis* sp. n.**
– Snout pointed with a small prominence on tip; a pair of symmetrical large dark patches present on chest; single external vocal sac ..... ***K. idiootocus***
11 Snout rounded or somewhat pointed; chin and breast smooth ..... ***K. verrucosus***
– Snout obviously pointed; chin and breast granular **12**
12 Dorso-lateral fold fairly distinct ..... ***K. naso***
– No obvious dorso-lateral fold **13**
13 Venter uniformly cream to tan with no black spots ..... ***K. appendiculatus***
– Black spots present on ventral surface **14**
14 Single internal vocal sac; omosternum unforked ..... ***K. odontotarsus***
– Paired lateral vocal sacs or single internal vocal sac and omosternum forked ..... ***K. bisacculus***

Comparative material examined

Kurixalus idiootocus: YGH 140215, 140217–140220, Xinbei, Taiwan.
Kurixalus odontotarsus: YGH 090130–090137, Caiyanghe, Puer, Yunnan.
Kurixalus bisacculus: YGH 080166, 080168–080170, 140013, Pingbian, Yunnan; YGH 090045, 140020, Wenshan, Yunnan; YGH 090081, Libo, Guizhou; YGH 090202, Longmeng, Guangdong; YGH 090268, 090270, Nanning, Guangxi; THNHM 10051, 10052, Nan, Thailand.
Kurixalus verrucosus: CAS 225128, 231489, 231491, 224563, Kachin, Myanmar.

Acknowledgements

We are indebted to S. Lin for the donation of specimens of *K. idiootocus* from Taiwan and to T. Chan-ard for the loan of specimens of *K. bisacculus* from Thailand. Thanks also to E. J. Ely for assistance with taking measurement of *K. verrucosus*, to R. Min for her help with laboratory work, and to two reviewers for their valuable comments on the manuscript. This work was supported by the National Natural Science Foundation of China (No. 31301870), CAS "Light of West China" Program to G. Yu, and Natural Science Foundation of Yunnan Province (No. 2015FB176) to J. Wang.

References

Annandale N (1912) Zoological results of the Abor expedition. Part I. Batrachia. Records of the Indian Museum 8: 7–36. https://doi.org/10.5962/bhl.part.1186

Boettger O (1895) Neue Frösche und Schlangen von den Liukiu-Inseln. Zoologischer Anzeiger 18: 266–270.

Bossuyt F, Dubois A (2001) A review of the frog genus *Philautus* Gistel, 1848 (Amphibia, Anura, Ranidae, Rhacophoridae). Zeylanica 6: 1–112.

Boulenger GA (1893) Concluding report on the reptiles and batrachians obtained in Burma by Signor L. Fea, dealing with the collection made in Pegu and the Karin Hills in 1887–1888. Annali del Museo Civico di Storia Naturale di Genova Serie 2 13: 304–347.

Boulenger GA (1904) Descriptions of new frogs and snakes from Yunnan. Annals and Magazine of Natural History Series 7 13: 130–135. https://doi.org/10.1080/00222930408562447

Bourret R (1939) Notes herpétologiques sur l'Indochine française. XVII. Reptiles et batraciens reçus au Laboratoire des Sciences Naturelles de l'Université au cors de l'année 1938. Descriptions de trois espèces nouvelles. Annexe au Bulletin Général de l'Instruction Publique 6: 13–34.

Fei L (1999) Atlas of Amphibians of China. Henan Publishing House of Science and Technology, Zhengzhou, China, 432 pp.

Fei L, Ye C, Jiang J (2010) Colored Atlas of Chinese Amphibians. Sichuan Publishing House of Science and Technology, Chengdu, China, 519 pp.

Fouquet A, Gilles A, Vences M, Marty C, Blanc M, Gemmell NJ (2007) Underestimation of species richness in Neotropical frogs revealed by mtDNA analyses. PLoS ONE 2(10): e1109. https://doi.org/10.1371/journal.pone.0001109

Frost DR (2017) Amphibian Species of the World: and Online Reference. Version 6.0. American Museum of Natural History, New York, USA. http://research.amnh.org/herpetology/amphibia/index.html [accessed 22 June 2017].

Günther ACLG (1858) Neue Batrachier in der Sammlung des britischen Museums. Archiv für Naturgeschichte 24: 319–328. https://doi.org/10.5962/bhl.part.5288

Huelsenbeck JP, Ronquist F (2001) MrBayes: Bayesian inference of phylogeny. Bioinformatics 17: 754–755. https://doi.org/10.1093/bioinformatics/17.8.754

Inger RF, Orlov N, Darevsky I (1999) Frogs of Vietnam: a report on new collections. Fieldiana Zoology, New Series 92: 1–46.

Jerdon TC (1870) Notes on Indian herpetology. Proceedings of the Asiatic Society of Bengal 1870: 66–85

Kou Z (1990) A new species of genus *Philautus* (Amphibia: Rhacophoridae) from Yunnan, China. In: Zhao E (Ed.) From Water onto Land. China Forestry Press, Beijing, 210–212.

Kuramoto M, Wang C (1987) A new rhacophorid treefrog from Taiwan, with comparisons to *Chirixalus eiffingeri* (Anura, Rhacophoridae). Copeia 1987: 931–942. https://doi.org/10.2307/1445556

Mathew R, Sen N (2008) Rediscovery of *Rhacophorus naso* Annandale, 1912 (Amphibia: Anura: Rhacophoridae) from Mizoram, North East India. Records of the Zoological Survey of India 108: 41–42.

Matsui M, Orlov NL (2004) A new species of *Chirixalus* from Vietnam (Anura: Rhacophoridae). Zoological Science 21: 671–676. https://doi.org/10.2108/zsj.21.671

Myers CW, Duellman WE (1982) A new species of *Hyla* from Cerro Colorado, and other tree frog records and geographical notes from western Panama. American Museum Novitates 2752: 1–32.

Nguyen TT, Matsui M, Eto K (2014a) A new cryptic tree frog species allied to *Kurixalus banaensis* (Anura : Rhacophoridae) from Vietnam. Russian Journal of Herpetology 21: 295–302.

Nguyen TT, Matsui M, Duc HH (2014b) A new tree frog of the genus *Kurixalus* (Anura: Rhacophoridae) from Vietnam. Current Herpetology 33: 101–111. https://doi.org/10.5358/hsj.33.101

Orlov NL, Murphy RW, Ananjeva NB, Ryabov SA, Cuc HT (2002) Herpetofauna of Vietnam, a checklist. Part 1. Amphibia. Russian Journal of Herpetology 9: 81–104.

Posada D, Crandall KA (1998) Modeltest: testing the model of DNA substitution. Bioinformatics 14: 817–818. https://doi.org/10.1093/bioinformatics/14.9.817

Silvestro D, Michalak I (2012) RAXMLGUI: a graphical front-end for RAxML. Organisms Diversity & Evolution 12: 335–337. https://doi.org/10.1007/s13127-011-0056-0

Tamura K, Peterson D, Peterson N, Stecher G, Nei M, Kumar S (2011) MEGA5: molecular evolutionary genetics analysis using maximum likelihood, evolutionary distance, and maximum parsimony methods. Molecular Biology and Evolution 28: 2731–2739. https://doi.org/10.1093/molbev/msr121

Taylor EH (1962) The amphibian fauna of Thailand. University of Kansas Science Bulletin 43: 265–599. https://doi.org/10.5962/bhl.part.13347

Thompson JD, Gibson TJ, Plewniak F, Jeanmougin J, Higgins DG (1997) The CLUSTAL X windows interface: flexible strategies for multiple sequence alignment aided by quality analysis tools. Nucleic Acids Research 25: 4876–4882. https://doi.org/10.1093/nar/25.24.4876

Vogt T (1911) Beitrag zur Amphibien-fauna der Insel Formosa. Sitzungsberichte der Gesellschaft Naturforschender Freunde zu Berlin 1911: 179–184.

Wu S, Huang C, Tsai C, Lin T, Jhang J, Wu S (2016) Systematic revision of the Taiwanese genus *Kurixalus* members with a description of two new endemic species (Anura, Rhacophoridae). ZooKeys 557: 121–153. https://doi.org/10.3897/zookeys.557.6131

Ye C, Fei L, Hu S (1993) Rare and Economic Amphibians of China. Sichuan Publishing House of Science and Technology, Chengdu, China, 412 pp.

Yu G, Zhang M, Yang J (2010) A species boundary within the Chinese *Kurixalus odontotarsus* species group (Anura: Rhacophoridae): New insights from molecular evidence. Molecular Phylogenetics and Evolution 56: 942–950. https://doi.org/10.1016/j.ympev.2010.05.008

Yu G, Zhang M, Yang J (2013) Molecular evidence for taxonomy of *Rhacophorus appendiculatus* and *Kurixalus* species from northern Vietnam, with comments on systematics of *Kurixalus* and *Gracixalus* (Anura: Rhacophoridae). Biochemical Systematics and Ecology 47: 31–37. https://doi.org/10.1016/j.bse.2012.09.023

Zhao E, Wang L, Shi H, Wu G, Zhao H (2005) Chinese rhacophorid frogs and description of a new species of *Rhacophorus*. Sichuan Journal of Zoology 24: 297–300.

ZooKeys 694: 95–108 (2017)
doi: 10.3897/zookeys.694.12513
http://zookeys.pensoft.net

RESEARCH ARTICLE

A peer-reviewed open-access journal
ZooKeys
Launched to accelerate biodiversity research

A new species of the genus *Rana* from Henan, central China (Anura, Ranidae)

Haipeng Zhao[1,2,3], Junxiao Yang[1,2], Chunping Wang[4], Pipeng Li[5], Robert W. Murphy[2,6], Jing Che[1], Zhiyong Yuan[7]

1 *Kunming Institute of Zoology, Chinese Academy of Sciences, Kunming 650223, Yunnan, China* **2** *Kunming College of Life Science, University of Chinese Academy of Sciences, Kunming 650204, Yunnan, China* **3** *School of Life Science, Henan University, Kaifeng 475004, Henan, China* **4** *Henan Forestry Survey and Planning Institute, Zhengzhou 450045, Henan, China* **5** *Center for Chinese Endemic Herp-breeding and Conservation Research, and Liaoning Key Laboratory of Evolution and Biodiversity, Shenyang Normal University, Shenyang 110034, Liaoning, China* **6** *Centre for Biodiversity and Conservation Biology, Royal Ontario Museum, 100 Queen's Park, Toronto M5S 2C6, Canada* **7** *College of Forestry, Southwest Forestry University, Kunming 650224, Yunnan, China*

Corresponding author: *Jing Che* (chej@mail.kiz.ac.cn); *Zhiyong Yuan* (yuanzhiyongkiz@126.com)

Academic editor: *J. Penner* | Received 3 March 2017 | Accepted 8 June 2017 | Published 29 August 2017

http://zoobank.org/C5F1430E-FD70-49E3-8A95-57BCDCEE491D

Citation: Zhao H, Yang J, Wang C, Li P, Murphy RW, Che J, Yuan Z (2017) A new species of the genus *Rana* from Henan, central China (Anura, Ranidae). ZooKeys 694: 95–108. https://doi.org/10.3897/zookeys.694.12513

Abstract

A new species of brown frog *Rana luanchuanensis* Zhao & Yuan, **sp. n.** is described from Luanchuan County, western Henan, central China. The mitochondrial genealogy suggests that the new species is the sister taxon to the clade including *R. amurensis* and *R. coreana*, and is separated by uncorrected pairwise distances more than 12.5%. Morphologically, this new species differs from its congeners by a suite of characters. Analyses of partial sequences of cytochrome oxidase subunit I (COI) resolve the new species as a single matriline.

Keywords

Brown frog, DNA barcode, genealogy, *Rana luanchuanensis* sp. n.

Introduction

Frogs in the genus *Rana* Linnaeus, 1758 (type species: *Rana temporaria* Linnaeus, 1758), are commonly known as brown or wood frogs. Currently, the genus *sensu* Yuan et al. (2016) contains 101 species (AmphibiaWeb 2017). It is a widespread, complex, and diverse group that crosses Eurasia and the Americas. They share prominent dorsolateral folds, a dark temporal mask, and a body that is counter-shaded in various shades of brown, which lead to the common English name "brown frogs" (Boulenger 1920; Liu and Hu 1961). The conservative morphology of Eurasian *Rana* makes many species notoriously difficult to identify (Che et al. 2007a, b; Liu and Hu 1961). In this case, molecular assessments have resulted in the description of new species (e.g. Lu et al. 2007; Yan et al. 2011; Matsui 2011; Ryuzaki et al. 2014). Additional cryptic new species were suggested to occur in the New World (Hillis and Wilcox 2005).

Five of seven clades of *Rana* (Yuan et al. 2016) exist in China (AmphibiaChina 2017), including 23 species. Among others, *R. chensinensis* David, 1875, *R. culaiensis* Li, Lu & Li, 2008, and *R. zhenhaiensis* Ye, Fei, & Matsui, 1995 occur in Henan (AmphibiaChina 2017). Recent herpetofaunal surveys in Henan (August 2007, November 2013, and May 2014) led to the discovery of three new populations of *Rana* in western areas (Figure 1). These populations show distinct and curved dorsolateral folds and their males do not possess subgular vocal sacs. These characters are similar to those of the *R. amurensis* species group, which contains *R. amurensis* Boulenger, 1886 and *R. coreana* Okada, 1928 (Fei et al. 2009; Yang et al. 2010; Zhou et al. 2015). Further, these frogs possess several distinct morphological characters that differ from *R. amurensis* and *R. coreana*. Taken together, these data suggest that the new populations might be a new species.

Herein, the identity of a new brown frog is investigated by comparing morphological and molecular characteristics with Eurasian congeners. Analyses determine that the frogs constitute a new species, which is described here.

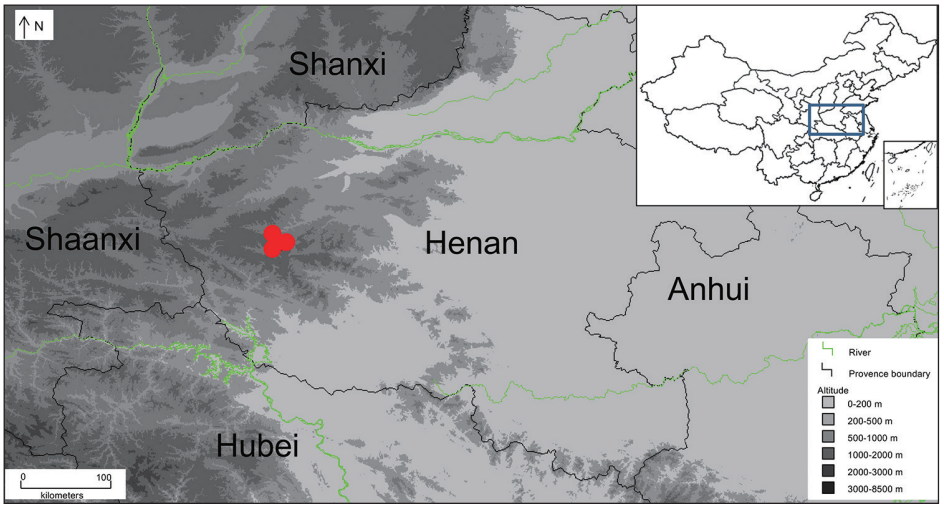

Figure 1. Map showing the collecting locations of *Rana luanchuanensis* sp. n. indicated by red cycles.

Materials and methods

Sampling

From 2013 to 2014, field surveys conducted in Luanchuan, western Henan resulted in the collection of 38 adult frogs. Following euthanizing, muscle or liver tissue was dissected from specimens and then preserved in 95% ethanol. Voucher specimens were fixed in 10% buffered formalin, and then later transferred to 70% ethanol. All specimens were deposited in the Kunming Institute of Zoology (KIZ), Chinese Academy of Sciences. Tissues samples used in our comparative analyses were summarized in Table 1, along with locality data, voucher numbers, and GenBank accession numbers.

DNA extraction, amplification, and sequencing

Total genomic DNA was extracted from tissues of five individuals using the standard phenol-chloroform protocols (Sambrook et al. 1989). Partial sequences of the gene encoding cytochrome oxidase subunit I (COI) was amplified and sequenced.

Amplification was performed in a 25 μL volume as follows: initial denaturation step for 5 min at 95 °C followed by 35 cycles of denaturation for 1 min at 94 °C, primer-specific annealing temperature of 46 °C for 1 min, extension for 1 min at 72 °C; final extension at 72 °C was conducted for 10 min. The primers Chmf4 (5'-TYTCWACWAAYCAYAAAGAYATCGG-3') and Chmr4 (5'-ACYTCRGGRTGRCCRAARAATCA-3') (Che et al. 2012) were used for amplification and sequencing. PCR products were purified with Gel Extraction Mini Kit (Tiangen Biotech, Beijing). The cycle sequencing reactions were performed using BigDye Terminator Cycle Sequencing Kit (v.2.0, Applied Biosystems, Foster City, California, USA), using purified products as the template DNA. Sequences were determined using an ABI PRISM 3730 automated DNA sequencer with sequencing in both directions. The sequence data were submitted to a BLAST search in GenBank to confirm the identity. Considering geography and morphological similarity, 13 COI sequences of Eurasian *Rana* were retrieved from GenBank and included in the subsequent molecular analyses (Table 1). *Rana luteiventris* was chosen as outgroup based on the phylogeny of Yuan et al. (2016). Nucleotide sequences were aligned using MUSCLE v.3.6 (Edgar 2004) with default parameters.

Genetic analyses

Interspecific and intraspecific mean uncorrected pairwise distances were computed in MEGA v.6.0 (Tamura et al. 2013). Phylogenetic analyses of the sequences were conducted using Bayesian inference (BI) and maximum likelihood (ML). The BI analysis was executed in MrBayes v.3.1.2 (Ronquist and Huelsenbeck 2003) using GTR + I + G model determined using the Akaike Information Criterion (AIC) computed with

Table 1. Voucher specimens, localities, and GenBank accession numbers for brown frogs, *Rana*. "*" = type locality. GBN = GenBank Accession No.

Species	Voucher No.	Locality	GBN (COI)	Source
Rana amurensis	KIZ070423558	Shangzhi, Heilongjiang, China	JF939079	Yan et al. (2011)
Rana asiatica	XJ416	Forty seven Tuan, Xinjiang, China	MF149925	This study
Rana arvalis	KIZ04239	Haba River, Xinjiang, China	MF149926	This study
Rana arvalis	GBOL03518	Upper Bavaria, Bavaria, Germany	KP697924	Hawlitschek et al. (2015)
Rana chaochiaoensis	KIZ06425	Zhaojue, Sichuan, China*	JF939103	Yan et al. (2011)
Rana chensinensis	KIZRD05SHX01	Huxian, Shanxi, China*	JF939080	Yan et al. (2011)
Rana coreana	MMS223	South Korea	MF149928	This study
Rana coreana	KIZYPX2630	Mt. Kunyu, Shandong, China*	MF149927	This study
Rana culaiensis	KIZSD080501	Mt. Culai, Shandong, China*	JF939082	Yan et al. (2011)
Rana dybowskii	KIZ070423448	Huangnihe, Jilin, China	JF939078	Yan et al. (2011)
Rana hanluica	KIZYPXll72	Mt. Yangming, Hunan, China*	JF939099	Yan et al. (2011)
Rana huanrensis	SYNU040006	Huanren, Liaoning, China*	JF939072	Yan et al. (2011)
Rana japonica	KIZYPX11775	Japan	JF939101	Yan et al. (2011)
Rana jiemuxiensis	KIZ05263	Jiemuxi NR, Hunan, China*	JF939090	Yan et al. (2011)
Rana kukunoris	CJ06102001	Qinghai Lake, Qinghai, China*	JF939073	Yan et al. (2011)
Rana longicrus	KIZ15026	Nanzhuang, Miaoli, Taiwan, China	JF969067	Yan et al. (2011)
Rana luanchuanensis sp. n.	KIZ047393	Luanchuan, Henan, China*	MF149924	This study
Rana luanchuanensis sp. n.	KIZ047452	Luanchuan, Henan, China*	MF149923	This study
Rana luanchuanensis sp. n.	KIZ047476	Luanchuan, Henan, China*	MF149921	This study
Rana luanchuanensis sp. n.	KIZ047482	Luanchuan, Henan, China*	MF149920	This study
Rana luanchuanensis sp. n.	KIZ047487	Luanchuan, Henan, China*	MF149922	This study
Rana luteiventri	MVZ Herp 137417	Missoula, Montana, USA	KU985757	Chambers and Hebert (2016)
Rana omeimontis	KIZ02424	Mt. Emei, Sichuan, China*	JF939069	Yan et al. (2011)
Rana zhenhaiensis	KIZ0803271	Zhenhai, Zhejiang, China*	JF939065	Yan et al. (2011)
Rana zhengi	SCUM0405190CJ	Zhangcun, Hongya, Sichuan, China*	MF149929	This study

jModelTest 2 (Darriba et al. 2012). Consensus frequencies, termed Bayesian posterior probabilities, were used to estimate nodal support. Four separate runs were performed with four Markov chains. Each run was conducted for 10000000 generations while sampling every 1000 generations. Log likelihood scores were tracked for stabilization and the first 50% of the trees were discarded as burn-in. The sampled trees were analyzed using Tracer v.1.6 (Rambaut et al. 2014) to confirm satisfactory convergence of topological split frequencies. The ML analysis was conducted using RAxML v.8.0 (Stamatakis 2014). This analysis implemented the GTR + I + G model. Nodal support values were estimated from 1000 nonparametric bootstrap pseudoreplicates.

Morphometrics

A total of 38 specimens was examined (Appendix 1). Haipeng Zhao took all measurements of the specimens to minimize bias. Nineteen linear measurements following Fei et al. (2009) were made using digital dial calipers with a precision of 0.1 mm. These measurements were as follows:

SVL (snout-vent length),
HDL head length,
HDW head width,
SL snout length,
EYE diameter of exposed portion of eyeball,
IOD interorbital distance,
IND internarial distance,
UEW upper eyelid width,
TYE tympanum outer diameter,
LAL lower-arm length,
HL hand length,
LAHL lower-arm and hand length,
LAW lower-arm width,
FEL femur length,
TL tibia length,
TW tibia width,
FTL length of foot and tarsus,
FOL foot length, and
IMTL inner metatarsal tubercles length.

Dissections on five male specimens determined the presence or absence of vocal sacs which can be seen by the presence of openings on the mouth floor. Vocal sacs that are externally visible are defined as "external" vocal sacs, those that cannot be distinguished by external observation are defined as "subgular". All these morphological characters are defined following Fei et al. (2009).

Results

Ten new sequences with 558 base pairs (bp) were obtained and deposited in GenBank (Accession numbers MF149920–MF149929; Table 1). After trimming ends, the combined sequences contained 211 variable sites of which 187 were potentially parsimony-informative. The uncorrected *p*-distances between the new populations from Henan and congeners ranged from 12.54% (*R. amurensis*) to 17.92% (*R. longicrus*) (Table 2).

Table 2. The pairwise uncorrected *p*-distance (%) of the COI partial sequence used in this study (a, b). 1: *Rana amurensis*; 2: *R. asiatica*; 3. *R. arvalis*; 4: *R. chaochiaoensis*; 5: *R. chensinensis*; 6: *R. coreana*; 7: *R. culaiensis*; 8: *R. dybowskii*; 9: *R. hanluica*; 10: *R. huanrensis*; 11: *R. japonica*; 12: *R. jiemuxiensis*; 13: *R. kukunoris*; 14: *R. longicrus*; 15: *R. luanchuanensis* sp. n.; 16: *R. omeimontis*; 17: *R. zhenhaiensis*; and 18: *R. zhengi*. Bolded number highlights the distance between *R. luanchuanensis* sp. n. and the species of *Rana* analyzed in this study. "—" indicates genetic distance less than 1%.

(a)

	1	**2**	**3**	**4**	**5**	**6**	**7**	**8**	**9**
1	—								
2	0.1562	—							
3	0.1595	0.1113	—						
4	0.1631	0.14	0.1326	—					
5	0.1523	0.1436	0.1452	0.1613	—				
6	0.1093	0.1609	0.1455	0.1553	0.1699	0.0164			
7	0.1828	0.1364	0.1685	0.1308	0.1685	0.1843	—		
8	0.1685	0.1311	0.138	0.1595	0.1326	0.1626	0.1774	—	
9	0.1756	0.14	0.1577	0.1272	0.1595	0.1824	0.0717	0.1685	—
10	0.1487	0.1329	0.1344	0.1541	0.0502	0.1726	0.1703	0.129	0.1649
11	0.1685	0.1382	0.147	0.1308	0.1416	0.1518	0.147	0.1541	0.1308
12	0.172	0.14	0.1613	0.1398	0.1559	0.1798	0.0771	0.1756	0.0771
13	0.1613	0.1346	0.1487	0.1541	0.0609	0.1698	0.1703	0.1308	0.1649
14	0.1792	0.1472	0.1738	0.1434	0.1756	0.1852	0.0287	0.1792	0.0878
15	**0.1254**	**0.1346**	**0.1523**	**0.1523**	**0.1452**	**0.1464**	**0.1649**	**0.1505**	**0.1703**
16	0.1631	0.1436	0.1487	0.1487	0.1613	0.1725	0.0806	0.1505	0.0771
17	0.1846	0.1508	0.1685	0.138	0.1667	0.1969	0.0323	0.181	0.0806
18	0.1667	0.1382	0.1416	0.1452	0.1434	0.1716	0.1703	0.1523	0.1559

(b)

	10	**11**	**12**	**13**	**14**	**15**	**16**	**17**	**18**
11	0.1416	—							
12	0.1613	0.1487	—						
13	0.0484	0.1452	0.1577	—					
14	0.181	0.1541	0.086	0.181	—				
15	**0.1434**	**0.1362**	**0.1792**	**0.1487**	**0.1738**	**—**			
16	0.1649	0.1559	0.0932	0.1559	0.0932	**0.1559**	—		
17	0.181	0.1416	0.086	0.181	0.043	**0.1667**	0.0806	—	
18	0.1577	0.1667	0.1667	0.1541	0.1774	**0.1685**	0.1649	0.1703	—

The uncorrected pairwise distances between the two new populations from Henan were less than 0.1%.

Genealogical reconstructions by BI and ML were nearly identical (Figure 2). The monophyly of ingroup and major clades were similar to previous studies (Yan et al.

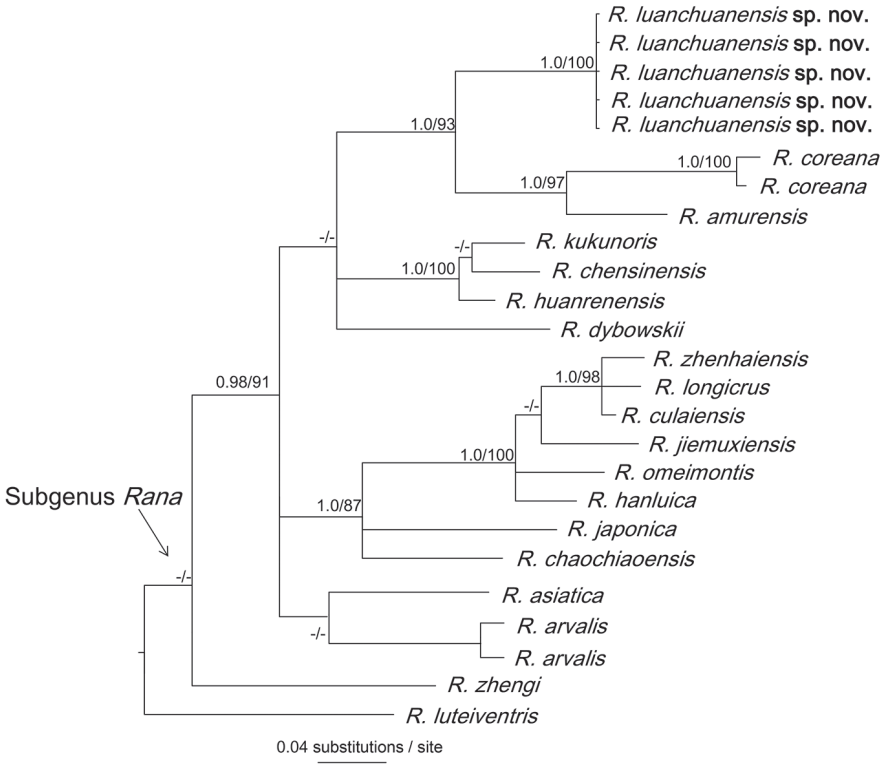

Figure 2. A Bayesian inference tree based on the COI partial sequence data. Numbers near the nodes are Bayesian posterior probabilities / ML bootstrap value but only when values are ≥ 0.95 and ≥ 70, respectively.

2011; Yuan et al. 2016). However, phylogenetic relationships among the five major clades were not recovered by our analyses likely due to limited data; future study using additional loci were deemed to be desirable. The new samples from Luanchuan, Henan shared a common matriline, which clustered as the sister-group of *R. amurensis* plus *R. coreana* with strong support (BI BPP= 100, ML BS = 93). This resolution and the extent of sequence divergence suggested that the new samples constituted a new species.

Morphological and morphometric analyses of the frogs (Table 3) identified several diagnostic morphological characters (see below).

***Rana luanchuanensis* Zhao & Yuan, sp. n.**
http://zoobank.org/3FF49AB8-95A4-4C30-8735-2B0C5778A683
Figures 3, 4

Holotype. KIZ016090, an adult male, collected by Haipeng Zhao and Ruiliang Wang on 4 May 2014 in Tongyi River near the village of Hanqiu (33.80°N, 111.80°E, elevation 810 m a.s.l.), Miaozi town, Luanchuan County, western Henan, central China.

Table 3. Linear measurements (in mm) of *Rana luanchuanensis*. The abbreviations are provided in text.

Character	Measurements		
		♂	♀
SVL	Range	27.2–33.0 ± 1.87	23.7–41.2 ± 4.25
HDL	Range	7.9–10.5 ± 0.69	8.5–13.5 ± 1.25
HDW	Range	9.7–11.8 ± 0.63	9.7–15.2 ± 1.47
SL	Range	4.3–5.7 ± 0.34	4.1–6.9 ± 0.7
EYE	Range	2.9–4.3 ± 0.35	3.3–5.3 ± 0.55
IOD	Range	2.4–3.4 ± 0.3	2.5–4.3 ± 0.39
IND	Range	2.3–3.6 ± 0.29	2.5–3.4 ± 0.27
UEW	Range	1.9–2.6 ± 0.26	1.9–3.1 ± 0.36
TYE	Range	1.4–2.4 ± 0.25	1.4–3.2 ± 0.44
LAL	Range	5.9–7.4 ± 0.44	5.3–8.5 ± 0.78
HL	Range	7.2–9.1 ± 0.54	6.8–11.2 ± 1.11
LAHL	Range	13.3–15.3 ± 0.6	11.7–18.2 ± 1.7
LAW	Range	2.3–3.6 ± 0.4	1.7–3.8 ± 0.5
FEL	Range	13.9–18.2 ± 1.35	13.5–21.7 ± 2.1
TL	Range	15.5–20.3 ± 1.35	14.7–22.8 ± 2.18
TW	Range	2.5–4.1 ± 0.52	2.1–4.9 ± 0.7
FTL	Range	21.0–26.4 ± 1.36	19.7–33.3 ± 3.26
FOL	Range	15.8–18.6 ± 0.93	13.2–23.4 ± 2.52
IMTL	Range	1.7–2.4 ± 0.23	1.4–2.8 ± 0.28

Paratypes. KIZ047446–047453, KIZ016089, with the same collection data as the holotype; KIZ047383, with the same locality as the holotype, collected on 16 November 2013; KIZ047470–047487, KIZ016086–016088, and KIZ016091 from Wangping village, Tantou town, Luanchuan County (33.95°N, 111.73°E, elevation 530 m a.s.l.) in the same river, collected on 5 May 2014; KIZ0093, KIZ0099, KIZ0101, KIZ0104, and KIZ0105, collected by Li Ding and Xiaobei Zhang from nearby Miaozi town (33.75°N, 111.72°E, elevation 1070 m a.s.l.) on 15 August 2007. A total number of 37 adult individuals included 12 males and 25 females.

Diagnosis. A small-sized species (SVL 27.2–33.0 mm in males; 23.7–41.2 mm in females) of *Rana*; temporal fold distinct; dark mask covering tympanum; curved dorsolateral fold thin, extending from posterior canthus to groin; tips of fingers not expanded; skin smooth with few small granules on dorsum and legs, distinct large tubercles absent; head length slightly less than head width; vocal sac absent in males; white rictal gland absent on the upper lip; ventral surface of throat, chest, and belly white with irregular black spots; poster part of abdomen and ventral surface of thighs and limbs reddish; distinct transverse grayish brown bars on dorsal surface of fingers and toes, lower arms, tarsus, thighs, and tibia; toes two-thirds webbed; gray-blackish nuptial pad prominent and forming two groups in males, with minute nuptial spines; three metacarpal tubercles, inner one close to the nup-

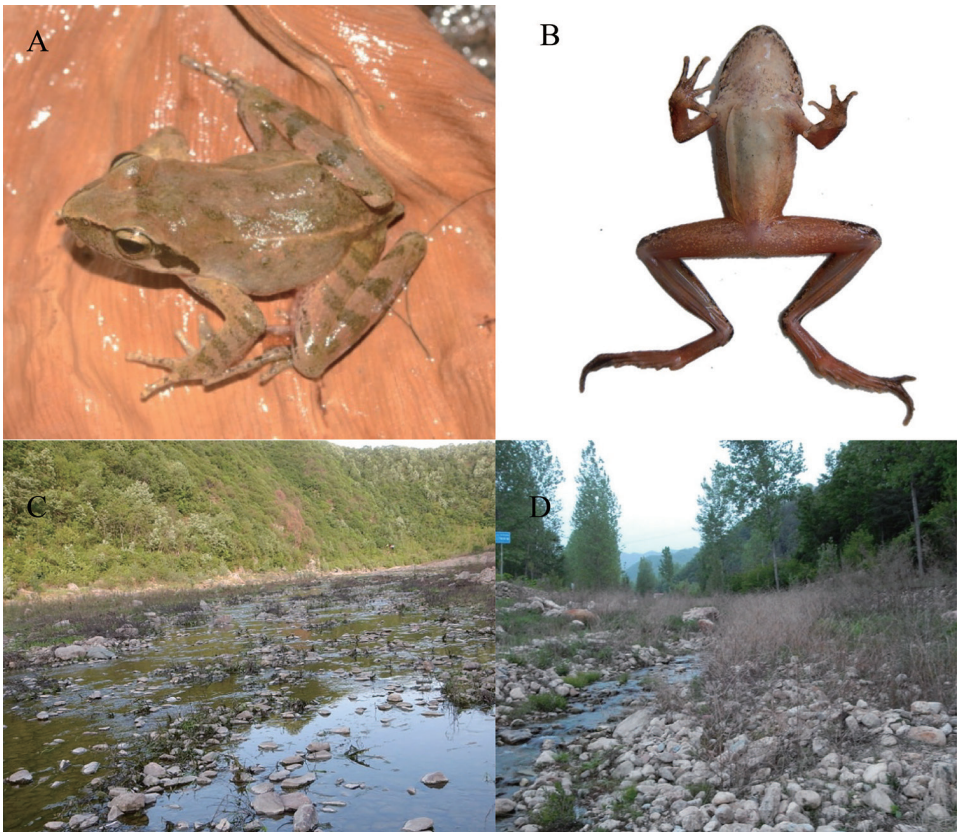

Figure 3. Photographs of a live specimen and its habitat near the type locality of *Rana luanchuanensis* sp. n. **A** Lateral view **B** Ventral view **C, D** Habitat of the type locality of *R. luanchuanensis* showing a live individual.

tial pad at the base of finger I, the two outer ones closed together at the base of fingers III and IV.

Description of holotype. SVL 32.8 mm. *Head* slightly shorter than broad (HL\HW = 0.87), snout pointed and projecting; snout length much longer than eye diameter (SL\EYL = 1.35); interorbital space equal to internasal space and both wider than upper eyelid width; tympanum diameter about half of eye diameter, loreal region concave, sloping outwards; vomerine teeth in short oblique series, anterior edges in line with centers of choanae; tongue deeply notched posteriorly; vocal sacs absent.

Forearm robust, fingers slender, unwebbed; tips of fingers not expanded, with no circum-marginal grooves; relative length of fingers: II < I < IV < III; one prominent subarticular tubercle on fingers I and II, two small subarticular tubercles on fingers III and IV; distinct supernumerary tubercles below the base of fingers; inner metacarpal tubercle strong and large, ovoid, close to the nuptial pad at base of finger I; two outer tubercles close together at base of fingers III and IV, flat, long elliptic and obvious. Nuptial pad covered densely by small grey-blackish spines and divided into two groups, one near tip larger than the other one.

Hindlimb long (8.7 mm), heels well overlapping when limb held at right angles to body; tibiotarsal articulation of adpressed limb reaching far anterior to eyes; inner metatarsal tubercle weak and small, smooth, about 0.37 of the first toe; tips of toes similar to fingers; relative length of toes: I < II < III < V < IV; toes two-thirds webbed, webbing formula: I 1–2 II 1–2 ½ III 2–3 IV 3–1 V; web of toe III reaching the first joint from tip and on other toes nearly extending to tip; subarticular tubercles small, but visible; distinct supernumerary tubercles below the base of toes; inner metatarsal tubercle ovoid, small but distinct; outer metatarsal tubercle absent.

Skin rather smooth, except for some small granules near vent and ventral femoral region; temporal fold distinct, extending from posterior margin of eye above and behind tympanum to above arm insertion, a large triangular black and brown patch behind the eye and anterior to temporal fold; thin dorsolateral fold from posterior canthus to groin, obviously curved at upper tympanum and crossing temporal fold; ventral surface smooth, reddish; few granules on the posterior ventral surface of thighs.

Color of holotype. In life, dorsum gray-brown, with few scattered black spots and grayish brown blotches; dorsolateral fold reddish brown and darker than ground dorsal color; distinct grayish brown crossbars on dorsal surface of fingers and toes, lower arms, tarsus, thighs and tibia; narrow black stripe on edge of canthus rostralis from tip of snout along margin of upper eyelid and across eye continuing along supratympanic ridge; large triangular black and brown patch behind the eye and anterior to temporal fold; lower lip whitish with black spots and bars; throat, chest, and belly white with irregular black spots; poster part of abdomen reddish; ventrally limbs reddish with faint yellow nebulous mottling; faint yellow granules on ventral thigh; foot webbing brownish red with few indistinct black spots; nuptial pad blackish gray. In preservative, dorsal surface dark gray-brown with slightly paler limbs (Fig. 4); all grayish brown crossbars and grayish brown blotches fade to black; throat, chest, and abdomens fade to creamy white, with gray spots.

Habitat and life history. All specimens of the new species were collected in shallow slow-flowing streams with large gravel beds (Figure 3). Streams were near the mountains with well-preserved forests. Females with mature eggs were collected from Hanqiu village on 16 November 2013, which indicated its breeding season may occur in the winter. However, we did not observe any breeding pairs, egg clutches, or tadpoles. More field work is needed to observe its breeding behavior and other phenomena of life history.

Variation in the type series. Morphometric data were summarized in Table 3. Individuals varied in their dorsal ground color by ranging from being pinkish orange to dark brown. Number and shape of the spots and grayish brown blotches on dorsum varied. Number of grayish brown crossbars on dorsal surface of fingers, toes, lower arms, tarsus, thighs, and tibia varied. Forearm are much more robust in males than in females; nuptial pads are absent in females.

Etymology. The specific epithet "luanchuanensis" is in reference to the type locality.

Comparisons. *Rana luanchuanensis* sp. n. closely resembles the *R. amurensis* Boulenger, 1886 and *R. coreana* Okada, 1928, within the *R. amurensis* species group, but

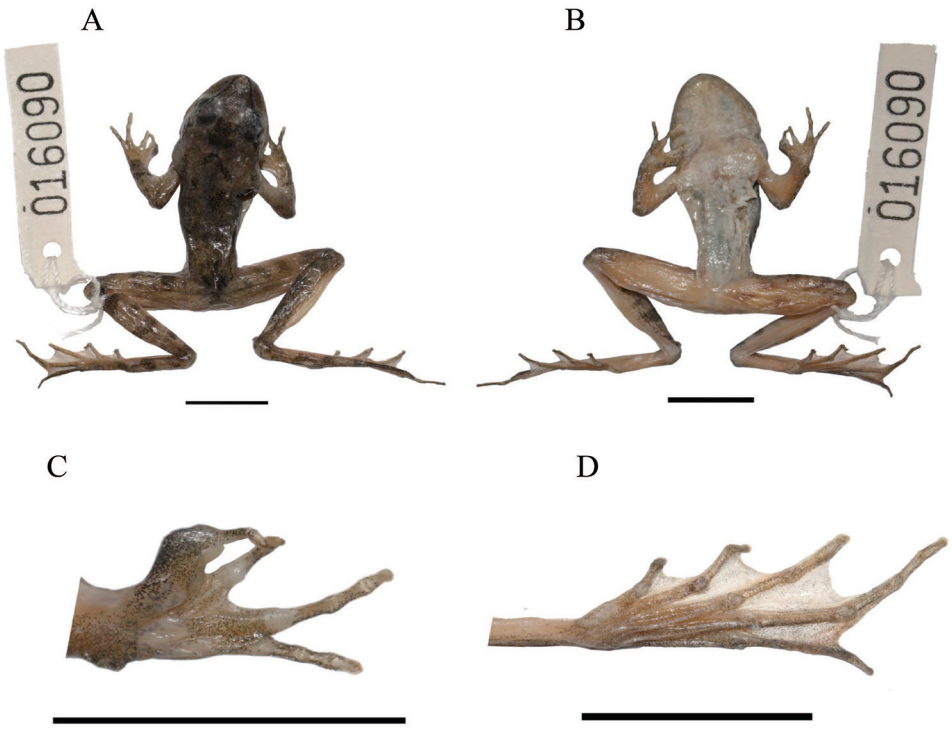

Figure 4. Holotype (KIZ016090) of *Rana luanchuanensis* sp. n. **A** Dorsal view **B** Ventral view **C** Details of left hand showing the nuptial pad **D** Details of left foot showing the extent of webbing. Scale bar 10 mm.

differs from them by the following morphological characters: 1) skin smooth (vs. many tubercles on the dorsum and dorsolateral surfaces of *R. amurensis* and many tubercles on the dorsolateral surface of *R. coreana*); 2) upper white rictal gland absent (vs. present in *R. amurensis* and *R. coreana*); 3) small size, SVL 27.2–33.0 mm in males and 23.7–41.2 mm in females (vs. SVL 48.8–66.4 mm in males and 51.2–70.4 mm in females of *R. amurensis*); 4) nuptial pad forming two groups in males (vs. nuptial pad forming four groups in males of *R. amurensis*); 5) toes two-thirds webbed (vs. toes half webbed in *R. coreana*); 6) transverse grayish brown bars on dorsal surface of fingers and toes, lower arms, tarsus, thighs, and tibia (vs. absent in *R. coreana*); and 7) ventral surface of throat, chest, and belly white with irregular black spots (vs. absence of black spots in *R. coreana*).

Distribution. The species is currently only known from Luanchuan, Henan, China.

Acknowledgements

We thank Li Ding and Yang Lu for specimens collection or providing tissues; Yunyu Wang and Jieqiong Jin for laboratory work; and Yongzhao Huang for providing mor-

phometric data of *R. amurensis*. Weiwei Zhou and Xiaohong Chen provided valuable comments during the manuscript preparation. This work was supported by the grants from the National Natural Science Foundation of China (31401966), the Animal Branch of the Germplasm Bank of Wild Species, Chinese Academy of Sciences (the Large Research Infrastructure Funding), and Innovation Scientists and Technicians Troop Construction Projects of Zhengzhou City (131PLJRC654), the first-class discipline construction project for Forestry in Yunnan (No.51600625).

References

AmphibiaWeb (2017) http://amphibiaweb.org University of California, Berkeley, CA, USA. [Accessed 9 Jan 2017]

AmphibiaChina (2017) The database of Chinese amphibians. Electronic Database accessible at http://www.amphibiachina.org/. Kunming Institute of Zoology (CAS), Kunming, Yunnan, China. [Accessed 9 Jan 2017]

Boulenger GA (1920) A monograph of the American frogs of the genus *Rana*. Proceedings of the American Academy of Arts and Sciences 55: 413–480. https://doi.org/10.2307/20025810

Chambers EA, Hebert PDN (2016) Assessing DNA barcodes for species identification in North American reptiles and amphibians in natural history collections. PLoS ONE 11(4): e0154363. https://doi.org/10.1371/journal.pone.0154363

Che J, Chen HM, Yang JX, Jin JQ, Jiang K, Yuan ZY, Murphy RW, Zhang YP (2012) Universal COI primers for DNA barcoding amphibians. Molecular Ecology Resources 12: 247–258. https://doi.org/10.1111/j.1755-0998.2011.03090.x

Che J, Pang JF, Zhao EM, Matsui M, Zhang YP (2007a) Phylogenetic relationships of the Chinese brown frogs (Genus *Rana*) inferred from partial mitochondrial 12S and 16S rRNA gene sequences. Zoological Science 24: 71–80. https://doi.org/10.2108/zsj.24.71

Che J, Pang JF, Zhao H, Wu GF, Zhao EM, Zhang YP (2007b) Phylogeny of Raninae (Anura: Ranidae) inferred from mitochondrial and nuclear sequences. Molecular Phylogenetics and Evolution 43: 1–13. https://doi.org/10.1016/j.ympev.2006.11.032

Darriba D, Taboada GL, Doallo R, Posada D (2012) JMODELTEST 2: more models, new heuristics and parallel computing. Nature Methods 9: 772. https://doi.org/10.1038/nmeth.2109

Edgar RC (2004) MUSCLE: multiple sequence alignment with high accuracy and high throughput. Nucleic Acids Research 32: 1792–1797. https://doi.org/10.1093/nar/gkh340

Fei L, Hu SQ, Ye CY, Huang YZ (2009) Fauna Sinica. Amphibia. Vol. 3. Anura. Science Press, Beijing, China, 959–1847. [In Chinese]

Hawlitschek O, Moriniere J, Dunz AR, Franzen M, Rodder D, Glaw F, Haszprunar G (2015). Comprehensive DNA barcoding of the herpetofauna of Germany. Molocular Ecology Resources 16(1): 242–253. https://doi.org/10.1111/1755-0998.12416

Hillis DM, Wilcox TP (2005) Phylogeny of the New World true frogs (*Rana*). Molecular Phylogenetics and Evolution 34: 299–314. https://doi.org/10.1016/j.ympev.2004.10.007

Liu CC, Hu SQ (1961) Chinese Tailless Amphibians. Science Press, Peking (Beijing), China, 364 pp. [In Chinese]

Lu YY, Li PP (2002) A new wood frog of the genus *Rana* in Mt. Kunyu, Shandong province, China. Acta Zootaxonomica Sinica 27: 162–166. [In Chinese]

Lu YY, Li PP, Jiang DB (2007) A new species of *Rana* (Anura, Ranidae) from China. Acta Zootaxonomica Sinica 32: 792–801.

Matsui M (2011) On the brown frogs from the Ryukyu Archipelago, Japan, with descriptions of two new species Amphibia, Anura. Current Herpetology 302: 111–128. https://doi.org/10.5358/hsj.30.111

Rambaut A, Suchard MA, Xie D, Drummond AJ (2014) Tracer v1. 6. Available from: http://beast.bio.ed.ac.uk/Tracer [accessed 30 August 2016]

Ronquist F, Huelsenbeck JP (2003) MrBayes 3: Bayesian phylogenetic inference under mixed models. Bioinformatics 19: 1572–1574. https://doi.org/10.1093/bioinformatics/btg180

Rujirawan A, Stuart BL, Aowphol A (2013) A new tree frog in the genus *Polypedates* (Anura: Rhacophoridae) from southern Thailand. Zootaxa 3702: 545–565. https://doi.org/10.11646/zootaxa.3702.6.3

Ryuzaki M, Hasegawa Y, Kuramoto M (2014) A new brown frog of the genus *Rana* from Japan (Anura: Ranidae) revealed by cytological and bioacoustic studies. Alytes 31: 49–58.

Sambrook J, Fritsch EF, Maniatis T (1989) Molecular Cloning: A laboratory Manual, Sec Ed. Cold Spring Harbor Laboratory Press, Cold Springs Harbor, NY, 1659 pp.

Stamatakis A (2014) RAxML version 8: a tool for phylogenetic analysis and post-analysis of large phylogenies. Bioinformatics 30: 131–1313. https://doi.org/10.1093/bioinformatics/btu033

Tamura K, Stecher G, Peterson D, Filipski A, Kumar S (2013) MEGA6: Molecular evolutionary genetics analysis (MEGA) software version 6.0. Molecular Biology and Evolution 30: 2725–2729. https://doi.org/10.1093/molbev/mst197

Yan F, Jiang K, Chen HM, Fang P, Jin JQ, Li Y, Wang SN, Murphy RW, Che J, Zhang YP (2011) Matrilineal history of the *Rana longicrus* species group (*Rana*, Ranidae, Anura) and the description of a new species from Hunan, southern China. Asian Herpetological Research 2: 61–71. https://doi.org/10.3724/SP.J.1245.2011.00061

Yang JX, Zhou WW, Rao DQ, Poyarkov AN, Kuzmin SL, Che J (2010) Validity and systematic position of *Rana altaica* (*Rana*: Ranidae): Results of a phylogenetic analysis. Zoological Science 31: 353–360.

Yuan ZY, Zhow WW, Chen X, Poyarkov NA, Chen HM, Jang-Liaw NH, Chou WH, Matzke NJ, Iizuka K, Min MS, Kuzmin SL, Cannatella DC, Hillis DM, Zhang YP, Che J (2016) Spatiotemporal diversification of the true frogs (genus *Rana*): a historical framework for a widely studied group of model organisms. Systematic Biology 65(5): 824–842. https://doi.org/10.1093/sysbio/syw055

Zhou Y, Yang BT, Li PP, Min MS, Fong JJ, Dong BJ, Zhou ZY, Lu YY (2015) Molecular and morphological evidence for *Rana kunyuensis* as a junior synonym of *Rana coreana* (Anura: Ranidae). Journal of Herpetology 49(2): 302–307. https://doi.org/10.1670/13-111

Appendix 1

Specimens examined

Rana luanchuanensis (n = 38): KIZ016090, KIZ04744-53, KIZ016089, KIZ047383, KIZ047470-87, KIZ016086-88, KIZ016091, KIZ023276, KIZ023282, KIZ023284, KIZ023287-88.

ZooKeys 694: 109–133 (2017)
doi: 10.3897/zookeys.694.15001
http://zookeys.pensoft.net

RESEARCH ARTICLE

A peer-reviewed open-access journal
ZooKeys
Launched to accelerate biodiversity research

Revision of *Massylaea* Möllendorff, 1898 (Stylommatophora, Helicidae)

Houria Bouaziz-Yahiatene[1], Beat Pfarrer[2], Ferroudja Medjdoub-Bensaad[1], Eike Neubert[2]

1 *Laboratoire de Production, sauvegarde des espèces menacées et des récoltes. Influence des variations climatiques. Département de Biologie. Faculté des sciences Biologiques et des Sciences Agronomiques. Université Mouloud Mammeri de Tizi-Ouzou. 15000. Algérie* **2** *Natural History Museum of the Burgergemeinde Bern, Bernastr. 15, CH-3005 Berne, Switzerland*

Corresponding author: *Eike Neubert* (eike.neubert@nmbe.ch)

Academic editor: *Ton de Winter* | Received 11 July 2017 | Accepted 8 August 2017 | Published 29 August 2017

http://zoobank.org/D5786387-3344-4BF1-BF0D-8B12CF666427

Citation: Bouaziz-Yahiatene H, Pfarrer B, Medjdoub-Bensaad F, Neubert E (2017) Revision of *Massylaea* Möllendorff, 1898 (Stylommatophora, Helicidae). ZooKeys 694: 109–133. https://doi.org/10.3897/zookeys.694.15001

Abstract

In this paper some helicoid species from eastern Algeria are investigated using a morphological and molecular approach. The investigation of the genital organs of *M. massylaea* (Morelet, 1851), the type species of the genus *Massylaea* Möllendorff, 1898, showed the same autapomorphic character states as are considered typical for *Eobania* P. Hesse, 1913. These findings are fully supported by the genetic analysis using two mitochondrial and three nuclear markers. Thus, the latter genus has to be considered a synonym of the former. Currently, three species are known to comprise the genus, viz. *M. massylaea*, *M. constantina* (E. Forbes, 1838), and *M. vermiculata* (O. F. Müller, 1774). Several nominal taxa from northern Africa are synonymised with one of the species mentioned here under *Massylaea*. The generic position of the so-called "*Massylaea*" species from the High Atlas Mountains in southern Morocco remains unresolved.

Résumé

Dans cet article, certaines espèces d'Helicidae de l'est de l'Algérie sont étudiées par une approche morphologique et moléculaire. L'étude des organes génitaux de *M. massylaea* (Morelet, 1851), espèce de type du genre *Massylaea* Möllendorff, 1898, a montré les mêmes caractères autapomorphiques que ceux considérés comme typiques pour *Eobania* P. Hesse, 1913. Ces résultats sont pleinement soutenus par l'analyse génétique utilisant deux marqueurs mitochondriaux et trois nucléaires. Ainsi, ce dernier genre doit être

considéré comme un synonyme de l'ancien. Actuellement, trois espèces sont connues pour comprendre le genre, à savoir *M. massylaea*, *M. constantina* (E. Forbes, 1838) et *M. vermiculata* (O. F. Müller, 1774). Plusieurs taxons nominaux de l'Afrique du Nord sont synonymes avec l'une des espèces mentionnées ici sous *Massylaea*. La position générique des espèces dites «*Massylaea*» des montagnes du Haut Atlas dans le sud du Maroc reste non résolue.

Keywords
Massylaea, *Eobania*, Algeria, Kabylie, revision

Mots clé
Massylaea, *Eobania*, Algérie, Kabylie, révision systématique

Introduction

The north-eastern part of Algeria, which is called "La Grand Kabylie", is an area seldom in the focus of malacological research. After the main active period in the second half of the 19th century, which culminated in the monumental work of Bourguignat (1863-1864) on Algeria as a whole, and the very detailed list for the Kabylie published by Letournex (1870). Additional information was then supplied by Péchaud (1880), while the activities of Paul Pallary, who dominated the research on Northafrican molluscs after the death of Bourguignat in 1892 focused mainly on north-west Algeria and Morocco. It is the aim of the senior author of this paper to re-activate the malacological research in the area. Consequently, a combination of freshly collected specimens and a reworking of historical collections were chosen to approach this goal. On the long run, the establishment of a modern checklist for the area summarising and implementing the results of the latest research is planned.

Kobelt (1887) listed his findings of *Massylaea* in Algeria under the generalised genus *Helix* as was the use in these times. Later, Möllendorff (1898) established the genus *Massylaea* including the species *Helix massylaea* Morelet, 1851 and *Helix punica* Morelet, 1851 in this new group. Kobelt (1904: 34, etc.) in his biogeographical analysis used this new name for these two species, but erroneously related them with species from the Greek helicoid genus *Codringtonia* Kobelt, 1898 because of a superficially similar shell morphology. However, he also indicated (1904: 100) that particularly *H. punica* could also be considered as an aberrant form of *Alabastrina* Kobelt, 1904. This statement illustrates the uncertainty of how to define the genus, and which species to allocate there. Hesse (1911: 104) cites Pallary, who suggested to place *Helix bailloni* Kobelt, 1888 [from between Tiut und Mograr (= SW Algeria close to the Moroccan border) also under *Massylaea* and adds that this species was also found close to Constantine, the latter being a confusion with the true *M. massylaea*. Latest in 1915, Pallary started to use the name *Massylaea* also for the large and flat helicoid species living in the High Atlas of Morocco southwest of Marrakesch, like for example *Helix rerayana*

Mousson, 1873, a use that pertains until today. In his anatomical work, Hesse (1915) restricted the use of *Massylaea* to species from east Algeria, but included the Westalgerian *Helix soluta* Terver, 1839 [currently *Alabastrina soluta*], although he found considerable differences even in the outer morphology of the genital organs. In the same work, Hesse also investigated *Eobania*, a generic name he had introduced earlier (1913: 13), and which is based on *Helix vermiculata* O. F. Müller, 1774. Interestingly, he already concluded that *Helix constantina* E. Forbes, 1838 belongs to his genus *Eobania*. However, he never noticed the high morphological similarity between *Massylaea* and *Eobania*. Schileyko (2006) listed *Massylaea* without further comment as a group near Helix Linnaeus, 1758, with 2-3 species from Tunisia, Algeria and Morocco.

Based on specimens collected by the first author of this paper and supplemented by museum's specimens, a new try to disentangle the unclear taxonomic situation is taken using traits derived from shell morphology, anatomy of the genital organs as well as the results of an analysis of partial sequences of the genes COI, 16S, H3, 28S and ITS2.

Material and methods

Living specimens as well as empty shells were collected in the Kabylie (eastern Algeria) during the last two years. For subsequent anatomical and molecular analysis, specimens were preserved and stored in 80% ethanol until dissection and DNA extraction. Specimens used in this study (both shells and preserved animals) are housed in the voucher collection of the first author and in the wet collection of the Natural History Museum of the Burgergemeinde Bern. Some of the sequences used in this study were downloaded from GenBank (https://www.ncbi.nlm.nih.gov).

First assessments of the shell morphological characters were done by using simple magnifying glasses. Preserved animals were dissected under LEICA M212 stereo microscope using thin tweezers. The genital organs of the specimens were removed from the body, the situs and further morphological details were investigated. After that, shells, genital situs and later details of the genital organs were photographed with a LEICA DFC 425 camera combined with a LEICA M205 C. The multifocal images were processed by using an imaging software (Imagic Switzerland).

Molecular study

1.1. Sampling

The specimens from Algeria used in this study were all collected by H. Bouaziz. Species from outside Algeria originate from the collections of Hutterer, Jochum, and Neubert. Data on sampling sites, voucher numbers, GenBank acession numbers and the identification of the specimens used are compiled in the Table 1.

Table 1. Species data.

Family	Species	Locality	Longitude	latitude	Voucher	GenBank acession number CO1	GenBank acession number 16S	GenBank acession number H3	GenBank acession number 28S	GenBank accession number 5.8S-ITS2-28S
Helicidae	*Allognathus* (*Iberellus*) *hispanicus hispanicus*	Ma 10 km 26 road. Escorca, Mallorca, 31SDE8608			EHUMC-1053	KM592543	KM592633			KM592718
Helicidae	*Eobania vermiculata*	Makouda, Tizi Ouzou/ Kabylie, DZ	36.7909	4.0659	NMBE 540544	MF564159	MF564112	MF564174	MF564128	MF564144
Helicidae	*Eobania vermiculata*	Beach between Agia Napa and Capo Greco, CY	34.9728	34.0427	NMBE 549959	MF564160	MF564113	MF564175	MF564129	MF564145
Helicidae	*Eobania vermiculata*	Kusadasi/ Izmir, TR	37.86	27.26	NMBE 549961	MF564161	MF564114	MF564176	MF564130	MF564146
Helicidae	*Helix melanostoma*	Kasserine, TN	35.1722	8.8307	NMBE 520822		MF564115	MF564177	MF564131	MF564147
Helicidae	*Helix melanostoma*	between Rabieux and Saint-Félix-de-Lodez/ Herault, F	43.6628	3.4409	NMBE 540550	MF564162	MF564116	MF564178	MF564132	MF564148
Helicidae	*Helix vladika*	Mokro close to Savnik, MNE	42.95	19.08	NMBE 23348	MF564163	MF564117	MF564179	MF564133	MF564149
Helicidae	*Hemicycla bidentalis*	Anaya, Tenerife, Canary Islands			MVHN-2160	KM592619	KJ458528			KJ458615
Helicidae	*Massylaea constantina*	Draâ-Ben Khedda/ Tizi Ouzou/ Kabylie, DZ	36.7318	3.9654	NMBE 534211a	MF564164	MF564118	MF564181	MF564134	MF564150
Helicidae	*Massylaea constantina*	Draâ-Ben Khedda/ Tizi Ouzou/ Kabylie, DZ	36.7318	3.9654	NMBE 534211b	MF564165	MF564119	MF564182	MF564135	MF564151
Helicidae	*Massylaea constantina*	Azaghar d'Ait Bouaddou, Bounouh, Tizi Ouzou, DZ	36.5214	3.9425	NMBE 540542	MF564166	MF564120	MF564183	MF564136	MF564152

Family	Species	Locality	Longitude	latitude	Voucher	GenBank acession number CO1	GenBank acession number 16S	GenBank acession number H3	GenBank acession number 28S	GenBank accession number 5.8S-ITS2-28S
Helicidae	*Massylaea constantina*	Makouda, Tizi Ouzou/ Kabylie, DZ	36.7909	4.0659	NMBE 540543	MF564167	MF564121	MF564184	MF564137	MF564153
Helicidae	*Massylaea constantina*	Ighil Bourmi, DZ	36.4872	4.0613	NMBE 540545	MF564168	MF564122	MF564185	MF564138	MF564154
Helicidae	*Massylaea massylaea*	Aurès Mountains/ Batna/ Kenchela, DZ			NMBE 519961	MF564169	MF564123	MF564180	MF564139	
Helicidae	*Otala punctata*	Tlemcen, DZ			MVHN-2186	KM592621	KJ458545			KJ458628
Helicidae	*Otala punctata*	Makouda, Tizi Ouzou/ Kabylie, DZ	36.7909	4.0659	NMBE 534228a	MF564170	MF564124	MF564186	MF564140	MF564155
Helicidae	*Otala punctata*	Makouda, Tizi Ouzou/ Kabylie, DZ	36.7909	4.0659	NMBE 534228b	MF564171	MF564125	MF564187	MF564141	MF564156
Helicidae	*Theba subdentata subdentata*	West of Aoulouz/ Souss-Massa-Draa, MA	30.7094	-8.2683	NMBE 549949	MF564172	MF564126	MF564188	MF564142	MF564157
Helicidae	*Tingitana "decussata"*	Montes de Kebdana, Djebel Sebaa Reyal/ Rif, MA	35.0297	-2.6134	NMBE 549840	MF564173	MF564127	MF564189	MF564143	MF564158

Table 2. list of primer pairs used in PCR and sequencing.

Gene	Primer	Sequence	Reference
CO1	LCO1490	5'-GGTCAACAAATCATAAAGATATTGG-3'	Folmer et al. 1994
	HCO2198	5'-TAAACTTCAGGGTGACCAAAAAATCA-3'	
16S	16sF	5'-CGGCCGCCTGTTTATCAAAAACAT-3'	Palumbi et al. 1991
	16sR	5'-GGAGCTCCGGTTTGAACTCAGATC-3'	
28S	LSU-2	5'-GGGTTGTTTGGGAATGCAGC-3'	Wade and Mordan 2000
	LSU-4	5'-GTTAGACTCCTTGGTCCGTC-3'	
5.8S-ITS2-28S	LSU-1	5'-CTAGCTGCGAGAATTAATGTGA-3'	Wade and Mordan 2000
	LSU-3	5'-ACTTTCCCTCACGGTACTTTG-3'	
5.8S-ITS2-28S	ITS2ModA	5'-GCTTGCGGAGAATTAATGTGAA-3'	This work
	ITS2ModB	5'-GGTACCTTGTTCGCTATCGGA-3'	
H3	H3AD	5'-ATGGCTCGTACCAAGCAGACVGC-3'	Colgan et al.2013
	H3BD	5'-ATATCCTTRGGCATRATRGTGAC-3'	

1.2 DNA extraction, PCR amplification and sequencing

Total genomic DNA was extracted from the foot muscle tissue using Qiagen Blood and Tissue Kit (Qiagen cat nr. 69506) in combination with an QIAcube extraction robot (Protocol 430, DNeasy Blood Tissue and Rodent tails Standard). For this work we decided to use the following markers: Two mitochondrial gene fragments, Cytochrome c oxidase subunit I (COI) of 710 bp length and the 16S ribosomal RNA subunit (16S rRNA) for an approximately 480 base-pair segment. Three nuclear genes: the RNA (rRNA) cluster 5.8S-ITS2-28S of approx. 900 bp length (5.8S and 28S only partial, complete internal transcribed spacer 2), 28S ribosomal RNA partial sequence and the Histone 3 (H3) fragment. Primer pairs used in the PCR and sequencing are listed in Table 2.

PCR mixtures consisted of 12.5 µl of GoTaq G2 HotStart Green Master Mix (Promega M7423), 6.5 µl nuclease free H2O (Sigma-Aldrich, W4502), 1 µl of each primer and 2µl template DNA. The 25µl vol. mixtures passed through following listed reaction conditions. For COI, the cycling protocol begins with 3min at 95°C, followed by 35cycles of 1min at 95°C, 1min at 40°C and 1min at 72°C and finally, 5min at 72°C. For 16S the amplification conditions were 3min at 95°C, followed 35 cycles of 1min at 95°C, 1min at 50°C and 1min at 72°C, and finally, 5min at 72°C. ITS-2 and 28S shared the same cycle conditions: 1min at 96°C, followed 35 cycles of 30sec at 94°C, 30sec at 55°C and 1min at 72°C, and finally, 10min at 72°C. For H3, 3min at 95°C, followed 45 cycles of 45sec at 95°C, 45sec at 50°C and 45sec at 72°C, and finally, 10min at 72°C. The PCR condition for the new primer pair ITS2ModA and ITS2ModB are virtually the same as for the LSU-1/3 and varies only in the annealing temperature of 43°C.

The PCR product purification and sequencing was performed by LGC (LGC Genomics Berlin) and difficult/delicate sequences were sent for single tube sequencing to Microsynth (Microsynth Balgach Switzerland).

1.3 Phylogenetic analyses

Geneious Ver.9.1.8 (Biomatters Ltd.) was used for Sequence processing and editing. MAFFT v.7.222 plugin of Geneious (Katoh and Standley 2013), was used with the default setting and the automated algorithm search setting. We decided defining the 16S fragment, ITS2 and 28S as single data blocks. The protein coding gene CO1 and H3 fragments were defined each in 2 data blocks: the first two codon positions as one block and the third codon position as a second. Partitionfinder Ver. 2.1 (Lanfear et al. 2012) was implemented to search the optimal evolutionary models for the partitions using the corrected Akaike Information Criterion (AICc). From the resulting evolutionary models, GTR +G was chosen for further Maximum Likelihood (ML) analysis. ML inference was computed with RAxML (Stamatakis, 2006), using Geneious 's plugin with the rapid bootstrapping setting, the search for the best scoring ML tree and 1000 bootstrapping replicates.

Bayesian Inference (BI) was performed using Mr Bayes v3.2.2 x64 (Huelsenbeck and Ronquist 2001; Ronquist and Huelsenbeck 2003; Ronquist et al. 2012) calculated through the UBELIx (http://www.id.unibe.ch/hpc) the HPC cluster at the University of Bern. The nucleotide model was set to 4by4 and a mixed evolution model with G+I rates was chosen, considering this to be the model best suited for the data of the concatenated sequences of 5 different genes (CO1, 16S, H3, ITS2, 28S). The Monte Carlo Markov Chain (MCMC) parameter was set as follow: starting with four chains and four separate runs for 20 × 106 generations with a tree sampling frequency of 1000 and a burn in of 25%. Trees were displayed on FigTree v1.4.3 (Rambaut 2012).

Abbreviations of shell measurements: D: shell diameter; H: shell height; PD: peristome diameter; PH: peristome height; W: number of whorls.

Abbreviations of collections used

EHUMC	Euskal Herriko Unibersitatea Malacological Collection
MHNG-MOLL	Muséum d'Histoire Naturelle Genève, collection Bourguignat, Switzerland
MHNL	Musée des Confluences, Lyon, France
MNHN	Muséum National d'Histoire Naturelle, Paris, France
MVHN	Museo Valenciano de Historia Natural
NMBE	Natural History Museum of the Burgergemeinde Bern, Switzerland
NMSZ	National Museums of Scotland, Edinburgh
SMF	Senckenberg Research Institut, Frankfurt am Main, Germany

Results

Molecular study

The p-distances of all markers of different *Massylaea* taxa are supplied as electronic supplementary files. The BI and RAxML analyses of the concatenated data set recovered the genus *Massylaea* and separated it from the *Otala*-clade with a maximal statistical support (Figs 1, 2).

Within *Massylaea*, the separation of species was relatively well supported. Although originating from Algeria, Cyprus and northwestern Turkey, the genetic difference between *vermiculata* populations was very low. In the Bayesian analysis (Fig. 1), the *constantina*-clade, however, detected an irregularity: the node that differentiated NMBE 540542 from NMBE 540545 showed only a low support, although both populations are only separated by a distance of 20 km. In the ML tree (Fig. 2), however, the same branching point was highly supported. In both trees, the position of *M. massylaea* within the clade is beyond any doubt.

Similar problems occurred in the *Otala*-clade. The specimens investigated included a species that is here identified as "*Tingitana decussata* Pallary, 1936", which clustered within a group of *punctata*. In both trees, the two *punctata*-specimens NMBE 534228a and b had a low support, although they originate from the same population in eastern Algeria.

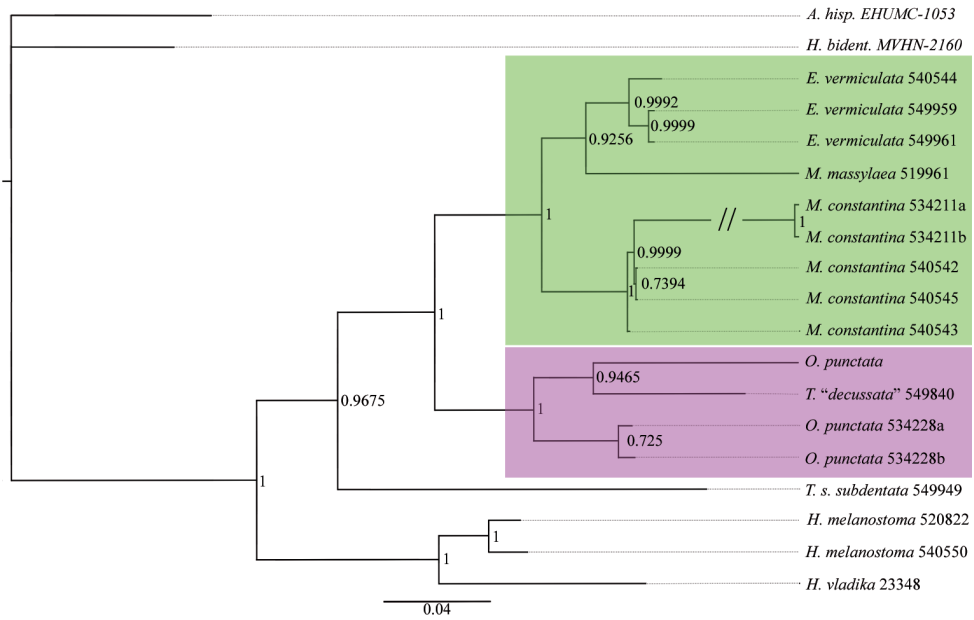

Figure 1. Bayesian Inference tree based on concatenated set of sequences (CO1 16S, H3, 28S, ITS2). Number on the nodes refer to posterior probabilities provided by the BI analysis.

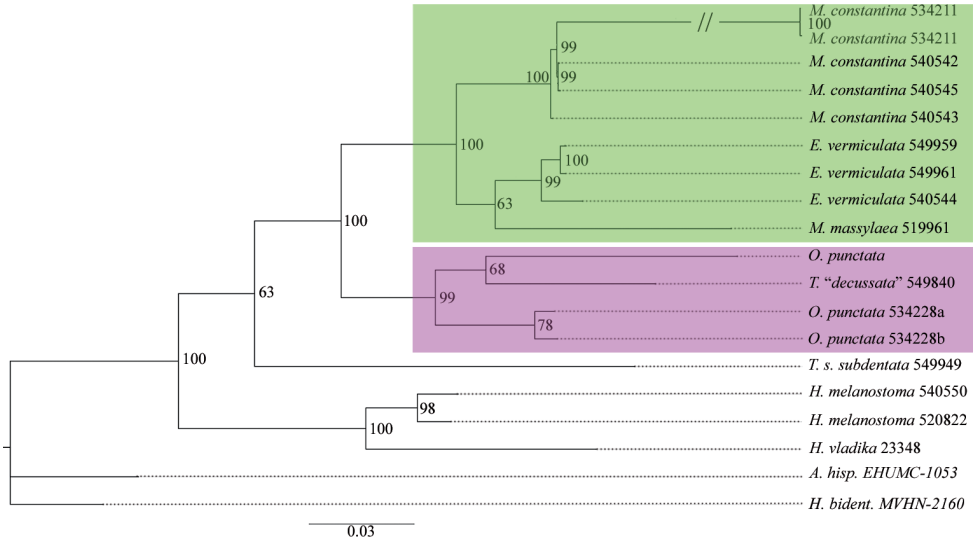

Figure 2. Maximum Likelihood (RAxML) tree based on the concatenated dataset (CO1 16S, H3, 28S, ITS2) Number on the nodes represent bootstrap support values from the ML analysis.

Taxonomic implications

Genus *Massylaea* Möllendorff, 1898

Massylaea Möllendorff, 1908; Nachrichtsblatt der Deutschen Malakozoologischen Gesellschaft 30 (9/10): 120.

Vermiculatiana Caziot, 1908; Mémoires de la Société Zoologique de France 20 (4): 439. Type species (by monotypy): *Helix vermiculata* O.F. Müller, 1774.

Eobania Hesse, 1913; Nachrichtsblatt der Deutschen Malakozoologischen Gesellschaft 45(1): 13. Type species (by monotypy): *Helix vermiculata* O.F. Müller, 1774.

Type species. *Helix massylaea* Morelet, 1851 by tautonymy.

Diagnosis. Large shells, spire flat to considerably raised, with or without a malleate surface structure, aperture without or only with a small labial ridge; penial chamber with a solid "false" penial papilla, epiphallus entering the penial chamber through a laterally situated pore, glandulae mucosae with many subdivided tubules, diverticulum very long.

Massylaea massylaea (Morelet, 1851)

Figs 3–8

Helix massylaea Morelet, 1851; Journal de Conchyliologie 2: 354, pl. 9, fig. 1, 2 [La province de Constantine].

Helix punica Morelet, 1851; Journal de Conchyliologie 2: 352, pl. 9, fig. 3, 4 [habite la grande plaine de Temlouk, au sud-est de Constantine].

Helix massylaea var. *concolor* Bourguignat, 1863; Malacologie de l'Algérie I: 109, plate 9 fig. 9 [no type locality given].

Helix massylaea var. *conoïdea* Bourguignat, 1863; Malacologie de l'Algérie I: 109 [Ouled-Sultan (Deshayes)].

Helix nitefacta Bourguignat in Péchaud 1883; Excursions malagologiques dans le nord de l'Afrique de La Calle a Alger, d'Alger a Tanger: 99 [l'Aurès oriental à Aïn-Tamagra, au sud de Khenchala].

Helix massylaea var. *zenatia* Kobelt, 1887; Iconographie, (2) 3(1): 3 [Wed Zenati].

Helix punica var. *speculatorum* Kobelt, 1887; Iconographie, (2) 3(1): 6, Taf. 63, fig. 320–322 [El Kantara].

Massylaea (?) *severinae* Pallary, 1918; Bulletin de la Société d'histoire naturelle d'Afrique du Nord 9(7): 148 [Aïn el Bey (Constantine) (Philippe Thomas)].

Type specimens. *massylaea*: 2 syntypes NHMUK 1893.2.4.43.5-6; *concolor*: syntypes MHNG-MOLL 118330/3 (Constantine on label in coll.); *conoidea*: not found in coll. Bourguignat; *nitefacta*: syntype MHNG-MOLL 118331/1; *zenatia*: not researched; *speculatorum*: not researched; *punica*: 3 syntypes NHMUK 1893.2.4.1240-1242; *severinae*: no type specimens found so far.

Other records. Sigus, 36.1202°N 6.7849°E (Hesse 1920: 41); Tebessa, 35.4142°N 8.1010°E (Hesse 1920: 43, sub *punica*).

Diagnosis. large grey-yellowish shells with maximum four brown spiral bands, aperture whitish to reddish brown, strong surface sculpture of longitudinal grooves.

Description. Shell large, spire depressed to slightly broad conical, basic colour cream grey-yellowish with brown spiral bands; protoconch large (diameter ca. 5 mm), white; teleoconch whorls regularly increasing, with the last whorl considerably expanding before the aperture, rapidly declining at the aperture; suture deep, surface of teleoconch rough, covered by longitudinal, spirally arranged grooves, sometimes intersected by growth riblets and thus producing a pattern of longitudinal rectangles; spiral bands may be fully developed with maximum four spirals, but all variations including complete fusion of spirals may occur; aperture whitish to reddish brown with a thick lip, columellar part of aperture seldom with a ridge; peristome slightly thickened, umbilicus completely covered by a large reflection of the columellar part of aperture.

Genital organs (only the single subadult specimen (NMBE 519961, sequenced specimen) could be investigated, Fig. 3): Penis short, bulbiform; epiphallus reaching twice the length of penis, with the penis retractor muscle inserting in the distal third of epiphallus; tubiform flagellum reaching the length of penis + epiphallus; penial lumen filled with longitudinal fleshy pilasters; penial chamber with a solid penial papilla (pp2, see also Neubert and Bank 2006); epiphallus opening into the penial chamber via a small pore opposite the "false papilla".

Female part almost undeveloped, the glandulae mucosae only represented by a few small tubules; all other female structures only weakly developed.

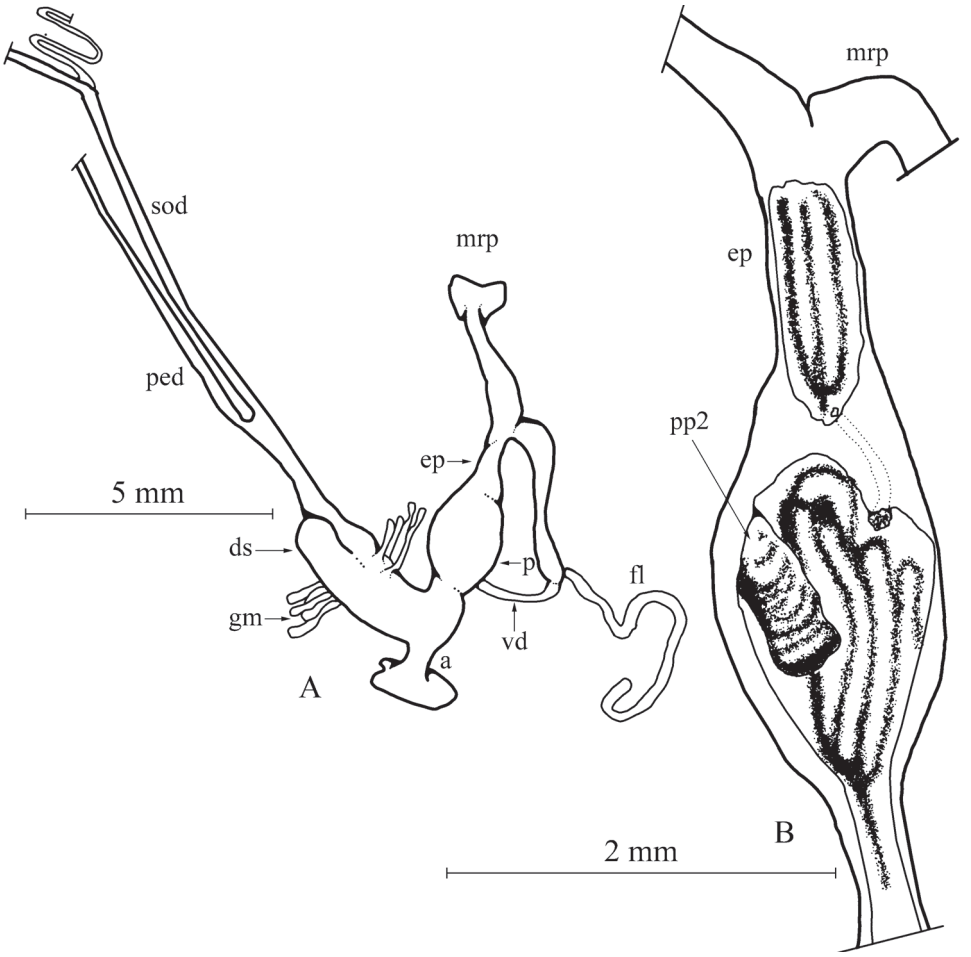

Figure 3. *Massylaea massylaea*, morphology of the genital organs; NMBE 519961/1, Aurés Mountains (sequenced specimen). **A** situs of the hermaphroditic genitals **B** penis opened to show internal structure.

Measurements: Syntype *massylaea*: H = 28.4 mm; D = 40.1 mm; PH = 12.6 mm; PD = 20.5 mm; W = 4.75.

Distribution. Kobelt (1887) supplied data on the distribution of both, *massylaea* and *punica*, and stated that they may occur in hundreds of specimens in a single locality. Given the fact that we here consider *punica* a synonym of *massylaea*, this taxon turns out to be one of the most widespread helicoid species in the southern part of the Eastalgerian mountain range covering southwestern parts of the province of Constantine, and parts of the provinces of Biskra and Blida westwards to Schott el Hodna.

Remarks: The variation in shell morphology mainly concerns the elevation of the spire, which may be rather flat to considerably raised. The second character state that varies is the formation, number and colour of the spiral bands. These may be reddish- to chestnut-brown, some may miss completely or in parts, or are fused to form

Figures 4–8. *Massylaea massylaea* (Morelet, 1851). **4** syntype *Helix massylaea* NHMUK 1893.2.4.43.5, D = 40.1 mm **5** syntype *Helix punica* NHMUK 1893.2.4.1240, D = 36.8 mm **6** syntype *concolor* MHNG-MOLL 118330, D = 36.9 mm **7** syntype *nitefacta* MHNG-MOLL 118331, D = 35.5 mm **8** NMBE 519961, Aurés Mountains, D = 33.65 mm (sequenced specimen). All figures Neubert, natural size.

a cloudy brownish surface. Although Kobelt (1887: 3) states that his specimens usually had spiral bands he separated one form without spiral bands under the name *zenati*, claiming that this form only occurs at this single locality, from which already Bourguignat named his var. *concolor*. According to the specimens known today, spiral banding is quite stable, but there are all variations seen from five bands to completely unicoloured shells.

Hesse (1920: 43, sub *punica*) reports that he received three specimens of this species from Tunisia "Redyef im südlichen Tunis [= Al Rudayyif, Gafsa]. This record has not been reconfirmed by modern collections and is probably based on a confusion with *vermiculata*.

Massylaea constantina (E. Forbes, 1838)

Figs 9–12

Helix constantina E. Forbes, 1838; Annals of Natural History, II: 251, pl. XI, fig. 1 [In waste places among nettles at Bougia].
Helix cirtae Terver, 1839; Catalogue des Mollusques...: 11, pl. 1, fig. 1 [Bone].
Helix constantinae var. *bifasciata* Bourguignat, 1863; Malacologie de l'Algérie I: 114 [La Calle].
Helix constantinae var. *conoidea* Bourguignat, 1863; Malacologie de l'Algérie I: 114, plate 10 fig. 7 [Constantine].
Helix constantinae var. *depressa* Bourguignat, 1863; Malacologie de l'Algérie I: 114 [Ouled-Sultan].
Helix constantinae var. *maxima* Bourguignat, 1863; Malacologie de l'Algérie I: 114 [Constantine].
Helix constantinae var. *minima* Bourguignat, 1863; Malacologie de l'Algérie I: 114 [Bone].
Helix constantinae var. *trifasciata* Bourguignat, 1863; Malacologie de l'Algérie I: 114 [La Calle].

Type specimens. *constantina*: no type specimens could be identified in the E. Forbes collection in NMSZ; *cirtae*: syntype MHNL 45001107; the type specimens for the varietal names of Bourguignat are not identifiable in his collection.

Additional specimens. Ighil Bourmi, 36.4872 4.0613, 1297 m alt., 24.5.2015, Bouaziz, NMBE 540545/1, Makouda, Tizi Ouzou/ Kabylie, 36.7909 4.0659, 440 m alt., 22.3.2015, Bouaziz, NMBE 540543/3, Azaghar, Bounouh, Tizi Ouzou, 36.5214 3.9425, 432 m alt., 26.4.2015, Bouaziz, NMBE 540542/9, Draa Ben Khedaa/ Tizi Ouzou, 36.7318 3.9654, 50 m alt., 6.1.2015, Bouaziz, NMBE 534211/20.

Diagnosis. Medium sized shell, teleoconch smooth, and aperture with a raised columellar ridge.

Description. Shell medium sized, with a globular or broad conical spire, basic colour white to grey, always with up to five brown spiral bands; protoconch large (diameter ca. 4 mm), white; all teleoconch whorls regularly increasing, with the last whorl rapidly declining at the aperture; suture of moderate depth, surface of teleoconch

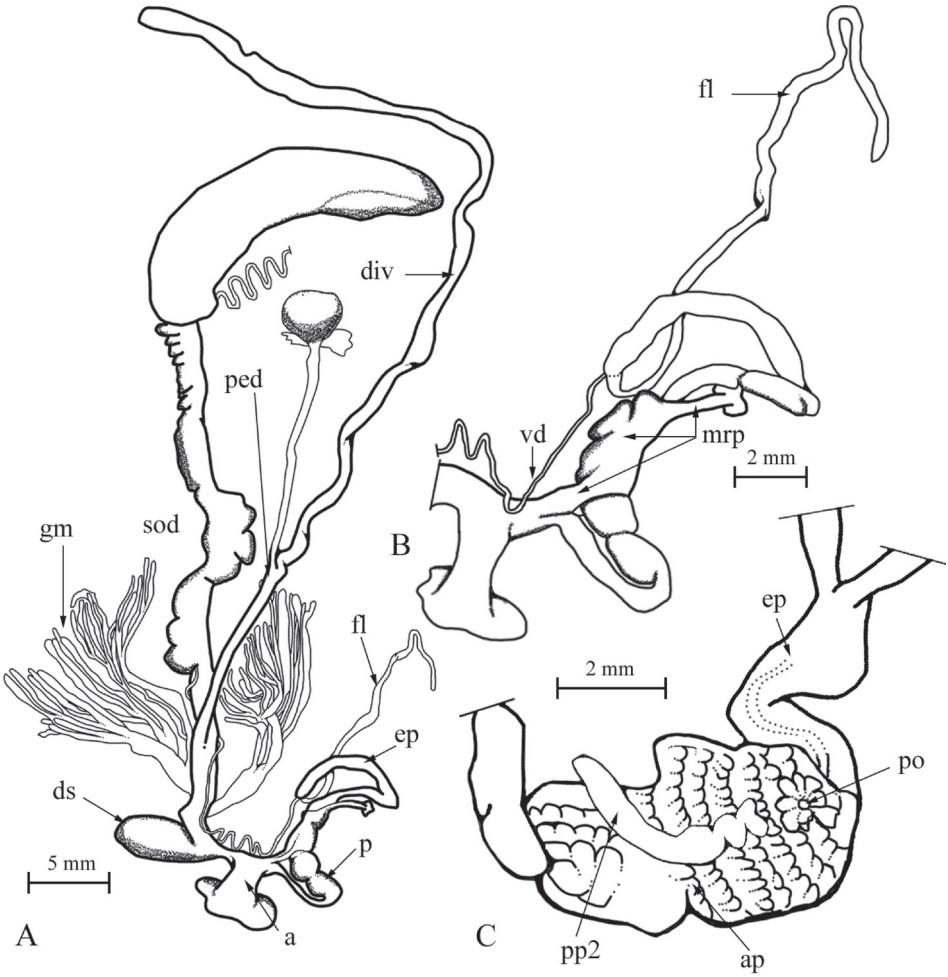

Figure 9. Genital organs of *M. constantina*; NMBE 540542, Azaghar; **A** situs **B** outer morphology of male organ **C** interior of penis. Abbreviations used: a = atrium; ap = annular pad; div = diverticulum; ds = dart sac; ep = epiphallus; fl = flagellum; gm = glandulae mucosae; mrp = penial retractor muscle; p = penis; ped = pedunculus; po = pore of penial papilla; pp2 = second penial papilla; sod = spermoviduct; vd = vas deferens.

smooth; usually with five spiral bands with spiral 2+3 often very close or almost merging; aperture always porcelain white with a thick lip, columellar part of aperture with a raised ridge; peristome slightly thickened, umbilicus completely covered by a large reflection of the columellar part of aperture.

Genital organs (Fig. 9A–C): penis subdivided in three parts, with an elongate distal tube connecting to the atrium, and a bilobed muscular proximal part with the internal boundary marked by an annular pad (Giusti et al. 1995); epiphallus longer than penis, enveloped by a strong penial retractor muscle that connects with a fascicle to the atrium, flagellum a long, simple tube; internally, the proximal penial chamber filled by

Figures 10–12. *Massylaea constantina* (E. Forbes, 1838). **10** Original figure of E. Forbes, pl. XI, Figure 1 [1839], size adopted to next figure **11** syntype *cirtae* MHNL 45001107, D = 27.2 mm **12** NMBE 534211, Draa Ben Khedaa, D = 30.25 mm. All figures Neubert/Bochud, natural size.

a solid penial papilla (pp2, see also Neubert & Bank 2006); epiphallus opening into the penial chamber via a small pore.

Dart sac opening laterally into the short vagina; glandulae mucosae with two central stems giving rise to at least three subsequent branches with at least 40 tubules; diverticulum branches off in a central position from the pedunculus reaching a length of at least 30 mm.

Measurements: syntype *cirtae*: H = 21.3 mm; D = 27.2 mm; PH = 8.6 mm; PD = 12.9 mm; W = 4.75.

Distribution. This species is known from Tizi Ouzou in the Grand Kabylie towards the northern parts of the province of Constantine. In many places it lives in sympatry with *M. vermiculata*.

Remarks. This species proved to be quite stable in terms of conchological traits. The number of five spiral bands is very stable as well as the white and smooth teleoconch. Some colour morphs of *M. vermiculata* look quite similar; however, so far all shells of the latter species could be differentiated by presence of the malleate teleoconch surface. This surface structure may be reduced to a small area above and around the aperture, but it is always clearly discernible. It differs from *M. massylaea* by its considerably smaller shell, the high globular spire, and the smooth teleoconch surface.

***Massylaea vermiculata* (O. F. Müller, 1774)**
Figs 13–16

Helix vermiculata O. F. Müller, 1774; Vermium terrestrium et fluviatilium 2: 21 [In Italia sabulosis juxta torrentes].
Helix bonduelliana Bourguignat, 1863; Mollusques nouveaux, litigieux ou peu connus, fasc. 1: 9, plate 3 figs 1–4 [Province d'Oran].
Helix vermiculata var. *albida* Bourguignat, 1863; Malacologie de l'Algérie I: 112, plate 8 fig. 10 [La Calle].
Helix vermiculata var. *aspersa* Bourguignat, 1863; Malacologie de l'Algérie I: 112 [Cherchell].
Helix vermiculata var. *expallescens* Bourguignat, 1863; Malacologie de l'Algérie I: 112 [Environs d'Alger, Blidah].
Helix vermiculata var. *minuta* Bourguignat, 1863; Malacologie de l'Algérie I: 112 [Ile de Galite].
Helix vermiculata var. *trizonata* Bourguignat, 1863; Malacologie de l'Algérie I: 112 [Philippeville].
Helix fleurati Bourguignat, 1868; Histoire Malacologique de la Régence de Tunis: 12, plate 1 fig. 1–3 [Env. de Tunis (Champs au sud et au sudest de Tunis, entre un vieux puits espagnol et les collines de Sidi ben Hassen et de la forteresse Bordj el Raïs. Ruines d'Oudena. Ruines d'Utique et de Carthage. non loin de la chapelle Saint-Louis]
Helix fleurati var. *obesa* Bourguignat, 1868; Histoire Malacologique de la Régence de Tunis: 13 [no locality information given].
Helix fleurati var. *subcarinata* Bourguignat, 1868; Histoire Malacologique de la Régence de Tunis: 13, plate 1 fig. 4 [no locality information given].
Helix (*Macularia*) *vermiculata* var. *conoidea* Issel, 1880; Annali del Mus. Civ. di St. Nat. di Genova, Vol. XV: 263 [Sahel, fra Susa e Bir el Buita e fra Susa ed El Gem].
Helix (*Macularia*) *vermiculata* var. *depressa* Issel, 1880; Annali del Mus. Civ. di St. Nat. di Genova, Vol. XV: 263 [Cartagine].
Helix (*Macularia*) *vermiculata* var. *minuta* Issel, 1880; Annali del Mus. Civ. di St. Nat. di Genova, Vol. XV: 264 [Is. Galita, Galitone, Aguglia, Gallina (Violante, 1877). Cartagine (Bellucci, 1875)].
Helix toukriana Bourguignat in Péchaud, 1883; Excursions malagologiques dans le nord de l'Afrique de La Calle a Alger, d'Alger a Tanger: 37 [hauts plateaux du Sersou, entre Aïn-Toukria et le Nahr-Ouassel, dans la direction de Sebaïn-Aïoun].
Helix aecouria Letourneux et Bourguignat, 1887; Prodrome de la malacologie terrestre et fluviatile de la Tunisie: 7 [Environs d'Houmt-Souk dans l'ile de Djerba].
Helix vermiculata var. *saharica* Kobelt, 1887; Iconographie, (2) 3(1): 9, Taf. 6, fig. 343–345 [Biskra].

Type specimens. *bonduelliana*: 1 syntype MHNG-MOLL 118415; *aecouria*: 3 syntypes MHNG-MOLL 118413; *fleurati*: syntypes MHNG-MOLL 118440/7 (Env. de Tunis); *toukriana*: syntype MHNG-MOLL 118487; *saharica*: not researched.

Diagnosis. Medium sized shell, teleoconch with a malleate surface sculpture, and aperture with a slightly raised columellar ridge.

Description. shell medium sized, with a globular to depressed conical spire, basic colour white to grey, up to five brown spiral bands may be present or completely missing; protoconch large (diameter ca. 4 mm), corneous to white; whorls regularly increasing, the last whorl declining at the aperture; teleoconch suture of moderate depth, surface of teleoconch with a characteristic malleate sculpture (sometimes only present close to the aperture!); spiral bands 2+3 often merging, and bands may fuse to a large brown area on the last whorl before the aperture; aperture usually porcelain white with a thick lip, columellar part of aperture with a raised ridge; peristome slightly thickened, umbilicus completely covered by a large reflection of the columellar part of aperture.

Genital organs (after Giusti et al. 1995; Neubert and Bank 2006; Holyoak and Holyoak 2017): penis clubshaped, bipartite; the bilobed muscular proximal part not visible in outer morphology; epiphallus longer than penis; penial retractor muscle simple, attaching at the boundary of penis and epiphallus; internally, the proximal penial chamber filled by a solid penial papilla, epiphallus opening into the penial chamber via a small pore or on top of a flat papilla.

Dart sac opening laterally into the short vagina; glandulae mucosae with two central stems giving rise to at least three subsequent branches with at least 40 tubules; diverticulum branches off in a central position from the pedunculus surpassing the bursa copulatrix enormously.

Distribution. This species is widely recorded throughout Tunisia and eastern Algeria.

Remarks. The synonymy list and illustrations only cover synonyms of *M. vermiculata* important for the area from east Algeria and Tunisia. Here, this species inhabits Mediterranean shrublands as well as the wooded hinterland. It also tolerates coastal dunes with salty spray, and semiarid steppes. Holyoak and Holyoak (2017) justify the synoynmisation of *constantina* with *vermiculata* with the similar morphology of the genital organs and the wide overlap in shell size and banding pattern. However, in many land-snails, closely related species cannot be differentiated by the morphology of their genital organs. More attention should be paied to the construction of the penis (bilobed muscular proximal part visible from outside or not) and the variability of attaching system of the retractor muscle, which is much larger (and also connects to the atrium) in the specimen of *constantina* than in any *vermiculata* seen so far. The most important character state that separates the species is the absence of any malleation on the shell surface in *constantina*. Additionally, the phenotypic plasticity of the shells of *vermiculata* is markedly contrasted by the congeneric *M. constantina*, which is extremely stable in respect of the spiral banding pattern.

One species mentioned by Kobelt (1887) as a closely related species to his *vermiculata-constantina*-complex is *Helix bonduelliana* Bourguignat, 1863, with the type locality "Province d'Oran" in western Algeria. Kobelt doubts the correctness of this locality, and speculates that it might originate from Tunisia. According to his personal experience in Algeria, *M. vermiculata* reaches the Isser, but does not expand much to the west of this river. The only exception he found was Cherchell west of Algiers,

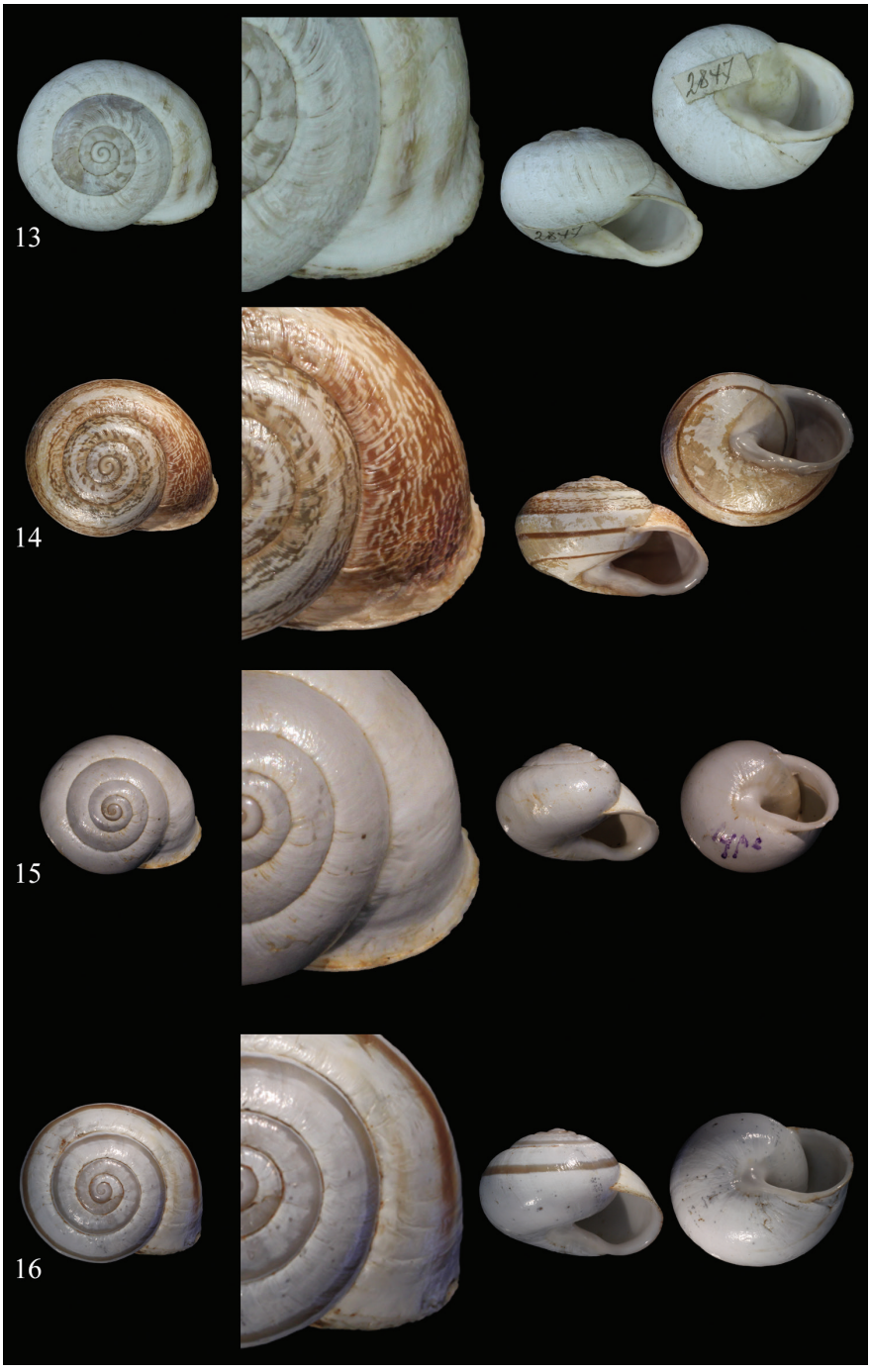

Figures 13–16. *Massylaea vermiculata* (O. F. Müller, 1774). **13** syntype *Helix toukriana* MHNG-MOLL 118487, D = 29.7 mm **14** syntype *Helix aecouria* syntype MHNG-MOLL 118413, D = 28.4 mm **15** syntype *Helix fleurati* MHNG-MOLL 118440, D = 23.9 mm **16** *Helix bonduelliana* Bourguignat, 1863 syntype MHNG-MOLL 118415, D = 27.0 mm. — All figures Neubert/Bochud, natural size.

where the species occurred in large numbers, but restricted to and around the harbour, so it can be considered being introduced there. It is not clear how the situation is today along the central and western Algerian coast, but Kobelt's lines can be seen as an information on the natural range of this species in northern Africa. In the same year, Bourguignat (1887: 8) records *H. bonduelliana* from Ghardimaou (Tunisia) (= MHNG-BBT 118417/3). Bourguignat's collection has another record from "environs de Tunis" under MHNG-MOLL 18416/1. Later, Pallary (1898) mentions his and Debeaux's unsuccessful attempts to recollect the species in Oran. Summarising it can be said that the type locality of *H. bonduelliana* is apparently wrong, and the specimens are very probably of Tunisian offspring. This nominal taxon fully falls into the colour variation of *M. vermiculata*, which can reach from completely white shells as exemplified by *H. fleurati* (Fig. 15) to the typical morph as seen in *H. aecouria* (Fig. 14). The shell shape, however, is quite stable in most of these forms, and typical for *M. vermiculata*. The synonymisation of *saharica* Kobelt, 1887 needs reconfirmation by study of the type specimens.

Discussion

The results of our study strongly support the monophyly of the genus *Massylaea*. This is evidenced by traits of the genital organs as well as by the genetic analysis, which is based on two mitochondrial and three nuclear markers.

Although only a subadult specimen of *M. massylaea* was available for investigation, the autapomorphic character states of presence of a "blind" penial papilla in combination with a separate epiphallial pore could clearly be detected (Fig. 3). This type of internal penial construction is also seen in *M. constantina* (Fig. 9) and in *M. vermiculata* (Neubert and Bank 2006). It differs profoundly from other helicoid genera like for example the syntopic *Otala punctata* (O. F. Müller, 1774), which shows the plesiomorphic type of a bipartite penis with two subsequent penial papillae (De Mattia and Mascia 2011).

In the genetic analysis, the *Massylaea*-clade is supported by high bootstrap values (Figs 1, 2). Within the clade, a separation of *M. constantina* from a combined cluster *vermiculata-massylaea* can be seen. The *constantina* population NMBE 534211 shows an enormous number of base-pair substitutions if compared to the other three congeners. The distance matrixes show that the generated 5.8S-ITS2-28S sequence is responsible for the caused deviation. In an ITS2 alignment, the NMBE 534211 population showed a higher variation, often up to 84bp, in the complete second Internal Transcriber Spacer region, in comparison to the congeners. NMBE 534211 from Draâ-Ben Khedda seems to be constituted by a faster evolving population, indicated by the much longer branch reflecting the higher base pair substitutions. We could hypothesize that we probably are witnessing the beginning of a speciation process, but we have to collect more specimen from the complete distribution area to be more conclusive about the existing species boundaries.

Figure 17. *Helix boghariensis* Debeaux, 1857 [Rochers en face le village arabe Ksar·el-Boghari]; syntype MNHN IM-2000-31714, D = 34.0 mm. Figure 17 by courtesy of MNHN, Paris, natural size.

The generic name *Massylaea* Möllendorff, 1898 has been widely used for a number of species and thus cannot be treated as a nomen oblitum. It has precedence over *Eobania* Hesse, 1913, and the widespread species *Helix vermiculata* O. F. Müller, 1774, has to be classified under this generic name. Currently, the use of *Massylaea* should be restricted to the three species treated here; the so-called "*Massylaea*" species from the High Atlas Mountains in southern Morocco are widely unknown, and probably form a separate generic entity. At least 12 nominal taxa can be affiliated to this radiation, but species delimitation poses a major problem at the moment.

Already Kobelt (1887) remarked the similarity of *Helix boghariensis* Debeaux, 1857 (syntype Fig. 17), with the *constantina-vermiculata*-group. In fact the shell of this species is close to *M. constantina*, and lacks the teleoconch sculpture of *M. vermiculata*. Kobelt remarked that the type locality Boghar is far from the range of *M. constantina*, which was true at his time. Due to the collections of the senior author we now know that *M. constantina* also inhabits the area of Tizi Ouzou. The distance (as the crow flies) between these localities is about 150 km. From a shell morphological point of view there is no evidence for any major difference between *constantina* and *boghariensis* supporting the separation of the latter as a species in its own rights. This question can only be sorted out by an investigation of animals from Boghar. Holyoak and Holyoak (2017) synonymise this taxon with *E. vermiculata* without further comments.

The enormous radiation of Helicid species and genera in northern Africa is poorly understood and still in a chaotic state, and often complained about like recently in Holyoak and Holyoak (2017). Although not in the centre of the helicoid radiation in northern Africa, our results may contribute to some clarifications like for example in the "*Otala*-clade". By chance, a specimen of *T.* "*decussata*" (nomen nudum) could be included in our study. This taxon is conchologically similar to *Archelix minettei* Pallary, 1917 from "Tarzout-du-Guigou", which is the type species of *Tingitana* Pallary, 1918, a genus used to accommodate a number of helicoid species from all over Morocco. The position of *T.* "*decussata*" in our concatenated trees (see Figs 1, 2) indicates that *Tingitana* is close to or even identical with *Otala*. This result coincides with Razkin et al. (2015), who found that *T. orientalis* Pallary, 1918 from Berkane clusters within the *Otala* clade. However, it is not clear whether this species is a *Tingitana* in its original sense, or rather a classical *Otala*. Although we have a more clear evidence for a synonymisation of *Tingitana* with *Otala* we still consider this synonymy as premature as

long as evidence through study of anatomical and genetic data of the type species of the genera is supplied. It should be mentioned that the form "*decussata*" lives in the summit area of the Kebdana (leg. R. Hutterer); the population consists exclusively of strongly keeled specimens.

Holyoak and Holyoak (2017) revisited the problems within *Otala* and *Eobania* in northern Africa adding valuable distribution data. However, some details are astonishing. The authors cover the complete distribution area of the genus *Massylaea* and collect (and synonymise) a reasonable number of available species-level names, but completely omit *Helix massylaea* Morelet, 1851! The only reference to the genus is restricted to a note, where it is mentioned as a host of *Helix soluta* Michaud, 1833, perpetuating the erroneous ideas of Kobelt (see introduction). A concept for *Massylaea* is completely missing, and all taxa are lumped under *Eobania vermiculata*. Puzzlingly, the only exception is *Helix punica* (from south of Constantine), which is affiliated by the authors to *Loxana* Pallary, 1899. This genus is based on *Helix beaumieri* Mousson, 1873, which lives in the High Atlas south of Marrakech. It is currently considered to constitute a subgenus of *Alabastrina* Kobelt, 1904; the new concept of *Loxana* is not explained, delimited or justified. Under the same generic name *Loxana*, the enigmatic *Helix rerayana* Mousson, 1873 is treated, a species which originates from the same larger area as *H. beaumieri*, but differs enormously in shell shape, so a congeneric position for these two taxa will require good arguments (which are not supplied in this paper). All names allocated by us to the three accepted taxa under *Massylaea* (and scrutinized by checking and presenting the type specimens), are lumped by Holyoak and Holyoak (2017) under *E. vermiculata*, a concept, which does not comply with our genetic data.

Concluding it can be said that still, the chaos is not fully disentangled, and that the rigorous lumping of taxa is probably not fully supported. We agree with Holyoak and Holyoak (2017: 420) that "it has been taken as axiomatic that the species recognised should be identifiable from morphological characters, of shells, genital anatomy, or both". But then, prior to any decision taken, the initial point should be the study and presentation of type specimens. This is a major service to other students of the fauna and greatly facilitates the understanding of subsequent decisions made. It could help to clarify the identity of species-level taxa used in genetic studies, and thus constitute a major contribution towards stabilisation of taxonomy and nomenclature.

Acknowledgements

We are very grateful to Estée Bochud, NMBE, for preparing several of the photos used in this paper. We are very grateful to Jean Mariaux and Emanuel Tardy, MHNG Genève, for providing access to the Bourguignat collection. This contribution could only be realised by support through GBIF.CH (Neufchâtel, Switzerland). Eike Neubert would like to thank R. Janssen for years of access to the collection of SMF, which greatly helped to understand the malacological diversity in Northern Africa. We are very grateful to P. Bouchet, and V. Héros, MNH, Paris, for the permission to use a pic-

ture from the database of MNHN, to Vincent Prié for a specimen of *H. melanostoma* from southern France, to S. Pye for searching for type specimens of *H. constantina* in the collection of the National Museums of Scotland, Edinburgh, and C. Audibert from the Musée des Confluences, Lyon for his interest and valuable support of H. Bouaziz-Yahiatene.

References

Bourguignat J-R (1863–1864) Malacologie de l'Algérie ou histoire naturelle des animaux mollusques terrestres et fluviatiles recueillis jusqu'à ce jour dans nos possessions du nord de l'Afrique. — 1: fasc. 1: 1–80, pls I–VIII [May 1863]; fasc. 2: 81–192, pl. IX, X, XIII–XVIII [June 1863]; fasc. 3: 193–294 pls XI, XII, XIX–XXXII [Nov. 1863]; [described species extracted] 2: fasc. 4: 1–144, pl. I–V, VII [Jan. 1864]; fasc. 5: 145–232, pl. VI, VII, IX–XI, XV, XVI, XVIII–XXVI [Apr. 1864]; fasc. 6: I–XII [to be bound prior to fasc. 1] [with replacement pages 9–32 in fasc. 1] 233–380, pls. XII–XIV, XVII [Dec. 1864]. Paris (Challamel ainé).

Bourguignat J-R (1863–1870) Mollusques nouveaux, litigieux ou peu connus. — Vol. 1 (Première Centurie): Tit. + 324 pp., pls 1–45 (1863–1868); Vol. 2 (inachevée): 1–55, pls 1–4 (1870). Paris (F. Savy, Bouchard-Huzard). Vol. 1: l[ère] décade, l[er] mars 1863: pp. 1–22, pl. 1–4 [= Revue et Magasin de Zoologie, (2) 15 (3): 100–111, (4): pl. 5–8]; 2[e] décade, l[er] mai 1863: pp. 23–49, pl. 5–7 [= Revue et Magasin de Zoologie, (2) 15 (5): 179–187, pl. 18–19, (7): 252–261; pl. 7 est supplémentaire dans le livre]; 3[e] décade, l[er] décembre 1863: pp. 51–82, pl. 8–11; 4[e] décade, mai 1864: pp. 83–130, pl. 12–19; [= Revue et Magasin de Zoologie, (2) 16 (6): 161–179, pl. 11–13, (7): 193–212, pl. 14, (8): pl. 15–16, (9): pl. 17, (11): pl. 18]; 5[e] décade, 1[er] novembre 1865: pp. 131–170, pl. 20–28; [= Revue et Magasin de Zoologie, (2) 17 (11): 337–347, pl. 16–21, (12): pl. 22–24 (1865), 18: (1): 6–23 (1866); l'ordre de quelques planches a été changé: pl. 24 = pl. 23, pl. 25 = pl. 21, pl. 26 = pl. 22, pl. 27 = pl. 20, pl. 28 = pl. 24]; 6[e] décade, 1[er] janvier 1866: pp. 171–198, pl. 29–31; 7[e] décade, 1[er] février 1866: pp. 199–221, pl. 32–34; 8[e] décade, 1[er] décembre 1867: pp. 223–257, pl. 31 [réimpression], pl. 35–38; 9[e] décade, 1[er] séptembre 1868: pp. 259–294, pl. 39–41; 10[e] décade, l[er] décembre 1868: [3] pp. + pp. 295–324 [319–324: Table alphabétique], pl. 42–45. — Vol. 2: 11[e] décade 1[er] janvier 1870: 1–27, pl. 1–2 [= Revue et Magasin de Zoologie, (2) 22 (1): 14–30, pl. 14–15]; 12[e] décade 1[er] février 1870: 29–55, pl. 3–4 [= Revue et Magasin de Zoologie, (2) 22 (3): 87–97, (5): 166–171, pl. 16–17.] [Du vol. 2 a paru seulement une livraison de la 11[e] et 12[e] décade ensemble]

Bourguignat J-R (1868) Souvenirs d'une exploration scientifique dans le nord de l'Afrique, III. Histoire malacologique de la Régence de Tunis. 36 pp, 1 pl., 2 cartes. Paris (Challamel ainé).

Caziot E (1908) Compte rendu d'une excursion malacologique dans la partie supérieure de la Vallée de la Roya, et dans le voisinage de la mer, sur la rive droite du Var, près Nice. Mémoires de la Société Zoologique de France 20(4) [1907]: 435–469. [6 June]

Colgan D, McLauchlan A, Wilson GDF, Livingston SP, Edgecombe GD, et al. (1998) Histone H3 and U2 snRNA DNA sequences and arthropod molecular evolution. Australian Jour-

nal of Zoology 46: 419–437. https://doi.org/10.1071/ZO98048 https://doi.org/10.1071/ZO98048

De Mattia W, Mascia F (2011) *Otala punctata* (O. F. Müller, 1774) in Italy. Iberus 29(1): 39–46.

Debeaux O (1857) Catalogue des mollusques vivants observés aux environs de Boghar (Algérie). Recueil trav. Societe d'agriculture d'Agen 8: 317–329.

Folmer O, Black M, Hoe W, Lutz R, Vrijenhoek R (1994) DNA primers for amplification of mitochondrial cytochrome c oxidase subunit I from diverse metazoan invertebrates. Molecular Marine Biology and Biotechnology 3(5): 294–299.

Forbes E (1838) On the land and freshwater mollusca of Algiers and Bougia. Annals of Natural History II: 250–255, pl. XI, XII [plates published in Feb. 1839] https://doi.org/10.1080/00222933809496670

Giusti F, Manganelli G, Schembri, PJ (1995) The non-marine molluscs of the Maltese Islands. Torino, 607 pp.

Hesse P (1908–1911) In: Rossmässler E A, Iconographie der Land- & Süßwasser-Mollusken mit vorzüglicher Berücksichtigung der europäischen noch nicht abgebildeten Arten, Taf. 421–450 [1909–1911]; Wiesbaden (Kreidel), (2) 14 (5/6): 129–172, Taf. 381–390 [1908]; (2) 16 (1/6): 1–119.

Hesse P (1913) Neue Funde aus der Umgebung von Philipoppel. Nachrichtsblatt der Deutschen Malakozoologischen Gesellschaft 45(1): 12–16.

Hesse P (1915–1920) In: Rossmässler EA Iconographie der Land- und Süßwasser-Mollusken, mit vorzüglicher Berücksichtigung der europäischen noch nicht abgebildeten Arten. C.W. Kreidel's Verlag, Berlin & Wiesbaden, (2) 23 (1/2): 1–72, pl. 631–640 [1915]; (2) 23 (3/4): 73–152, pl. 641–650 [1919]; (2) 23 (5/6): 153–262, pl. 651–660 [1920].

Holyoak DT, Holyoak GA (2017) A revision of the land-snail genera *Otala* and *Eobania* (Gastropoda, Helicidae) in Morocco and Algeria. Journal of Conchology 40(6): 419–490.

Huelsenbeck JP, Ronquist F (2001) MRBAYES: Bayesian inference of phylogeny. Bioinformatics 17: 754–755. https://doi.org/10.1093/bioinformatics/17.8.754

Issel A (1880) Molluschi terrestri et d'aqua dolce viventi e fossili. Annali del Museo Civico di Storia Naturale di Genova 15: 259–282.

Kearse M, Moir R, Wilson A, Stones-Havas S, Cheung M, Sturrock S, Buxton S, Cooper A, Markowitz S, Duran C, Thierer T, Ashton B, Mentjies P, Drummond A (2012) Geneious Basic: an integrated and extendable desktop software platform for the organization and analysis of sequence data. Bioinformatics 28:1647–1649. https://doi.org/10.1093/bioinformatics/bts199

Kobelt W (1887–1888) In: Rossmässler EA: Iconographie der Land- & Süßwasser-Mollusken mit vorzüglicher Berücksichtigung der europäischen noch nicht abgebildeten Arten. Kreidel, Wiesbaden, (2) 3 (1/2): 1–12, Taf. 61–70 [1887]; (2) 3 (3/4): 13–36, Taf. 71–80 [1887]; (2) 3 (5/6): 37–60, Taf. 81–90 [1888].

Kobelt W (1904) Register. In: Rossmässler EA: Iconographie der Land- & Süßwasser- Mollusken mit vorzüglicher Berücksichtigung der europäischen noch nicht abgebildeten Arten, Karten, (2) 11: I–XII., 1–342, 6.

Lanfear R, Frandsen PB, Wright AM, Senfeld T, Calcott B (2016) PartitionFinder 2: new methods for selecting partitioned models of evolution for molecular and morphological

phylogenetic analyses. Molecular biology and evolution. https://doi.org/10.1093/molbev/msw260

Letourneux A, Bourguignat J-R (1887) Prodrome de la malacologie terrestre et fluviatile de la Tunisie. Imprimerie nationale, Paris, 1–166. https://doi.org/10.5962/bhl.title.132280

Letourneux A (1870) Excursions malacologiques en Kabylie et dans le Tell Oriental. Paris, Annales de Malacologie 1: 258–322. [pl. 6]

Katoh, Misawa, Kuma, Miyata (2002) MAFFT: a novel method for rapid multiple sequence alignment based on fast Fourier transform. Nucleic Acids Res. 30: 3059–3066.

Möllendorff Ov (1898) Studien zur Zoogeographie von Dr. W. Kobelt. II. Band. Die Fauna der Meridionalen Sub-Region. C. W. Kreidel, Wiesbaden 898, gr. 8°, 368 pp. Nachrichtsblatt der Deutschen Malakozoologischen Gesellschaft 30(9/10): 112–121.

Morelet A (1851) Appendice à la conchyliologie de l'Algérie; description d'espèces nouvelles. Paris, Journal de Conchyliologie 2: 351–361.

Mousson A (1873) Diagnosen neuer Mollusken aus West-Marokko, von Dr. von Fritsch und Dr. Rein gesammelt. Malakozoologische Blätter 21: 149–157.

Müller OF (1774) Vermium terrestrium et fluviatilium, Havniae et Lipsiae, 2, 214 pp + X; .

Neubert E, Bank RA (2006) Notes on the species of *Caucasotachea* C. Boettger 1909 and *Lindholmia* P. Hesse 1919, with annotations to the Helicidae (Gastropoda: Stylommatophora: Helicidae). Archiv für Molluskenkunde, Frankfurt am Main, 135(1): 101–132; .

Pallary P (1899) Deuxième contribution à l'étude de la faune malacologique du Nord-Ouest de l'Afrique. Supplement à «La faune malacologique du Maroc» de A. Morelet. Journal de Conchyliologie, Paris 46 (2) [1898]: 49–170, pl. 5–9. [9 February]

Pallary P (1915) Description de quelques mollusques nouveaux du Grand Atlas. Bulletin du Muséum Nationale d'Histoire naturelle, Paris, 21(1): 21–28.

Pallary P (1917) Hélicidées nouvelles du Maroc. Journal de Conchyliologie 63(2): 126–141, pl. 5. Paris. [31 August].

Pallary P (1918) Diagnoses d'une cinquantaine de mollusques terrestres nouveaux du Nord de l'Afrique. Le Bulletin de la Société d'histoire naturelle d'Afrique du Nord 9(7): 137–152. Alger. [15 July]

Palumbi S, Martin A, Romano S, McMillan W, Stine O, Grabowski G (1991) The simple fool's guide to PCR version 2.0 Honolulu, University of Hawaii.

Péchaud J (1883) Excursions malacologiques dans le nord de l'Afrique de la Calle a Alger, d'Alger a Tanger. I, 112 pp.

Rambaut A (2012) FigTree v1. 4. Molecular evolution, phylogenetics and epidemiology. Edinburgh, University of Edinburgh, Institute of Evolutionary Biology.

Razkin O, Gómez-Moliner BJ, Prieto CE, Martínez-Ortí A, Arrébola JR, Muñoz B, Chueca LJ, Madeira MJ (2015) Molecular phylogeny of the western Palaearctic Helicoidea (Gastropoda, Stylommatophora). Molecular Phylogenetics and Evolution 83: 99–117. https://doi.org/10.1016/j.ympev.2014.11.014

Ronquist F, Huelsenbeck JP (2003) MRBAYES 3: Bayesian phylogenetic inference under mixed models. Bioinformatics 19: 1572–1574. https://doi.org/10.1093/bioinformatics/btg180

Ronquist F, Teslenko M, Van Der Mark P, Ayres DL, Darling A, Höhna S, Larget B, Liu L, Suchard MA, Huelsenbeck JP (2012) MrBayes 3.2: efficient Bayesian phylogenetic inference and model choice across a large model space. Systematic biology 61(3): 539–542. https://doi.org/10.1093/sysbio/sys029

Schileyko AA (2006) Treatise on recent terrestrial pulmonate molluscs. Ruthenica Supplement, Moscow, 2 13: 1765–1906.

Stamatakis A (2006) RAxML-VI-HPC: maximum likelihood-based phylogenetic analyses with thousands of taxa and mixed models. Bioinformatics 22(21): 2688–2690. https://doi.org/10.1093/bioinformatics/btl446

Terver A-P (1839) Catalogue des mollusques terrestres et fluviatiles observés dans les possessions françaises au nord de l'Afrique. Lyon, 40 pp. [4 pl.]

Wade CM, Mordan PB (2000) Evolution within the gastropod molluscs; using the ribosomal RNA gene-cluster as an indicator of phylogenetic relationships. Journal of Molluscan Studies 66: 565–570. https://doi.org/10.1093/mollus/66.4.565

ZooKeys 694: 135–156 (2017)
doi: 10.3897/zookeys.694.14871
http://zookeys.pensoft.net

RESEARCH ARTICLE

A peer-reviewed open-access journal
ZooKeys
Launched to accelerate biodiversity research

Notes on two crabs (Crustacea, Brachyura, Dynomenidae and Iphiculidae) collected from red coral beds in northern Taiwan, including a new species of *Pariphiculus* Alcock, 1896

Peter K. L. Ng[1], M.-S. Jeng[2]

1 *Lee Kong Chian Natural History Museum, Faculty of Science, National University of Singapore, 2 Conservatory Drive, Singapore 117377, Republic of Singapore* **2** *Biodiversity Research Center, Academia Sinica, 128 Academia Road, Section 2, Nankang, Taipei 11529, Taiwan, R.O.C.*

Corresponding author: *Peter K. L. Ng* (peterng@nus.edu.sg)

Academic editor: *S. De Grave* | Received 4 July 2017 | Accepted 6 August 2017 | Published 29 August 2017

http://zoobank.org/C6FB5FE4-A6F0-47A4-AFBA-3ABC59350D07

Citation: Ng PKL, Jeng M-S (2017) Notes on two crabs (Crustacea, Brachyura, Dynomenidae and Iphiculidae) collected from red coral beds in northern Taiwan, including a new species of *Pariphiculus* Alcock, 1896. ZooKeys 694: 135–156. https://doi.org/10.3897/zookeys.694.14871

Abstract

Two brachyuran species of the families Dynonemidae and Iphiculidae are reported from red coral beds in northern Taiwan. The dynonemid *Acanthodromia margarita* (Alcock, 1899) has hitherto been reported from the Andaman Sea, Japan, and Philippines and the species is here recorded for the first time from Taiwan. A new species of iphiculid, *Pariphiculus stellatus* **sp. n.**, is also described. The new *Pariphiculus*, which also occurs in the Philippines, is superficially similar to *P. agariciferus* Ihle, 1918, a species known from Indonesia, Japan, Philippines, South China Sea, Taiwan, and Vanuatu, but can be distinguished by distinct carapace, pleonal and male first gonopod features.

Keywords

Brachyuran crab, Dromioidea, East China Sea, Leucosioidea, new *Pariphiculus* species, taxonomy

Introduction

The small seamount associated with Peng-Chia-Yu Island, a small outcrop 60 km northeast of Keelung in Taiwan, is a special area with controlled commercial fishing for precious red corals (MOJ 2014). One endemic new species, *Corallium carusrubrum*

Tu, Dai & Jeng, 2012 (Anthozoa: Octocorallia: Coralliidae) was recently described from this site.

Recently, two crab species were obtained from the area where the precious red corals are collected. One is the rarely reported dromioid *Acanthodromia margarita* (Alcock, 1899) (Dynomenidae), hitherto reported from India, Japan, and Philippines. The second is a new species of leucosioid of the genus *Pariphiculus* Alcock, 1896 (Iphiculidae), which is superficially similar to *P. agariciferus* Ihle, 1918, from Indonesia, Japan, Philippines, South China Sea, Taiwan, and Vanuatu. The taxonomy of these two species is discussed. The new species of *Pariphiculus*, here named *P. stellatus*, is described and compared at length with *P. agariciferus*. *Pariphiculus stellatus* sp. n. is also reported from the Philippines.

Materials and methods

The measurements provided (in millimetres) are of the maximum carapace width and length (including spines), respectively. The abbreviations G1 and G2 are used for the male first and second gonopods, respectively.

Specimens examined are deposited in the collections of the Institute of Zoology, Biodiversity Research Center, Academia Sinica (**ASIZ**), Taipei, Taiwan; Muséum national d'Histoire naturelle (**MNHN**), Paris, France; and the Zoological Reference Collection (**ZRC**) of the Lee Kong Chian Natural History Museum, National University of Singapore. The terminology used follows that in Tan and Ng (1995) and Davie et al. (2015).

Systematics

Family Dynomenidae Ortmann, 1892
Genus *Acanthodromia* A. Milne-Edwards, 1880

***Acanthodromia margarita* (Alcock, 1899)**
Figs 1A–C, 2, 3

Dynomene margarita Alcock, 1899: 19, pl. 2: fig. 3.
Acanthodromia margarita – Alcock 1900: 134; Sakai 1965: 43; Sakai 1976: 31, pl. 7: fig. 2; Nagai 1989: 43; McLay 1999: 539, fig. 31; Marumura and Kosaka 2003: 20; McLay and Ng 2005: 18, fig. 5; Ng et al. 2008: 37.

Material examined. Taiwan: 1 female (17.8 × 18.3 mm) (ASIZ 75484), waters of Zone A (precious coral fishing ground), Peng-Chia-Yu Island, 60 km northeast of Keelung, 25°37.901'N, 122°28.577'E, 175 m, Taiwan, coll. Fishing Vessel "De-Cheng 136", M.-L. Chang, 14 May 2017. **Philippines**: 1 male (14.7 × 17.7 mm) (ZRC 2001.358), Balicasag Island, 200–300 m, coll. December 2000; 1 male

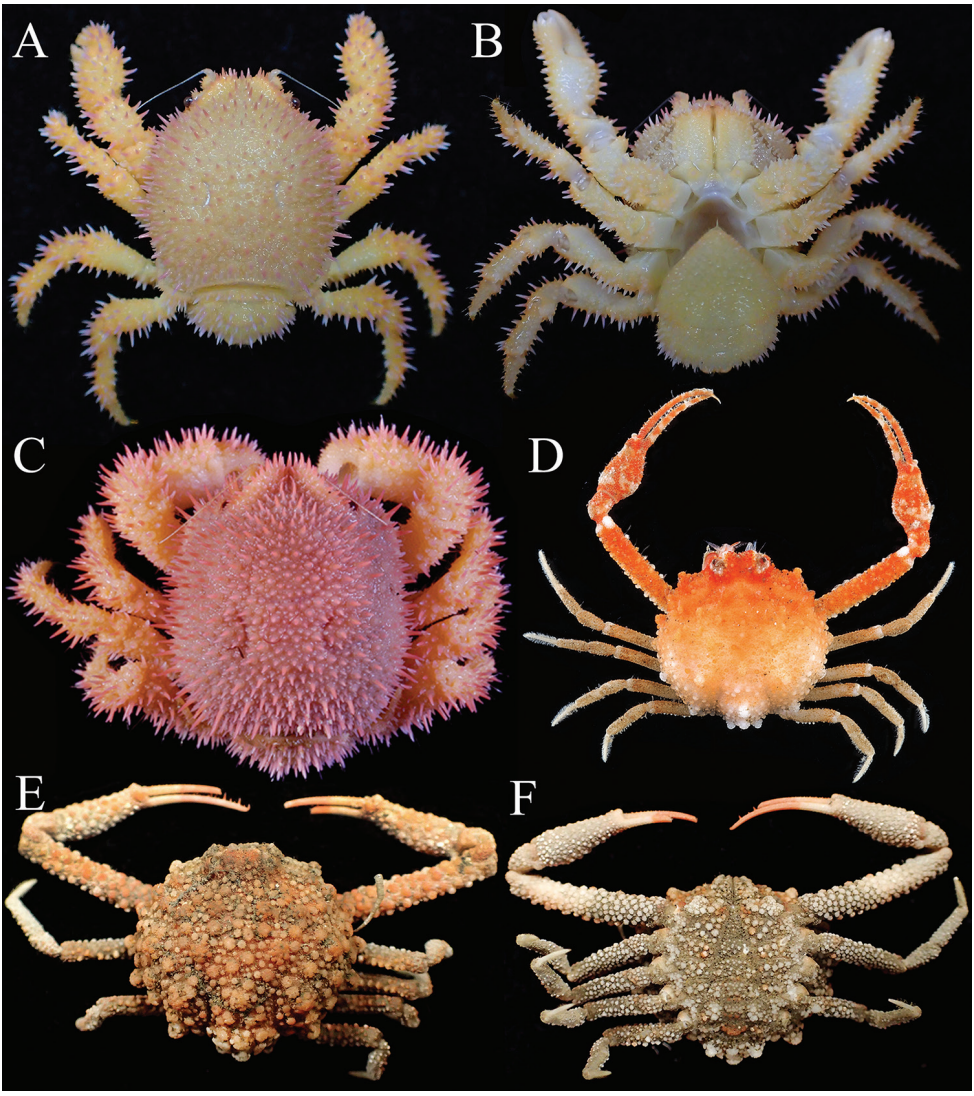

Figure 1. Colour in life. **A, B** *Acanthodromia margarita* (Alcock, 1899), female (17.8 × 18.3 mm) (ASIZ 75484), Taiwan **C** *Acanthodromia margarita* (Alcock, 1899), female (17.7 × 19.2 mm) (ZRC 2008.1420), Philippines **D** *Pariphiculus agariciferus*, Ihle, 1918, male (11.9 × 12.1 mm) (ZRC 2009.471), Vanuatu **E, F** *Pariphiculus stellatus* sp. n., holotype male (27.7 × 24.5 mm) (ASIZ 75485), Taiwan. **A, C, D, E** overall dorsal view; **B, F** ventral view.

(10.5 × 11.5 mm), 2 females (7.8 × 8.3 mm, 11.2 × 12.2 mm), 2 ovigerous females (14.7 × 16.7 mm, 17.0 × 18.5 mm) (ZRC 2003.668), 1 male (9.9 × 10.6 mm), 1 female (12.3 × 13.4 mm) (MNHN); Balicasag Island, 200 –300 m, 25 –30 Jul 2003; 1 male (14.7 × 15.8 mm) (ZRC 2008.1425), station PN1, Balicasag Island,

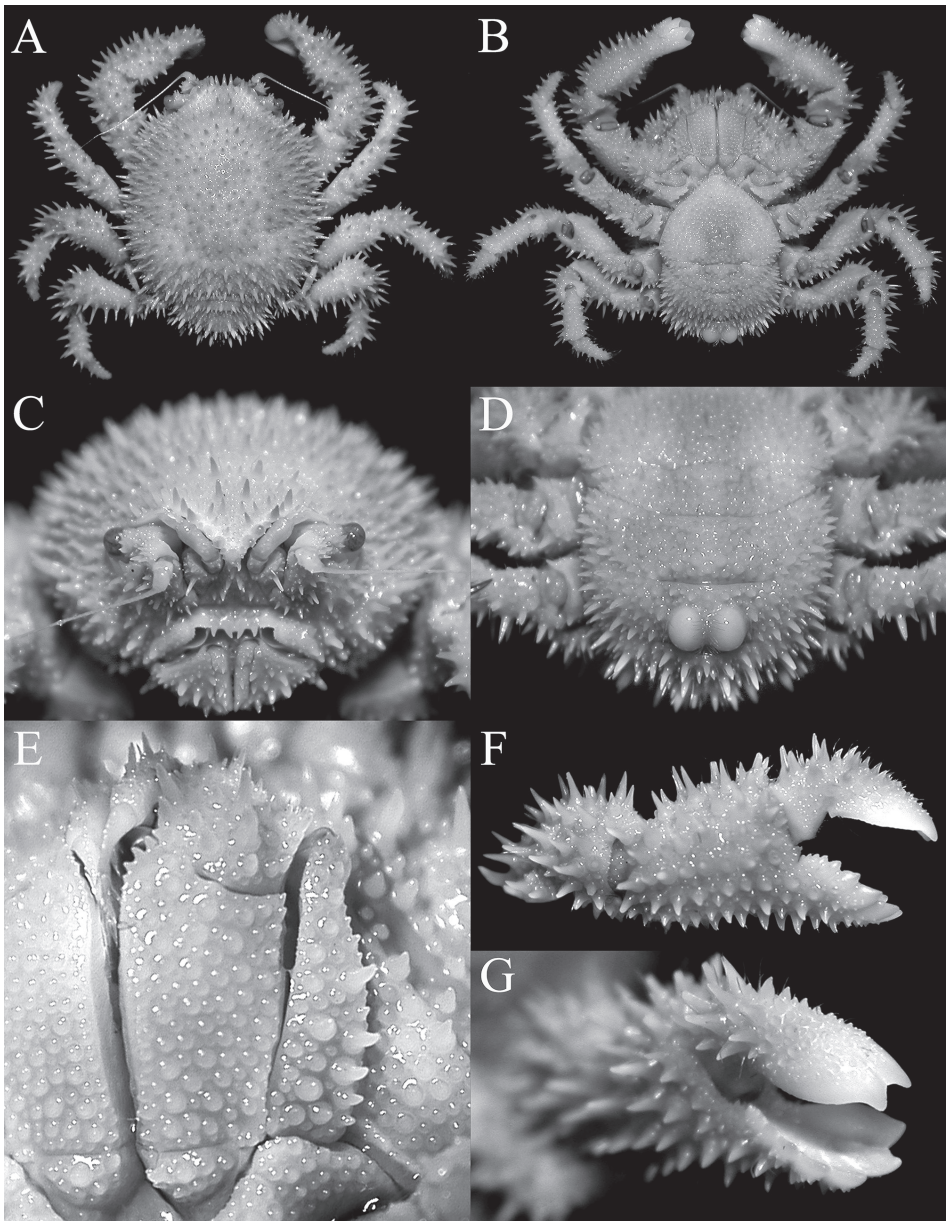

Figure 2. *Acanthodromia margarita* (Alcock, 1899), female (17.8 × 18.3 mm) (ASIZ 75484), Taiwan. **A** overall dorsal view **B** ventral view of cephalothorax **C** frontal view of cephalothorax **D** pleon showing tubercles on somite 4 **E** outer view of left third maxilliped **F** outer view of right chela **G** sublateral view of fingers of right chela.

200–300 m, coll. November 2003; 1 female (no pereopods left, 11.2 × 12.0 mm) (ZRC 2008.1426), Balicasag Island, 200–300m, coll. November 2003–April 2004; 1 male (15.3 × 16.7 mm) (ZRC 2008.1419), station PN1, Balicasag Island, coll.

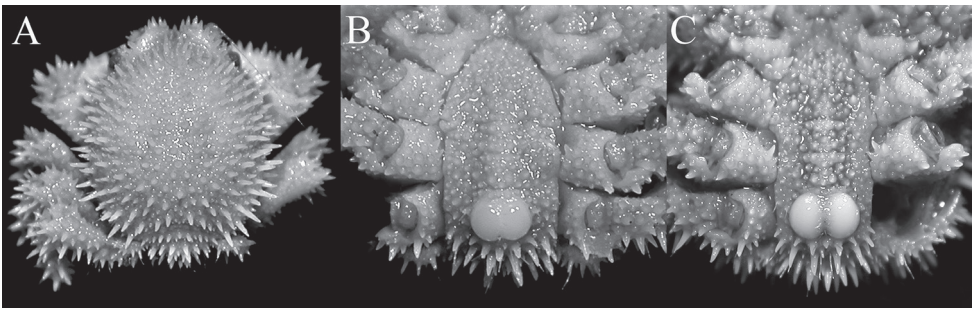

Figure 3. *Acanthodromia margarita* (Alcock, 1899). **A**, **B** male (11.6 × 12.0 mm) (ZRC 2003.668), Philippines **C**, male (13.5 × 14.2 mm) (ZRC 2004.596), Philippines. **A** overall dorsal view **B, C** pleon showing tubercles on somite 4.

29 May 2004; 1 female (17.7 × 19.2 mm) (ZRC 2008.1420), Balicasag Island, coll. 29 March 2004; 5 males (8.8 × 10.6 mm, 11.2 × 12.5 mm, 11.3 × 13.0 mm, 13.5 × 14.2 mm, 14.1 × 16.2 mm), 2 females (15.4 × 17.2 mm, 15.8 × 17.0 mm), 1 female (carapace cracked) (ZRC 2004.596), Balicasag Island, coll. 2 March 2004; 1 male (11.3 × 12.7 mm) (ZRC 2008.1043), Balicasag Island, coll. May 2004 [all above locations at 9.518891°N, 123.680511°E, Panglao, Bohol, Visayas, Philippines; purchased from local shell fishermen, obtained by tangle nets]; 1 male (13.9 × 15.3 mm), 2 females (14.2 × 15.0 mm, 15.7 × 16.1 mm) (ZRC 2013.372), Maribojoc Bay, Panglao, Bohol, Philippines, coll. J. Arbasto, 30 May 2004; 1 female (14.2 × 15.0 mm) (ZRC 2007.207), Maribojoc Bay, Panglao, Bohol, Philippines, coll. J. Arbasto, July-May 2005.

Description. *Colour*. McLay and Ng (2005: 18) described the fresh colour of Philippine specimens as "light pink spines on carapace and the pereopods with golden yellow dactyli". The present Taiwan specimen is orange-yellow on all its dorsal surfaces, with the spines orange-pink with white tips (Fig. 1A, B). In some Philippine specimens, the carapace can be a more striking pink and the pereopods orange-yellow with the spines pink (Fig. 1C).

Remarks. The present female specimen from Taiwan is one of the largest on record and agrees well with published descriptions and figures of the species. The frontal margin appears to vary in form due to the relative strength of the frontal spines, particularly the median pseudorostral one. The two large rounded, basally fused tubercles on pleonal somite 4 is distinct in both sexes; with those in some of the smaller specimens appearing almost completely fused, forming one structure (Fig. 3B). The posterior margin of the epistome always has four spines, but the structure of the two median ones varies slightly, from directly pointing downwards (e.g., McLay and Ng 2005: fig. 5B) to curving medially (Fig. 2C).

Distribution and depth. *Acanthodromia margarita* was described from the Andaman Sea in the eastern Indian Ocean, and has been also reported from Japan, Philippines, and now Taiwan. The Indian Ocean specimen was from relatively shallow water (135 m), but the series from the Philippines was from 120–300 m depth. The present Taiwan specimen was collected from a depth of 175 m.

Family IPHICULIDAE Alcock, 1896
Pariphiculus Alcock, 1896

Pariphiculus stellatus sp. n.

http://zoobank.org/7EC3869E-1F27-4C50-8EE3-DCEB4817630C
Figs 7–10, 11B, D, F, 12B, D, F, 13E–H

Pariphiculus sp. – Ikeda 1998: 84, pl. 2.
Pariphiculus agariciferus – Galil and Ng 2007: 87 (part) (not *Pariphiculus agariciferus* Ihle, 1918).

Material examined. Holotype: male (27.7 × 24.5 mm) (ASIZ 75485), waters of Zone A (precious coral fishing ground), Peng-Chia-Yu Islands, 60 km northeast of Keelung city, 25°37.765'N, 122°28.623'E, 170 m, Taiwan, coll. Fishing Vessel "De-Cheng 136", M.-L. Chang, 7 May 2017. **Philippines**: Non-types: 1 female (31.1 × 26.2 mm) (ZRC 2017.188), Balicasag Island, coll. J. Arbasto, July 2004–May 2005; 1 male (24.3 × 21.6 mm), 1 female (35.1 × 29.6 mm) (ZRC 2007.590), Balicasag Island, coll. 2 March 2004; 1 male (15.4 × 13.8 mm) (ZRC 2017.184), station PN1, Balicasag Island, coll. November 2003; 1 female (32.3 × 27.6 mm) (ZRC 2017.185), Balicasag Island, Panglao, Philippines, 80–140 m, in tangle nets, coll. March 2004 [all above locations at 9.518891°N, 123.680511°E, Panglao, Bohol, Visayas, Philippines; purchased from local shell fishermen, obtained by tangle nets].

Comparative material of *Pariphiculus agariciferus* Ihle, 1918. Taiwan: 1 male (12.9 × 12.3 mm) (ASIZ 75113), 22°14.74'N, 118°43.69'E 141 m, southern Taiwan, coll. M.-L. Chang, 14 May 2011. **Philippines**: 1 male (16.6 × 16.2 mm) (ZRC 2015.436), Balicasag Island, coll. J. Arbasto, July 2004–May 2005; 2 females (19.5 × 18.9 mm, 19.8 × 18.9 mm) (ZRC 2017.181), Balicasag Island, coll. J. Arbasto, 2006; 1 female (19.3 × 17.6 mm), 1 broken female (ZRC 2001.559), Balicasag Island, 50–500 m, coll. 28 November 2001; 1 male (14.4 × 13.3 mm), 1 female (21.0 × 19.1 mm) (ZRC 2009.297), Balicasag Island, coll. June 2002; 2 males (13.4 × 13.3 mm, 15.8 × 15.8 mm), 1 female (19.5 × 18.4 mm) (ZRC 2007.588a), station PN1, Balicasag Island, coll. November 2003; 1 male (13.9 × 13.3 mm) (ZRC 2009.1164), Balicasag Island, coll. December 2003; 1 female (16.6 × 18.6 mm) (ZRC 2017.180), station P2, Balicasag Island, 2004; 1 male (14.0 × 13.5 mm) (ZRC 2015.437), Balicasag Island, coll. 2 March 2004; 1 male (15.8 × 15.0 mm) (ZRC 2017.187), Balicasag Island, Panglao, Philippines, 80–140 m, in tangle nets, coll. March 2004; 1 male (15.5 × 14.4 mm) (ZRC 2012.484), Balicasag Island, coll. May 2004; 1 female (22.0 × 21.6 mm) (ZRC 2017.183), station P1, Balicasag Island, coll. 6 July 2004; 1 young female (15.0 × 14.7 mm) (ZRC 2017.182), station P4, Balicasag Island, coll. 2 July 2004; 2 females (18.4 × 18.0 mm, 22.1 × 21.3 mm) (ZRC 2009.288), Balicasag Island, coll. J. Arbasto, July 2004–May 2005; 1 male (12.8 × 13.7 mm), 1 female (19.0 × 19.0 mm) (ZRC 2017.186), Balicasag Island, Panglao, Philippines, 80–140 m, in tangle nets, coll. J. Arbasto, 2004–2005; 1 male (15.4 × 16.0 mm) (ZRC 2009.185), Balicasag

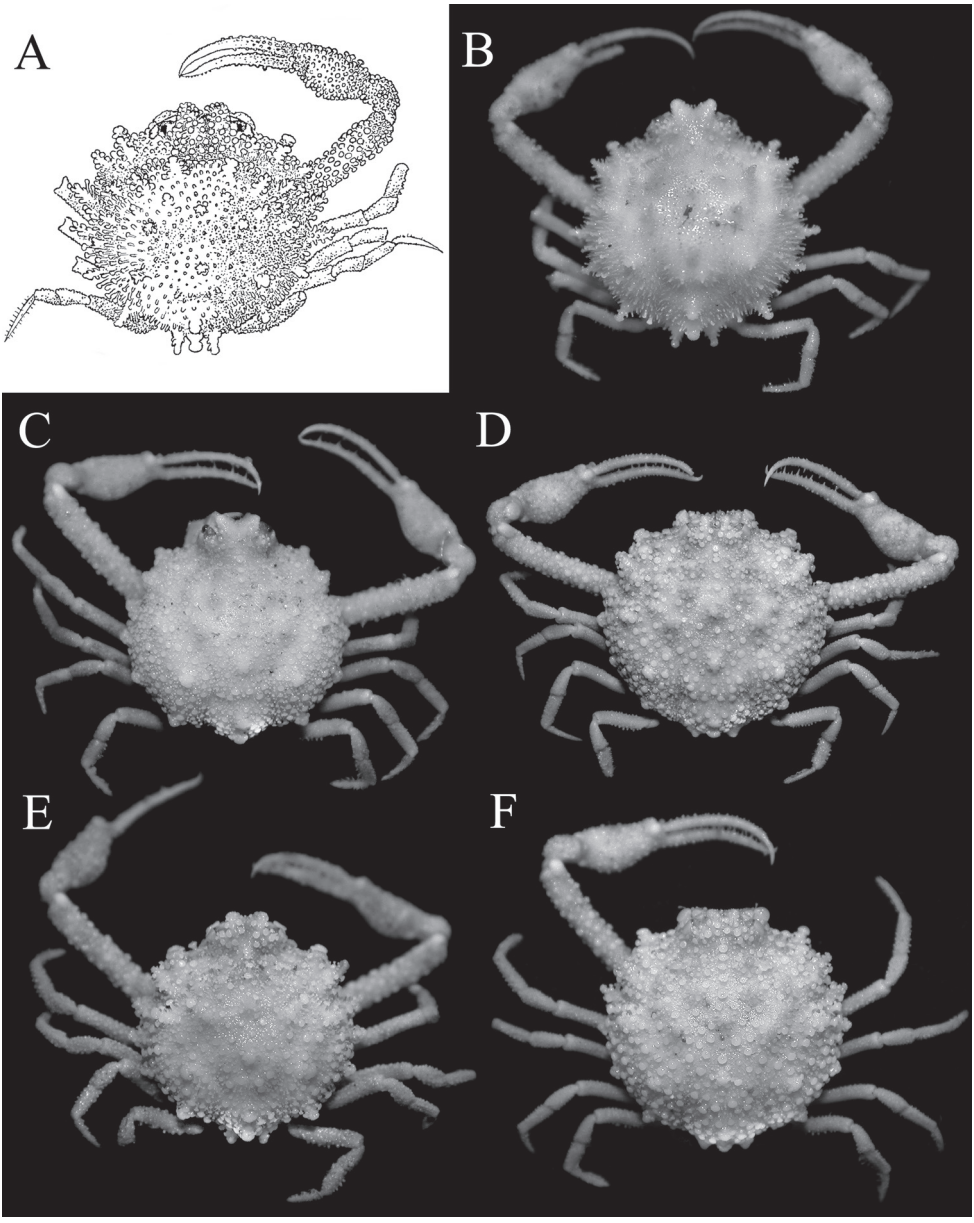

Figure 4. *Pariphiculus agariciferus* Ihle, 1918, overall dorsal view. **A** holotype male (9.0 × 9.3 mm), after Ihle (1918: fig. 230) **B** young male (10.2 × 9.6 mm) (ZRC 2009.470), Vanuatu **C** male (11.9 × 12.1 mm) (ZRC 2009.471), Vanuatu **D** female (22.1 × 21.3 mm) (ZRC 2009.288), Philippines **E** male (15.5 × 14.4 mm) (ZRC 2012.484), Philippines **F** female (19.0 × 19.0 mm) (ZRC 2017.186), Philippines.

Island, 120–160 m, coll. J. Arbasto, January–December 2007 [all above locations at 9.518891°N, 123.680511°E, Panglao, Bohol, Visayas, Philippines; purchased from local shell fishermen, obtained by tangle nets]; 1 male (17.2 × 16.9 mm), 2 females (16.1

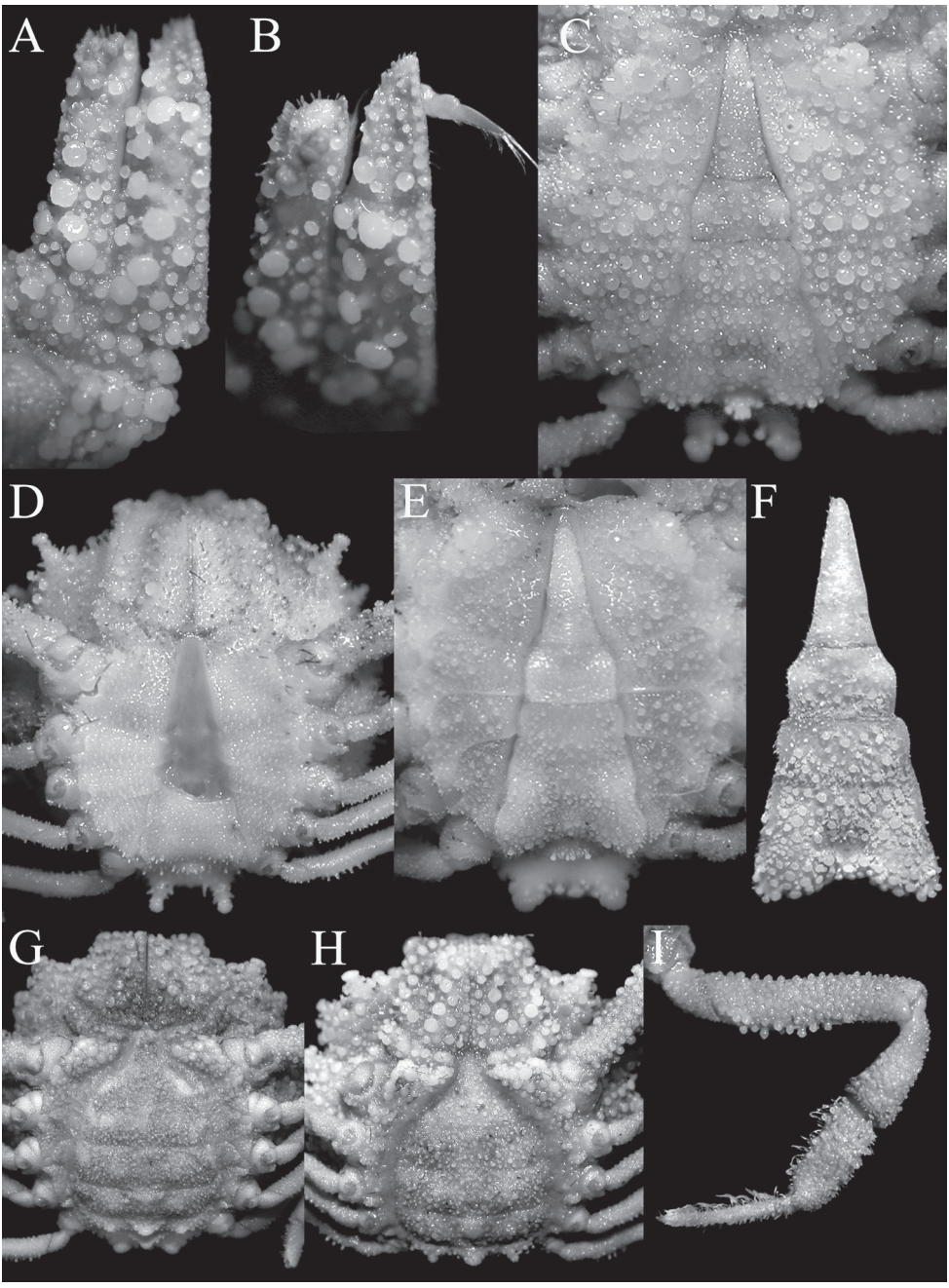

Figure 5. *Pariphiculus agariciferus* Ihle, 1918. **A**, **B** female (19.8 × 18.9 mm) (ZRC 2017.181), Philippines **C** male (15.5 × 14.4 mm) (ZRC 2012.484), Philippines **D** young male (10.2 × 9.6 mm) (ZRC 2009.470), Vanuatu **E** male (11.9 × 12.1 mm) (ZRC 2009.471), Vanuatu **F** male (15.8 × 15.0 mm) (ZRC 2017.187), Philippines **G, I** female (22.1 × 21.3 mm) (ZRC 2009.288), Philippines **H** female (19.0 × 19.0 mm) (ZRC 2017.186), Philippines. **A, B** outer view of right third maxilliped **C–E** male thoracic sternum and pleon **E** female thoracic sternum and pleon **G, H** female thoracic sternum and pleon **E** female thoracic sternum and pleon **I** right fourth ambulatory leg.

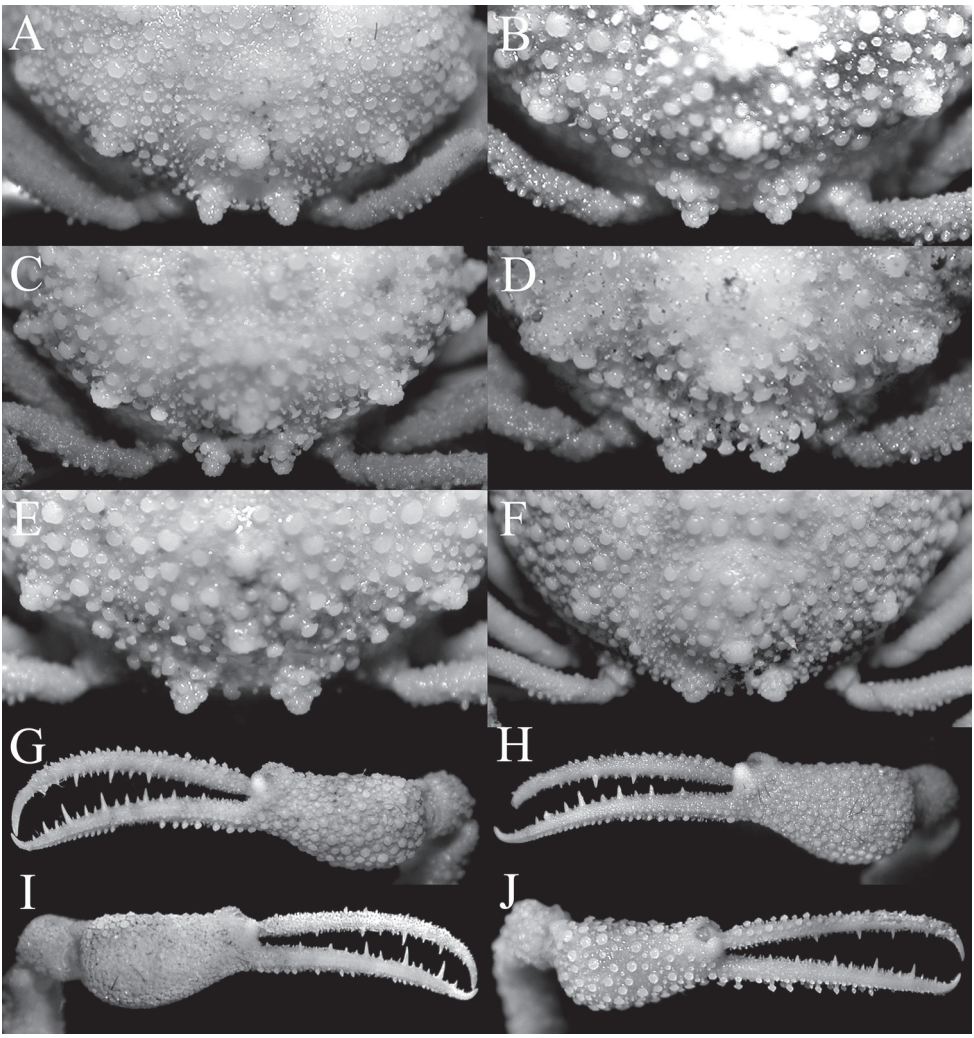

Figure 6. *Pariphiculus agariciferus* Ihle, 1918. **A** male (11.9 × 12.1 mm) (ZRC 2009.471), Vanuatu **B** male (15.8 × 15.0 mm) (ZRC 2017.187), Philippines **C, J** male (15.5 × 14.4 mm) (ZRC 2012.484), Philippines **D** male (12.8 × 13.7 mm) (ZRC 2017.186), Philippines **E, G** female (19.0 × 19.0 mm) (ZRC 2017.186), Philippines **F, H** female (22.1 × 21.3 mm) (ZRC 2009.288), Philippines **I** male (11.9 × 12.1 mm) (ZRC 2009.471), Vanuatu. **A–F** intestinal region and posterior margin of carapace **G, H** outer view of left chela **I**, **J** outer view of right chela.

× 15.4 mm, 18.5 × 18.7 mm) (ZRC 2013.104), Maribojoc Bay, Panglao, Bohol, Philippines, coll. J. Arbasto, November 2003–April 2004. **Vanuatu**: 1 male (10.2 × 9.6 mm), 1 female (13.0 × 13.5 mm) (ZRC 2009.470), station AT13, south of Aésé Island, Palikulu Bay, 15°27.8S 167°15.7E, 146–153 m, Santo, coll. N.O."Alis", SANTO Expedition, 19 September 2006; 1 male (11.9 × 12.1 mm) (ZRC 2009.471), station AT61, south of Urélapa Island, West Malo Island, 15°39'S 167°01'E, 266–281 m, Santo, coll. N.O."Alis", SANTO Expedition, 4 October 2006; 2 juvenile females (10.3 × 9.4 mm, 13.4 × 13.6 mm), 1 carapace only (17.9 × 17.4 mm) (ZRC 2009.472), station AT63,

south of Urélapa Island, West Malo Island, 15°40'S 167°01'E, 290–334 m, Santo, coll. N.O."Alis", SANTO Expedition, 4 October 2006; 1 male (11.9 × 11.8 mm) (ZRC 2009.473), station AT64, south of Urélapa Island, West Malo Island, 15°40'S 167°02'E, 249–252 m, Santo, coll. N.O."Alis", SANTO Expedition, 19 September 2006.

Diagnosis. Carapace 1.12–1.19 times broader than long; with relatively low mushroom-shaped tubercles on carapace, chelipeds and ambulatory legs with margins of tops distinctly asteriform (Figs 7, 8A, G, 9A, B, 11D, F, 12B); gastric and branchial regions inflated (Figs 8A, G, 11D, F); in lateral view, surface behind postfrontal region gently concave, forming shallow depression (Fig. 11F); suborbital tubercle relatively low, not protruding (Figs 8A, G, 9C, 11D); palms of chelae relatively long, slender, with fingers long, gently curved (Figs 9E–H, 12F); dorsal margin of dactylus and ventral margin of pollex of chela lined with low granules, never serrated (Figs 9E–H, 12F); tubercles and granules on surface of male and female pleons relatively large, tend to be fused, forming semi-eroded structures (Figs 8D, E, 9D, 12D); male telson proportionately shorter (Figs 8D, E, 12D); G1 relatively long, slender (Fig. 13E).

Description of male. *Carapace* 1.12–1.19 times broader than long, regions not well-defined; dorsal surface with numerous low mushroom-shaped tubercles and granules, edges of raised tubercle with short slender spinules, asteriform from dorsal view, with scattered short setae between them; postfrontal region raised, prominent; surface behind postfrontal region with shallow depression; gastric regions convex, separated from swollen branchial regions by shallow, partially granulated groove; branchial regions with numerous large and small tubercles, separated from intestinal and cardiac regions by relatively broad granulated groove; cardiac and intestinal regions barely distinguishable, intestinal region with 2 prominent large tubercles, one dorsal in position, another directed obliquely posteriorly; hepatic region gently concave, with distinct low lateral tubercle, surface granulated; pterygostomial and suborbital regions with numerous mushroom-shaped, asteriform tubercles; branchiostegite region with numerous low, rounded tubercles (Figs 7, 8A, G, 9A–C, 11B, D–F, 12B). posterolateral border adjacent to cardiac region prominently protruded to form large tooth. Front slightly produced, not protruding beyond anterior edge of buccal cavity and closed third maxillipeds, gently upturned, weakly bilobed (distinct in frontal view) (Figs 7, 8A, G, 11B, D, 12B). Antero- and posterolateral margins not cristate, not clearly demarcated, with structures gradually merging medially on carapace; subdorsal margins lined with numerous large mushroom-shaped tubercles with asteriform tops, with interspersed smaller granules of similar form; posterior carapace margin with 3 broad, stout tubercles, each covered with smaller granules, median one smallest (Figs 7, 9A, B, 11B, 12B).

Basal article of *antenna* subquadrate, surface gently convex, fused with epistome; short flagellum lodged in orbital hiatus (Fig. 9C). Basal segment of antennule occupies entire fossa when closed, with folded articles hidden behind basal article; margins of fossae almost smooth (Figs 8A, G, 9C). Orbit rounded; eyes small with short ocular peduncle, mobile; suborbital tubercle relatively low, not prominent, asteriform (Figs 8A, G, 9C, 11D).

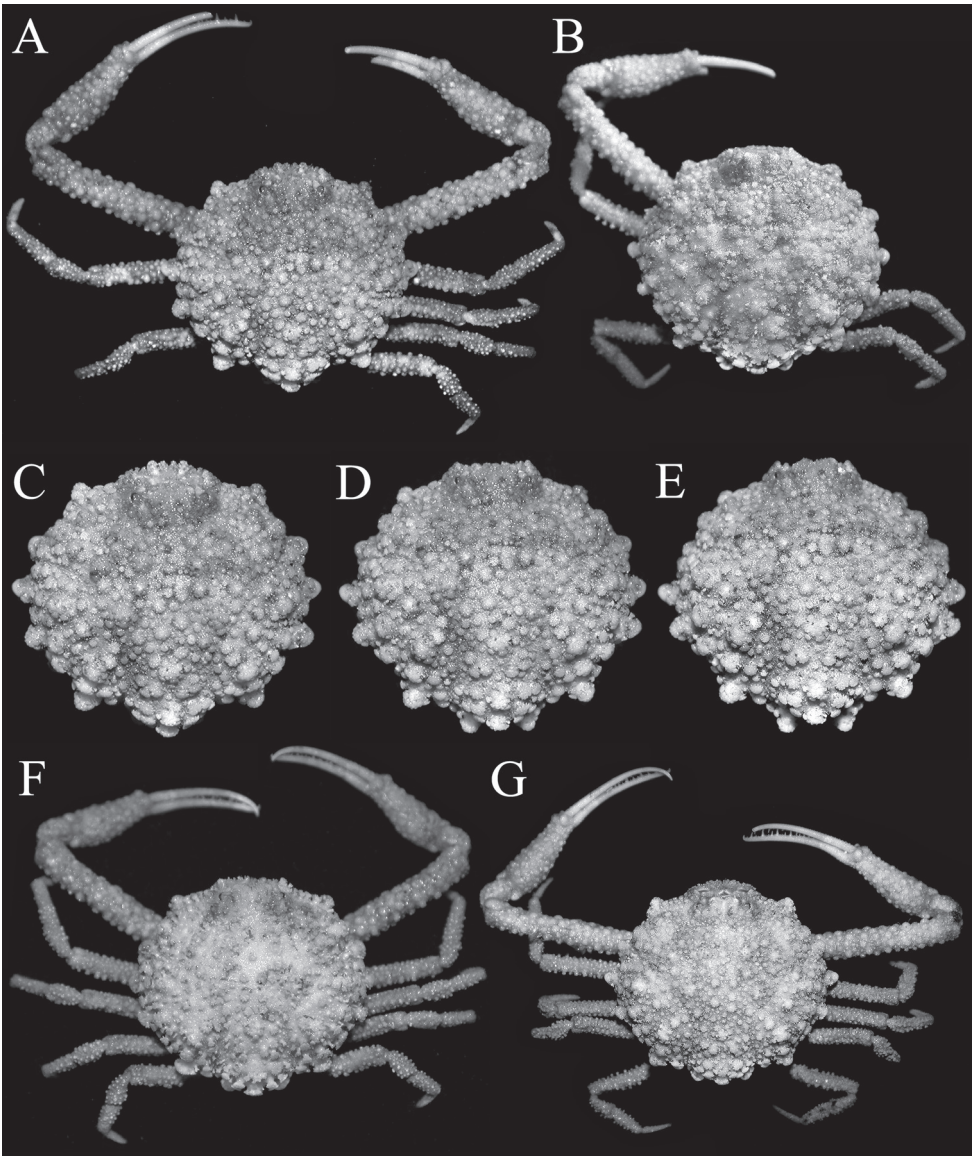

Figure 7. *Pariphiculus stellatus* sp. n. **A, C–E** holotype male (27.7 × 24.5 mm) (ASIZ 75485), Taiwan **B** female (32.3 × 27.6 mm) (ZRC 2017.185), Philippines **F** male (24.3 × 21.6 mm) (ZRC 2007.590), Philippines **G** female (35.1 × 29.6 mm) (ZRC 2007.590), Philippines. **A, B, F, G** overall dorsal view **C–E** dorsal view of carapace photographed from slightly different angles.

Third maxillipeds relatively short; outer surfaces of merus, ischium, basis and exopod densely covered with mushroom-shaped tubercles and granules, many with asteriform tops; merus triangular with broadly pointed apex, inner edge straight, outer edge gently convex, with large, low rounded tubercle on proximal margin; ischium ca.

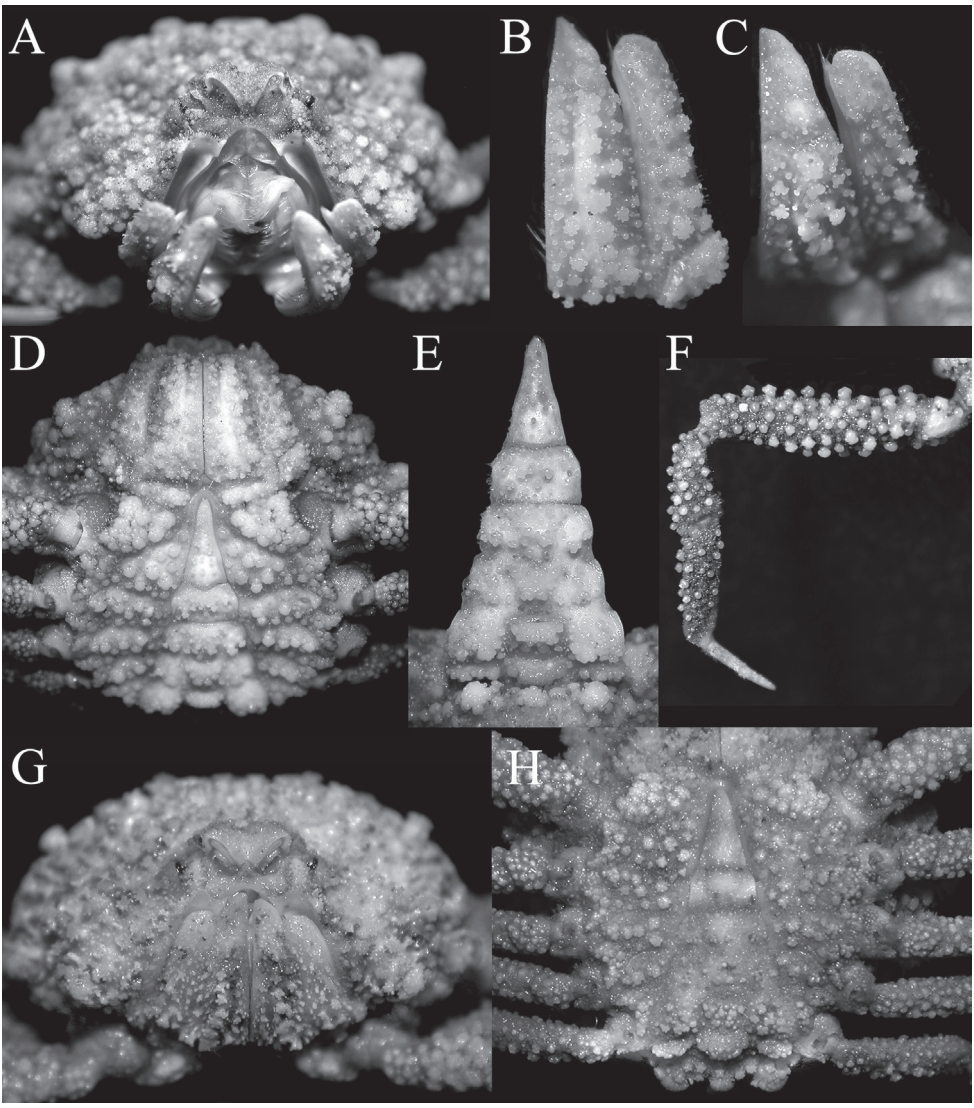

Figure 8. *Pariphiculus stellatus* sp. n. **A–F** holotype male (27.7 × 24.5 mm) (ASIZ 75485), Taiwan **G, H** male (24.3 × 21.6 mm) (ZRC 2007.590), Philippines. **A, G** frontal view of cephalothorax showing orbit, antennae, antennules and buccal cavity **B, C** outer view of left third maxilliped **D, H** male thoracic sternum and pleon **E** male pleon **F** left third ambulatory leg.

2 times longer than merus along inner margin, with prominent submedian ridge of tubercles; palp (carpus, propodus and dactylus, short, completely hidden behind ischium when folded; exopod relatively broad, reaching beyond distal margin of ischium, tip rounded, without flagellum (Figs 8B, C, G 11D).

Chelipeds slender, elongate, subequal; surfaces with numerous large, round or low mushroom-shaped tubercles, some with asteriform tops (Figs 7A, F, G, 9E–H, 11B, 12F).

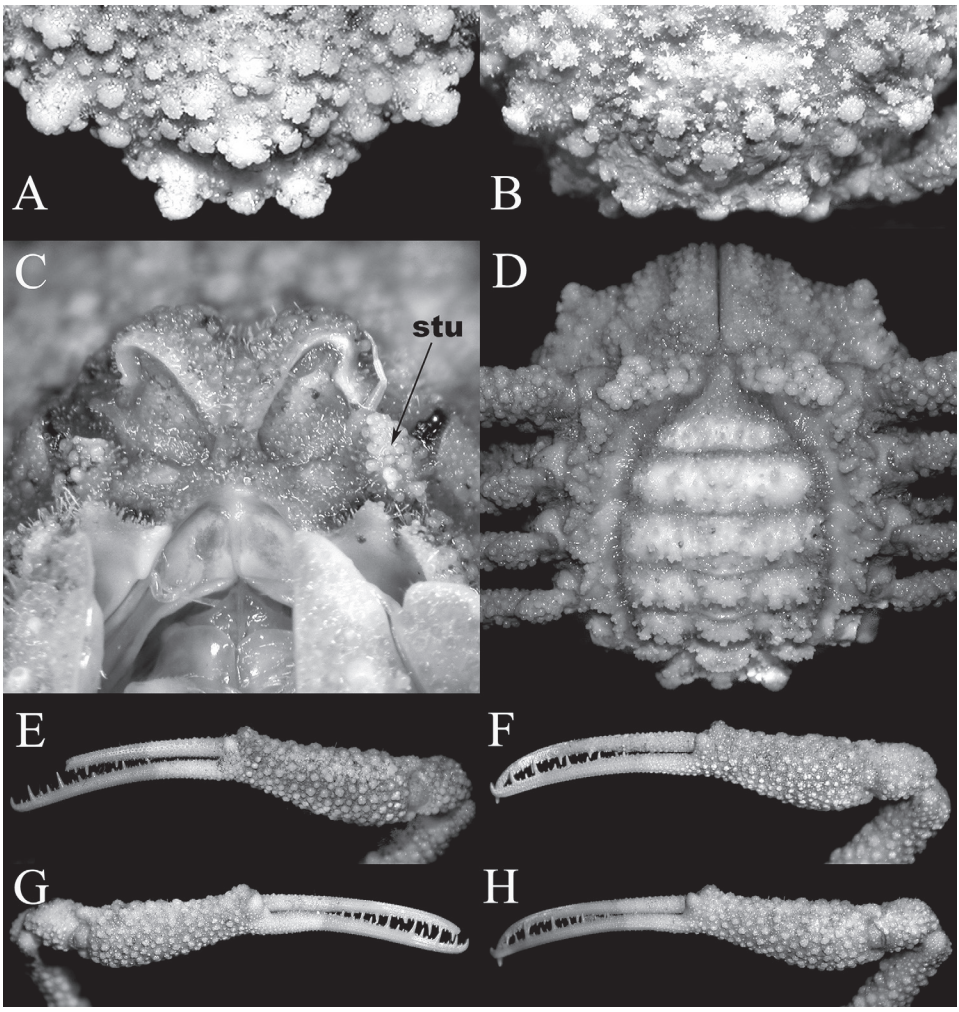

Figure 9. *Pariphiculus stellatus* sp. n. **A, C, E** holotype male (27.7 × 24.5 mm) (ASIZ 75485), Taiwan **B** female (32.3 × 27.6 mm) (ZRC 2017.185), Philippines **F** male (24.3 × 21.6 mm) (ZRC 2007.590), Philippines **D, G, H** female (35.1 × 29.6 mm) (ZRC 2007.590), Philippines. **A, B** intestinal region and posterior margin of carapace **C** antennae, antennules and orbit **D** female thoracic sternum and pleon **E, F, H** outer view of left chela **G** outer view of right chela. Abbreviation: stu = suborbital tubercle.

Merus cylindrical in cross-section; carpus small, subtriangular (Figs 7A, F, G, 9E–H, 11B). Chela with proximal half relatively stouter, gradually tapering to more slender distal part, margins granulated but not serrated; fingers elongate, just longer than palm, surface with very small granules, gently curved, distal two-thirds more darkly pigmented, rest of structure white in preservative; cutting edges of both fingers with long and short sharp vertical spines (Figs 9E–H, 12F).

Ambulatory legs relatively short, first leg longest; surfaces of merus, carpus and propodus covered with small rounded or mushroom-shaped tubercles, some with

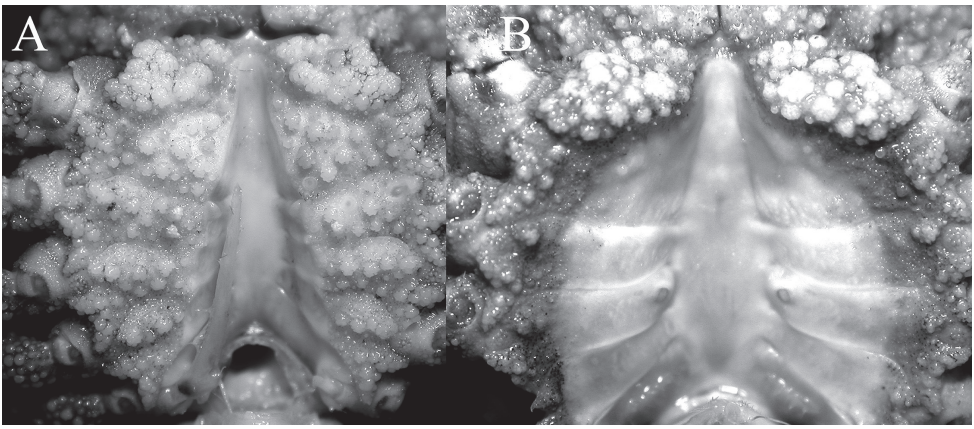

Figure 10. *Pariphiculus stellatus* sp. n. **A** holotype male (27.7 × 24.5 mm) (ASIZ 75485), Taiwan **B** female (31.1 × 26.2 mm) (ZRC 2017.188), Philippines. **A** male sternopleonal cavity showing right G1 and pleonal locking tubercle on sternite 5 **B** female sternopleonal cavity showing vulvae on sternite 6.

asteriform tops (Figs 7A, F, G, 8F, 11B); dactylus styliform, almost straight, surfaces smooth, margins lined with setae (Fig. 8F).

Thoracic sternum relatively narrow transversely; surfaces of sternites 1–4 covered with round or low mushroom-shaped tubercles, some with asteriform tops, some coalescing to form ridges and clusters; surfaces of sternites 5–8 with more individual tubercles and granules; sternites 1 and 2 separated by low ridge, longitudinally very narrow, lateral surfaces of sternite 2 with thick row of coalesced tubercles; separated from coalesced row of tubercles on sternite 3 by deep groove; tubercles on sternite 3 separated from cluster of coalesced tubercles on sternite 4 by deep groove; sternites otherwise not clearly demarcated; small part of sternite 8 just visible when pleon closed; sternopleonal cavity narrow, deep, nearly reaching buccal cavity at level of sternite 2 (Figs 8D, H, 12D); all sutures from sternites 3–8 medially interrupted; peg-like tubercle of pleonal locking mechanism relatively large, semicircular, directed anteriorly (Fig. 10A); penis short, tubular with dilated tip, arising from condyle of coxa of fourth ambulatory leg (Fig. 10A).

Pleon triangular, covered with large rounded tubercles, many coalescing to form semi-eroded structure on somites 1–6; surface of telson with scattered small, narrow mushroom-shaped; somites 1, 2 free; somites 3–5 functionally fused although somites can still be approximately distinguished; somites 2–6 trapezoidal; somite 6 free, broadly subrectangular with lateral margin convex; telson triangular, elongate; surface of somite 3 with subrectangular cluster of fused granules; surface of somite 2 with 3 uneven clusters of fused granules (Figs 8D, E, H, 12D).

G1 ca. 2 times length of G2, relatively slender, slightly sinuous basally, becoming almost straight distally; margins lined with dense soft long setae; tip sharp (Fig. 13E–G). G2 with with elongate subpetaloid terminal process which is slightly shorter than basal segment (Fig. 13H).

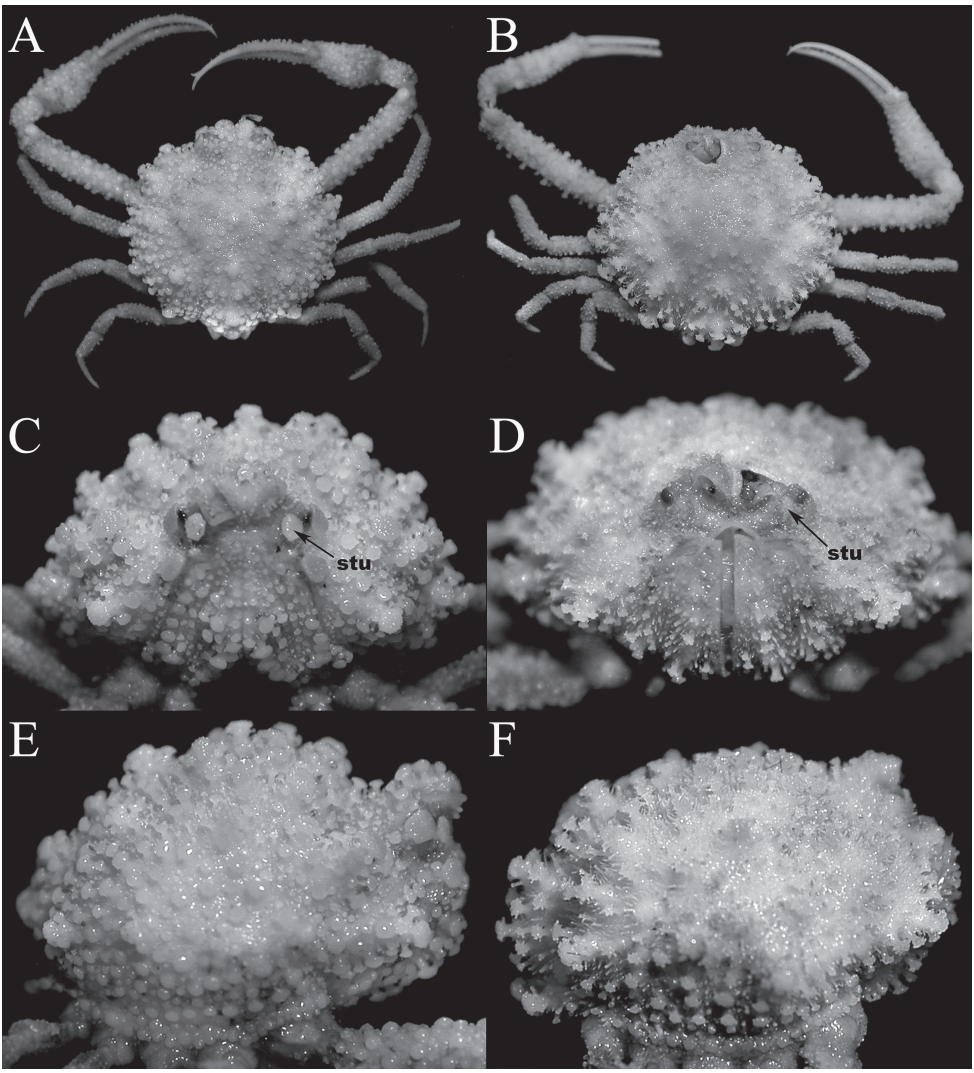

Figure 11. Comparisons between similar sized *Pariphiculus agariciferus* Ihle, 1918, and *P. stellatus* sp. n. **A, C, E** *P. agariciferus*, male (15.8 × 15.8 mm) (ZRC 2007.588), Philippines **B, D, F** *P. stellatus*, male (15.4 × 13.8 mm) (ZRC 2017.184), Philippines [left frontal margin damaged]. **A, B** overall dorsal view **C, D** frontal view of cephalothorax showing orbit, antennae, antennules and buccal cavity **E, F** right lateral view of cephalothorax. Abbreviation: stu = suborbital tubercle.

Females and variations. Female specimens are similar to males in almost all non-sexual aspects. The female pleon is of the typical iphiculid condition, with all the somites and telson freely articulating, none swollen or forming a dome-like structure covering the egg mass (Fig. 9D). The vulva is relatively small and simple with around opening, covered by an operculum, and directed obliquely posteriorly (Fig. 10B).

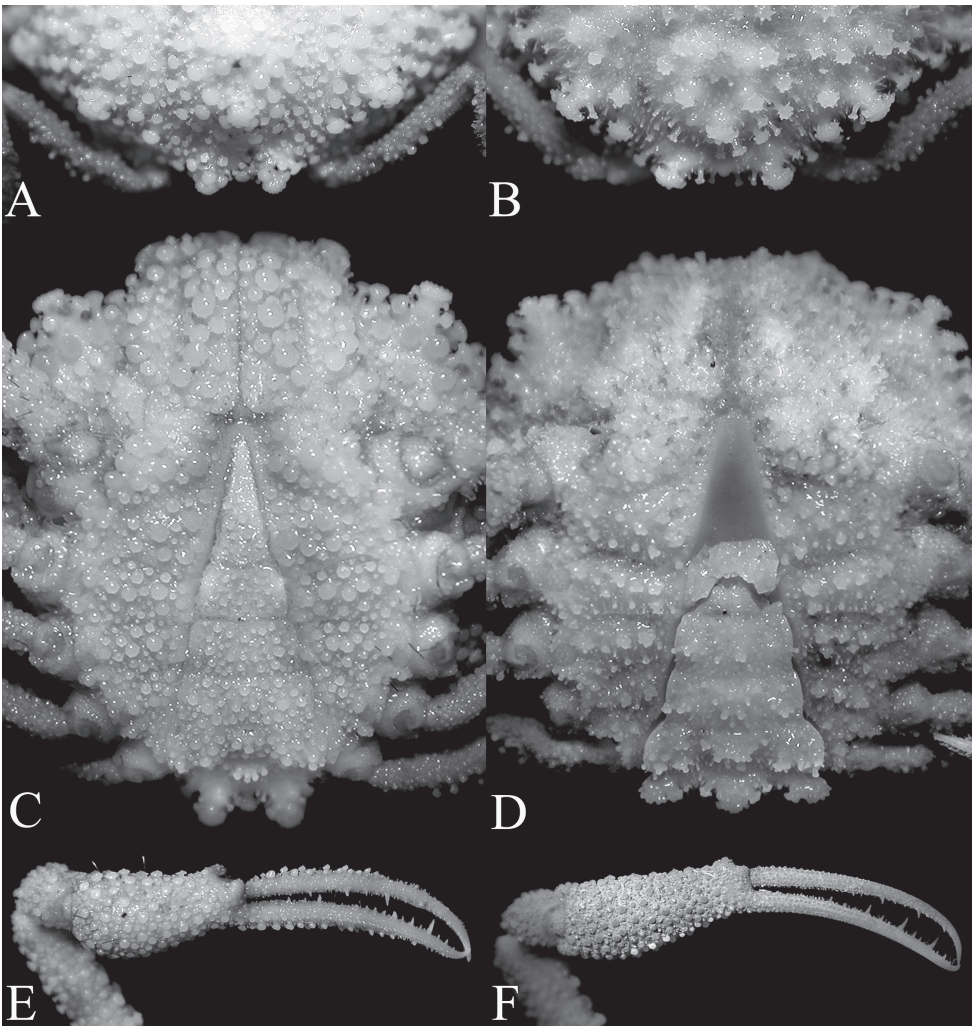

Figure 12. Comparisons between similar sized *Pariphiculus agariciferus* Ihle, 1918, and *P. stellatus* sp. n. **A, C, E** *P. agariciferus*, male (15.8 × 15.8 mm) (ZRC 2007.588), Philippines **B, D, F** *P. stellatus*, male (15.4 × 13.8 mm) (ZRC 2017.184), Philippines [telson missing, approximate shape and proportions as indicated by space on sternopleonal cavity]. **A, B** intestinal region and posterior margin of carapace **C, D** male thoracic sternum and pleon (somite 6 damaged and telson missing in D) **E, F** outer view of right chela.

Small specimens have proportionately shorter meri of the chelipeds although in all other aspects, the structures are similar (Figs 7B, F, 11B).

Colour. The fresh holotype of *P. stellatus* was a dull orange throughout, with some of the large posterior tubercles white; the distal two-thirds of fingers bright orange and basal third cream (Fig. 1E). The ventral surfaces are generally dirty white to light brown (Fig. 1F). A relatively larger fresh specimen of *P. agariciferus* (18. 1 mm carapace width) was figured by Galil and Ng (2007: fig. 3B) and its colour was similar to that

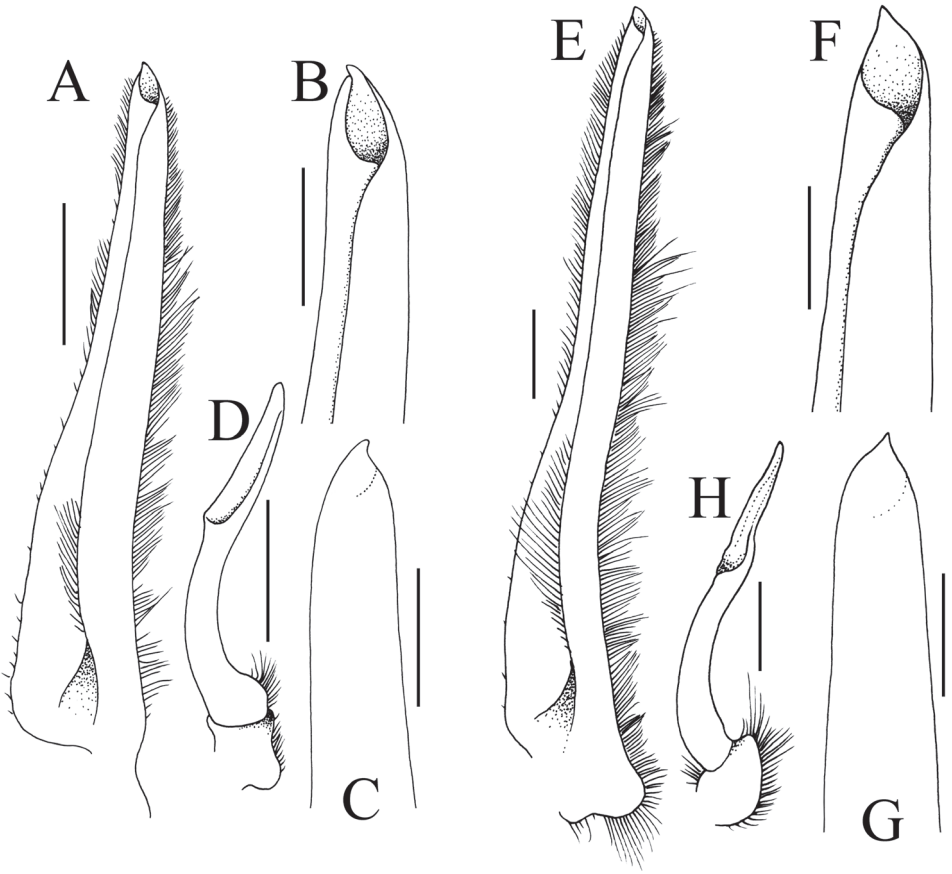

Figure 13. Gonopods. **A**–**D** *Pariphiculus agariciferus* Ihle, 1918, male (15.8 × 15.0 mm) (ZRC), Philippines **E–H** *P. stellatus* sp. n., holotype male (27.7 × 24.5 mm) (ASIZ 75485), Taiwan. **A–C, E–G** left G1 **D, H** left G2. Scale bars **A, E, D, H** 1.0 mm; **B, C, F, G** 0.5 mm.

of *P. stellatus*, being orange throughout. A smaller male specimen from Taiwan (12.9 × 12.3 mm, ASIZ 75113), however, had most of the carapace and chelipeds white and pale orange (Shih et al. in press). A similar sized male from Vanuatu (11.9 × 12.1 mm, ZRC 2009.471) had a similar colour pattern as the Taiwan specimen except that the colour is more intense (Fig. 1D)

Etymology. The species is named after the prominent asteriform or "star-like" mushroom-shaped tubercles and granules on the carapace and chelipeds.

Remarks. The large specimen from Taiwan is interesting as it is almost identical with a large female specimen measuring 36.2 × 30.3 mm figured by Ikeda (1998: 84) from Sagami Bay which he identified as "*Pariphiculus* sp.". Ng (1999: 718), in his review of the book, noted that this was almost certainly a new species although he incorrectly suggested it may be a species of *Parilia* Wood-Mason in Wood-Mason & Alcock, 1891, instead. Examination of the present Taiwanese specimen suggests it is

close to *Pariphiculus agariciferus* Ihle, 1918, a species known from Indonesia, Japan, Philippines, Taiwan, South China Sea and Vanuatu (Ihle 1918: 250; Balss 1922: 131; Yokoya 1933: 129; Sakai 1937: 131; Sakai 1965: 43; Serène and Vadon 1981:124; Sakai 1976: 104; Chen 1989: 231; Tan 1996: 1023; Komatsu et al. 2005: 106; Galil and Ng 2007: 87; Galil and Ng 2010: 143; Ng et al. 2008: 37; Shih et al. in press). The size of the Taiwanese (and Ikeda's Japanese) specimen, however, is much larger (almost twice) that what is known for *P. agariciferus* which averages 15–20 mm in carapace width. The Taiwanese specimen differs from typical *P. agariciferus* in a number of carapace, cheliped, male pleonal and G1 characters that suggests that it is a different taxon, but its large size makes comparisons difficult.

Fortunately, there is a good series of specimens of what had been identified as "*P. agariciferus*" from Philippines and Vanuatu by Galil and Ng (2007, 2010), as well as additional material in the ZRC not reported by them. While the majority of the specimens are *P. agariciferus* s. str., there are several specimens mixed among this material (cf. Galil and Ng 2007) that are clearly conspecific with the Taiwan specimen. This includes a small male specimen of the new species which allows for size-equivalent comparisons between the two taxa to be made. We can now be confident that the present Taiwanese male, Ikeda's (1998) specimen, and some of the Philippine material represent a new species, here named *Pariphiculus stellatus* sp. n.

Pariphiculus agariciferus Ihle, 1918, is a smaller species, with all specimens less than 22 mm in carapace length. The holotype male from seas around Timor and Rotti islands in Indonesia measured 9.0 × 9.3 mm (not measured to tip of spines). The carapace of the holotype male has all the lateral spines relatively slender and long, all of which are covered with additional spinules and tubercles; with the tubercles and granules on the carapace and chelipeds mushroom-shaped (Fig. 4A). A slightly larger male from Vanuatu has a very similar in carapace morphology (Fig. 4B). These characters are almost certainly juvenile features; the small Vanuatu specimen is still subadult, with the gonopods poorly chitinised; and the holotype male is probably a young individual as well. In the larger male specimens from the Philippines, Taiwan and Vanuatu, the lateral spines (including those on the posterior carapace margin) are relatively shorter and stouter (Figs 4C–F, 6A–F). The ambulatory meri and dactyli of the smallest specimens are also proportionately more slender and elongate (Fig. 4A, B). As specimens get larger (regardless of sex), the carapace becomes proportionately wider and rounder, and the spines shorter and blunter (Fig. 4C–F). The ambulatory meri and dactyli of these larger specimens are also relatively stouter and shorter (Fig. 4C–F). As the specimens increase in size, the tops of the mushroom-shaped tubercles on the carapace and chelae also become more mushroom-shaped, with the margins more gently serrated and distinctly asteriform (Figs 4C–F, 6A–F).

Pariphiculus stellatus sp. n. can be distinguished from *P. agariciferus* in having the gastric and branchial regions of the carapace proportionately less inflated (Figs 8A, G, 11D, F) (vs. prominently inflated in frontal view in *P. agariciferus*; cf. Fig. 11C, E); the tubercles on the carapace, chelipeds and third maxillipeds are prominently mushroom-shaped but relatively lower, with the tops of the large tubercles distinctly asteriform

(Figs 8A–C, G, 9A, B, 11D, F, 12B) (vs. tubercles on the carapace are relatively higher and mushroom-shaped, with the margins of the tops of the tubercles uneven but not distinctly asteriform in *P. agariciferus*; cf. Figs 5A, B, 6A–F, 11C, E, 12A); in lateral view, the surface behind the postfrontal region is gently concave, forming a shallow depression (Fig. 11F) (vs. area behind postfrontal region deeply concave, with a marked depression between frontal and gastric regions in *P. agariciferus*; cf. Fig. 11E); the suborbital tubercle is relatively low, not protruding and not conspicuous (Figs 8A, G, 9C, 11D) (vs. suborbital tubercle is large and prominently protrudes anteriorly in *P. agariciferus*; cf. Fig. 11C); the palms of the chelae are relatively long, slender with the fingers gently curved (Figs 9E–H, 12F) (vs. palms relatively short, swollen with the fingers distinctly curved in *P. agariciferus*; cf. Figs 6G–J, 12C); the dorsal margin of the dactylus and ventral margin of the pollex of the chela is lined with low granules, never serrated (Figs 9E–H, 12F) (vs. non-cutting margins of dactylus and pollex with prominent sharp and/or mushroom-shaped granules, appears serrated in *P. agariciferus*; cf. Figs 6G–J, 12C); the tubercles and granules on the surface of the male and female pleons are larger, tend to be fused, forming semi-eroded structures (Figs 8D, E, H, 9D, 12D) (vs. tubercles and granules tend to be smaller, discrete and packed in *P. agariciferus*; cf. Figs 5C–H, 12C); the male telson is proportionately shorter, even in small specimens (Figs 8D, E, H, 12D) (vs. male telson more elongate in *P. agariciferus*; cf. Figs 5C–F, 12C); and the G1 is relatively longer and more slender (Fig. 13E) (vs. G1 proportionately stouter and shorter in *P. agariciferus*; cf. Fig. 13A). It is important to note also that the single male specimen of *P. stellatus* sp. n. (Figs 11B–F, 12B–F) similar in size to adult *P. agariciferus* (Figs 11A, C, E, 12A, C, E) is still subadult, with the G1 soft and not well developed.

All the specimens of *P. stellatus* sp. n. have been collected by tangle nets in Taiwan and the Philippines. This is also true for all the *P. agariciferus* collected from the Philippines, with only a few specimens obtained by trawls (e.g. those in Vanuatu and Taiwan). The material from the Philippines was collected from deeper waters along steep cliffs, areas which can neither be sampled by divers, trawls or dredges (Ng et al. 2009). These heretofore rare species almost certainly prefer such inaccessible habitats and are thus rarely collected by dredges and trawls (see Mendoza et al. 2010).

Distribution and depth. Ikeda's (1998) Japanese specimen was collected from 180–200 m of water off Nagai in Sagami Bay. The holotype male from Taiwan was obtained from a depth of 170 m, with the series from the Philippines collected from 80–140 m.

Acknowledgements

This study was partially sponsored by the Fisheries Agency, Council of Agriculture, Executive Yuan, R.O.C. (106AS-10.2.1-FA-F1). We are grateful to Bella Galil, Hironori Komatsu, and Sammy De Grave for their many constructive comments. Thanks are also due to Cheng Anyi (ASIZ) for her help with the manuscript.

References

Alcock A (1896) Materials for a carcinological fauna of India. No. 2. The Brachyura Oxystoma. Journal of the Asiatic Society of Bengal 65(2): 134–296. [pls 6–8]

Alcock A (1899) An account of the deep-sea Brachyura collected by the marine survey ship "Investigator". Trustees of the Indian Museum, Calcutta, 85 pp. [4 pls.]

Alcock A (1900) Materials for a carcinological fauna of India. No. 5. Brachyura Primigenia or Dromiacea. Journal of the Asiatic Society, Bengal 1899(1900) 68: 123–169.

Balss H (1922) Ostasiatische Decapoden. III. Die Dromiaceen, Oxystomen und Parthenopiden. Archiv für Naturgeschichte 88A(3): 104–140. [figs 1–9]

Chen H (1989) Leucosiidae (Crustacea, Brachyura). In: Forest F (Ed.) Résultats des Campagnes MUSORSTOM, Volume 5. Mémoires du Muséum National d'Histoire Naturelle, Paris (A) 144: 181–263.

Davie PJF, Guinot D, Ng PKL (2015) Anatomy and functional morphology of Brachyura.. In: Castro P, Davie PJF, Guinot D, Schram FR, von Vaupel Klein JC (Eds) Treatise on Zoology – Anatomy, Taxonomy, Biology. The Crustacea. Volume 9C-I. Decapoda: Brachyura (Part 1), 11–163. https://doi.org/10.1163/9789004190832_004

Galil BS, Ng PKL (2007) Leucosiid crabs from Panglao, Philippines, with descriptions of three new species (Crustacea: Decapoda: Brachyura). Raffles Bulletin of Zoology, Supplement 16: 79–94.

Galil BS, Ng PKL (2010) On a collection of calappoid and leucosioid crabs (Decapoda, Brachyura) from Vanuatu, with description of a new species of Leucosiidae. In: Castro P, Davie PJF, Ng PKL, Richer de Forges B (Eds) Studies on Brachyura: a homage to Danièle Guinot. Crustaceana Monographs 11: 139–152.

Ihle JEW (1918) Die Decapoda Brachyura der Siboga-Expedition. III. Oxystomata: Calappidae, Leucosiidae, Raninidae. Siboga Expeditie 39b2: 1–322.

Ikeda H (1998) The Deep-Sea Crabs of Sagami Bay. Hayama Shiosai Museum, Kanagawa, Japan, 180 pp.

Komatsu H, Manuel MR, Takeda M (2005) A small collection of leucosiid crabs (Crustacea; Decapoda; Brachyura) from Balicasag Island, Bohol, Philippines. Species Diversity 10: 105–123.

Marumura M, Kosaka A (2003) Catalogue of the brachyuran and anomuran crabs donated by the late Mr. Seiji Nagai to the Wakayama Prefectural Museum of Natural History. Wakayama Prefectural Museum of Natural History, Kainan, 73 pp.

McLay CL (1999) Crustacea Decapoda: Revision of the family Dynomenidae. In: Crosnier A (Ed.) Résultats des Campagnes MUSORSTOM Volume 20. Mémoires du Muséum national d'Histoire naturelle 180: 427–569. [figs 1–40]

McLay CL, Ng PKL (2005) On a collection of Dromiidae and Dynomenidae from the Philippines, with description of a new species of *Hirsutodynomene* McLay, 1999 (Crustacea: Decapoda: Brachyura). Zootaxa 1029: 1–30. https://doi.org/10.11646/zootaxa.1029.1.1

Mendoza JCE, Naruse T, Tan SH, Chan T-Y, Richer de Forges B, Ng PKL (2010) Case studies on decapod crustaceans from the Philippines reveal deep, steep underwater slopes as prime habitats for 'rare' species. Biological Conservation 19: 575–586. https://doi.org/10.1007/s10531-009-9744-x

Milne-Edwards A (1880) Études préliminaires sur les Crustacés, 1ère Partie. In: Reports on the results of dredging under the supervision of Alexander Agassiz, in the Gulf of Mexico, and the Caribbean Sea, 1877, 1878, 1879, by the U. S. coast survey steamer "Blake". Lieut.-Commander C. D. Sigsbee, U.S.N., and Commander J. S. Bartlett, U.S.N. commanding. Bulletin of the Museum of Comparative Zoology, Harvard 8(1): 1–68. [pls. 1, 2]

MOJ (Ministry of Justice, Taiwan) (2014) Laws and Regulations Database of The Republic of China. Management approach to fishing vessels engaging in coral fisheries in Taiwan. Dated 26 September 2014. http://law.moj.gov.tw/LawClass/LawOldVer.aspx?Pcode=M0050038&LNNDATE=20140210&LSER=001

Nagai S (1989) Brachyuran fauna of Wakayama Prefecture II, Nankiseibutu 31(1): 39–44.

Ng PKL (1999) Book review: The Deep-Sea Crabs of Sagami Bay. H. Ikeda, 1998. Hayama Shiosai Museum, Kanagawa, Japan. Crustaceana 72(7): 717–718.

Ng PKL, Guinot D, Davie PJF (2008) Systema Brachyurorum: Part I. An annotated checklist of extant brachyuran crabs of the world. Raffles Bulletin of Zoology, Supplement 17: 1–286.

Ng PKL, Mendoza JCE, Manuel-Santos M (2009) Tangle net fishing, an indigenous method used in Balicasag Island, central Philippines. Raffles Bulletin of Zoology, Supplement 20: 39–46.

Ortmann AE (1892) Die Abtheilungen Hippidea, Dromiidea und Oxystomata. Die Decapoden-Krebse des Strassburger Museums, mit besonderer Berücksichtigung der von Herrn Dr. Döderlein bei Japan und bei den Liu-Kiu-Inseln gesammelten und zur Zeit im Strassburger Museum aufbewahrten Formen. Theil V [= Part V]. Zoologische Jahrbücher, Abtheilung für Systematik Geographie und Biologie der Thiere 6(4): 532–588. [pl. 26]

Sakai T (1937) Studies on the Crabs of Japan. II. Oxystomata. Science Reports of the Tokyo Bunrika Daigaku, Section B, 3 (Supplement 2): 67–192. [figs 1–45, pls 10–19, Table I]

Sakai T (1965) The Crabs of Sagami Bay, collected by His Majesty the Emperor of Japan. Tokyo, Maruzen Co., 206 pp. [figs 1–27 (English text), pls 1–100, pp 1–92 (Japanese text), pp 1–26 (references and index in English), pp 27–32 (index in Japanese), 1 map]

Sakai T (1976) Crabs of Japan and the adjacent seas. Tokyo, Kodansha Ltd. [3 volumes: (1) English text, xxxix + 773 pp, figs, 1–379; (2) Plates, 16 pp., pls 1–251; (3) Japanese text, 461 pp, figs 1–2]

Serène R, Vadon C (1981) Crustacés Décapodes. Brachyoures. Liste préliminaire, description de formes nouvelles et remarques taxonomiques. Résultats des Campagnes MUSORSTOM, 1. Philippines (18-28 Mars 1976). Memoires ORSTOM, No. 91 1981: 117–140. [pls 1–4]

Shih Y-J, Ho H-P, Jeng M-S (in press) Two new records of the leucosioid genus *Pariphiculus* (Alcock, 1896) from Taiwan (Decapoda, Brachyura, Iphiculidae). Crustaceana.

Tan CGS (1996) Leucosiidae of the *Albatross* expedition to the Philippines, 1907–1910 (Crustacea: Brachyura: Decapoda). Journal of Natural History 30: 1021–1058. https://doi.org/10.1080/00222939600770551

Tan CGS, Ng PKL (1995) A revision of the Indo-Pacific genus *Oreophorus* Rüppell, 1830 (Crustacea: Decapoda: Brachyura: Leucosiidae). In: Richer de Forges B (Ed.) Les fonds meubles des lagons de Nouvelle-Calédonie (Sédimentologie, Benthos), Etudes & Thèses, Volume 2, ORSTOM, 101–205. [pls 1–16]

Tu T-H, Dai C-F, Jeng M-S (2012) Precious corals (Octocorallia: Coralliidae) from the northern West Pacific region with descriptions of two New Species. Zootaxa 3395: 1–17.

Yokoya Y (1933) On the Distribution of Decapod Crustaceans inhabiting the Continental Shelf around Japan, chiefly based upon the Materials collected by S. S. Sôyô-Maru, during the Year [sic] 1923–1930. Journal of the College of Agriculture, Tokyo Imperial University 12(1): 1–226. [figs 1–71]